The Dark Side of Polar Day

The influence of coastal run-off
on Arctic kelp communities

Sarina Niedzwiedz

Dissertation

In fulfilment of the requirements
for the degree of
Doctor of natural sciences (Dr. rer. nat)

at the Faculty 02 – Biology and Chemistry
of the University of Bremen, Germany

July 2024

_____

Cover figures: *Saccharina latissima* under different run-off influences in the Arctic.

© Sarina Niedzwiedz

Thesis submission: 26.07.2024

Colloquium: 20.09.2024

Thesis reviewers:

First reviewer: Prof. Dr. Kai Bischof
Marine Botany; University of Bremen
Bremen, Germany

Second reviewer: Prof. Dr. Lars Chresten Lund-Hansen
Department of Biology – Aquatic Biology; Aarhus University
Aarhus, Denmark

Third reviewer: Prof. Dr. Katrin Iken
College of Fisheries and Ocean Sciences
University of Alaska Fairbanks
Fairbanks, USA

Examination commission:

Commission chair: Prof. Dr. Marko Rohlfs
Population and Evolutionary Ecology; University of Bremen
Bremen, Germany

Examiner: Prof. Dr. Kai Bischof
Marine Botany; University of Bremen
Bremen, Germany

Examiner: Prof. Dr. Lars Chresten Lund-Hansen
Department of Biology – Aquatic Biology; Aarhus University
Aarhus, Denmark

Examiner: Prof. Dr. Laurie Hofmann
Shelf Sea System Ecology; Alfred-Wegener-Institute
Bremen, Germany

Student member: Florian Stahl
PhD student; Marine Botany; University of Bremen
Bremen, Germany

Student member: Milena Söhnen
M.Sc. student; Marine Botany; University of Bremen
Bremen, Germany

Table of content

_____

_____

Summary

Arctic coastal ecosystems are currently facing severe environmental transformations due to ongoing climate change. Rates of Arctic sea surface temperature rise are far beyond the global average. Glacial, snow and permafrost melt are accelerating and precipitation rates are expected to increase, leading to extensive run-off plumes covering fjords. Run-off plumes alter many water column parameters, e.g., high concentrations of suspended particles reduce the flux of photosynthetically active radiation (PAR) and spectral composition; terrestrial and lithogenic material alter dissolved element concentrations. Along Arctic rocky coastlines, brown macroalgae, so called kelps (Laminariales), act as foundation species, providing the basis of life for many associated species. Recently, it was found that the thermal tolerance of kelps alone acts as weak predictor for their cold-distribution limit. Contributing to the knowledge of what defines the distribution of Arctic kelp populations, I combined *in-situ* monitoring with experimental approaches to analyse the acclimatisation potential and responses of kelps to environmental changes. Altered kelp performances can have cascading consequences to associated biota and is essential for the dynamics and functioning of future Arctic coastal ecosystems.

In two *in-situ* studies, I found run-off plumes to significantly condition kelp populations, having the potential to change Arctic coastal ecosystem functioning. While run-off influenced kelps were characterised by higher nitrogen contents (**publ. I**), they also accumulated harmful elements (**publ. II**). As both changes have the potential to alter susceptibilities and responses of kelps towards environmental drivers, the local conditioning of populations has to be considered in climate projections. I further found the kelps' microbiome to significantly respond to differences in run-off intensity, influencing the health, nutritional value and element cycling of kelp holobionts (**publ. II**). In three experimental studies, I focussed on the effect of changing PAR × temperature interactions. I showed that temperature influences are highly interactive with the prevailing PAR conditions (**publ. III**): Being exposed to high PAR levels, kelps overall experienced high-light stress, and acclimatised by a reduction of the light harvesting complex. Warm temperatures mitigated high-light stress and cold temperatures enhanced it. In **publ. IV**, I showed that the interaction of high-PAR × cold temperatures is detrimental for the temperate kelp *Laminaria hyperborea*, preventing its spread to higher latitudes. When kelps were exposed to low PAR levels, I found their overall physiological stress level to be reduced. However, kelps were also characterised by an overall low carbon content when PAR intensities are too low to maintain a positive net carbon balance, potentially resulting in habitat loss. The temperature impact under low-PAR availabilities was species dependent. Warm temperatures had the potential to further decrease the net carbon content of kelps, resulting in a temperature driven reduction of the lower depth distribution limit (**publ. V**).

These strong physiological and biochemical responses of kelps towards changes in PAR × temperature interactions, have consequences for the seasonal performance of kelps. The results of my studies suggest that high-PAR availabilities during polar spring cause high physiological stress levels, eventually being mitigated in summer by increasing temperatures and a reduction of PAR by run-off (**publ. III**). The response towards polar winter is likely to be strongly species dependent, being defined by a species' net carbon balance. As run-off plumes establish a steep spatial gradient, PAR × temperature conditions vary greatly within a fjord. Generally, the run-off influence is highest in the inner fjord, decreasing towards the outer fjord. I found run-off to lead to an accumulation of harmful elements in kelps, which might cause a reduced algal performance in the inner fjord (**publ. II**). Further, limited PAR intensities in run-off plumes reduce the maximum distribution depth of the kelps (**publ. V**). Towards the outer fjord, PAR availability increases, eventually causing physiological and biochemical changes in kelps to counteract high-PAR stress. As outer fjord boundaries have a great influence on the fjord environment, conditioning kelp populations (**publ. I**), research efforts must aim for a pan-Arctic approach to increase the understanding on general Arctic ecosystem functioning. The high spatial variability of present-day fjords makes it difficult to model future developments of Arctic coastal ecosystems. While extreme events such as marine heatwaves, cold spells, or the crossing of climate tipping points can lead to severe and immediate disruptions of ecosystems, gradual environmental changes alter the interspecific competition balance of kelps (**publ. III, IV, V**), which might lead to large scale changes of the ecosystem. While I argue that the presence and intensity of run-off plumes act as integrating predictor for kelp forest distribution, more undescribed parameters have to be explored, e.g., substrate availability.

On a global scale, kelp forest losses at their warm distribution limit seem to outpace their expansion at high latitudes. Hence, the area of wild kelp forests and their contribution to global carbon sequestration might decline in the near future. A possibility to increase kelp carbon sequestration might be the implementation of kelp maricultures. High-latitude kelp maricultes might also provide a sustainable livelihood possibility. However, when farmed kelps are used for food production, the accumulation of heavy metals from run-off has to be considered (**publ. II**).

Concluding, climate change induced Arctic run-off, and especially varying PAR availability, has drastic consequences on the performance of kelps, with the potential to limit Arctic kelp distribution. While I investigated the responses of kelp sporophytes, kelps have to complete their entire life cycle to establish stable populations. Hence, I propose future research to investigate the susceptibilities of the microscopic life stages. Further, it is crucial to understand and compare present-day spatial variability of abiotic conditions in fjords. Therefore, I propose the implementation of long-term monitoring stations, covering the fjord gradient.

Zusammenfassung

Durch den Klimawandel ändern sich die Umweltbedingungen in arktischen Küstenökosystemen drastisch. Der Anstieg der Meeresoberflächentemperatur in der Arktis liegt weit über dem globalen Durchschnitt. Gletscher, Schnee und Permafrostböden schmelzen und es wird erwartet, dass die Niederschlagsmenge zunimmt. Dies führt zum Eintrag großer Mengen terrestrischer Sedimente in die Fjorde, verbunden mit der Änderung vieler Wasserparamter: hohe Schwebstoffkonzentrationen dämpfen die Intensität photosynthetisch aktiver Strahlung (PAR) und ihre spektrale Zusammensetzung; terrestrisches und lithogenes Material ändert die Elementkonzentrationen des Wassers. Entlang arktischer Felsküsten bilden braune Makroalgen (Laminariales) Kelpwälder und bieten die Lebensgrundlage für viele Organismen. Die Verbreitung von arktischen Kelps wird durch Temeraturtoleranz alleine nur unzulänglich beschrieben. Daher habe ich *in-situ* Beobachtungen mit experimentellen Ansätzen kombiniert, um die Verbreitung von arktischen Kelps und ihr Anpassungspotential auf sich verändernde Umweltbedingungen besser zu verstehen. Eine Veränderung der Kelpwälder kann weitreichende Folgen für das gesamte Ökosystem haben. Daher sind Kelpwälder von entscheidender Bedeutung für die Dynamik und Funktionalität zukünftiger Küstenökosysteme in der Arktis.

In zwei *in-situ* Studien habe ich nachgewiesen, dass Sedimentfahnen Kelppopulationen und die Funktion arktischer Küstenökosysteme erheblich beeinflussen. Kelps unter starkem Sedimentfahneneinfluss waren durch höhere Stickstoffgehalte gekennzeichnet (**Publ. I**), akkumulierten jedoch auch schädliche Elemente (**Publ. II**). Beide Veränderungen haben das Potential, die Reaktionsfähigkeit von Kelps auf Umweltveränderungen zu beeinflussen. Daher müssen lokale Unterschiede zwischen Kelppopulationen in Klimawandelmodellen berücksichtigt werden. Zudem konnte ich zeigen, dass das Kelp-Mikrobiom von dem Sedimentfahneneinfluss abhängt, was die Ökosystem Leistungen des Kelp Holobionten beeinflusst (**Publ. II**). In drei experimentellen Studien, habe ich nachgewiesen, dass der Temperatureinfluss auf Kelps von der Interaktion mit den vorherrschenden Lichtbedingungen abhängt (**Publ. III**): Waren Kelps Starklicht ausgesetzt, zeigten sie ein hohes physiologisches Stresslevel, was zu einer Anpassung des photosynthetischen Lichtsammelkomplexes führte. Höhere Temperaturen minderten Starklichtstress, während niedrige Temperaturen ihn verstärkten. Für die Kelpart *Laminaria hyperborea* lagen niedrige Temperaturen in Verbindung mit Starklicht außerhalb des Toleranzbereiches, was ihre arktische Ausbreitung unter aktuellen Bedingungen verhindert (**Publ. IV**). Waren Kelps Schwachlicht ausgesetzt, sank ihr physiologisches Stresslevel. Allerdings zeigten diese Populationen einen geringen Kohlenstoffgehalt, was zu einem potentiellen Lebensraumverlust führt. Der Temperatureffekt unter Schwachlichteinfluss ist artenabhängig. Erhöhte Temperaturen hatten das Potential den Kohlenstoffgehalt der Kelps zu reduzieren (**Publ. V**).

Die starken physiologischen und biochemischen Reaktionen der Kelps auf unterschiedliche PAR × Temperatur Interaktionen hat Auswirkungen auf ihre Reaktionen im Jahreszeitenverlauf. Die Ergebnisse meiner Studien deuten darauf hin, dass hohe PAR Intensitäten im polaren Frühjahr Starklichtstress auslösen. Steigende Temperaturen im Sommer und gedämpfte PAR Intensitäten in Sedimentfahnen mindern den Starklichtstress (**Publ. III**). Die Reaktion während des polaren Winters ist vermutlich stark artabhängig und wird von dem Kohlenstoffhaushalt der Arten bestimmt. Da Sedimentfahnen einen ausgeprägten räumlichen Gradienten bilden, variieren PAR- und Temperaturbedingungen stark innerhalb eines Fjordes. Grundsätzlich ist der Einfluss der Sedimentfahnen im Fjordinneren am stärksten. Eine hohe Anreicherung von schädlichen Elementen in Kelps, könnte zu einer geringeren Produktivität der Kelps im Fjordinneren führen (**Publ. II**). Schwachlichtintensitäten begrenzen zudem die maximale Verteilungstiefe des Kelpwaldes (**Publ. V**). Äußere Fjordbereiche sind durch höhere PAR Intensitäten gekennzeichnet, was zu physiologischen und biochemischen Veränderungen der Kelps führt, um Starklichtstress zu reduzieren. Da Umweltbedingungen zwischen Fjorden stark variieren, müssen wissenschaftliche Aktivitäten einen pan-arktischen Ansatz verfolgen, um das Verständnis für arktische Küstenökosysteme zu erhöhen. Die hohe räumliche Variabilität der Fjorde erschwert die Modellierung zukünftiger arktischer Küstenökosysteme. Extremereignisse, wie marine Hitze- und Kältewellen oder Klimakipppunkte führen zu schwerwiegenden und unmittelbaren Ökosystemstörungen. Graduelle Veränderungen beeinflussen die interspezifische Konkurrenz der Kelps (**Publ. II, IV, V**). Während meine Ergebnisse zeigen, dass das Ausmaß von Sedimentfahnen als integrativer Indikator für die Verbreitung arktischer Kelpwäldern dienen kann, müssen weitere Faktoren untersucht werden, z. B. die Verfügbarkeit von Substrat.

Weltweit scheint der Verlust von Kelpwäldern an ihrer warmen Verbreitungsgrenze ihre Ausbreitung in der Arktis zu übertreffen. Daher könnten sowohl die Fläche von natürlichen Kelpwäldern, als auch ihr Beitrag zur Kohlenstoffbindung in naher Zukunft abnehmen. Eine Möglichkeit die Kohlenstoffbindung durch Kelps zu erhöhen, könnte die Einführung von Kelp Marikulturen sein. Diese könnten auch einen nachhaltigen Lebensunterhalt bieten. Bei der Nutzung der Kelps als Nahrungsmittel muss die Schwermetallanreicherung berücksichtigt werden (**Publ. II**).

Klimawandel-induzierte Sedimentfahnen und die Änderung in der PAR Verfügbarkeit haben drastische Auswirkungen auf das Ökosystem und die Verbreitung arktischer Kelpwälder. Während ich die Reaktionen von Kelp Sporophyten untersucht habe, muss die Reaktion von mikroskopischen Lebensstadien ein Forschungsschwerpunkt werden, da Kelps ihren gesamten Lebenszyklus durchlaufen müssen, um stabile Populationen zu etablieren. Zudem muss die gegenwärtige räumliche Variabilität zwischen Fjorden verstanden und verglichen werden. Daher schlage ich die Einrichtung von Langzeit-Messstationen über den Fjordgradienten vor.

List of figures and tables in the synoptic chapters

1 General introduction

7 Synoptic discussion

8 Conclusion

Abbreviations

AA	Arctic Amplification
Acc	Accessory pigments
	$= chlorophyll\ c + \beta\ carotene + fucoxanthin$
AMAP	Arctic Monitoring and Assessment Programme
AMOC	Atlantic Meridional Overturning Circulation
AOA	Antioxidant activity (Re et al. 1999)
C	Total carbon content
C:N	Carbon to nitrogen ratio
CO_2	Carbon dioxide
CTD	Oceanographic instrument to measure conductivity, temperature and water depth
DW	Dry Weight
DPS	De-epoxidation state of xanthophyll cycle pigments after Colombo-Pallotta et al. (2006)
	$= \dfrac{Zeaxanthin + (0.5 * Antheraxanthin)}{Violaxanthin + Antheraxanthin + Zeaxanthin}$
F_v/F_m	Maximum quantum yield of photosystem II
FW	Fresh weight
gbif	Global Biodiversity Information Facility; https://www.gbif.org/
I_λ	Spectrally downwelling irradiance (µmol photon m^{-2} s^{-1} nm^{-1})
IPCC	Intergovernmental Panel on Climate Change
K_d	Light attenuation coefficient after Hanelt et al. (2001)
	$= \dfrac{1}{depth_1\ (m) - depth_2\ (m)} * \ln(\dfrac{PAR_{depth\ 2}\ (\mu mol\ photons\ m^{-2}\ s^{-1})}{PAR_{depth\ 1}\ (\mu mol\ photons\ m^{-2}\ s^{-1})})$
MHW	Marine heatwave
N	Total nitrogen content
PAR	Photosynthetically active radiation (also: photosynthetically available radiation)
	$= \sum_{400}^{700} I_\lambda$ = µmol photons m^{-2} s^{-1}
Publ.	Publication
S_A	Salinity
SST	Sea surface temperature
VAZ	Pool of xanthophyll cycle pigments
	$= Violaxanthin + Antheraxanthin + Zeaxanthin$
×	Symbol to mark interacting drivers

_____

Glossary
(Extended after Niedzwiedz 2021)

Acclimation refers to the coordinated, fast and reversible adjustment of the *phenotype* in response towards one single environmental driver, while **acclimatisation** is the response towards several interacting environmental drivers (Collier et al. 2019). Thereby, a constant or increased *performance* is facilitated (Collier et al. 2019). Acclimation / Acclimatisation occurs in two phases: 1) short-term / acute response. 2) long-term / chronic response (Horowitz 2002).

Adaption occurs across generations through natural selection of heritable *phenotypic* traits. The shift of the allele frequency potentially results in an increased *performance* in the prevailing environment and eventually a shift of the populations *tolerance limits* (Donelson et al. 2019).

Albedo describes the fraction of incoming solar radiation being reflected by a surface, often expressed as percentage. High albedo: snow-covered surfaces; Low albedo: vegetation-covered surfaces or open water (IPCC 2018).

Antioxidative response describes a defence system against *oxidative stress*, consisting of enzymatic and non-enzymatic (e.g., phlorotannins) processes (Rezayian et al. 2019).

Arctic amplification describes the Arctic warming faster than the global average, being a prominent phenomenon of anthropogenic *climate change* (England et al. 2021; Previdi et al. 2021).

Blue carbon refers to the inorganic carbon taken up by living organisms of coastal and marine ecosystem that is stored as biomass or in sediments (IPCC 2018).

Climate change describes a phenomenon in which climatic properties change in mean value or variability over an extended period, typically decades or longer (IPCC 2018). While climate change can be caused naturally, I generally refer to anthropogenic activities causing climatic changes, if not stated otherwise.

Climate feedback describes a relationship between two climate quantities, where a perturbation of one leads to changes in a second climate quantity, which has an additional effect on the first (IPCC 2018).

Climate forcing refers to the change of an external driver of climate change, e.g., the rise of atmospheric greenhouse gas concentration (Previdi et al. 2021)

Compensation irradiance describes the *PAR* intensity at which photosynthetic processes balance respiration rates (Falkowski and Raven 2007). **Compensation depth** relates to the depth in which the light intensity matches the compensation irradiance (Falkowski and Raven 2007).

Coastal darkening in the Arctic refers to the reduced PAR transmission through the water column due to extensive coastal run-off plumes covering fjords, carrying a high concentration of suspended particles. The run-off plumes originate from *climate change* induced glacial and permafrost melt, as well as higher precipitation rates (Konik et al. 2021; **publication V**).

Ecosystem engineer is a species that structures a species community, and modifies environmental conditions, species interactions, and the availability of resources. Ecosystem engineers can be both keystone and *foundation species* (Jones et al. 1977).

Fitness describes the ability of an individual to survive and produce fertile offspring in the ambient environment (Orr 2009).

Foundation species is a species that acts as *ecosystem engineer* by their presence not actions (Wernberg et al. 2024).

Genotype is the sum of allele-pair types of a diploid organism (Mahner and Kary 1997).

Kelp is used *sensu stricto*, referring to brown algae of the order Laminariales (Steneck et al. 2002; Bartsch et al. 2008).

Marine heatwave describes a prolonged discrete event of anomalously warm water, lasting for a minimum of five consecutive days with temperatures warmer than the 90th percentile of a 30-year historical baseline (Hobday et al. 2016).

Niche (Malanson et al. 1992; Severtsov 2013)**:**
- **Fundamental niche**: the entire suitable range of abiotic environmental conditions for a species; defined by *adaptation*
- **Realised niche**: actual distribution area of a species; usually smaller than the fundamental niche, as it is bound by limits, e.g., physical dispersal barriers or biological interactions
- **Thermal niche**: a species' *performance curve* in response to temperature; often based on the response of one single, central population (King et al. 2017; Bennett et al. 2019)

Optimum describes the environment / environmental condition at which a *performance curve* for a *phenotypic* trait expression is at its maximum (Wahl et al. 2020).

Performance is a measure of the *phenotypic* expression of a *fitness*-related trait (Kingsolver and Huey 2003). A performance of zero marks the *tolerance limits* of an individual for an environment.
Performance curve (= tolerance curve; Chevin et al. 2010) is a graph that describes the expected *phenotypic* trait expression (i.e., *performance*) of a *genotype* as a function of an environmental factor (Wahl et al. 2020).

Phenotype is the set of trait characteristics of an organism that is influenced by the *genotype* and the environment (Mahner and Kary 1997).

_____

Phenotypic plasticity (= acclimatisation potential; Somero et al. 2010) is the ability of a single *genotype* to produce different *phenotypes* in response towards the environment (Fox et al. 2019).

Photosynthetically active ration (PAR; also: photosynthetically available radiation) is electromagnetic waves between 400–700 nm (Falkowski and Raven 2007). **PAR availability** refers to the combination of PAR intentsity, photoperiod and spectral composition.

Sea surface temperature is the subsurface bulk temperature in the top few metres of the ocean (IPCC 2018).

Stress:

- **cellular stress response**: genetically conserved mechanism to protect cells from sudden environmental changes, threatening the damage of macromolecules (Kültz 2003; 2005).
- **core stress proteome**: response to survive environmental fluctuations (Kültz 2003) and maintain a high *performance* (→ *acclimation / acclimatisation*).
- **oxidative stress**: major component of cellular stress caused in an oxygenated environment. Can be the consequence of any kind of environmental stress, when electrons are transferred to oxygen, forming reactive oxygen species (ROS), destroying macromolecules → triggers *antioxidative response* (Bischof and Rautenberger 2012).
- **stressor**: any kind of environmental driver moving away from the optimum of a species, triggering cellular stress response (Collier et al. 2019; Wahl et al. 2020).

Temperature: In the frame of this thesis, I use the terms
- 'cold temperatures' for suboptimal temperatures with regard to the reported temperature optimum of a species and
- 'warm temperatures' as temperatures near a species reported thermal *optimum*

Tolerance range is the width of a *performance curve*, which is determined by the *genotype* and can only be modified by *adaptation*. The **tolerance limits** are described by a *performance* of zero (Chevin et al. 2010).

Scientific Curriculum vitae

Education

10.2021–09.2024	PhD position within the EU project FACE-IT at the University of Bremen
10.2019–09.2021	Master degree program "Marine Biology" at the University of Bremen Final grade: 1.48
10.2016–09.2019	Bachelor degree program "Biologie" (Biology) at the University of Bremen Final grade: 1.43

Publications

Published

2024 **Publication III**		Light-mediated temperature susceptibility of kelp species (*Agarum clathratum*, *Saccharina latissima*) in an Arctic summer heatwave scenario **Niedzwiedz S**, Vonnahme TR, Juul-Pedersen T, Bischof K, Diehl N Cambridge Prisms: Coastal Future
2024		The sugar kelp *Saccharina latissima* II: recent advances in farming and applications Sæther M, Diehl N, Monteiro C, Li H, **Niedzwiedz S**, Burgunter-Delamare B, Scheschonk L, Bischof K, Forbord S Review article; Journal of Applied Phycology
2024		The sugar kelp *Saccharina latissima* I: recent advances in a changing climate Diehl N, Li H, Scheschonk L, Burgunter-Delamare B, **Niedzwiedz S**, Forbord S, Sæther M, Bischof K, Monteiro C Review article; Annals of Botany
2023 **Publication V**		Glacial retreat and rising temperatures are limiting the expansion of temperate kelp species in the future Arctic **Niedzwiedz S**, Bischof K Limnology and Oceanography
2022		Biocrusts from Iceland and Svalbard: Does microbial community composition differ substantially? Pushkareva E, Elster J, Holzinger A, **Niedzwiedz S**, Becker B Frontiers in Microbiology
2022		Seasonal and inter-annual variability in the heatwave tolerance of the kelp *Saccharina latissima* (Laminariales, Phaeophyceae) **Niedzwiedz S**, Diehl N, Fischer P, Bischof K Phycological Research

_____

Submitted

07.2024 **Publication II**	Run-off impacts on Arctic kelp holobionts have strong implications on ecosystem functioning and bioeconomy **Niedzwiedz S**, Schmidt CE, Yang Y, Burgunter-Delamare B, Andersen S, Hildebrandt L, Pröfrock D, Thomas H, Zhang R, Damsgård B, Bischof K
06.2024 **Publication IV**	Photoperiod and temperature interactions drive the latitudinal distribution of kelps under climate change Diehl N, Laeseke P, Bartsch I, Bligh M, Buck-Wiese H, Hehemann J-H, **Niedzwiedz S**, Plag N, Karsten U, Shan T, Bischof K
05.2024 **Publication I**	Local environmental settings condition biochemistry of Arctic kelp populations **Niedzwiedz S**, Voigt C, Andersen S, Diehl N, Damsgård B, Bischof K

In preparation; expected submission in 2024

	Kelp and phytoplankton in Arctic fjord: drivers and future trajectories – a toolbox for ecosystem comparisons **Niedzwiedz S** / Vonnahme TR, Holding J, Schlegel R, Duarte P, Bailey A, Lund-Hansen LC (main author team; more co-authors will be invited to contribute)
	Impact of climate change on the kelp *Laminaria digitata* – simulated Arctic winter warming Trautmann M, Bartsch I, Bligh M, Buck-Wiese H, Hehemann J-H, **Niedzwiedz S**, Plag N, Shan T, Bischof K, Diehl N
	Shaping the plasticity of *Saccharina latissima* – the potential of thermal priming and genetic lines Gauci C, Bartsch I, **Niedzwiedz S**, Hill G, Hoarau G, Jüterbock A
	Quantifying Arctic kelp carbon reservoirs: an empirical approach to kelp standing stocks Castro de la Guardia L, Hop H, Düsedau L, Ager TG, Krause-Jensen D, Sejr M, Schlegel RW, Gattuso J-P, Lebrun A, Bartsch I, **Niedzwiedz S**, Diehl N, Filbee-Dexter K, Miller CA, Wiktor J jr., Duarte P (prelim.)

Conferences

02.2024	Kick-off Meeting of the EU project SEA-Quester; Lynby, Denmark
11.2023	Svalbard Science Conference (SSC); Oslo, Norway Poster presentation: Run-off increases heavy metal content in Arctic kelps
09.2023	FACE-IT annual meeting; Bodø, Norway Poster presentation: The Dark Side of Polar Day
08.2023	European Phycological Congress (EPC); Brest, France Poster presentation: Run-off increases heavy metal content in Arctic kelps
02.2023	Arctic Science Summit Week (ASSW); Vienna, Austria Oral presentation: Rising temperatures and a deteriorating light climate are limiting the expansion of temperate kelp species in the Arctic
11.2022	FACE-IT annual meeting; Bremen, Germany
11.2021	Svalbard Science Conference (SSC); Oslo, Norway

Expeditions

08.2024	Planned expedition to Woodfjorden, Svalbard, with RV Oceania (3 weeks)
06-07.2023	Nuuk, Greenland; Greenland Institute for Natural Resources (6 weeks)
08-09.2022	Longyearbyen, Svalbard; The University Centre in Svalbard (4 weeks)
08.2022	Circum Svalbard; Ship-based expedition (2 weeks)
06-07.2021	Kongsfjorden, Svalbard; AWIPEV (4 weeks)
06-07.2019	Kongsfjorden, Svalbard; AWIPEV (7 weeks)

Grants and Prices

10.2023	Winner of the poster award for best poster at the Svalbard Science Conference
08.2023	Winner of the poster award for best poster at the European Phycological Congress
2022	Recipient of the "Arctic Field Grant" by the Research Council of Norway of 92,000 NOK for the Svalbard Field Campaign in 2022

Teaching experience

2023	Supervision of Bachelor thesis of Clara Voigt
	"Impacts of different underwater light climates in Svalbard fjords on the photosynthetic pigments of the kelp *Saccharina latissima*"
2021-2024	Co-supervision of laboratory work during the Bachelor course "Pflanzenphysiologie"

Outreach activities

10.2023	Invited talk: Kelps along a fjord gradient
	Nord University, Bodø, Norway
09.2023	Invited talk: Die dunkle Seite des Polartags
	Haus der Wissenschaft, Bremen
	Publicly available on YouTube
03.2023	Article on homepage of University of Bremen
08.2022	Public talk: Melting glaciers, sediment and underwater forests
	Hurtigruten Expeditions
07.2022	Podcast: Sarina Niedzwiedz unterwegs in den Algenwäldern
	Das Ozean Projekt
	Publicly available on Spotify
05.2022	Invited talk: Von schmelzenden Gletschern, Sediment und Wäldern unter Wasser
	Ocean Chat; Naturwissenschaftlicher Verein Bremen

_____

1   General introduction

1.1   The Arctic

The Arctic describes a region at the northernmost part of the Earth, including the Arctic Ocean and its surrounding land masses of Europe, Asia and North America (Timmermans and Marshall 2020). Its southern boundary varies depending on definition. The Arctic circle is often defined by the tilt of the earth's axis, at approx. 66°32'N (**Figure 1.1A** green line; Murray et al. 1998), which marks the southern latitude at which at least one day of Polar Day (sun does not set for 24 consecutive hours) and Polar Night (sun does not rise for 24 consecutive hours) prevail. However, this definition is neglecting climatologic (e.g., temperature, permafrost occurrence), geographic (e.g., presence of mountains) and oceanographic (e.g., currents) features. In this thesis, I will use the definition of the Arctic Monitoring & Assessment Programme (AMAP), as it includes the "Arctic circle, political boundaries, vegetation boundaries, permafrost limits and major oceanographic features" (**Figure 1.1A** yellow line; Murray et al. 1998).
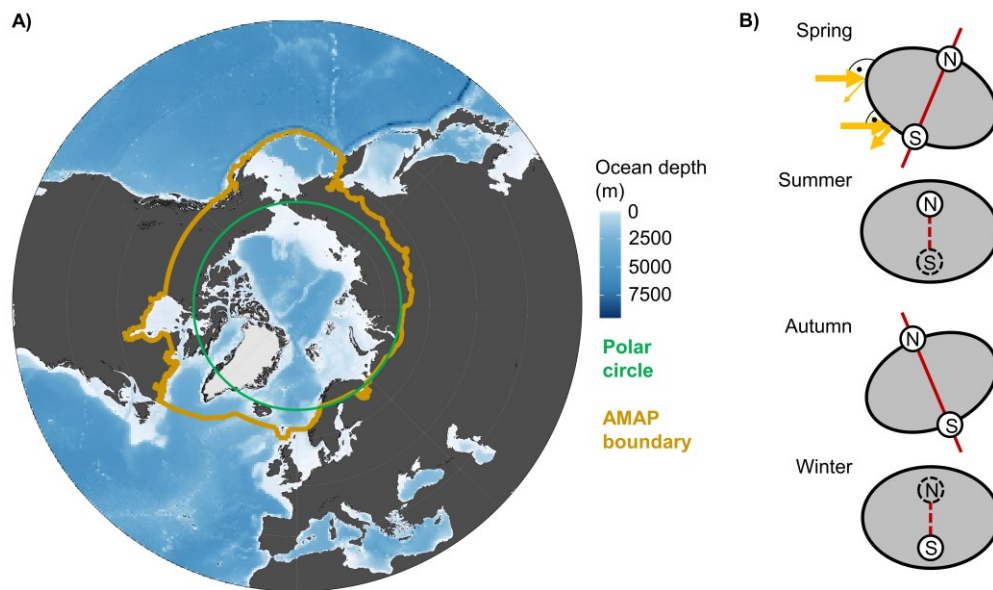
Figure 1.1: **A)** Map of the Arctic and southern boundary. Colour gradient: ocean depth (m). Green line: polar circle at approx. 66°32'N. Yellow line: southern boundary of the Arctic geographical coverage according to the Arctic Monitoring & Assessment Programme (AMAP). Map was created with ggOceanMaps (Vihtakari 2024). **B)** Schematic display of factors influencing the global heat imbalance; modified after Fedorov et al. (2020). View from the sun. Polar regions (N: North Pole; S: South Pole) are less heated due to a smaller angle of incoming irradiance (schematically displayed in spring scenario). Polar regions are characterised by a high albedo (schematically displayed in spring scenario). The tilt of the earth's axis (red line) causes extreme seasonality (northern hemishere perspective: Polar Day in summer; Polar Night in winter).

Arctic weather and climate are characterised by extreme environmental conditions. Polar regions are less heated by the sun compared to the equator, due to the smaller angle of incoming irradiance (**Figure 1.1B**; Fedorov et al. 2020). Hence, the Arctic is characterised by low

_____

temperatures throughout the year (Timmermans and Marshall 2020), leading to a year-round cover of large areas with snow and ice. The resulting high albedo is further reducing the energy uptake of polar regions (**Figure 1.1B**; Previdi et al. 2021). The global heat imbalance is enhanced by the tilt of the earth's axis, leading to an extreme seasonality (**Figure 1.1B**; Fedorov et al. 2020). Arctic winters are characterised by monthlong periods of darkness (Polar Night), while in summer monthlong periods of light (Polar Day) prevail (Gattuso et al. 2020). The heat imbalance drives global atmospheric and oceanic circulations. In the North Atlantic, warm and saline surface water masses from the equator are transported poleward, cooling down by atmospheric heat loss (Eldevik and Nilsen 2013). Near the North Pole, cold, high-salinity water masses sink down, contributing to the global thermohaline circulation (Eldevik and Nilsen 2013; Rahmstorf 2024). Precipitation rates in the Arctic are highest over coastal areas that are influenced by warmer water masses and a high evaporation, usually decreasing towards the north and east (Serreze et al. 2003). Additional to precipitation and melt water drainage, the Arctic Ocean receives ~11 % of the worldwide river discharge (McClelland et al. 2012). In the past 40 years, the abiotic conditions have changed drastically in the Arctic. I will review underlying mechanisms and consequences in **chapter 1.3**.

Even though weather and climate conditions are outside of the tolerance range (**chapter 1.3.3**) for many species, the Arctic provides unique ecosystems and habitats. Species living under Arctic conditions year-round are often characterised by specific adaptations, enabling them to thrive under extreme environmental conditions (Callaghan et al. 2004), e.g., Arctic microorganisms were found to metabolise at temperatures of -20°C (Rivkina et al. 2000). Further, many species, including insects, birds, and mammals, are migrating to the Arctic in summer months to breed, and to take advantage of Polar Day, the high food availability, and reduced predation and parasitism (Kubelka et al. 2022).

Overall, Arctic coastlines comprise ~34 % of the world's coastlines (Lantuit et al. 2012). While being highly productive (Attard et al. 2024), Arctic coastlines are also highly dynamic (Irrgang et al. 2022). They show a great geomorphic diversity, resulting from the interplay of various factors, i.a., cryolithogenic characteristics, glaciation effects, sea ice dynamics, sea-level changes, coast morphology, wave energy, erosion, air and sea temperature and storm intensities (Irrgang et al. 2022). While tides only have little influence on Arctic coasts (ESA 2019), ice berg scouring can cause severe mechanical damage (Krause-Jensen et al. 2012). Coastlines along fjords are considered as a link between land and ocean. Inner fjord boundaries in the Arctic are usually dominated by glacial influences, while the outer fjord region is characterised by an oceanic compound (Cottier et al. 2010). Despite the extreme and dynamic environments, a large proportion of Arctic coastlines are suitable for marine forests (Filbee-Dexter et al. 2019).

1.2   Kelp forests

Along rocky shores from temperate to polar regions, macroalgae form marine forests, dominating a total of ~25 % of the global coastlines (Krumhansl et al. 2016; Wernberg et al. 2019). Intertidal marine forests on the northern hemisphere are often dominated by brown algal species of the order Fucales, while brown algae of the order Laminariales thrive in the subtidal (Bringloe et al. 2020). Tilopterales and Desmarestiales have also been described as habitat forming orders (Bringloe et al. 2020). As all of these species act as foundation species for marine forests, they can be referred to as "kelps" in a functional sense (Fraser 2012). In a stricter sense however, the term "kelp" is only referring to brown algae of the order Laminariales (Steneck et al. 2002; Bartsch et al. 2008). As I focus on Laminariales in this dissertation, I use the term "kelp" *sensu stricto*, not excluding that it can also be used otherwise.

1.2.1   Ecological role of kelps

Kelps act as ecosystem engineers, providing complex three-dimensional structures above the seafloor. Kelp forests are built by diploid sporophytes that can grow several tens of metres in height (Teagle et al. 2017; Wernberg et al. 2019). Sporophytes can have a lifespan of several years (Bartsch et al. 2008) and are structured into three main organs (**Figure 1.2**). Kelps are attached with a holdfast (rhizoid), typically to hard substrate, although exceptions can be found of specimens being attached to gravel on overall soft sediment (Bluhm et al. 2022; Filbee-Dexter et al. 2022). Castro de la Guardia et al. (2023) have found mixed substrata to support the same kelp cover, but with a lower canopy height compared to rocky shores. With the flexible stipe (cauloid), kelps become resistant against wave action and currents (Lüning 1990). Sporophyte growth is restricted to the meristem at the base of the blade (phylloid; Kain 1979). The phylloid is the area of photosynthesis and generally also of reproduction, although there are exceptions, e.g., sporophylls in *Alaria esculenta* (Munda and Lüning 1977). A schematic life cycle of the kelp *Saccharina latissima* can be seen in **Figure 1.2** (modified after Diehl et al. 2024). When the sporophyte is becoming mature, sporangia accumulate into sori, producing microscopic meiospores, which develop into haploid gametophytes (Liu et al. 2017). If conditions do not allow fertility, gametophytes may remain vegetative for months or even years (tom Dieck 1993). Gametophytes show sexually dimorphic traits, with the females producing large eggs in oogonia and the males producing small, motile sperm in antheridia (Liboureau et al. 2024). Eggs and sperm fuse into a zygote, which grows to a sporophyte (Liboureau et al. 2024). The general life cycle sequence is conveyable to other kelp species (Liu et al. 2017), although recently variations in the kelp sexual system have been described (e.g., Liboureau et al. 2024).
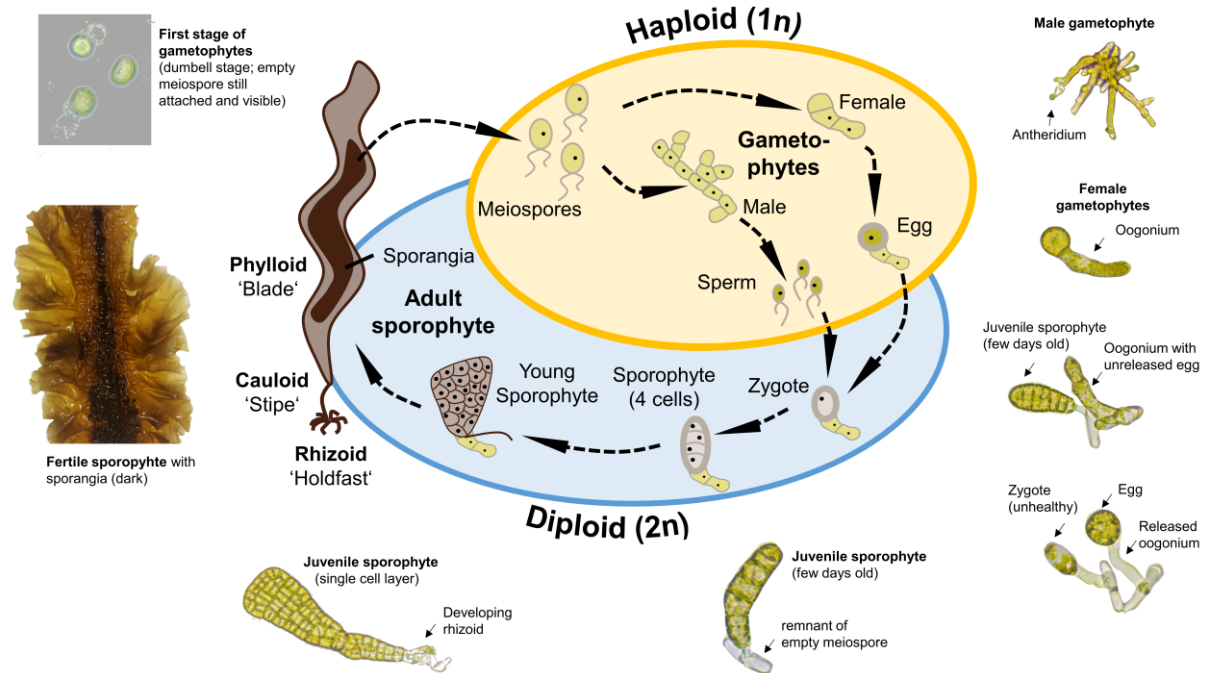
Figure 1.2: Schematic kelp life cycle (here: *Saccharina latissima*). Blue: diploid phase. Yellow: haploid phase. Adult sporophytes (2n) release meiospores (1n), which develop to either female or male gametophytes (1n). Female gametophytes release eggs (1n); male gametophytes release sperm. Egg and sperm fuse to form a zygote (2n), which grows into a sporophyte. Microscopic pictures (I. Bartsch) are provided for additional information on the morphology of developmental stages. Sporophyte photograph: S. Forbord. Modified after: Diehl et al. (2024).

It has to be considered that both diploid and haploid stages of the life cycle have to be completed to establish a population in a specific environment, even though sporophytes represent the life cycle stage that is ecologically and economically most relevant. The sporophyte thallus itself provides habitat for a variety of endo- and epibionts, with a large interspecific diversity. Christie et al. (2003) found 8000 individuals of 130 species on one single *Laminaria hyperborea* sporophyte. Thereby, rhizoid, cauloid and phylloid vary distinctly in the microhabitats they provide, with most species being found in the rhizoid (**Figure 1.3A**; Christie et al. 2003). Further, kelps are a hotspot for microscopic diversity, as they provide an attractive surface for heterotrophic microbial communities by generating oxygen and carbon rich mucus (Egan et al. 2013). The kelp-associated microbial community is composed of prokaryotes (viruses, Archaea, bacteria) and eukaryotes (fungi) (Burgunter-Delamare et al. 2024). The relationships between macroalgae and their associated microbiome is based on metabolite exchange (Burgunter-Delamare et al. 2023, 2024). The community of the kelp-associated microbiome depends on season and abiotic environmental factors (Bengtsson et al. 2010). As the microbiome shapes the development, morphology, fitness and physiology of the (kelp) host, it has been suggested to consider the kelp holobiont as one unit (Rosenberg and Zilber-Rosenberg 2016). The kelp-

_____

associated microbiome can further be an indicator for the health status and the ecosystem services of kelps (Burgunter-Delamare et al. 2023, 2024). Multiple kelp individuals act as foundation species, creating a unique environment by altering the surrounding physio-chemical environment (**Figure 1.3B**, **C**). The kelp canopy reduces the incoming irradiance, which provides habitat for low-light adapted species (Laeseke et al. 2019). Particle transport was shown to be significantly reduced in kelp forests, possibly having benefits for suspension feeders inhabiting kelp understory environments (Eckman et al. 1989). When photosynthesis exceeds respiration, the pH can significantly increase within kelp forests, which might be beneficial for calcifying species (Krause-Jensen et al. 2016). Further, kelps provide protection from predators and nursery ground for many ecological or economically important organisms (Teagle et al. 2017).

As primary producers with a fast production of biomass, kelps are at the base of the benthic food web. Kelps were shown to have a high biosorption potential for cations from their surrounding seawater (Davies et al. 2003), incorporating them intercellularly during growth or via cell wall incorporated fucoidan and alginates (Zeraatkar et al. 2016). This accumulation makes seaweeds good food source for macromolecules for grazers (Kreissig et al. 2021), but, also posing the risk for accumulation of harmful elements (Costa et al. 2016). Many herbivore species, including snails, urchins, crustaceans and fish directly feed on kelps (Christie et al. 2009; Teagle et al. 2017). As those attract larger piscivores and top predators, e.g., birds and sharks, kelp forests support complex food webs (Graham 2004) and a high secondary production (Krumhansl and Scheibling 2012; Teagle et al. 2017). Given the rapid production of biomass, but their ephemeral nature, the role of kelps in carbon sequestration remains controversial and subject of active research (e.g., Gallagher et al. 2022; Filbee-Dexter et al. 2023).
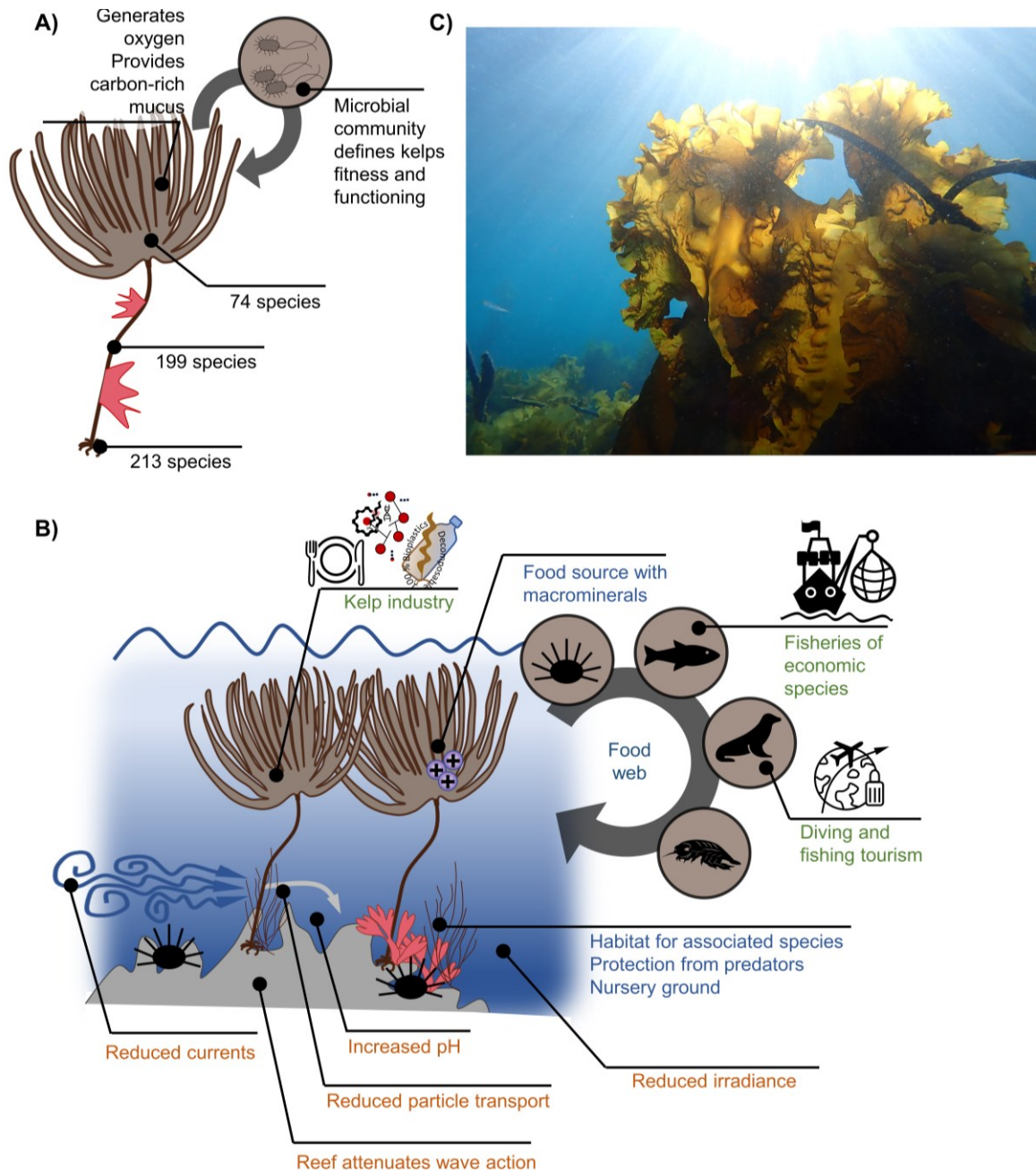
Figure 1.3: **A)** Kelp sporophyte as habitat. Associated species numbers for Norwegian *Laminaria hyperborea* after Christie et al. (2003). **B)** Kelp sporophytes as foundation species alter the physio-chemical properties of the water column (orange text). They provide the basis for many associated species (blue text). Many of their ecosystem services (green text) are economically relevant. **C)** Kelp forests around Nuuk, Greenland in June 2023. *Saccharina latissima*. © Sarina Niedzwiedz

_____

1.2.2   Economic role of kelps

In addition to their crucial ecological role, the ecosystem services provided by kelps are of great economic value (Sæther et al. 2024). Global estimates value the ecosystem services of kelp forests at an average of 500 billion US dollars per year (Eger et al. 2023). Kelp forests have a positive effect on fisheries of economically valuable fish and invertebrate species (Wernberg et al. 2019). Further, the high biodiversity associated to kelps attracts fishing and diving tourism (Wernberg et al. 2019). The effect of coastal protection of kelp forests by damping wave action has long been discussed (e.g., Mork et al. 1996; Dubi and Tørum 1996). However, in more recent studies, the positive effect of wave attenuation of kelps, has been found to be modest (Elsmore et al. 2024) and is rather attributed to coastal geometry and geology rather than the kelps themselves (Morris et al. 2020). Harvested kelps can be used for animal feed, fertiliser and human consumption (**Figure 1.3B**; Sæther et al. 2024). Fascinatingly, resources provided by kelp forests are thought to have facilitated the early colonisation of America from northeast Asia, by people following the "kelp highway" (Erlandson et al. 2007).

Traditionally, kelps have been harvested from the wild. As the industrial interest in chemical compounds, as well as their utilisation in biomedicin, -material and -fuel increases, recent research has been focussing on optimising farming efforts (reviewed by Sæther et al. 2024).

1.2.3   Cold-temperate species forming Arctic kelp forests

Arctic kelp forests are mainly formed by cold-temperate kelp species, such as *Alaria esculenta*, *Agarum clathratum*, *Eualaria fistulosa*, *Laminaria digitata*, *Laminaria hyperborea*, *Nereocystis luetkeana*, *Saccharina latissima*, *Hedophyllum nigripes*, *Saccorhiza dermatodea*, *Alaria elliptica*, and *Alaria oblonga* (Filbee-Dexter et al. 2019). Only one truly Arctic endemic species was reported: *Laminaria solidungula* (Wilce and Dunton 2014). In studies of this disseration, I worked with *S. latissima*, *A. esculenta*, *A. clathratum* and *L. hyperborea*. An overview of their thallus, biogeographical distribution and thermal optimum in the European Arctic is displayed in **Figure 1.4**.
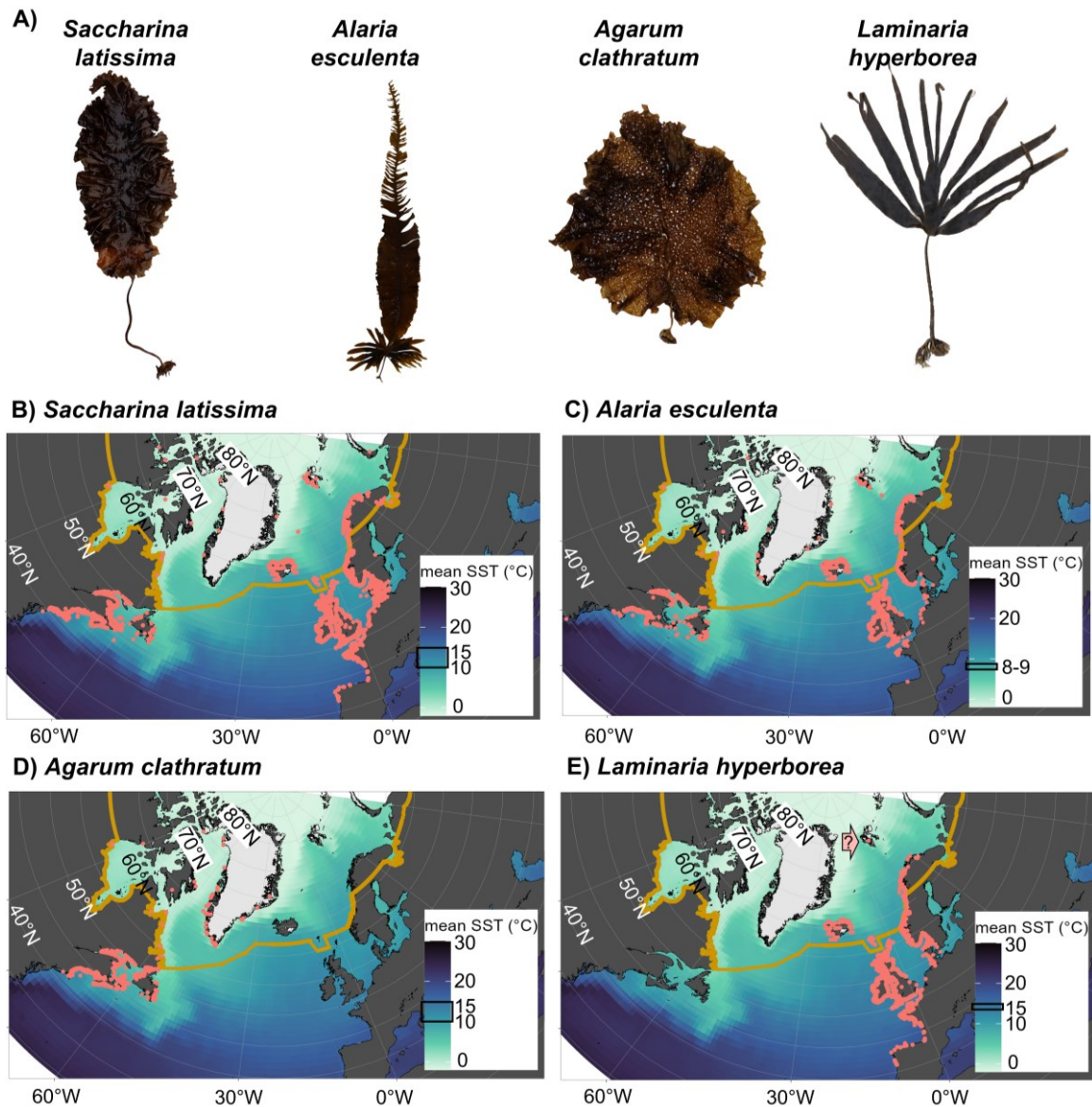
Figure 1.4: **A)** Kelp thalli (not to scale). ©: *S. latissima*, *A. clathratum*: Sarina Niedzwiedz. *A. esculenta*: Luisa Düsedau. *L. hyperborea*: Florian Stahl. **B–E)** Red points: distribution data of kelp species from Global Biodiversity Information Facility (gbif). Maps were created with ggOceanMaps (Vihtakari 2024). Yellow line: southern Arctic boundary after AMAP. Colour gradient: sea surface temperature (SST) of 2023 from the National Oceanic and Atmospheric Administration (NOAA) database. SST was averaged over the year in in grids of 1° lat×lon (mean SST [°C]). Rectangle in SST legend: species' thermal optimum (after A) Bolton and Lüning (1982); B) Munda and Lüning (1977); C) Simson et al. (2015); D) Bolton and Lüning (1982). Data download: 29.05.2024. **B)** *Saccharina latissima*, **C)** *Alaria esculenta*, **D)** *Agarum clathratum*, **E)** *Laminaria hyperborea*; single observation on Svalbard is questionable, as the species is easily mis-identified.

Saccharina latissima (Linneaus; Lane et al. 2006; sugar kelp) is one of the best-studied kelps, thereby serving as model to understand trait performance of kelps as response towards climate changes (Diehl et al. 2024). Its essential ecological (Diehl et al. 2024) as well as economical (Sæther et al. 2024) role has recently been reviewed. *S. latissima* is a cold-temperate kelp with a temperature optimum between 10–15°C (Bolton and Lüning 1982). It tolerates temperatures

from 0–25°C for >1 week (Diehl et al. 2021). It is distributed along the entire European coast, from northern Portugal to Svalbard (**Figure 1.4B**; Araújo et al. 2016). *S. latissima* tolerates salinities from S_A 5–60 for several days (Karsten 2007) with an optimal growth between S_A 23–31 (Bartsch et al. 2008). Generally, *S. latissima* has a high tolerance towards environmental changes, with a high phenotypic plasticity (Diehl et al. 2024). Based on genetic evidence (McDevit and Sauders 2010) and a similar physiological reaction (Egan et al. 1989), *Saccharina longicruris* has been synonymised with *S. latissima*.

Alaria esculenta (Linnaeus; Greville 1830; winged kelp) was reported to grow best at temperatures between 8–9°C, with temperatures of 16–17°C being reported as lethal (Munda and Lüning 1977). Hence, its warm distribution limit is farther north compared to *S. latissima*. Araújo et al. (2016) described the southern species limit in France, although a single observation in northern Spain was in the gbif.org database (**Figure 1.4C**). It can exhibit high performance at salinities of S_A 10-50 (Karsten 2007).

The temperature optimum of *Agarum clathratum* (Durmontier 1822; sieve kelp) has been described between 10–15°C (Simonsen et al. 2015). It is only occurring on the west coast of the Atlantic (**Figure 1.4D**). *A. clathratum* was classified as cryotolerant by Bringloe et al. (2022), thriving in areas with long-term minimum annual temperatures below 0°C. *A. clathratum* is reported to be a weak interspecific competitor in shallow waters (Gagnon et al. 2005). Vadas (1977) and Gagnon et al. (2005) described sea urchins to avoid feeding on *A. clathratum*.

The kelp *Laminaria hyperborea* (Gunnerus, Foslie 1885) is widespread along the eastern Atlantic coasts (**Figure 1.4E**). Its temperature optimum is reported at 15°C (Bolton and Lüning 1982). Its northernmost distribution has been described at 71°N (Lüning 1985). On the gbif.org database, one single record of "*Laminaria hyperborea*" has been found on Svalbard, classified as human observation. *L. hyperborea* is easily mis-identified as either *Laminaria digitata* or *Hedophyllum nigripes*, due to similar morphological appearance (Dankworth et al. 2020). Despite extensive observational and molecular surveys in Kongsfjorden, Svalbard (Bartsch et al. 2016; Düsedau et al. 2024.), presence of *L. hyperborea* has not been confirmed. Hence, it is questionable whether *L. hyperborea* has yet spread to the Arctic. Hopkin and Kain (1978) reported a similar salinity tolerance for *L. hyperborea* and *S. latissima*. Sporophytes showed no growth reduction down to a salinity of S_A 19.

Being highly responsive to environmental changes, kelps are important indicator species (Wernberg et al. 2013; Krumhansel et al. 2016). Given their essential ecological role, their response can have cascading consequences for the entire ecosystem, making them important to study. Especially the direct comparison of the four introduced kelp species, covering different tolerances and geographical regions, allows conclusions to be drawn on ecological changes.

1.3   Climate change in the Arctic

While the environmental conditions in fjords are highly dynamic, e.g., due to inner and outer fjord boundaries and geology (**chapter 1.1**), recently Arctic fjords have been subject to drastic environmental changes due to ongoing anthropogenic climate change. Although climate change is of global consequences, with drastic ecological as well as socio-economic impacts (IPCC 2023), the magnitude and direction of change greatly vary between regions (Burrows et al. 2011; Krumhansl et al. 2016). The Arctic has been monitored to be one of the fastest changing regions, as a result of climate forcings, climate feedbacks, as well as changes in the poleward energy transport (**chapter 1.3.1**; Previdi et al. 2021). In this chapter, I will elaborate why Arctic coastal ecosystems are expected to be among the most affected areas worldwide (Lantuit et al. 2012) and introduce the physical and chemical drivers that are most important for kelps. **Figure 1.5A** gives an overview of forces driving the abiotic environment in fjords.
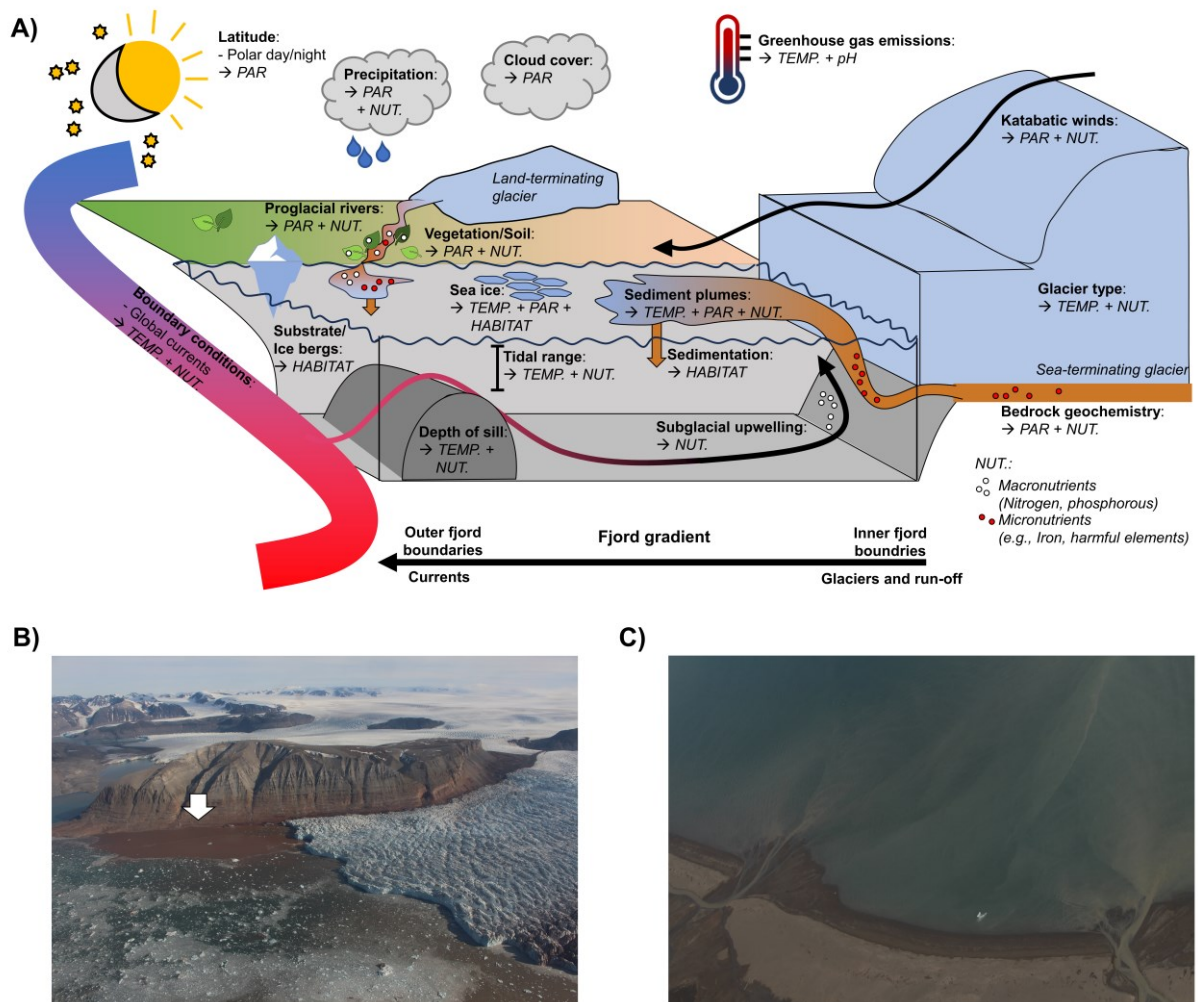
Figure 1.5: **A)** Schematic overview of forces affecting the abiotic environment in fjords for kelps, here habitat (*HABITAT*), temperature (*TEMP.*), the photosynthetically active radiation (*PAR*), pH (*pH*), and the chemical water composition (*NUT.*, including macronutrients and (potentially harmful) micronutrients). The inner fjord boundaries are dominated by glaciers and run-off. Outer fjord boundaries are dominated by

the global current system. A fjord gradient is established. **B)** Aerial picture of a sea-terminating glacier in Kongsfjorden, Svalbard. Due to calving, many ice bergs can be seen. White arrow points to area of subglacial upwelling; visible by an area of brownish water (high concentration of suspended particles), which is lacking ice bergs as the upwelling current is pushing them away from the glacier front. © Sarina Niedzwiedz. **C)** Aerial picture of proglacial rivers, discharging run-off from land-terminating glacier and precipitation to the water columns' surface in Kongsfjorden, Svalbard. Only one drift ice berg can be seen along the shore line (no calving). © Sarina Niedzwiedz.

1.3.1   Physical changes

The effect of increasing concentrations of atmospheric greenhouse gases has been described as the most important driver for global **temperature** rises (IPCC 2023). However, temperature changes in Arctic regions exhibit a different pattern compared to the rest of the world. For a large part of the 20th century, Arctic surface air temperatures have been decreasing, while the average global temperature has risen. This has been attributed to internal climate variability and regional cooling effects, e.g., of aerosols (England et al. 2021). Since the 1980s, however, the rate of temperature increases in Arctic regions is far beyond the global average (Arctic amplification, AA). Depending on the considered time frame and definition of the southern Arctic boundary, studies have reported that temperatures increase two to four times faster compared to the global average (Rantanen et al. 2022). Considering 1979-2021 and the area north of 66.5°N, Rantanen et al. (2022) found an average four-fold increase of temperature, with local variations. External drivers of climate change (climate forcings), such as atmospheric greenhouse gas concentrations, changes in solar irradiance and aerosols, have been found to attribute but not fully explain the extent of AA. Therefore, the contribution of climate feedback mechanisms to AA has to be considered (reviewed by Previdi et al. 2021): Differences in surface and tropospheric temperature changes cause altered energy fluxes (temperature feedback). Melting snow and ice decrease the surface albedo (surface albedo feedback). Cloud cover and moisture are predicted to increase (cloud and water vapour feedback). The overall increase in Arctic terrestrial vegetation cover further reduces the albedo, changes heat fluxes, as well as influences the atmospheric water vapour content (vegetation feedback). Additional to climate feedbacks, global changes in atmospheric and oceanic energy transport also contribute to AA. Not all regions of the Arctic are experiencing the same increase in temperature (Rantanen et al. 2022). Svalbard belongs to the fastest warming regions in the Arctic, warming at a rate twice as high as the Arctic average (Nordli et al. 2020). Temperature differences between fjords can be explained by a combination of offshore boundary conditions (e.g., currents) and local conditions (e.g., presence and depth of a fjord sill). In fjords with an extensive iceberg calving, the melting of icebergs has been described to cool down the surface water layer (Meire et al. 2017). As temperatures become tolerable for temperate kelps species, opening up more habitat, an overall poleward range expansion has been modelled

_____

(Krause-Jensen et al. 2020; Assis et al. 2022). In a consequence, cryophilic kelp species are potentially outcompeted (Bringloe et al. 2022). Additional to the long-term temperature rise, marine heatwaves (MHWs) have been recorded to increase in frequency and intensity in the Arctic as result of abrupt sea ice melt (Schlegel 2020; Barkhordarian et al. 2024). MHWs are defined as a temperature increase above the 90th percentile of the 30-year climatology for more than five consecutive days (Hobday et al. 2016; Oliver et al. 2018). MHWs can have drastic consequences on ecosystems and might be the tipping point for alternative ecosystem states (Wernberg et al. 2016; Filbee-Dexter and Wernberg 2018; Straub et al. 2019). Filbee-Dexter et al. (2020) monitored massive kelp forest declines and replacement with low productive small filamentous (turf) algae after MHW events in southern Norway. Generally, MHWs have been classified as a major threat for kelp forests (Wernberg et al. 2013; Smale 2019).

Compared to lower latitudes, the Arctic is characterised by low annual cumulative **irradiance** levels (Gattuso et al. 2006; 2020), due to the tilt of the earth's axis and the consequential monthlong period of darkness in winter (**Figure 1.1**). The rhythm between Polar Night and Polar Day is one of the few abiotic factors not influenced by climate change. However, climate change has an effect on the PAR availability during Polar Day. Even though Schlegel et al. (2024) showed that for most Arctic fjords these changes are not significant due to high interannual variations, three clear overall patterns can be observed: 1) Elevated temperatures result in the loss of sea ice and in consequence a longer period of open water and a higher PAR availability in spring (Nicolaus et al. 2012; Payne and Roesler 2019; Ivanov 2023). 2) Glacial (Milner et al. 2017) and permafrost (Bintanja 2018) melt, as well as higher precipitation rates (Bintanja and Andry 2017) lead to increased run-off and a higher concentration of suspended particles, darkening the water column in summer (Konik et al. 2021). 3) With Arctic warming, cloudiness increases, reducing the irradiance that is transferred through the atmosphere and might penetrate the water column (Laliberté et al. 2021). Being primary producers, kelps use photosynthetically active radiation (PAR; λ 400–700 nm) to ultimately convert inorganic to organic carbon (primary production). They require an annual cumulative PAR of 49 mol photons m^{-2} yr^{-1} (Castro de la Guardia et al. 2023) to maintain a net positive carbon balance, i.e., their carbon gain (photosynthetic rate) has to be higher than their carbon loss (respiration rate). In the Arctic, kelps are restricted to summer months to gain enough carbon to balance carbon loss during winter months.

1.3.2   Chemical changes

Additional to changes in temperature and irradiance, freshwater input by run-off reduces the **salinity** of the water column. Low salinities at glacier fronts play an important role in the fjord food web, as zooplankton experiencing osmostic shock are easy, high-energy prey for higher trophic levels (Zajączkowski and Legeżyńska 2001). Low salinities can have an effect on the kelps' ion levels and osmotic regulation, as well as the photosynthetic apparatus (Kirst 1990, Kirst and Wiencke 1995). Goldsmit et al. (2021) have found salinity to be among the top three predictors for kelp distribution in the Canadian Arctic, with a high variability between species. However, kelps in general have a high halotolerance (**chapter 1.2.3**). Fredersdorf et al. (2009) reported only few significant salinity effects in sporophyte responses of *A. esculenta*, however highlighting a higher sensitivity of microscopic life stages.

In a typical fjord, temperature and salinity gradients stratify fjords into a surface layer, intermediate water masses and deep-water masses (Cottier et al. 2010). In spring and summer, freshwater run-off and temperatures of the surface layer increase, enhancing the stratification. In fjords that are covered by sea ice in winter, vertical mixing is restricted to autumn, when the surface layer loses heat to the atmosphere (Cottier et al. 2010). After a phytoplankton bloom in spring, the surface layer is generally nutrient depleted, leading to a high seasonal variation in **nutrient** concentration (Juul-Pedersen et al. 2015). To which extent surface nutrients are re-supplied largely depends on the fjord's glacier type. In fjords that are influenced by sea-terminating glaciers, the glacial meltwater plume enters the fjord at depth, rising buoyantly to the surface. The buoyant plume creates a subglacial upwelling of nutrient rich deep-waters (**Figure 1.5A, B;** Meire et al. 2017; Hopwood et al. 2020), having the potential to fuel a second phytoplankton bloom in summer (Juul-Pedersen et al. 2015). Katabatic and down-fjord winds further facilitate the mixture of water masses in front of sea-terminating glaciers (Hopwood et al. 2020). In fjords that are influenced by land-terminating glaciers, the freshwater run-off is directly discharged to the surface by proglacial rivers (**Figure 1.5A, C**). Hence, the fjord system lacks the subglacial upwelling (Meire et al. 2017) and consequently the re-supply of nutrients from deep-waters. Run-off plumes have been shown to be an important source for silica and iron from bedrock weathering; however, this applies only to a reduced extent for other nutrients, such as nitrate and phosphate (Meire et al. 2016). Therefore, the sources of macronutrients in land-terminating glacier systems are terrestrial sources, which can be rich in inorganic and organic matter (McGovern et al. 2020). It has been suggested that the greening of the tundra may increasingly preclude terrestrial nutrients from reaching coastal ecosystems (Sørgaard et al. preprint). Overall, Meire et al. (2017) showed that the productivity of fjords with a sea-terminating glacier was higher compared to fjords with a land-terminating glacier. Hence, they suggested that the fjords' productivity decreases with climate change related glacial retreat.

Similar to other algae, kelps require nitrogen and phosphorous for photosynthesis and growth. Nitrogen is generally considered to be primarily limiting (Roleda and Hurd 2019). The nitrogen availability has been shown to influence thermal tolerance of kelps (Fernández et al. 2020). However, some kelp species can accumulate nutrients (Mortensen 2017), and use them during periods of low nutrient concentrations (Wernberg et al. 2019).

Additional to macronutrients, primary producers require **micronutrients**, such as metals, for many physiological and biochemical processes, e.g., to stabilise protein structures, facilitate electron transport or catalyse enzymatic reactions (Torres et al. 2008). For instance, iron is involved in carbon and nitrogen fixation, reductive processes, chlorophyll synthesis and electron transport chains (Twining and Baines 2013). Manganese is required in photosystem II in the oxygen evolving complex (Twining and Baines 2013). Overall, the oceanic concentrations of these essential trace elements are low and often even limiting (Ash and Stone 2003). Arctic run-off plumes are characterised by high concentrations of particulate and dissolved elements, as they carry lithogenic material from bedrock weathering (Krause et al. 2021). Depending on run-off origin, the lithogenic material has different compositions, changing the water columns' concentration of macrominerals and harmful elements, such as heavy metals, and legacy pollutants (Pittino et al. 2023). Kelps were shown to take up harmful elements intercellularly during their growth phase or via cell wall-incorporated fucoidan and alginates (Davis et al. 2003; Zeraatkar et al. 2016). This process is highly dependent on many factors, such as exposure time, temperature and pH (Zeraatkar et al. 2016). The impacts of run-off-induced increased concentration of harmful elements in the water column on Arctic kelp ecosystem functioning are unknown.

The **ocean's CO_2 chemistry** is a complex interplay of various physical and biological factors with temporal and local differences (Lauvset et al. 2020). With the atmospheric CO_2 concentration rising due to anthropogenic activities, the dissolved inorganic carbon and pH of the ocean are changing. Since 1980, an overall surface water pH decline of 0.017 ± 0.001 pH units per decade was observed, with spatial differences (Ma et al. 2023). Generalising the impact of the seawater CO_2 chemistry on organisms is difficult, as it is highly species-specific and varies regionally. For calcifying organisms, e.g., bivalves, echinoderms or corals, severe negative effects have been recorded, due to a reduced ability to produce calcium carbonate structures (Fabry et al. 2008). As lower water temperatures further increase the solubility of calcium carbonate (Ma et al. 2023), Arctic ecosystems are generally considered to be especially vulnerable. Here, kelp forests have been proposed to provide potential refugia for calcifying organisms, as long photoperiods during Polar Day resulted in an increase of the pH (Krause-Jensen et al. 2016).

_____

1.3.3 Biological changes depend on ecological niches

The fundamental niche describes all combinations of environmental conditions suitable for a species, which is determined by adaptation (Malanson et al. 1992; Severtsov 2013). The realised niche refers to the actual biogeographical distribution of a species, being influenced by physical boundaries or competition. Hence, it is often a subset of the fundamental niche (Malanson et al. 1992; Severtsov 2013). Climate change causes the realised niche of species to shift by changing the local environmental conditions. In response, a species can either migrate, acclimatise and/or adapt to the altered conditions (Donelson et al. 2019). Being sedentary, kelps cannot actively escape stressors by moving and had to develop a variety of physiological and biochemical strategies to maintain a high performance, e.g., survival, growth or reproduction, under varying environmental conditions. Here, I will conceptually introduce adaptation and acclimatisation in response to a single environmental parameter, as they are relevant for the ability of cold-temperate kelps to respond to environmental changes (**Figure 1.6**). All important terms are defined in the glossary.
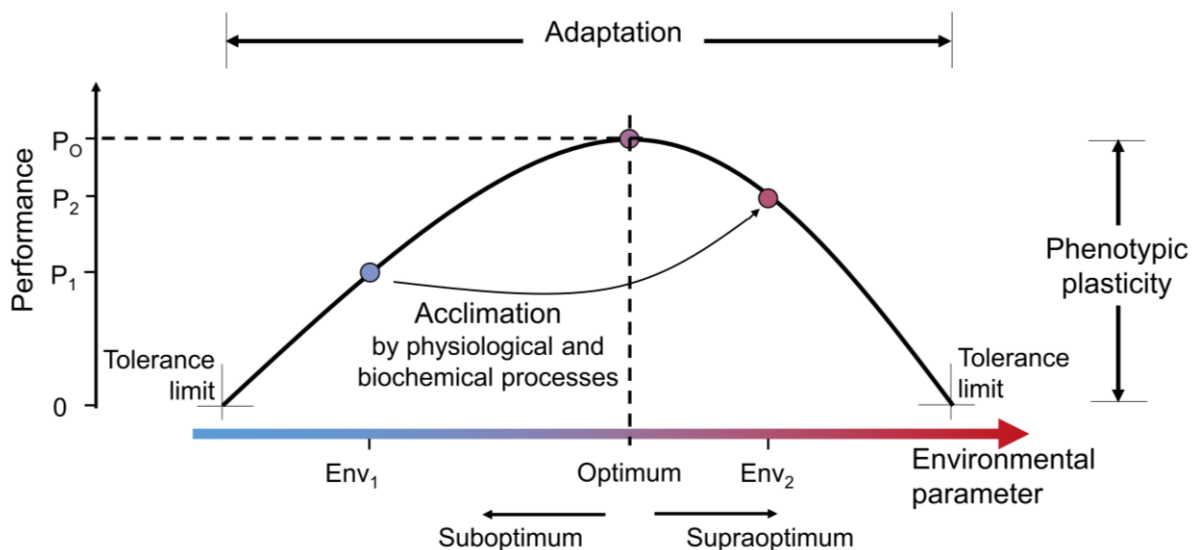
Figure 1.6: Schematic performance curve in response to a gradient of a single environmental parameter. The performance curve represents the phenotype of a single genotype as function of maximised trait performance (e.g., growth; performance curve). The form and width of the performance curve is defined by adaptive processes. When the environmental parameter changes within the the tolerance limits of a species (Env$_1$ → Env$_2$), it can acclimate to maintain a maximised performance (P$_1$ → P$_2$). When the environmental parameter is optimal, the performance reaches its absolute maximum (P$_0$). Conditions below the optimum: suboptimum. Conditions above the optimum: supraoptimum.

Adaptative processes are based on differences between genotypes, i.e., allele-pairs, defining different phenotypes, i.e., sets of trait characteristics. Should the differences in phenotypes relate to differences in performance in a prevailing environment, heritable beneficial traits are subject to natural selection. Over generations, a population can change the form of its performance curve

_____

and/or shifts its tolerance limits and adapt to an altered environment (King et al. 2017; Collier et al. 2019). Theoretically, adaptations can occur to any environmental condition, leading to highly specialised species. However, adaptive processes might be restricted when (1) the availability of beneficial genes is limited in marginal, fragmented populations, or (2) when continual immigration from central populations suppresses the establishment of local adaptation (Bridle and Vines 2006). Further, the rate of environmental change can outpace the change of genotype by natural selection, i.e., adaptive capacity (Martin et al. 2023). For example, Vranken et al. (2021) have shown that the rate of environmental change in western Australia occurs too fast for adaptive processes in the local kelp population.

When the environment changes within the adapted tolerance limits of a species, an individual can modify its phenotype (phenotypic plasticity) to maximise trait performance under prevailing conditions (acclimatisation). Acclimatisation is achieved by a fast and reversible modification of the physiology and biochemistry of an individual (phenotype) (Collier et al. 2019). In an optimal environment, the species' performance reaches its absolute maximum (Wahl et al. 2020). Towards the tolerance limits, the cellular stress level is increasing, and acclimatisation and repair mechanisms require cellular resources to mitigate negative effects of stressors, e.g., the damage of macromolecules (Kültz 2005). At the tolerance limits, acclimatisation mechanisms cannot counteract the stress inflicted damage, causing apoptosis and the organism's death (Kültz 2005).

1.4   Objectives and research questions

With ongoing climate change, Arctic coastlines are experiencing drastic environmental changes (**chapter 1.3**). With temperatures rising at a rate far beyond the global average, accelerating run-off rates darken the water column and change the concentration of dissolved elements in fjords during summer months. To be able to maintain a stable population, kelps have to acclimatise to the changing environment, as they cannot actively migrate and climate change may outpace their adaptive potential (Vranken et al. 2021). To predict the performance and responses of a species towards climate change, models often use the fundamental thermal niche, potentially neglecting within-species variations (Bennett et al. 2019) and interacting drivers. Recently, Laeseke et al. (2024) have shown that the fundamental thermal niche alone has limited predictive power for the the biogeographical distribution (realised niche) of >70 % of seaweed species. They further highlighted that especially the physiological cold-tolerance limit was a weak predictor for distribution of seaweeds in polar regions.

The overarching aim of my doctoral thesis is to assess what defines the boundaries of the realised niche of Arctic kelp forests. A shift of the kelps' realised niche has cascading ecological and economical consequences. Hence, an increased understanding of kelp drivers and dynamics contributes to improving future local management and climate change mitigation guidelines. To target this aim, I investigate the performance of kelps towards three major abiotic factors potentially driving shifts in Arctic kelp forest ecosystems, namely temperature, PAR and an altered chemical composition in coastal run-off (**Figure 1.7**). To be able to draw reliable conclusions, I combine *in-situ* monitoring studies (**publication I, II**) with experimental studies (**publication III, IV, V**): I monitor the spatial variation in performance of kelps, responding to a latitudinal gradient of temperature × PAR interactions (**publication I**). I investigate variability in kelp holobiont functioning along coastal run-off gradients, focussing on the impact of the chemical composition of the water column (**publication II**). I assess the impact of marine heatwaves on kelp performance, under varying PAR intensities, mimicking different run-off influence (**publication III**). I explore the temperature × PAR tolerance limits of kelps to establish a two-dimensional fundamental niche (**publication IV, V**). The experimentally determined temperature × PAR tolerance limits are the basis for a species distribution model (**publication IV**), and a model of the realised niche for the depth distribution of kelp forests along the fjord gradient (**publication V**).
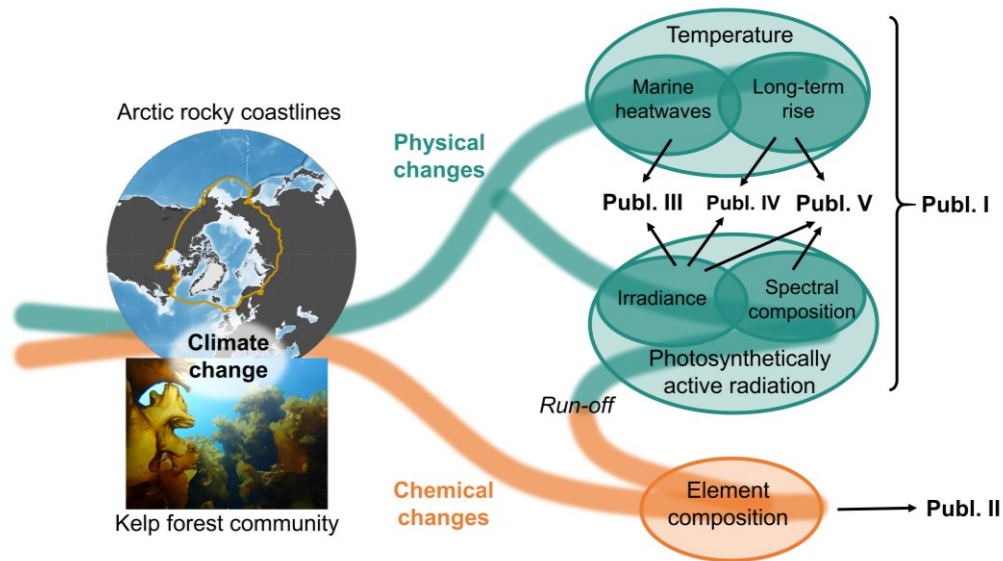
Figure 1.7: Structure of this dissertation and drivers of **publication I–V**, contributing to assess what defines the boundaries of the realised niche of Arctic kelp forests. I assess the performance of kelps towards three major abiotic factors potentially driving shifts in Arctic kelp forest ecosystem, namely temperature, PAR and an altered chemical composition in coastal run-off. I monitor the spatial variation in performance of kelps, responding to a latitudinal gradient of temperature × PAR interactions (**publication I**). Further, I investigate performance variability of kelps along coastal run-off gradients, focussing on the impact of the chemical composition of the water column (**publication II**). I assess the impact of marine heatwaves on kelp performance, under varying PAR inetensities, mimicking run-off influence (**publication III**). I explore the temperature × PAR boundaries of kelps to establish a two-dimensional fundamental niche (**publication IV, V**). The experimentally determined boundaries are the base for a species distribution model (**publication IV**), and a model of the realised niche for kelp forests along the fjord gradient (**publication V**).

I designed and contributed (**chapter 1.5**; **Table 1.1**) to five peer-reviewed research articles (**chapters 2–6**) to answer the following major research questions:

Research question I: Can Arctic kelp populations be treated as one biochemical unit in climate projections?

Using the kelp *S. latissima* as a model kelp, I analysed the biochemical composition of eight populations from fjords along the west coast of Svalbard. The different fjords were characterised by temperature and PAR differences. I hypothesised that kelps are acclimatised to and, therefore, conditioned by their local environment, which has possible consequences for their susceptibility towards environmental changes. → **chapter 2 Publication I**

Research question II: How are heavy metals in run-off affecting kelp holobiont functioning?

Kelp tissue samples from three areas with different run-off influence were sampled in Billefjorden, Svalbard, and analysed for their elemental mass fraction, biochemical response and associated microbiome. I used the kelp *Saccharina latissima* as model kelp. I hypothesised that the elemental mass fraction of kelps correlated positively with the dissolved elemental concentration of the

_____

water column, which has consequences on physiological and biochemical processes. I hypothesised that an accumulation of harmful elements would result in an antioxidative response of the kelp. I hypothesised that the kelp-associated microbial community will respond to spatial differences in abiotic and host conditions, resulting in altered microbial species composition and potentially different ecosystem services of the kelp holobiont. → **chapter 3 Publication II**

Research question III: How are *Agarum clathratum* and *Saccharina latissima* responding to marine heatwaves, being exposed to either high- or low-PAR availabilities?

After acclimation of meristematic discs of *A. clathratum* and *S. latissima* to different PAR availabilities (3 vs. 120 µmol photons m^{-2} s^{-1}), mimicking run-off intensities, the performance of samples was analysed in response to experimental marine heatwave scenarios (4–10°C). Based on its natural distribution, I hypothesised *A. clathratum* to perform better under low-light conditions. As the thermal optimum of both species was described between 10–15°C, I hypothesised that the performance of both species will increase with rising temperatures. Shifts in interspecific competition balances can have cascading consequences on the ecosystem. → **chapter 4 Publication III**

Research question IV: Why has *Laminaria hyperborea* not yet spread to Svalbard?

In a three-month experiment, non-meristematic discs of *Laminaria hyperborea* were exposed to Polar Day (24 h L), long day (16:8 h L:D) and Polar Night (24 h D) light regimes under three different temperatures (0, 5, 10°C) to assess the boundaries of the species' two-dimensional fundamental niche. I hypothesised that the interaction of Polar Day with cold temperatures is limiting and restricts the spread of *L. hyperborea* to higher latitudes. Given the thermal optimum of the species, I hypothesised rising temperatures to have beneficial effects on its performance. To assess the potential of *L. hyperborea* to spread to higher latitudes (realised niche), a species distribution model was created based on the experimental results. → **chapter 5 Publication IV**

Research question V: How are temperature rises and run-off plumes affecting the realised niche of *Alaria esculenta* and *Saccharina latissima* along the fjord?

Meristematic discs of *A. esculenta* and *S. latissima* from Kongsfjorden, Svalbard, were exposed to different temperatures (3–11°C). After acclimation to each temperature, I analysed their light-use characteristics to define the boundaries of their fundamental niche. I hypothesised to find increasing dark respiration and photosynthetic rates with rising temperature, due to higher enzymatic and metabolic activities. To be able to draw conclusions about both species' future realised niche, I mapped the PAR availabilities along the fjord gradient and modelled their compensation depth. Given the complex run-off plume dynamics, I hypothesised to find strong spatial differences in the PAR availability and the kelps' compensation depth. → **chapter 6 publication V**

1.5   List of publications and declaration of own contribution

The contribution of the candidate to each publication is provided in % of the total workload (up to 100 % of each category) in **Table1.1**.

Table 1.1 Contribution of the candidate to publications of this dissertation in % of the total workload (up to 100 % of each category).

Category	Publication I	Publication II	Publication III	Publication IV	Publication V
Experimental concept & design	~ 70 %	~ 95 %	~ 50 %	~ 5 %	~ 70 %
Experimental work & data acquisition	~ 90 %	~ 60 %	~ 50 %	~ 30 %	~ 80 %
Data analysis & interpretation	~ 70 %	~ 80 %	~ 80 %	~ 10 %	~ 90 %
Preparation of figures & tables	100 %	100 %	~ 90 %	~ 20 %	100 %
Drafting of the manuscript	~ 85 %	~ 90%	~ 85 %	~ 5 %	~ 90 %

Publication I (submitted May 2024)

Sarina Niedzwiedz, Clara Voigt, Sebastian Andersen, Nora Diehl, Børge Damsgård, Kai Bischof (submitted May 2024) **Local environmental settings condition biochemistry of Arctic kelp populations**.

SN and ND conceptualised the study under the supervision of KB. SN and SA conducted the field work with advice and supervision of BD. Parameter analyses and evaluation were conducted as follows: physical water parameters: SN, CV and SA. Biochemical parameter: SN and CV. Data interpretation: SN, ND and KB. SN wrote the manuscript, which was revised and reviewed by all co-authors.

Publication II (submitted July 2024)

Sarina Niedzwiedz, Claudia Elena Schmidt, Yunlan Yang, Bertille Burgunter-Delamare, Sebastian Andersen, Lars Hildebrandt, Daniel Pröfrock, Helmuth Thomas, Rui Zhang, Børge Damsgård, Kai Bischof (submitted July 2024) **Run-off implications on Arctic kelp holobionts have strong implications on ecosystem functioning and bioeconomy**.

SN conceptualised the study under the supervision of KB. SN and SA conducted the field work with advice and support of BD. Parameter analyses and data evaluation was conducted as follows: physical water parameters: SN and SA. Biochemical parameters: SN. Elemental composition of

_____

kelps and water: SN, CS, LH, with advice and supervision of DP and TH. Microbial community of kelps and water: SN, YY, BB-D and RZ. SN wrote the manuscript, which was revised, reviewed and accepted by all co-authors.

Publication III (published)

Sarina Niedzwiedz, Tobias Reiner Vonnahme, Thomas Juul-Pedersen, Kai Bischof, Nora Diehl (2024) **Light-mediated temperature susceptibilities of kelp species (*Agarum clathratum*, *Saccharina latissima*) in an Arctic summer heatwave scenario**. *Cambridge Prisms: Coastal Futures*. 2, e6. doi: 10.1017/cft.2024.5

SN and ND designed, planned, and conducted the experiment. TRV and TJ-P assisted with sampling and provided advice and support during the design of the experimental set-up and methodology. SN, ND and TRV evaluated the data. SN wrote the manuscript, which was revised, reviewed and accepted by all authors. KB and ND supervised the study.

Publication IV (submitted June 2024)

Nora Diehl, Philipp Laeseke, Inka Bartsch, Margot Blight, Hagen Buck-Wiese, Jan-Hendrick Hehemann, Sarina Niedzwiedz, Niklas Plag, Ulf Karsten, Tifeng Shan, Kai Bischof (submitted June 2024). **Photoperiod and temperature interactions drive the latitudinal distribution of kelps under climate change.**

ND conceptualised the study under the supervision of IB and KB. ND and SN conducted the experimental work with advice and support of IB. Parameter analysis was conducted as follows: physiological and biochemical analysis: ND. Mannitol analysis: ND with support of NP and UK. Laminarin analysis: MB, HB-W and J-HH. DNA barcoding: TS. Data analysis with GL(M)M and geographic projections: PL. Statistical analysis: ND with support of SN. Data interpretation: ND, PL, IB and KB. ND wrote the manuscript, which was revised, reviewed and accepted by all authors.

Publication V (published)

Sarina Niedzwiedz, Kai Bischof (2023) **Glacial retreat and rising temperatures are limiting the expansion of temperate kelp species in the future Arctic**. *Limnology and Oceanography*. 68, 816-830. doi: 10.1002/lno.12312

SN conceptualised the study under supervision of KB. Sampling of field material, as well as experimental work was conducted by SN and KB. Analyses and presentation of the data was conducted by SN. SN drafted the manuscript, which was discussed and revised by KB.

_____

PUBLICATION I

Local environmental settings condition biochemistry of Arctic kelp populations

Sarina Niedzwiedz, Clara Voigt, Sebastian Andersen, Nora Diehl, Børge Damsgård

Arctic kelps are conditioned by local envrionment

Sarina Niedzwiedz[1], Clara Voigt[1], Sebastian Andersen[2], Nora Diehl[1], Børge Damsgård[2], Kai Bischof[1]

[1]University of Bremen, Germany; [2]UNIS, Svalbard, Norway
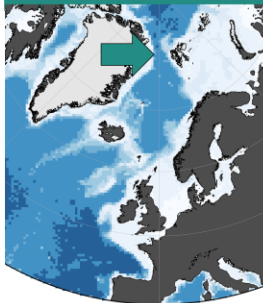
Climate change causes temperature and light to change drastically in Arctic fjords, being the main drivers for ecosystem engineering seaweeds (kelps). Climate projections on temperate kelps are often based on static reaction norms, treating species as one homogenous unit. It has been shown that the environmental conditions a species experienced changes its performance, which might lead to mis-extrapolations. We assessed how Arctic kelp populations react to their specific *in-situ* environment by sampling and analysing eight populations of the sugar kelp (*Saccharina latissima*) along the west coast of Svalbard, Norway in August 2022. This has consequences for their susceptibility towards climate change related stressors.

Research question: How is Arctic sugar kelp conditioned by its local environmental setting?

Sugar kelp

Abiotic conditions
**West coast of Svalbard
August 2022**

Warm
High

Medium
Medium

Cold
Low

Temperature:
Range 3-7 °C = below species optimum

Light:
Local run-off effect, depends on glacier influence

Kelp response

Photosynthetic pigments

Reduced pigment concentration ⇒Less intracellular stress

Less light availability, leads to a higher pigmentation to meet cellular energy needs

Altered elemental cycling

Photo-protection

High light availability causes photo-protection (little run-off influence)

No physiological stress response to low temperatures detected

Interacting stressors change kelp tolerances

Carbon to nitrogen ratio

Potentially higher content of storage compounds

Potentially higher food quality for grazers

Food web implications for higher trophic levels

Distinct differences in the biochemical composition of kelps correlated with sampling origin.
→ High phenotypic plasticity of the sugar kelp
→ Performance curves are not static, which has to be considered in climate projections

Get the publication:

_____

Title of article:

Local environmental settings condition biochemistry of Arctic kelp populations

Authors:

Sarina Niedzwiedz[a*], Clara Voigt[a], Sebastian Andersen[b], Nora Diehl[a], Børge Damsgård[b], Kai Bischof[a]

*corresponding author: sarina@uni-bremen.de

Affiliation:

[a]Marine Botany, Faculty of Biology and Chemistry and MARUM, University of Bremen, 28359 Bremen, Germany

[b]The University Centre of Svalbard (UNIS), Longyearbyen NO-9171. Norway

ORCIDs:

Sarina Niedzwiedz: 0000-0003-2604-2527
Clara Voigt: 0009-0000-8201-4075
Sebastian Andersen: 0009-0004-6622-8400
Nora Diehl: 0000-0002-7245-340X
Børge Damsgård: 0000-0002-7731-0168
Kai Bischof: 0000-0002-4497-1920

Running head:

Saccharina latissima in Svalbard

_____

Abstract

Climate change causes temperature and light to change drastically in Arctic fjords, being the main drivers for ecosystem engineering seaweeds (kelps; Laminariales, Phaeophyceae). Climate projections on temperate kelps are often based on static performance curve, treating species as one homogenous unit. This might lead to mis-extrapolations, as the environmental history might change biochemical compositions, physiological responses and consequently susceptibilities t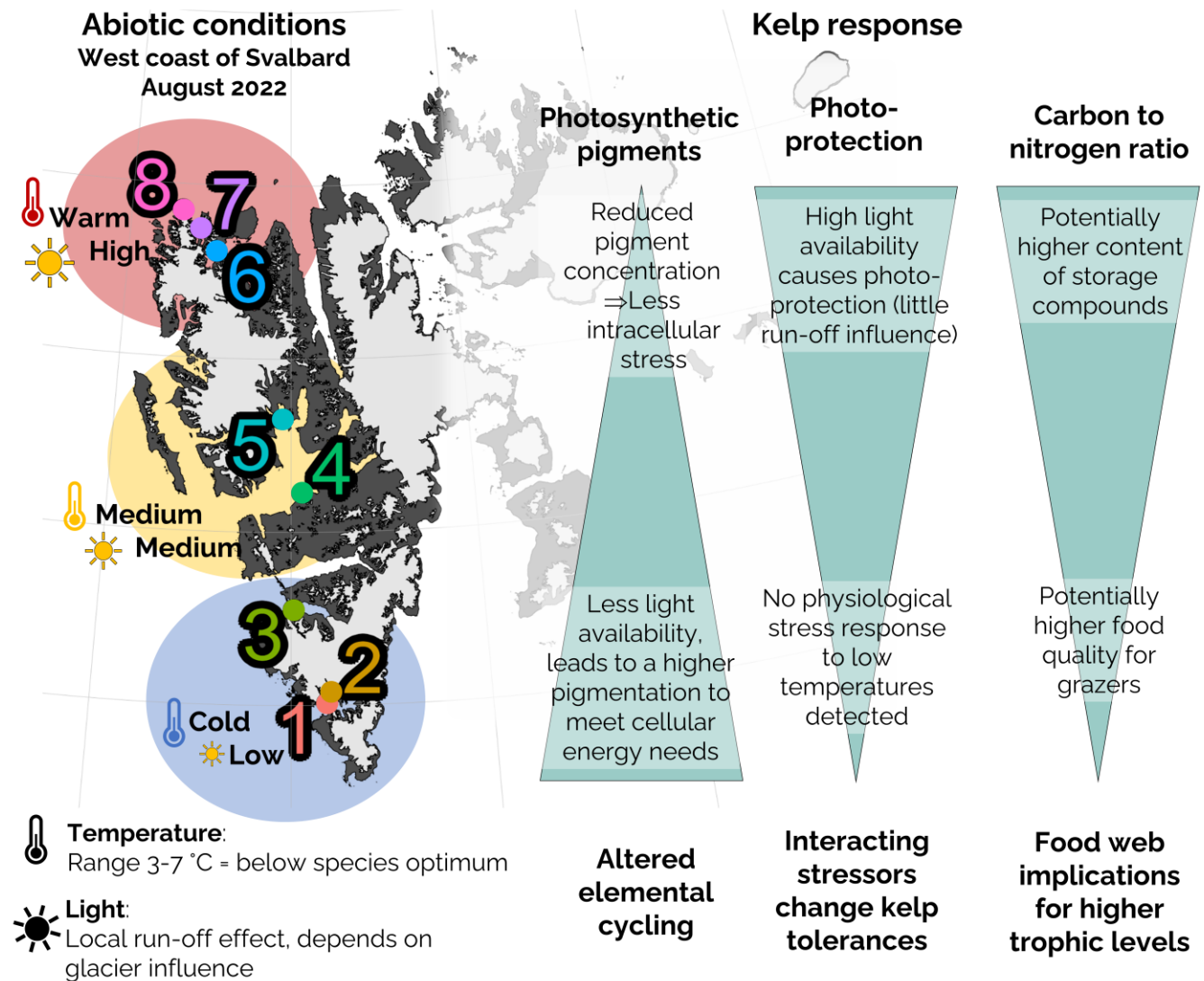owards stressors. We assessed how Arctic kelp populations react to their specific *in-situ* environment by sampling eight *Saccharina latissima* populations at several latitudes on the west coast of Svalbard, Norway. Analysing biochemical response variables (pigment content and composition; antioxidative activity; total carbon and nitrogen content) of sporophytes, we found a distinct clustering of the biochemical composition of *S. latissima* populations, which correlated significantly with their environmental setting. *S. latissima* responded strongly to changes in run-off induced turbidity, i.e., light availability. High light availability caused a significant reduction of photosynthetic pigments and a high de-epoxidation state of the photoprotective xanthophyll cycle, indicating high light stress. Nevertheless, the kelps' total carbon content increased. Their total nitrogen content increased with increasing turbidity, thus reacting to nutrients being washed into the fjord by run-off. We found no stress response to colder temperatures (3°C vs. 7°C), emphasising the importance of light as a driver of kelp distribution at high latitudes, and the necessity to include it in climate projections. Concluding, we found a high site-specific plasticity of Arctic *S. latissima* sporophytes, and high variation in biochemistry being strongly dependent on the sum of interacting environmental factors.

Graphical abstract
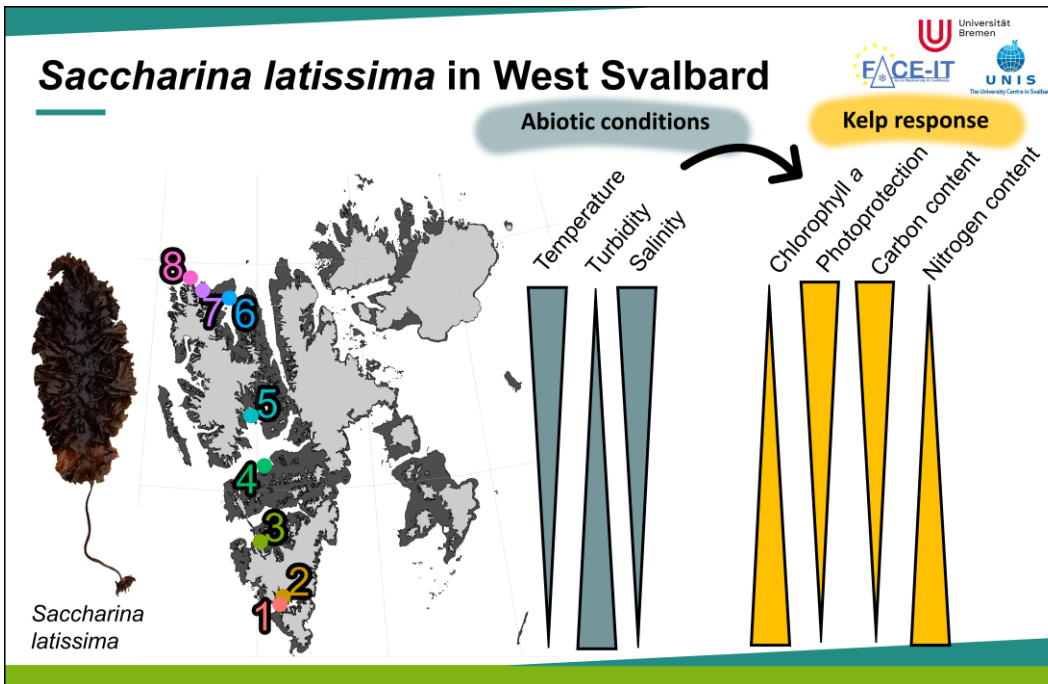
Keywords:

Antioxidative activity, C:N, Sea surface temperature, Tolerances, Pigments, Underwater light climate

_____

1. Introduction

Canopy-forming seaweeds of the order Laminariales, kelps, dominate temperate and Arctic rocky coastlines (Steneck et al., 2002, Wernberg et al., 2019). Kelp forests have been classified to be among the most productive ecosystems (Pessarrodona et al., 2022), acting as ecosystem engineers and foundation species, and thus providing habitat, nursery ground and food for many associated organisms (Eckman et al., 1989; Filbee-Dexter et al., 2019; Wernberg et al., 2019, 2024). Being sedentary, kelps cannot actively escape stressors and are susceptible to environmental changes. Within their genetically set tolerance limits, they have developed various physiological and biochemical mechanisms to respond to the sum of environmental changes, i.e., acclimatisation (Collier et al., 2019). Thereby, they maintain a high performance, e.g., growth and reproduction (phenotypic plasticity; King et al., 2017; Diehl et al., 2024). Energy requirements are lowest at a species optimum, increasing towards their tolerance limits, resulting in a reduced performance (Pörtner et al., 2005). A modification of the tolerance limits of species occurs over generations, by natural selection of favourable, heritable traits, i.e., adaptation (King et al., 2017; Collier et al., 2019).

The main driver for kelps' latitudinal distribution is temperature, while light is defining their vertical distribution over depth (Fragkopoulou et al., 2022). Both, temperature and light, are changing drastically in Arctic fjords with global climate change (Gattuso et al., 2020; Previdi et al., 2020, 2021; England et al., 2021; Konik et al., 2021). Vranken et al. (2021) have shown that the rate of change occurs too fast for adaptive responses in kelps. Given their key ecological role, the acclimatisation of kelps in future Arctic conditions has been subject to many recent studies. Increased water temperatures are predicted to result in an expansion of temperate kelp population to higher latitudes (e.g., Filbee-Dexter et al., 2019; Assis et al., 2022), while run-off induced deterioration of the underwater light climate has been shown to locally oppose this trend (e.g., Bartsch et al., 2016; Niedzwiedz and Bischof 2023; Düsedau et al., in revision). Studies projecting climate change developments are often based on tolerances from a single population and/or single-case experiment (Reed et al., 2011; Diehl et al., 2024). By this approach, it is assumed that populations along the entire biogeographical range react as one physiological and biochemical unit (King et al., 2017). However, Bennett et al. (2019) reviewed that susceptibilities towards abiotic stressors do not only vary between but also within one species, depending on a population's geographic location, which is supported by several studies: Liesner et al. (2020) highlighted the importance of cold-seasons for the plasticity towards warming of *Laminaria digitata*. Gauci et al. (2022) found that the performance of *L. digitata* sporophytes increased if their gametophytes were cold-primed. Assessing the effects of marine heatwaves on north Atlantic kelp populations, Filbee-Dexter et al. (2020) concluded that local temperature

_____

thresholds have to be considered in prediction on marine heatwave consequences. Niedzwiedz et al. (2022) showed that the susceptibility of the kelp *Saccharina latissima* towards experimental heatwaves strongly depends on the field conditions they experienced before the experiment. As cold-edge populations in general showed large within-species variation (Bennett et al., 2019), the upscaling of the responses of one, often temperate, population for the entire Arctic might pose some risk for mis-extrapolation due to local acclimatisation and adaptation processes.

Saccharina latissima is a widely distributed, cold-temperate kelp species, occurring from northern Portugal to Svalbard (Araújo et al., 2016), with its temperature optimum being described between 10–15°C (Bolton and Lüning, 1982). Given its essential ecological and economic role, it is well-studied, serving as model species (Diehl et al., 2024; Sæther et al., 2024). Our study was guided by the question of how Arctic *S. latissima* is conditioned by its local environmental setting, as this would have consequences for climate projections and, potentially, local management activities. We targeted this question with an *in-situ* approach, using the abiotic conditions and variations in fjords along western Svalbard, Norway, as a natural long-term laboratory to assess the effect of environmental history on the biochemistry of *S. latissima*. We mapped the abiotic conditions (temperature, light availability) and sampled *S. latissima* individuals in eight fjords along a latitudinal gradient, analysing their biochemical responses (pigment composition, antioxidant potential, carbon and nitrogen content).

_____

2. Material and Methods

2.1 Sampling

The Arctic Archipelago of Svalbard is located between ~77–80°N and characterised by strong environmental gradients. The sampling campaign was conducted from 05–16/08/2022 by ship (MS Spitsbergen). *Saccharina latissima* was collected at eight sampling stations along the west coast of Spitsbergen (**Figure 1**: 1–8; detailed map of different fjords with sampling locations: **Figure A1**). At each sampling station, similarly sized sporophytes (*n*=5) were collected from 5±2 m water depth using a plant rake (Plant rake 19.000, acc. to Sigurd Olsen, KC Denmark, Silkeborg, Denmark). Subsamples were taken from each sporophyte by cutting discs, 2 cm² in diameter, from the meristem, within two hours of sampling. All samples were dried in silica gel, which was replaced regularly.

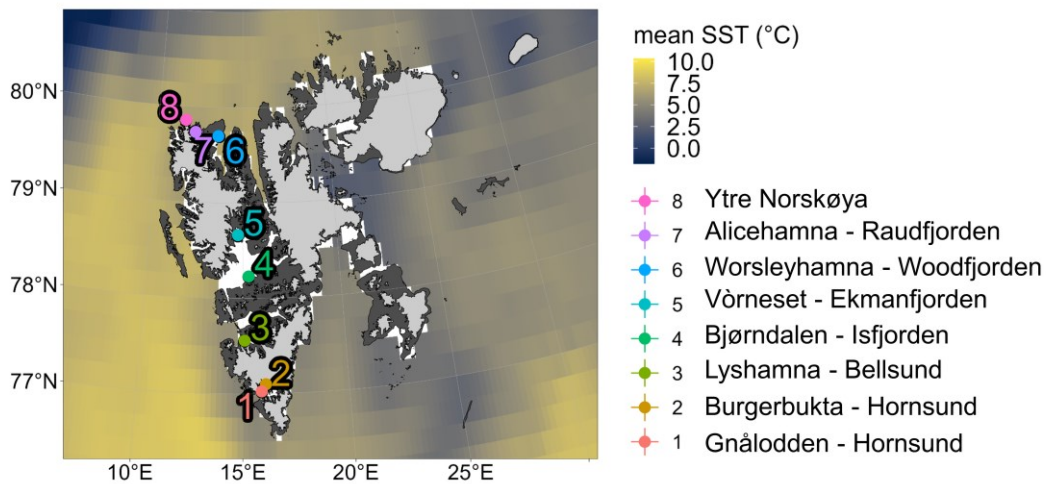**Figure 1**: Sampling stations (1–8) of *Saccharina latissima* along the west coast of Svalbard. Mean seasurface temperature (SST) data (color gradient) were downloaded from the NOAA database (https://coastwatch.pfeg.noaa.gov/erddap/, downloaded: 08/05/2024; Chamberlain, 2024), integrating the SST in 2022 until sampling (01/01/–16/08/2022). Maps were created with ggOceanMaps (Vihtakari, 2024).

_____

2.2 Abiotic parameters

CTD data. CTD profiles were run in open fjord water (except for station 4 and 5, where CTD and kelp sampling stations were the same). Water parameters (temperature [°C], salinity [S_A], turbidity [NTU]) of the water column were measured using an RBR Maestro3 (RBR Ltd., Ottawa, Canada). The downcast profile was used to monitor an undisturbed turbidity profile. The CTD was lowered at a speed of approx. 1 m s^{-1}. Data were smoothed by the mean for every meter interval. Values were reported as mean±SD of the upper 15 m of the water column.

Light data. The spectrally down-welling irradiance (λ 400–700 nm) was measured with a RAMSES-ACC-UV/VIS radiometer (TriOS Optical Sensor, Oldenburg, Germany; alternative calibration) above the kelp forest in water depths from the surface until the bottom was reached (max 10 m). The irradiance of each wavelength (I_λ) was measured in mW m^{-2} nm^{-1} and converted to μmol photons m^{-2} s^{-1} after Niedzwiedz and Bischof (2023). By integrating I_λ from 400–700 nm, the photosynthetically active radiation (PAR) was calculated (Niedzwiedz and Bischof, 2023). The light attenuation coefficient (K_d) was calculated between the surface and 3 m water depth after Hanelt et al. (2001). The spectrum peak (nm) on 3 m water depth was defined as the wavelength with the maximum irradiance transmission through the water column.

2.3 Kelp biochemistry

Biochemical measurements are based on dry weight (DW).

Pigment analyses. The kelp pigment composition reacts to cellular energy requirements and responds to light availability (Blain and Shears, 2019). Pigment concentrations were determined following Koch et al. (2015). Per specimen, two aliquots of 30–100 mg powdered material (*n*=3–5) were extracted in 1 mL 90 % acetone at 4°C for 24 h in darkness. The supernatant was filtered and analysed by a High-Performance Liquid Chromatography (HPLC; LaChromElite® system, L-2200 autosampler (chilled), DA-detector L-2450; VWR-Hitachi International GmbH, Darmstadt, Germany). After Wright et al. (1991), the pigments were separated in a Spherisorb® ODS-2 column (250 × 4.6 mm, 5 μm; Waters, Milford, MA, USA). Pigment peaks were identified and quantified using respective standards. Pigment concentrations were calculated as μg g$_{DW}^{-1}$. Accessory pigment content (Acc) was calculated as the sum of chlorophyll c, fucoxanthin and β-carotene. The ratio of accessory pigments to chlorophyll a (Acc:Chl*a*) was calculated. The pool of xanthophyll cycle pigments (VAZ; μg g$_{DW}^{-1}$) and its ratio to chlorophyll *a* was calculated (VAZ:Chl*a*). The de-epoxidation state of xanthophyll cycle pigments (DPS) was determined after Colombo-Pallotta et al. (2006).

Antioxidative activity. Bischof and Rautenberger (2012) reported antioxidants to be a protective mechanism against all types of abiotic stressors. Following the ABTS$^{·+}$ (2,2'-azino-bis-3-ethylbenzthiazoline-6-sulphonic acid, 7 mM in biDest H2O) assay (Re et al., 1999), the kelps antioxidative activity (AOA) was determined. One aliquot of 50 mg powdered material (*n*=3–5), was dark extracted in 1 mL 70 % ethanol for 4 h at 47°C. 10 µL of the supernatant were mixed with 1 mL ABTS$^{·+}$-working-standard (absorption range: 0.740±0.01;734 nm). After an incubation of 6 min, the absorption (λ 734 nm) was measured. AOA is reported as Trolox-equivalents (TE) by calibrating the ABTS$^{·+}$-working-solution with a Trolox dilution series (6-hydroxy-2,5,7,8-tetramethychroman-2-carboxylic acid; 2.5 mM in 70 % v/v ethanol).

Carbon and nitrogen content. The total carbon (C) and total nitrogen (N) content, as well as their ratio (C:N) was analysed to draw conclusions about nutrient availability at different sampling stations (Atkinson and Smith, 1983). C and N contents were analysed using powdered material (2–3 mg; *n*=3–5). Samples were weighed into tin cartridges (5×9 mm) and combusted at 1000°C. Acetanilide was used as standard (Verardo et al., 1990). An elemental analyser (Euro EA 3000 Elemental Analyser, EuroVector S.P.A., Milano, Italy) quantified the absolute C and N content automatically. Total C and N contents were expressed in mg g$_{DW}^{-1}$ and as ratio.

2.4 Statistical analyses

Data were evaluated, plotted and analysed in Rstudio (V 2023.12.1 using R-4.3.2-win; R Core Team, 2023), within "tidyverse" (Wickham et al., 2019). Maps were created with ggOceanMaps (Vihtakari 2024). As abiotic measurements were not independent from each other and often only point measurements, we did not evaluate them statistically, but only showed the mean and standard deviation over depth.

The raw data of the biochemical measurements and model residuals were tested for normality (Shapiro-Wilk test, p>0.05) and homoscedasticity (Levene's test, p>0.05). Outliers were removed from the dataset if they were classified as extreme (function: identify_outliers; package: rstatix; Kassambra, 2022). As prerequisites were met, a linear model was fit on each parameter (function: lm; package: stats; R Core Team, 2023). Sampling station was modelled as single-fixed effect to detect significant kelp responses to spatial variations. Analysis of variance was tested on the model (function: anova; package: stats; R Core Team, 2023). Pairwise performance (function: emmeans; package: emmeans; Lenth, 2024) was used to calculate the degrees of freedom, with Tukey'ø adjustment of the p-value. Pearson correlations were analysed (function: cor.test;

_____

package: stats; R Core Team, 2023). Correlogram was plotted using the ggcorr-function (package: GGally; Schloerke et al., 2024).

3. Results

3.1 Abiotic parameters

Water column measurements revealed a distinct latitudinal gradient of all parameters (**Figure 2**). Stations 1 and 2 in the south of Svalbard were characterised by cold temperatures (3.7±0.7°C) and highest turbidity values (2.8±2.0 NTU). At stations 3, 4 and 5 (mid of Svalbard) temperatures of 5.5±0.9°C, and turbidity values 1.8±0.7 NTU were measured. Stations 6 and 7 in the north of the Archipelago were characterised by highest temperatures (6.6±0.3°C) and lowest turbidity values (0.4±0.1 NTU). Mean salinity values across all stations ranged between S_A 32.0–33.8.

Highest K_d values were measured at station 2 (K_d = 1.8±0.4) and 5 (K_d = 1.0±0.1). Stations 6, 7, and 8 clustered very closely, being characteried by lowest K_d values (0.2±0.1). Spectrum peaks ranged between λ 510 and 580 nm, being highest at sampling station 2 (λ 577±3.7 nm) and 5 (λ 582±1.2 nm). Mean PAR intensities per sampling stations at 3 m water depth ranged between 2.3–137 µmol photons m^{-2} s^{-1}.

Complete CTD (temperature, salinity, turbidity) profiles over depth and the spectral resolution of PAR for each depth are provided in the appendix (**Figure A2**, **Figure A3**).
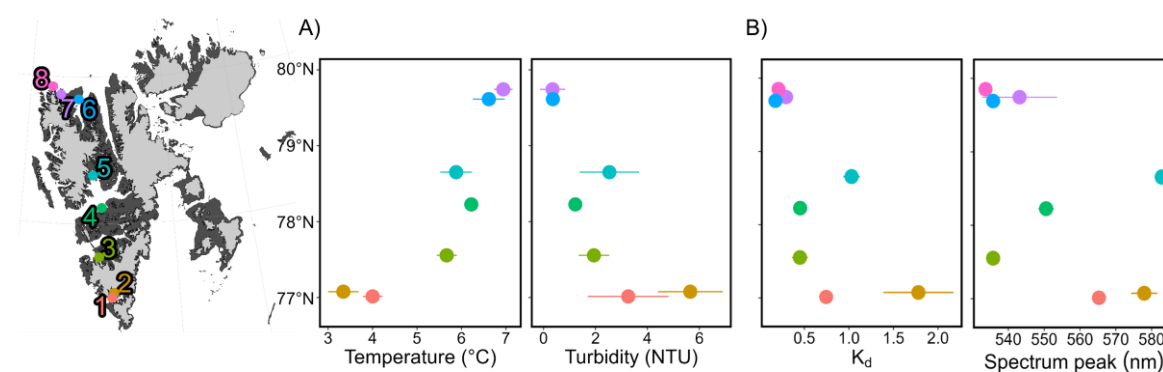
Figure 2: Abiotic parameters along the Svalbard latitudinal gradient. Stations: 1 – Gnålodden, Hornsund. 2 – Burgerbukta, Hornsund. 3 – Lyshamna, Bellsund. 4 – Bjørndalen, Isfjorden. 5 – Vòrneset, Ekmanfjorden. 6 – Worsleyhamna, Woodfjorden. 7 – Alicehamna, Raudfjorden. 8 – Ytre Norskøya. **A)** CTD data. Temperature (°C), Turbidity (NTU) of the upper 15 m of the water column (mean±SD over depth; n (per station) = 1). Note: Station 8 is missing in the CTD profiles. **B)** K_d: light attenuation coefficient between the water's surface and 3 m depth (mean±SD; *n*=1–3). Spectrum peak at 3 m water depth: wavelength (nm) with the highest irradiance (mean±SD; *n*=1–3).

_____

3.2 Kelp biochemistry

All statistical results are summarised in **Table 1** and are not given in the text for overview reasons.

Table 1: Statistics of biochemical parameters of kelps. Results of Analysis of Variance (ANOVA) to evaluate the effect of station as single fixed effect. Significant results are marked in bold. Acc:Chl*a*: ratio of accessory pigments to chlorophyll *a*. DPS: De-epoxidation state of xanthophyll cycle pigments. AOA: antioxidative activity. Total C: total carbon content. Total N: total nitrogen content. C:N: carbon to nitrogen ratio.

Parameter	numDF	denDF	*F* value	*p* value
Chlorophyll *a*	7	30	9.5	**<0.001**
Acc:Chl*a*	7	30	7.54	**<0.001**
DPS	7	27	2.9	**0.02**
AOA	7	26	5.2	**<0.001**
Total C	7	31	4.5	**0.001**
Total N	7	28	15.9	**<0.001**
C:N	7	28	12.5	**<0.001**

Note: numDF: numerator degrees of freedom. denDF: denominator degrees of freedom.

Pigments. The pigment composition differed significantly between stations (**Figure 3A**). Chlorophyll *a* (μg g_{DW}^{-1}) concentration of samples from station 2 was 50–87 % higher than in other fjords. Acc (μg g_{DW}^{-1}) and VAZ (μg g_{DW}^{-1}) showed similar patterns (**Figure A4**). The Acc:Chl*a* showed an increasing trend with higher latitude, being significantly lower at stations 1 and 2 compared to stations 6 and 7. While only the de-epoxidation state of xanthophyll cycle pigments (DPS) of station 1 was significantly lower compared to station 6, an overall increase of DPS values with higher latitude was observed.

Antioxidative activity. AOA (TE mM 100 mg_{DW}^{-1}; **Figure 3B**) was significantly affected by sampling stations; however no latitudinal trend was found for the significant differences.

Carbon and nitrogen content. The C and N content, as well as C:N were significantly affected by station (**Figure 3C**). Mean C content ranged between 280–345 mg g_{DW}^{-1} and increased with higher latitudes, with the C content of station 1, 2 being significantly lower compared to station 7. Mean N (7.1–20.1 mg g_{DW}^{-1}) showed a decreasing trend with higher latitude, although station 7 had the overall highest N content. Mean C:N (15.9–47.4) of station 6 was significantly higher, compared to the other stations (except station 4).
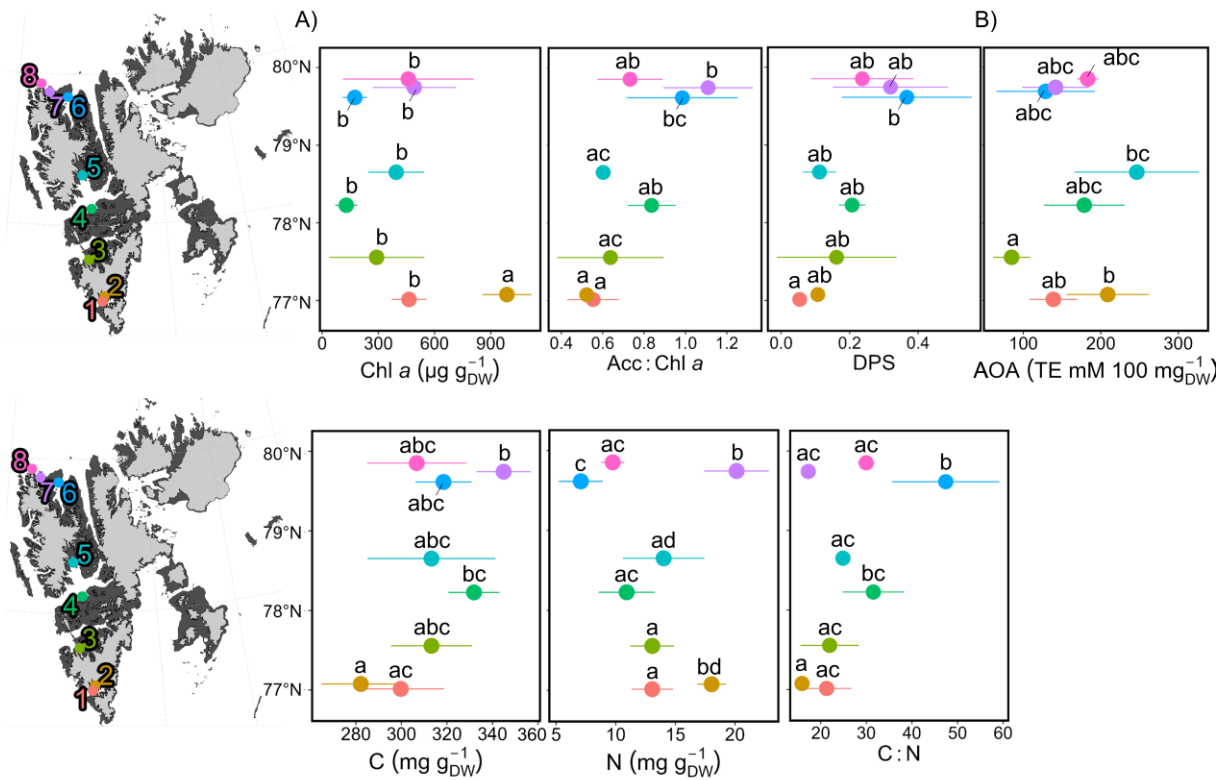
Figure 3: Kelp biochemistry along the Svalbard latitudinal gradient (mean±SD; *n*=3–5). Stations: 1 – Gnålodden, Hornsund. 2 – Burgerbukta, Hornsund. 3 – Lyshamna, Bellsund. 4 – Bjørndalen, Isfjorden. 5 – Vòrneset, Ekmanfjorden. 6 – Worsleyhamna, Woodfjorden. 7 – Alicehamna, Raudfjorden. 8 – Ytre Norskøya. Different letters indicate significant (*p*<0.05) differences between stations. Some error bars are within the diameter of the symbol. **A)** Chl *a*: chlorophyll *a* concentration (μg g$_{DW}$$^{-1}$). Acc:Chl*a*: ratio of accessory pigments to chlorophyll *a*. DPS: de-epoxidation state of xanthophyll cycle pigments. **B)** AOA: Antioxidative activity (TE mM 100 mg$_{DW}$$^{-1}$). **C)** C: total carbon content (mg g$_{DW}$$^{-1}$). N: total nitrogen content (mg g$_{DW}$$^{-1}$). C:N: carbon to nitrogen ratio.

_____

3.3 Correlations

Correlations between abiotic parameters and kelp responses are shown in **Figure 4**. Overall, a latitudinal gradient of environmental parameters was observed: temperature increased with higher latitude; turbidity decreased with higher latitude. Temperature correlated negatively with turbidity and K_d. High turbidity values correlated with high K_d values.

Kelp pigment concentrations (chlorophyll *a*, Acc, VAZ) correlated positively and pigment ratios (Acc:Chl*a*, DPS) correlated negatively with turbidity, the spectrum peak and K_d. DPS was found to correlate positively with temperature and latitude and negatively with turbidity. The chlorophyll *a* concentration, Acc and VAZ correlated positively with each other. Although AOA correlated positively with PAR, this correlation was not significant.

The total C correlated positively with temperature and latitude; and negatively with turbidity and K_d. Regarding total N these correlations were reversed, though not being significant.
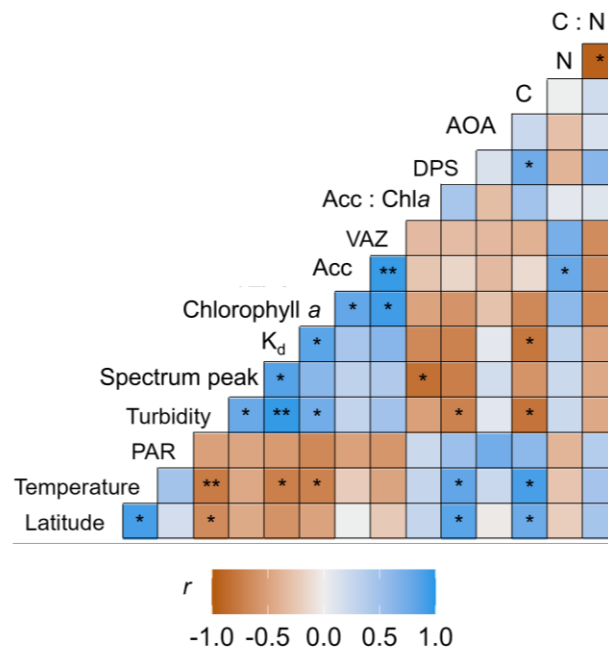
Figure 4: Linear dependency between kelp response parameters and abiotic conditions. Color scale: Pearson correlation co-efficient (*r*). PAR: photosynthetically active radiation. K_d: light attenuation coefficient. Acc: accessory pigments. VAZ: pool of xanthophyll cycle pigments. Acc:Chl*a*: ratio of accessory pigments to chlorophyll *a*. DPS: de-epoxidation state of xanthophyll cycle pigments. AOA: antioxidative activity. C: total carbon content. N: total nitrogen content. C:N: carbon to nitrogen ratio. Asterisks: significance of correlation (*: $p<0.05$; **: $p<0.01$; ***: $p<0.001$).

4. Discussion

The kelp *Saccharina latissima* is well-studied, being a key species in kelp forests along North Atlantic coasts (Araújo et al., 2016; Diehl et al., 2024). However, it is still unclear how its populations react to naturally occurring environmental variations at their cold-distribution limit. In this study, we analysed Arctic *S. latissima* populations from eight sampling stations along the west coast of Svalbard that were characterised by different environmental settings.

4.1 Biochemical composition responds strongly to the local environment

Using the environmental conditions along the west coast of Svalbard as natural laboratory, we assessed how local *S. latissima* populations were affected by naturally occurring abiotic variations. Therefore, we analysed their biochemical composition at each sampling station, relating them to differences in temperature and light availability, as they were described to be the most important drivers for kelp distribution (Fragkopoulou et al., 2022). We found clear spatial gradients along sampling stations for both drivers, increasing with higher latitude (**Figure 1**, **2**).

Fjord temperature patterns are influenced by currents (Cottier et al., 2010). Southern fjords in Svalbard were characterised by cold temperatures, being influenced by the Sørkapp Current carrying Arctic water masses (Konik et al., 2021). With higher latitude, we measured warmer temperatures, as the influence of the West Spitsbergen current increased, carrying warm Atlantic water masses (Svendsen et al., 2002). Thereby, all measured temperatures, ranging from 3–7°C, were well below the described growth optimum for *S. latissima* of 10–15°C (Bolton and Lüning, 1982).

Several experimental studies assessed how *S. latissima* responds to temperatures below their optimum: Monteiro et al. (2021) found an increasing trend of chlorophyll *a* and a significant decrease of the DPS between 0–15°C in young *S. latissima* of a temperate population (Roscoff, Brittany). Testing the same temperature range on young sporophytes from a Svalbard population, Li et al. (2020) also found decreasing DPS values with warmer temperature. As the DPS is part of the kelps' intercellular stress response (Gross and Jakob, 2010), these results indicate cold temperatures to inflict more physiological stress than temperatures closer to the optimum. We would have expected a similar response along the temperature gradient in Svalbard fjords. However, we found a contrary response; warmer temperatures correlated with higher DPS values. Thereby, it has to be noted that both Monteiro et al. (2021) and Li et al. (2020) worked with young sporophytes from stock cultures, while we worked on adult sporophytes. Generally, sporophytes of different ages can show different response patterns to stressors (Martins et al., 2017). However, we do not assume that these different responses were due to age differences or altered thermal

tolerances, but are rather due to interactive effects of stressors. Interpreting the biochemical composition of populations in this study, it has to be considered that warmer temperatures correlated with less run-off and a clearer water column (i.e., lower turbidity, K_d; **Figure 2**, **4**). Hence, we assume that high DPS values did not predominantly respond to changes in temperature but rather counteracted high-light stress. High-light availability might saturate the photosynthetic electron transport chain and deplete reductive equivalents (Bischof and Rautenberger, 2012). Excessive electrons contribute to form reactive oxygen species (ROS), which can destroy critical macromolecules (Sharma et al., 2012). DPS functions as protective mechanisms to dissipate excessive energy (Demmig-Adams and Adams, 1996), thereby reducing the potential of ROS formation. Kelps experiencing higher light availability were further characterised by a significantly lower chlorophyll *a* content, mitigating high light stress by reducing energy absorption. The ratio of Acc:Chl*a* confirmed this response pattern, increasing with higher light availability (**Figure 3**, **4**). This is indicating a reduction of the light harvesting antenna complex at photosynthetic reaction centres to prevent electrons being transmitted into the electron transport chain (Falkowski and Raven, 2007). As less electrons reduce the likelihood of ROS formation, oxidative stress is reduced (Kirk, 2011). Thereby, absolute PAR values, with a maximum of ~140 µmol photon m^{-2} s^{-1} at 3 m water depth are noteworthy, as they are well below PAR values that kelps experience in other regions, e.g., in the German Bight (400–500 µmol photons m^{-2} s^{-1}, Stahl et al., in revision). Niedzwiedz et al. (2024) argued that light stress at relatively low light intensities is caused by long photoperiod and the lack of a recovery phase. We found their experimental result confirmed by the responses to *in-situ* conditions.

This line of argumentat further explains the findings of Diehl et al. (2021). They described overall low DPS values and exceptionally high growth rates as a response to experimental temperatures between 0–6°C (including *in-situ* conditions). To be able to compare experiments across latitudes, they exposed the Svalbard samples to a 16:8 h L:D cycle. Thereby, samples likely recovered from the intense light exposure of Polar Day (comparable to high-light stress) and, therefore, showed no response to temperature changes. We hypothesise that the overall, temperature-independent increase in performance, Diehl et al. (2021) found, is due to a more optimal light regime. These findings emphasise the importance of interacting stressors, when considering a species tolerance towards environmental conditions. Besides variation in light intensity, qualitative shifts in spectral composition have been observed. With increasing run-off influence, we found a shift of the spectrum peak to longer wavelengths (**Figure 2**, **A3**), which was especially pronounced at station 1, 2, and 5. While stations 1 and 2 were characterised by overall high turbidity, indicating a relatively higher sediment load, station 5 was dominated by a very red sediment type ("Old red sandstone"; **Figure A5**; Kavan et al, 2022), leading to this strong wavelength shift. Accessory pigments are closing the green gap of chlorophyll *a*, increasing the absorption spectrum of kelps

_____

(Stomp et al, 2007). As Acc:Chl*a* correlated negatively with the spectrum peak, the pigment composition did not respond to spectrum shifts. Hence, we conclude that the reduction of the light harvesting complex predominantly responded to reduce high-light stress, and not related to spectral shifts.

We could not determine the same stress response in AOA as for DPS. As the samples were exposed to their respective environmental conditions during the whole growing season, we suggest that high-light stress was already effectively mitigated by changes in the pigment composition of the photosystem, preventing overall higher cellular stress response. As the AOA was significantly influenced by the sampling stations, we assume that parameters not quantified in this study might have triggered it.

We found a clear trend of increasing total C content with higher latitudes, i.e., with warmer temperatures and higher light availability, though we cannot identify the parameter that caused the increase in C content. A higher C content might indicate more storage compounds, e.g., mannitol and laminarin (Graiff et al., 2016). Scheschonk et al. (2019) showed that *S. latissima's* storage compounds were depleted by 96 % after three months of Polar Night. A reduced carbon content in run-off dominated fjord areas might increase the likelihood of *S. latissima* having an overall negative carbon balance, i.e., might run into starvation during winter months.

C:N ratios above 20 indicated that kelps from all sampling stations were N limited (Atkinson and Smith, 1983). In summer, Arctic water masses are stratified by strong temperature and salinity gradients (**Figure A2**), leading to the absence of vertical mixing and a re-supply of deep-water nutrients (Cottier et al., 2010). The total N content showed a decreasing trend with higher latitude (**Figure 3**). We attribute this to the higher influence of run-off in southern Svalbard fjords (higher turbidity; **Figure 2**), carrying nutrients from terrestrial sources (McGovern et al., 2020). Thereby, station 7 is an exception, being characterised by kelps with a high N content. At station 7, temperature gradients over depth were very weak (**Figure A2**), showing almost no variation within the upper 15 m of the water column (**Figure 2**, **A2**). As salinity and turbidity differences were likewise not very pronounced, we suggest that station 7 might have been influenced by local upwelling, leading to a resupply of nutrients. C:N ratios were described to define the food quality of kelps (Lowman et al., 2022). An altered food quality of primary producers changes the efficiency of energy transfer to higher trophic levels (Lowman et al., 2022), thereby having an effect on the ecosystems nutrient cycling. Grazing rates of invertebrates are predicted to increase with higher temperatures within their tolerance range (Brown et al., 2004). Further, Traiger (2019) showed that high sedimentation rates due to Arctic run-off, reduced the grazing pressure on kelps. In northern Svalbard fjords, we measured higher temperatures and less turbidity, which might increase grazing pressure, in comparison to southern Svalbard fjords. While further studies have

_____

to be conducted to assess these effects, it is highlighting the complexity of ecological responses towards climate change.

4.2 *Saccharina latissima* does not react as one biochemical unit

Bolton and Lüning (1982) described the temperature optimum for *S. latissima* between 10–15°C. Following the resulting performance curve, this indicates an increasing stress level as temperatures deviate from the optimum. Interacting with light, we found the opposite trend; stress levels increased with temperatures closer to the species optimum. Thereby, it has to be considered that temperature closer to the optimum might already have mitigated high-light stress, as was experimentally shown by Niedzwiedz et al. (2024). Further, we found kelps in most fjords to be N limited. Nutrient limitation was shown to weaken kelps, making them more susceptible for other stressors, such as UV radiation (Davison et al., 2007). We conclude that the sum of natural variation in present-day Arctic fjords leads to significant variations in the biochemical composition of kelps.

Comparing the biochemical composition of *S. latissima* along the entire European gradient, Diehl et al. (2023) found neither a clear latitudinal gradient nor a clustering of populations driven by abiotic conditions. In their study, they focussed on temperature and salinity as main drivers, not measuring light availability or light-dependent responses (e.g., pigments). Based on the results of our study, we hypothesise that the inclusion of light availability might have resulted in a more distinct clustering of sampling stations; especially, phlorotannin concentrations in the study of Diehl et al. (2023) indicated the significance of light on the biochemistry of kelps and population differences.

4.3 Concluding remarks

In this field study, we compared eight Arctic *S. latissima* populations. We analysed their biochemical composition and related their response to differences in temperature and light availability of their local environment. This approach had two advantages: (1) we studied the biochemical composition towards realistic abiotic conditions and (2) all kelp populations were acclimatised to their respective abiotic condition; hence, long-term biochemical responses are determined.

We found distinct differences in the biochemical composition of *S. latissima*, correlating with their sampling origin. While this indicates a high phenotypic plasticity of *S. latissima*, it also shows that it strongly depends on the local environmental history. Hence, the environmental history of field material and consequently the biochemical compositions have to be considered in climate

projections, as it changes susceptibilities towards (experimental) stressors. Further, our study highlights the necessity to consider the interaction of stressors, as it significantly changes tolerances (Wernberg et al., 2010). Hence, we conclude that performance curves must not be considered as static.

Author contribution

SN and ND conceptualised the study under the supervision of KB. SN and SA conducted the field work with advice and supervision of BD. Parameter analyses and evaluation were conducted as follows: physical water parameters: SN, CV and SA. Biochemical parameters: SN and CV. Data interpretation: SN, ND and KB. SN wrote the manuscript, which was revised and reviewed by all co-authors.

_____

Competing interests

The authors declare no conflict of interest.

Data availability

All data supporting this study are openly available on the Pangaea platform.

CTD data (temperature, salinity, turbidity) can be accessed:
https://doi.pangaea.de/10.1594/PANGAEA.968642

Light conditions (available light) can be accessed:
https://doi.pangaea.de/10.1594/PANGAEA.968464

Kelp responses (pigments, antioxidative potential, C:N ratio) are available:
https://doi.pangaea.de/10.1594/PANGAEA.968466

References

Araújo, R.M., Assis J., Aguillar, R., Airoldi, L., Bárbara, I., Bartsch, I., Bekkby, T., Christie, H., Davoult, D., Derrien-Courtel, S., Fernandez, C., Fredriksen, S., Gevaert, F., Gundersen, H., Le Gal, A., Lévêque, L., Mieszkowska, N., Norderhaug, K.M., Oliveira, P., Ouente, A., Rico, J.M., Rinde, E., Schubert, H., Strain, E.M., Valero, M., Viard, F., Sousa-Pinto, I., 2016. Status, trends and drivers of kelp forests in Europe: an expert assessment. Biodiversity and Conservation. 25, 1319-1348. https://doi.org/10.1007/s10531-016-1141-7

Assis, J., Serrão, E., Duarte, C.M., Fragkopoulou, E., Krause-Jensen, D., 2022. Major expansion of marine forests in a warmer Arctic. Frontiers in Marine Science. 9:850368. https://doi.org/10.3389/fmars.2022.850368

Atkinson, M.J., Smith, S.V., 1983. C:N:P ratios of benthic marine plants. Limnology and Oceanography. 28, 568-574. https://doi.org/10.4319/lo.1983.28.3.0568

Bartsch, I., Paar, M., Fredriksen, S., Schwanitz, M., Daniel, C., Hop, H., Wiencke, C., 2016. Changes in kelp forest biomass and depth distribution in Kongsfjorden, Svalbard, between 1996-1998 and 2012-2014 reflect Arctic warming. Polar Biology. 39, 2021-2036. https://doi.org/10.1007/s00300-015-1870-1

Bennett, S., Duarte C.M., Marbà, N., Wernberg, T., 2019. Integrating within-species variation in thermal physiology into climate change ecology. Philosophical Transactions of the Royal Society B. 374: 20180550. http://doi.org/10.1098/rstb.2018.0550

_____

Bischof, K., Rautenberger, R., 2012. Seaweed responses to environmental stress: reactive oxygen and antioxidant strategies, in: C. Wiencke and K. Bischof (Eds.) Seaweed Biology. Berlin-Heidelberg: Springer Verlag. pp. 109-132.

Blain, C.O., Shears, N.T., 2019. Seasonal and spatial variation in photosynthetic response of the kelp *Ecklonia radiata* across a turbidity gradient. Photosynthesis Research. 140, 21-38. http://doi.org/10.1007/s11120-019-00636-7

Bolton, J.J., Lüning, K., 1982. Optimal growth and maximal survival temperatures of Atlantic Laminaria species (Phaeophyta) in culture. Marine Biology. 66, 89-94. http://doi.org/10.1007/BF00397259

Brown, J.H., Gillooly, J.F., Allen, A.P., Savage, V.M., West, G.B., 2004. Toward a metabolic theory of ecology. Ecology. 85, 1771-1789. https://doi.org/10.1890/03-9000

Chamberlain, S., 2024. rerddap: General Purpose Client for 'ERDDAP' Servers. R package version 1.1.0. https://CRAN.R-project.org/package=rerddap

Collier, R.J., Baumgard, L.H., Zimbelman, R.B., Xiao, Y., 2019. Heat stress: physiology of acclimation and adaptation. Feature Article. 9, 12-19. https://doi.org/10.1093/af/vfy031

Colombo-Pallotta, M.F., García-Mendoza, E., Ladah, L.B., 2006. Photosynthetic performance, light absorption, and pigment composition of *Macrocystis pyrifera* (Laminariales, Phaeophyceae) blades from different depths. Journal of Phycology. 42, 1225-1234. http://doi.org/10.1111/j.1529-8817.2006.00287.x

Cottier, F.R., Nilsen, F., Skogseth, R., Tverberg, V., Skarðhamar, J., Svendsen, H., 2010. Arctic fjords: a review of the oceanographic environment and dominant physical processes. Geological Society London Special Publications. 344, 35-50. http://doi.org/10.1144/SP344.4

Davison, I.R., Jordan, T.L., Fegley, J.C, Grobe, C.W., 2007. Response of *Laminaria saccharina* (Phaeophyta) growth and photosynthesis to simultaneous ultraviolet radiation and nitrogen limitation. 43, 636-646. http://doi.org/10.1111/j.1529-8817.2007.00360.x

Demmig-Adams, B., Adams, W.W., 1996. Xanthophyll cycle and light stress in nature: uniform response to excess direct sunlight among higher plant species. Planta. 198, 460-470. https://doi.org/10.1007/BF00620064

Diehl, N., Roleda, M.Y., Bartsch, I., Karsten, U., Bischof, K., 2021. Summer heatwave impacts on the European kelp *Saccharina latissima* across its latitudinal distribution gradient. Frontiers in Marine Science. 8:695821. https://doi.org/10.3389/fmars.2021.695821

Diehl, N., Steiner, N., Bischof, K., Karsten, U., Heesch, S., 2023. Exploring intraspecific variability – biochemical and morphological traits of the sugar kelp *Saccharina latissima* along latitudinal and salinity gradients in Europe. Frontiers in Marine Science. 10:995982. https://doi.org/10.3389/fmars.2023.995982

Diehl, N., Li, H., Scheschonk, L., Burgunter-Delamare, B., Niedzwiedz, S., Forbord, S., Sæther, M., Bischof, K., Monteiro, C., 2024. The sugar kelp *Saccharina latissima* I: recent advances in a changing climate. Annals of Botany. 133, 183-211. https://doi.org/10.1093/aob/mcad173

Düsedau, L., Fredriken, S., Brand, M., Fischer, P., Karsten, U., Bischof, K., Savoie, A., Bartsch, I., n.d. Kelp forest dynamics in Kongsfjorden (Svalbard) across 25 years of Arctic warming. Ecology and Evolution (in revision).

_____

Eckman, J.E., Duggins, D.O., Sewell, A.T., 1989. Ecology of understory kelp environments. I. Effects of kelps on flow and particles transport near the bottom. Journal of Experimental Marine Biology and Ecology. 129, 173-187. https://doi.org/10.1016/0022-0981(89)90055-5

England, M.R., Eisenman, I., Lutsko, N.J., Wagner, T.J.W., 2021. The recent emergence of Arctic Amplification. Geophysical Research Letters, 48, e2021GL094086. https://doi.org/10.1029/2021GL094086

Falkowski, P. G., Raven, J.A., 2007. Aquatic photosynthesis, 2nd ed. Princeton Univ. Press.

Filbee-Dexter, K., Wernberg, T., Fredriksen, S., Norderhaug, K.M., Pedersen, M.F., 2019. Arctic kelp forests: diversity, resilience and future. Global and Planetary Change. 172, 1-14. https://doi.org/10.1016/j.gloplacha.2018.09.005

Filbee-Dexter, K., Wernberg, T., Grace, S.P., Thormar, J., Fredriksen, S., Narvaez, C.N., Feehan, C.J., Norderhaug, K.M., 2020. Marine heatwaves and the collapse of marginal North Atlantic kelp forests. Scientific reports. 10:13388. https://doi.org/10.1038/s41598-020-70273-x

Fragkopoulou, E., Serrão, E., De Clerck, O., Costello M.J., Araújo, M.B., Duarte, C.M., Krause-Jensen, D., Assis, J., 2022. Global biodiversity patterns of marine forests of brown macroalgae. 31, 363-348. https://doi.org/10.1111/geb.13450

Gattuso, J-P., Gentili, B., Antoine, D., Doxaran, D., 2020. Global distribution of photosynthetically available radiation on the seafloor. Earth System Science Data. 12, 1697-1709. https://doi.org/10.5194/essd-12-1697-2020

Gauci, C., Bartsch, I., Martins, N., Liesner, D., 2022. Cold thermal priming of *Laminaria digitata* (Laminariales, Phaeophyceae) gametophytes enhances gametogenesis and thermal performance of sporophytes. Frontiers in Marine Science. 9:862923. https://doi.org/10.3389/fmars.2022.862923

Graiff, A., Ruth, W., Kragl, U., Karsten, U., 2016. Chemical characterization and quantification of the brown algal storage compound laminarin – a new methodological approach. Journal of Applied Phycology. 28: 533–543. https://doi.org/10.1007/s10811-015-0563-z

Gross, R., Jakob, T., 2010. Regulation and function of xanthophyll cycle-dependent photoprotection in algae. Photosynthesis Research. 106, 103-122. https://doi.org/10.1007/s11120-010-9536-x

Hanelt, D., Tüg H., Bischof, K., Groß, C., Lippert, H., Sawall, T., Wiencke, C.,2001. Light regime in an Arctic fjord: a study related to stratospheric ozone depletion as a basis for determination of UV effects on algal growth. Marine Biology. 138, 649-658. https://doi.org/10.1007/s002270000481

Kassambara, A., 2023. rstatix: Pipe-Friendly Framework for Basic Statistical Tests. R package version 0.7.2. https://CRAN.R-project.org/package=rstatix

Kavan, J., Wieczorek, I., Tallentire, G.D., Demidionov, M., Uher, J., Strelecki, M.C., 2022. Estimating suspended sediment fluxes from the largest glacial lake in Svalbard to fjord system using Sentinel-2 data: trebrevatnet case study. Water. 14, 1840. https://doi.org/10.3390/ w14121840

King, N.G., McKeown N.J., Smale, D.A., Moore, P.J., 2017. The importance of phenotypic plasticity and local adaptation in driving intraspecific variability in thermal niches of marine macrophytes. Ecography. 41, 1469-1484. https://doi.org/10.1111/ecog.03186

Kirk, J. T. O. 2011. Light and photosynthesis in aquatic systems, 3rd ed. Cambridge Univ. Press.

_____

_____

Koch, K., Thiel, M., Tellier, F., Hagen, W., Graeve, M., Tala, F., Laeseke, P., Bischof, K., 2015. Species separation within the Lessonia nigrescens complex (Phaeophyceae, Laminariales) is mirrored by ecophysiological traits. Botanica Marina. 58, 91-92. https://doi.org/10.1515/bot-2014-0086

Konik, M., Darecki, M., Pavlov, A.K., Sagan, S., Kowalczuk, P., 2021. Darkening of the Svalbard fjords waters observed with satellite ocean color imagery in 1997–2019. Frontiers in Marine Science. 8:699318. https://doi.org/10.3389/fmars.2021.699318

Lenth, R., 2024. emmeans: Estimated Marginal Means, aka Least-Squares Means. R package version 1.10.0. https://CRAN.R-project.org/package=emmeans

Li, H., Monteiro, C., Heinrich, S., Bartsch, I., Valentin, K., Harms, L., Glöckner, G., Corre, E., Bischof, K., 2020. Responses of the kelp *Saccharina latissima* (Phaeophyceae) to the warming Arctic: from physiology to transcriptomics. Physiologia Plantarum. 168, 5-26. https://doi.org/10.1111/ppl.13009

Liesner, D., Sharma, L.N.S., Diehl, N., Valentin, K., Bartsch, I., 2020. Thermal plasticity of the kelp *Laminaria digitata* (Phaeophyceae) across life cycle stages reveals the importance of cold seasons for marine forests. Frontiers in Marine Science. 7:456. https://doi.org/10.3389/fmars.2020.00456

Lowman, H.E., Emery, K.A., Dugan, J.E., Miller, R.J., 2022. Nutritional quality of giant kelp declines due to warming ocean temperatures. Oikos. e08619. https://doi.org/10.1111/oik.08619

Martins, N., Tanttu, H., Pearson, G.A., Serrão, E., Bartsch, I., 2017. Interactions of daylength, temperature and nutrients affect thresholds for life stage transition in the kelp *Laminaria digitata* (Phaeophyceae). Botanica Marina. 60,109-121. https://doi.org/10.1515/bot-2016-0094

McGovern, M., Pavlov, A.K., Deininger, A., Granskog, M.A., Leu, E., Søreide, J., Poste, A.E., 2020. Terrestrial inputs drive seasonality in organic matter and nutrient biogeochemistry in a high Arctic fjord system (Isfjorden, Svalbard). Frontiers in Marine Science. 7: 542563. https://doi.org/10.3389/fmars.2020.542563

Monteiro, C., Li, H., Diehl, N., Collén, J., Heinrich, S., Bischof, K., Bartsch, I., 2021. Modulation of physiological performance by temperature and salinity in the sugar kelp *Saccharina latissima*. Phycological Research. 69, 48-57. https://doi.org/10.1111/pre.12443

Niedzwiedz, S., Diehl, N., Fischer, P., Bischof, K., 2022. Seasonal and inter-annual variability in the heatwave tolerance of the kelp *Saccharina latissima* (Laminariales, Phaeophyceae). Phycological Research. 70, 212-222. https://doi.org/10.1111/pre.12501

Niedzwiedz, S., Bischof, K., 2023. Glacial retreat and rising temperatures are limiting the expansion of temperate kelp species in the future Arctic. Limnology and Oceanography. 68, 816-830. https://doi.org/10.1002/lno.12312

Niedzwiedz, S., Vonnahme, T.R., Juul-Pedersen, T., Bischof, K., Diehl, N., 2024. Light-mediated temperature susceptibility of kelp species (*Agarum clathratum*, *Saccharina latissima*) in an Arctic summer heatwave scenario. Cambridge Prisms: Coastal Futures. 2, 1–13 https://doi.org/10.1017/cft.2024.5

Pessarrodona, A., Assis, J., Filbee-Dexter, K., Burrows, M.T., Gattuso, J.-P., Duarte, C.M., Krause-Jensen, D., Moore, P.J., Smale, D.A., Wernberg, T., 2022. Global seaweed production. Science Advances. 8, eabn2465. https://doi.org/10.1126/sciadv.abn2465

Pörtner, H.O., Lucassen, M., Storch, D., 2005. Metabolic biochemistry: its role in thermal tolerance and in the capacities of physiological and ecological function. Fish Physiology. 22, 79-154. https://doi.org/10.1016/S1546-5098(04)22003-9

Previdi, M., Tyler, T.P., Chiodo, G., Smith, K.L., Polvani, L.M., 2020. Arctic amplification: a rapid response to radiative forcing. Geophysical Research Letters. 47, e2020GL089933. https://doi.org/10.1029/2020GL089933

Previdi, M., Smith, K.L., Polvani, L.M., 2021. Arctic amplification of climate change: a review of underlying mechanisms. Environmental Research. 16, 093003. https://doi.org/10.1088/1748-9326/ac1c29

R Core Team, 2023. R: A language and environment for statistical computing. R Foundation for Statistical Computing, https://www.R-project.org/

Re, R., Pellegrini, N., Proteggente, A., Pannala, A., Yang, M., Rice-Evans, C., 1999. Antioxidant activity applying an improved ABTS radical cation decolorization assay. Free Radical Biology and Medicine. 26, 1231-1237. https://doi.org/10.1016/s0891-5849(98)00315-3

Reed, T.E., Schindler, D.E., Waples, R.S., 2011. Interacting effects of phenotypic plasticity and evolution on population persistence in a changing climate. Conservation Biology. 25, 56-63. https://doi.org/10.1111/j.1523-1739.2010.01552.x

Sæther, M., Diehl, N., Monteiro, C., Li, H., Niedzwiedz, S., Burgunter-Delamare, B., Scheschonk, L., Bischof, K., Forbord, S., 2024. The sugar kelp *Saccharina latissima*

II: recent advances in farming and applications. Journal of Applied Phycology. https://doi.org/10.1007/s10811-024-03213-1

Scheschonk, L., Becker, S., Hehemann, J.-H., Diehl, N., Karsten, U., Bischof, K., 2019. Arctic kelp eco-physiology during the polar night in the face of global warming: a crucial role for laminarin. Marine Ecology Progress Series. 611, 59-74. https://doi.org/10.3354/meps12860

Schloerke, B., Cook, D., Larmarange, J., Briatte, F., Marbach, M., Thoen, E., Elberg, A., Crowley, J., 2023. GGally: Extension to 'ggplot2'. R package version 2.2.0. https://CRAN.R-project.org/package=GGally

Sharma, P., Jha, A.B., Dubey, R.S., Pessarakli, M., 2012. Reactive oxygen species, oxidative damage and antioxidative defense mechanism in plants under stressful conditions. Journal of Botany. 217037, https://doi.org/10.1155/2012/217037

Stahl, F., Kappas, L., Uhl, F., Oppelt, N., Bischof K., n.d. Feasibility study for kelp afforestation in the German Bight: habitat availability and light requirements of Laminaria hyperborea. Journal of Sea Research (in revision).

Steneck, R.S., Graham, M.H., Bourque, B.J., Corbett, D., Erlandson, J.A., Estes, J.A., Tegner, M.J., 2002. Kelp forest ecosystems: biodiversity, stability, resilience and future. Environmental Conservation. 29, 436-459. https://doi.org/10.1017/S0376892902000322

Stomp, M., Huisman, J., Stal, L.J., Matthijs, H.C.P., 2007. Colorful niches of phototrophic microorganisms shaped by vibrations of the water molecule. The ISME Journal. 1, 271-282. https://doi.org/10.1038/ismej.2007.59

Svendsen, H., Beszczynska-Møller, A., Hagen, J.O., Lefauconnier, B., Tverberg, V., Gerland, S., Ørbæk, J.B., Bischof, K., Papucci, C., Zajaczkowski, M., Azzolini, R., Bruland, O., Wiencke, C., Winther, J-G.,

_____

Dallmann, W., 2002. The physical environment of Kongsfjorden-Krossfjorden, an Arctic fjord system in Svalbard. Polar Research. 21, 133-166. https://doi.org/10.3402/polar.v21i1.6479

Traiger, S.B., 2019. Effects of elevated temperature and sedimentation on grazing rates of the green sea-urchin: implications for kelp forests exposed to increase sedimentation with climate change. Helgoland Marine Research. 73:5. https://doi.org/10.1186/s10152-019-0526-x

Verardo, D.J., Froelich, P.N., McIntyre, A., 1990. Determination of organic carbon and nitrogen in marine sediments using the Carlo Erba NA-1500 Analyzer. Deep-Sea Research.37, 157-165. https://doi.org/10.1016/0198-0149(90)90034-S

Vihtakari, M., 2024. ggOceanMaps: Plot Data on Oceanographic Maps using 'ggplot2'. R package version 2.2.0, https://CRAN.R-project.org/package=ggOceanMaps

Vranken, S., Wernberg, T., Scheben, A., Severn-Ellis, A.A., Batley, J., Bayer, P.E., Edwards, D., Wheeler, D., Coleman, M.A., 2021. Genotype-environment mismatch of kelp forests under climate change. Molecular Ecology. 30, 3730-37446. https://doi.org/10.1111/mec.15993

Wickham, H., Averick, M., Bryan, J., Chang, W., McGowan, L.D., François, R., Grolemund, G., Hayes, A., Henry, L., Hester, J., Kuhn, M., Pedersen, T.L., Miller, E., Bache, S.M., Müller, K., Ooms, J., Robinson, D., Seidel, D.P., Spinu, V., Takahashi, K., Vaughan, D., Wilke, C., Woo, K., Yutani, H., 2019. Welcome to the tidyverse. Journal of Open Source Software. 4, 1686. https://doi.org/10.21105/joss.01686

Wernberg, T., Thomsen, M.S., Tuya, F., Kendrick, G.A., Staehr, P.A., Toohey, B.D., 2010. Decreasing resilience of kelp beds along a latitudinal temperature gradient: potential implications for a warmer future. Ecology Letters. 13, 685-694. https://doi.org/10.1111/j.1461-0248.2010.01466.x

Wernberg, T., Krumhansl, K., Filbee-Dexter, K., Pedersen, M.F., 2019. Status and trends for the world's kelp forests, in: C. Sheppard (Eds.), World seas: an environmental evaluation. Elsevier. pp. 57-78. https://doi.org/10.1016/B978-0-12 805052-1.00003-6

Wernberg, T., Thomsen, M.S., Baum J.K., Bishop, M.J., Bruno, J.F., Coleman, M.A., Filbee-Dexter, K., Gagnon, K., He, Q., Murdiyarso, D., Rogers, K., Silliman, B.R., Smale, D.A., Starko, S., Vanderklift, M.A., 2024. Impacts of climate change on marine foundation species. Annual Review of Marine Science. 16, 247-282. https://doi.org/10.1146/annurev-marine-042023-093037

Wright, S.W., Jeffrey, S.W., Mantoura, R.F.C., Llewellyn, C.A., Bjørnland, T., Repeta, D., Welschmeyer N., 1991. Improved HPLC method for the analysis of chlorophylls and carotenoids from marine phytoplankton. Marine Ecology Progress Series. 77, 183-196. https://doi.org/10.3354/meps077183

_____

Appendix

Figure A1: Locations of kelp and light sampling stations (circle) and CTD measuring stations (triangle); same location in subplot **C)** and **D)**. **A)** 1 – Gnålodden, Hornsund. 2 – Burgerbukta, Hornsund. **B)** 3 – Lyshamna, Bellsund. **C)** 4 – Bjørndalen, Isfjorden. **D)** 5 – Vòrneset, Ekmanfjorden. **E)** 6 – Worsleyhamna, Woodfjorden. 7 – Alicehamna, Raudfjorden. 8 – Ytre Norskøya. Blue colour gradient: water depth (m). Dark grey area: land. Light grey area: glaciers. Maps were created with ggOceanMaps (Vihtakari, 2022).

_____
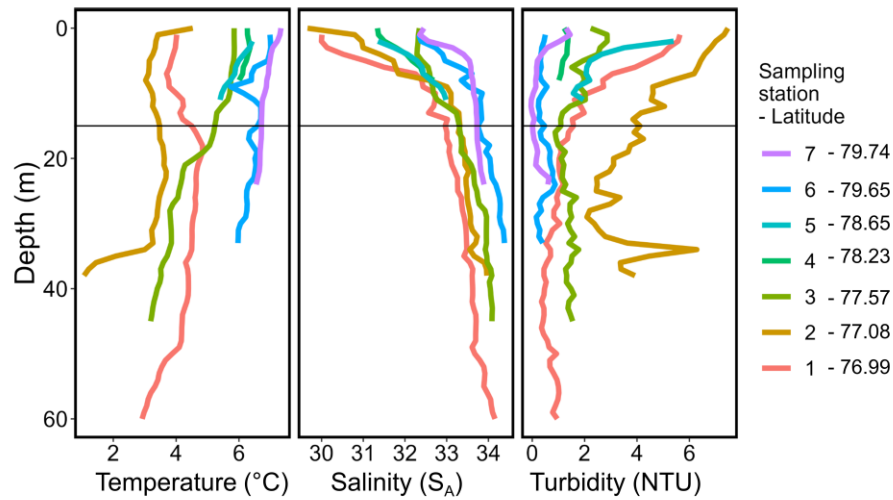
Figure A2: Complete CTD profiles (temperature [°C], salinity [SA], turbidity [NTU]) over depth (m) of each station. 1 – Gnålodden, Hornsund. 2 – Burgerbukta, Hornsund. 3 – Lyshamna, Bellsund. 4 – Bjørndalen, Isfjorden. 5 – Vòrneset, Ekmanfjorden. 6 – Worsleyhamna, Woodfjorden. 7 – Alicehamna, Raudfjorden. Data above 15 m (black line) were integrated for data in main text.
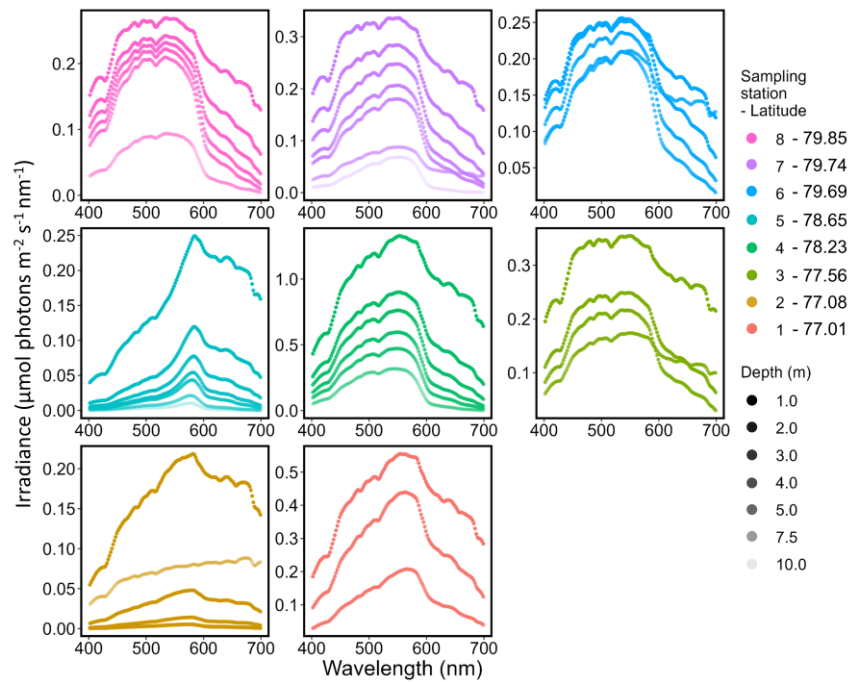
Figure A3: Spectral resolution (400–700 nm) of irradiance (µmol photons m-2 s-1 nm-1) from each station. 1 – Gnålodden, Hornsund. 2 – Burgerbukta, Hornsund. 3 – Lyshamna, Bellsund. 4 – Bjørndalen, Isfjorden. 5 – Vòrneset, Ekmanfjorden. 6 – Worsleyhamna, Woodfjorden. 7 – Alicehamna, Raudfjorden. 8 – Ytre Norskøya. Note: different y-axes of the subplots.
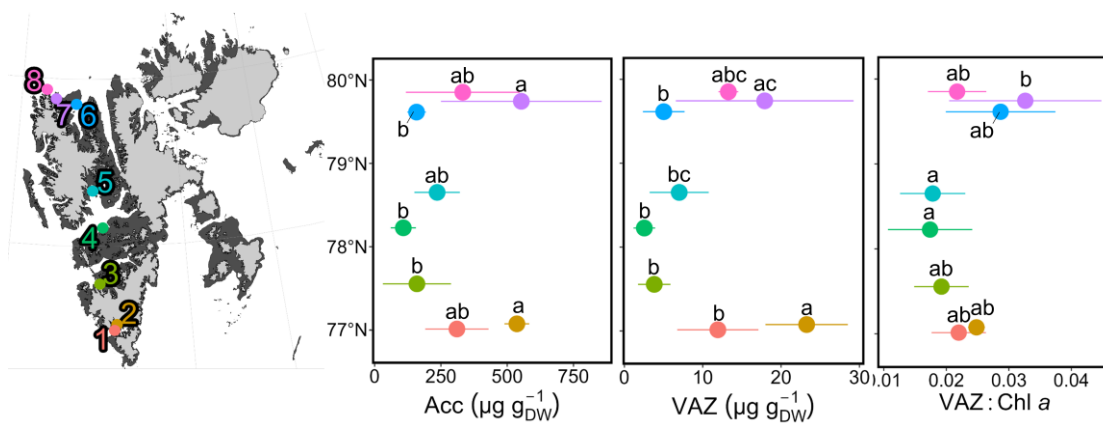
Figure A4: Kelp biochemistry along the Svalbard latitudinal gradient (mean±SD; *n*=3–5). Stations: 1 – Gnålodden, Hornsund. 2 – Burgerbukta, Hornsund. 3 – Lyshamna, Bellsund. 4 – Bjørndalen, Isfjorden. 5 – Vòrneset, Ekmanfjorden. 6 – Worsleyhamna, Woodfjorden. 7 – Alicehamna, Raudfjorden. 8 – Ytre Norskøya. Acc: accessory pigments (sum of chlorophyll c, fucoxanthin and β-carotene; µg gDW-1). VAZ: pool of xanthophyll cycle pigments (sum of violaxanthin, antheraxanthin, zeaxanthin; µg gDW-1). VAZ:Chl*a*: ratio of xanthophyll cycle pigments to chlorophyll *a*. Different letters indicate significant (*p*<0.05) differences between sampling stations.

_____

Figure A5: Run-off plume in Ekmanfjorden, Svalbard. The plume is dominated by "Old red sandstone"; Kavan et al. (2022), reflecting the red part of the light spectrum. Picture: 31/08/2022, ©Sarina Niedzwiedz.

_____

PUBLICATION II

Run-off impacts on Arctic kelp holobionts have strong implications on ecosystem functioning and bioeconomy

Sarina Niedzwiedz, Claudia E. Schmidt, Yunlan Yang, Bertille Burgunter-Delamare, Sebastian Andersen, Lars Hildebrandt, Daniel Pröfrock, Rui Zahng, Børge Damsgård, Kai Bischof

Run-off impacts on Arctic kelp holobionts

Sarina Niedzwiedz[1*], Claudia Elena Schmidt[2,3], Yunlan Yang[4], Bertille Burgunter-Delamare[5], Sebastian Andersen[6], Lars Hildebrandt[3], Daniel Pröfrock[3], Helmuth Thomas[2,3], Rui Zhang[4], Børge Damsgård[6], Kai Bischof[1]

[1] University of Bremen, Germany; [2] HEREON, Germany; [3] University of Oldenburg, Germany; [4] Xiamen University, China; [5] University Jena, Germany; [6] UNIS, Norway

81°N
80°N
79°N
78°N
77°N

10°E 15°E 20°E 25°E
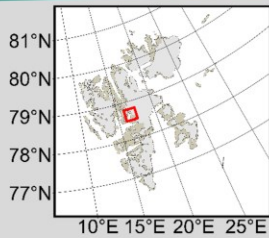
Rising temperatures in the Arctic result in run-off plumes in fjords. Within these run-off plumes, physical and chemical parameters are altered. In Arctic fjords, kelps are primary producers, hence, many species depend on them as food source. Kelps have a high heavy metals biosorption potential, with their associated microbial community depending on the host conditions.

Research question: How is meltwater run-off affecting the elemental concentration and associated microbial communities characteristics of kelps?

Meltwater plume in an Svalbard fjord

RUN-OFF SYSTEMS

Sea-terminating glacier

Control

Land-terminating glacier

CHEMISTRY

Cd   K   Lu
Hg   Na   La   Ce
Pb   Mg

Heavy metals

Macro-minerals

Rare earth elements

Stress response

Microbial community change

ECOLOGICAL RESPONSES AND FUNCTIONING

Bioaccu-mulation across the Arctic food web

High food quality

Altered availability of secondary metabolites for micrograzers

IMPLICATIONS

Area and harvest time for high-latitude kelp maricultures

Phytomining cultivated kelps from run-off areas?

Saccharina latissima

Ecosystem elemental cycles e.g. blue carbon

We found the biogenic element concentration, biochemistry and microbial community in *Saccharina latissima* to strongly respond to changes in run-off influences.
This relates both to present-day spatial differences and near-future temporal changes.

Get the publication

Bengtsson et al. (2010, 2011, 2012); Davies et al. (2003); Jaishankar et al. (2014); Zeraatkar et al. (2016).

_____

Title: Run-off impacts on Arctic kelp holobionts have strong implications on ecosystem functioning and bioeconomy

Running title: Run-off impacts on Arctic kelp holobionts

Author: Sarina Niedzwiedz[1*], Claudia E. Schmidt[2,3], Yunlan Yang[4], Bertille Burgunter-Delamare[5], Sebastian Andersen[6], Lars Hildebrandt[7], Daniel Pröfrock[7], Helmuth Thomas[2,3], Rui Zhang[4,8], Børge Damsgård[6], Kai Bischof[1]

***corresponding author**: sarina@uni-bremen.de

Affiliations: [1]Marine Botany, Faculty of Biology and Chemistry & MARUM, University of Bremen, 28359 Bremen, Germany.

[2]Institut für Chemie und Biologie des Meeres (ICBM), University of Oldenburg, 26111 Oldenburg, Germany.

[3]Helmholtz-Zentrum Hereon, Institute of Carbon Cycles, Department of Marine Carbon Cycles, 21502 Geesthacht, Germany.

[4]Institute for Advanced Study, Shenzhen University, 518052 Shenzhen, China.

[5]Matthias Schleiden Institute of Genetics, Bioinformatics and Molecular Botany, Friedrich Schiller University Jena, 07743 Jena, Germany.

[6]The University Centre of Svalbard (UNIS), 9171 Longyearbyen, Norway.

[7]Helmholtz-Zentrum Hereon, Institute of Coastal Environmental Chemistry, Department Inorganic Environmental Chemistry, 21502 Geesthacht, Germany.

[8]Southern Marine Science and Engineering Guangdong Laboratory, 519000 Zhuhai, China.

Abstract:

Kelps (Laminariales, Phaeophyceae) are foundation species along Arctic rocky shores, supporting a high secondary production. Currently, climate change induced glacial and terrestrial run-off is accelerating, changing water column parameters, e.g., dissolved concentrations of (harmful) element. We investigate the impact of run-off on Arctic kelps, as their responses have ecological and economic consequences.

We found the kelp *Saccharina latissima* to accumulate harmful elements (e.g., cadmium, mercury) originating from coastal run-off. As kelps are at the basis of the food web, this might lead to biomagnification, with potential consequences for high-latitude kelp maricultures. However, kelps might biomonitor environmental pollution or extract dissolved rare earth elements. We found the kelp's microbiome to significantly respond to run-off influence, being an indicator for kelp health, the holobionts nutritional value and elemental cycling. The accentuated responses of kelp holobionts to environmental variability implies high susceptibility of Arctic coastal ecosystems to future climate changes.

Keywords:

Introduction:

Kelps (Laminariales, Phaeophyceae) act as foundation species from temperate to polar rocky shores (1), governing ecosystem functioning, resilience and biodiversity (2). Kelps are important primary producers in coastal zones (2), supporting high secondary production, e.g., microbes, invertebrates, fish and mammals (3). However, kelps are sensitive to environmental changes, resulting in an alteration of their productivity and biomass production at local and global scales (4; 5). A change of kelp health has cascading ecological and economic consequences.

Global climate changes become especially evident in the Arctic, with temperatures increasing far beyond the global average rate (6; 7). Thereby, high Arctic coastlines have become habitable for cold-temperate kelps, such as *Saccharina latissima* (8–10) and an overall future range expansion of kelps to higher latitudes is expected (11–13). Rising temperatures also result in accelerated glacial melt, thawing permafrost and higher precipitation rates (14–16) leading to higher discharge of freshwater and terrestrial material into Arctic fjords (17). These run-off plumes alter physical water conditions. Temperature and salinity differences between the run-off and marine water masses stratify the fjord water column, establishing strong gradients (18). Increased concentrations of suspended particles result in a darkening of Arctic fjords in summer (19–21). Changes of physical water conditions affect benthic primary producers in the adjacent ecosystems, which resulted in a shift in the kelp forest community and a reduced depth distribution in an Arctic fjord system since 1996 (22).

Further, run-off alters the chemical properties of the water column, carrying nutrients, organic matter and littoral material into the fjord (23; 24) as well as a wide range of legacy pollutants stored during the last decades in the glacial ice (25). Increased dissolved element concentrations were shown in glacial run-off plumes in polar fjords (24), many of which act as micronutrients (26). Kelps were shown to have a high biosorption potential for ions from seawater (27). This results in high nutritional values of kelps due to the accumulation of bioactive compounds (28). However, increased concentrations of biologically harmful elements, such as dissolved mercury (dHg) were also detected in freshwater discharge (29) and fjord sediments (30). Kelps were shown to take up heavy metals (27; 31) intracellularly during their growth phase (32) or via cell wall incorporated alginates and fucoidan, which chelate heavy metals (27). The heavy metal ion uptake and accumulation are highly dependent on temperature, pH, dissolved metal concentration in the water column, presence of competing metal ions, and exposure time (reviewed by 32). A high mass fraction of biologically harmful metals (e.g., bCu, bPb) results in oxidative stress and could result in decreasing kelp performance, e.g., reduced growth rates (33).

Kelps are a hotspot for microscopic biodiversity (34). The kelp-associated microbial communities can serve as an indicator for kelps health, as it is largely dependent on host conditions, changing

when the kelp is stressed (35; 36). Further, the microbial communities depend on abiotic factors (37). Heterotrophic bacteria provide a crucial link in the food web, connecting kelp primary production with kelp consumers, by degrading released particulate organic matter (38; 39). Hence, environmental changes affecting the kelp holobiont might have consequences for the entire food web and ecosystem.

The aim of this *in-situ* study is to assess the impact of run-off on Arctic kelp holobionts functioning to draw conclusions on future Arctic coastal ecosystems and potential bioeconomic impacts. Therefore, we collected *S. latissima* sporophytes at the end of the run-off season in Billefjorden, Svalbard. We compared kelp samples that were influenced by glacial run-off (samples were collected with increasing distance to a sea-terminating glacier) or terrestrial run-off (samples were collected with increasing distance to a land-terminating glacier) to a control area (samples from relatively clear coastal water) (**Figure 1A**). We analysed the elemental composition of kelps, their biochemical response and associated microbial community and related these responses to physical and chemical water column mapping. The findings of our study have implications for present-day spatial as well as near-future temporal changes, and the work was guided by three hypotheses: I) We hypothesise that high concentrations of dissolved elements in run-off result in higher elemental mass fractions in kelps. II) As heavy metals, such as Cu and Pb, have been shown to lead to oxidative stress in algae (33), we expect high heavy metal mass fractions to correlate with higher antioxidant activities. III) We hypothesise that the kelp-associated microbial community will be influenced by different environmental and host conditions in the respective areas, resulting in altered microbial species composition.

We found kelps accumulating elements from run-off discharge, correlating with biochemical responses and microbial community changes within a few kilometres area, indicating a high spatial ecological variability. While samples from the glacial and terrestrial run-off areas were more similar to each other compared to the control area, differences between them relate to near-future changes in ecosystem functioning with glaciers retreating. High contents of biological harmful elements (e.g., *b*Hg, *b*Cd) in kelps at run-off dominated coastlines are likely to be bioavailable for the Arctic food web. Hence, harmful elements might biomagnify in higher trophic levels and be potentially passed on to humans. Changes in the kelp-associated microbial community indicated run-off to influence the holobionts health, their nutritional value, as well as changes in its elemental cycling. Concluding, we found kelps to be a potential biomonitor for the bioavailability of environmental metals and harmful elements in coastal ecosystems; the kelp-associated microbiome could serve as biomonitor for the kelp health status and the ecosystem services of the kelp holobiont.

_____

Results:

For overview reasons, all statistical results are displayed in **Table 1** (ANOVA) and are, therefore, not given in the text. Kelp parameters were analysed in response to sampling area (control area, glacial run-off area, terrestrial run-off area) and sampling station (A–I) (**Figure 1A**).

Table 1: **Statistical results of kelp responses**. Results of Analysis of Variance (ANOVA) to evaluate the effect of sampling area or station as single fixed effects. Significant results are marked in bold. DPS: De-epoxidation state of xanthophyll cycle pigments.

Parameter	Fixed effect	numDF	denDF	F value	P value
Elemental mass fraction in kelps					
Aluminium (Al)	Area	2	68	23.1	**<0.001**
	Station	8	61	10.6	**<0.001**
Iron (Fe)	Area	2	66	30.7	**<0.001**
	Station	8	61	9.1	**<0.001**
Manganese (Mn)	Area	2	67	20.6	**<0.001**
	Station	8	61	20.7	**<0.001**
Copper (Cu)	Area	2	69	13.2	**<0.001**
	Station	8	63	5.8	**<0.001**
Cobalt (Co)	Area	2	68	1.2	0.3
	Station	8	60	5.3	**<0.001**
Cadmium (Cd)	Area	2	69	5.6	**0.006**
	Station	8	63	2.9	**0.007**
Lead (Pb)	Area	2	68	16.1	**<0.001**
	Station	8	62	8.2	**<0.001**
Mercury (Hg)	Area	2	68	53.1	**<0.001**
	Station	8	61	28.8	**<0.001**
Biochemistry					
Chlorophyll *a*	Area	2	69	6.5	**0.002**
	Station	8	62	3.1	**0.006**
DPS	Area	2	68	14.5	**<0.001**
	Station	8	63	5.1	**<0.001**
Antioxidant activity	Area	2	69	8.5	**<0.001**
	Station	8	63	3.8	**0.001**
Biodiversity indices					
Shannon entropy	Area	2	64	7.0	**0.002**
	Station	8	57	5.4	**<0.001**
Pielou evenness	Area	2	63	15.5	**<0.001**
	Station	8	57	6.2	**<0.001**
Relative abundance of microbial taxa					
Bacteroidetes	Area	2	64	9.4	**<0.001**
	Station	8	58	5.77	**0.001**
Proteobacteria	Area	2	64	4.4	**0.02**
	Station	8	55	9.5	**<0.001**
Alphaproteo-bacteria	Area	2	64	0.07	0.93
	Station	8	56	4.82	**<0.001**
Gammaproteo-bacteria	Area	2	64	4.55	**0.01**
	Station	8	58	5.05	**<0.001**

Flavobacteria	Area	2	64	12.2	**<0.001**
	Station	8	58	6.8	**<0.001**
Tiotrichales	Area	2	62	18.2	**<0.001**
	Station	8	56	4.42	**<0.001**
Pirellulales	Area	2	61	17.3	**<0.001**
	Station	8	55	5.74	**<0.001**
Planctomycetes	Area	2	61	17.3	**<0.001**
	Station	8	55	5.74	**<0.001**
Saprospirales	Area	2	64	3.7	**0.03**
	Station	8	56	3.3	**0.003**
Rhodobacterales	Area	2	64	0.07	0.93
	Station	8	56	4.8	**<0.001**

Note: tested values are the means of replicates (Area: N=3; Station: N=6–9) numDF: numerator degrees of freedom. denDF: denominator degrees of freedom.

Abiotic parameters shown run-off influence

Water column mapping revealed area-specific differences in the underwater light climate (**Figure 1B**; PAR, K_d, turbidity), as well as in temperature and salinity (**Figure 1C**). The water column of the control area was not stratified. In the control area, we detected a comparably high photosynthetically available radiation (PAR) at 5 m water depth (42.2 ± 3.7 µmol photons m^{-2} s^{-1}), hence low light attenuation (K_d; 0.22 ± 0.01) as well as low turbidity values (0.5–1.6 NTU). Temperature ranges (6.3–6.7°C) were low. Highest salinities were measured in the control area ($S_A = 31.8$). In both glacial and terrestrial run-off area, light intensities at 5 m water depth were lower and K_d and turbidity higher than in the control area (Glacial run-off area: 35.4 ± 5.6 µmol photons m^{-2} s^{-1}, 0.30 ± 0.05; 1.0–3.6 NTU; Terrestrial run-off area: 30.7 ± 2.8 µmol photons m^{-2} s^{-1}, 0.25 ± 0.03; 0.9–3.0 NTU). Further, the water column was markedly stratified. Temperature and salinity values were lower towards the surface ($\sim$0–3 m), compared to 10 m water depth. Temperature amplitudes were highest in the glacier run-off area (6.0–6.8°C). Warmest temperatures were measured in the terrestrial run-off area (7.1°C). Salinity differences resembled temperature patterns, with lowest salinities close to the surface, increasing with increasing water depth. Lowest salinities were measured in the terrestrial run-off area ($S_A = 28.9$).
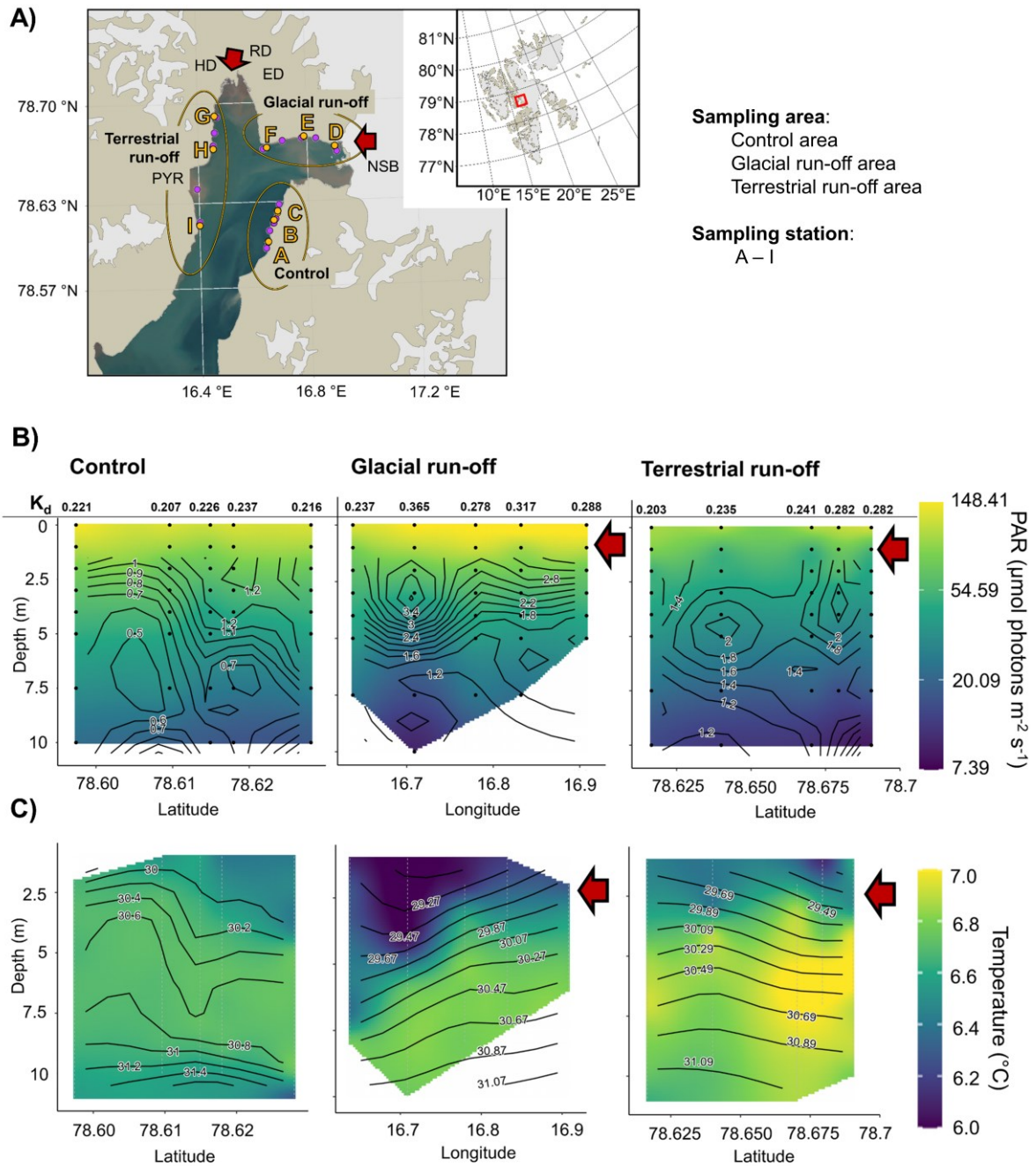
Figure 1: **Abiotic parameters at the study site in Billefjorden, Svalbard. A**) Map of Billefjorden, Svalbard. Right upper corner: overview map of Svalbard; red rectangle: Billefjorden. A–C: Control area. D–F: Glacial run-off area; NSB: Nordenskjölbreen. G–I: Terrestrial run-off area; ED: Ebbadalen; HD: Hørbyedalen; RD: Ragnardalen; PYR: Pyramiden (uninhabited miner's settlement). Yellow points, A–I: Position of kelp sampling. Purple points: Positions of CTD/light measurements. Red arrows: direction of run-off inflow. Map: RStudio, PlotSvalbard (100). Satellite image fjord water: toposvalbard.npolar.no; 06.02.2023. **B, C)** Section plots of abiotic conditions in sampling areas in Billefjorden (control, glacial run-off, terrestrial run-off) from 0–10 m depth on 30th August 2022. Red arrow: direction of run-off inflow to the run-off areas. Note the different x-axis. Black dots (**B**) / white vertical lines (**C**): actual light/CTD measurements in water column. White areas within section plots: insufficient data to support model. **B**) Colour gradient: photosynthetically available radiation (PAR; μmol photons m^{-2} s^{-1}; scale as log to highlight low PAR intensities). Contour: turbidity (NTU). Numbers above depth transects: light attenuation coefficient (K_d). **C**) Colour gradient: temperature (°C). Contour: salinity (S_A).

_____

Kelp elemental composition changes with run-off intensity

Dissolved elements in the water column are marked as *d*element (**Supplementary Figure 1**), while the biological elements in kelps are noted as *b*element (**Supplementary Figure 2**). Dissolved element concentrations at 5 m water depth correlated positively with *b*element mass fraction in kelps. This correlation was significant for Mn (**Figure 2A**). Over all sampling stations, the macrominerals *b*K > *b*Na > *b*Ca > *b*Mg were the most abundant *b*elements with mass fractions between ~5–80 mg g_{DW}^{-1} (**Figure 2B**). Rare earth elements (*b*La–*b*Lu) showed higher mass fractions in kelps that were influenced by run-off inflow, compared to the control area. The ratio between biological and dissolved rare earth elements ranged between 920 in Ho and 48500 in Ce (**Figure 2C**). The mean cumulative mass fraction of all rare earth elements ranged between 1.06–4.63 µg g_{DW}^{-1}.

The mass fractions of *b*Al, *b*Fe, *b*Mn, *b*Cu, *b*Co, *b*Cd, *b*Pb and *b*Hg (µg g_{DW}^{-1}) can be seen in **Figure 2D**. Except for *b*Co, all element mass fractions were significantly affected by sampling area. For each area, distinct overall patterns were observed: Control area: the mean mass fraction of all *b*elements was lowest. Except for *b*Co, there are no significant mass fraction differences within the area, independent of the sampling station. Glacial run-off area: The *b*elemental mass fraction at sampling station E was significantly lower compared to D or F for all elements except *b*Cd and *b*Hg. Except for *b*Al, *b*Mn and *b*Cd, there was a trend of decreasing element mass fraction with increasing distance to the meltwater run-off inflow. Terrestrial run-off area: compared to the other areas, mean element mass fractions were highest, except for *b*Fe, *b*Cd and *b*Pb. Within the area, elemental mass fractions were significantly decreasing with increasing distance to the meltwater run-off inflow, except for *b*Mn and *b*Cd. The *b*Hg mass fraction in the terrestrial run-off area had the highest relative difference to the other areas, being ~60 % higher compared to the glacial run-off area and ~72 % higher compared to the control area.
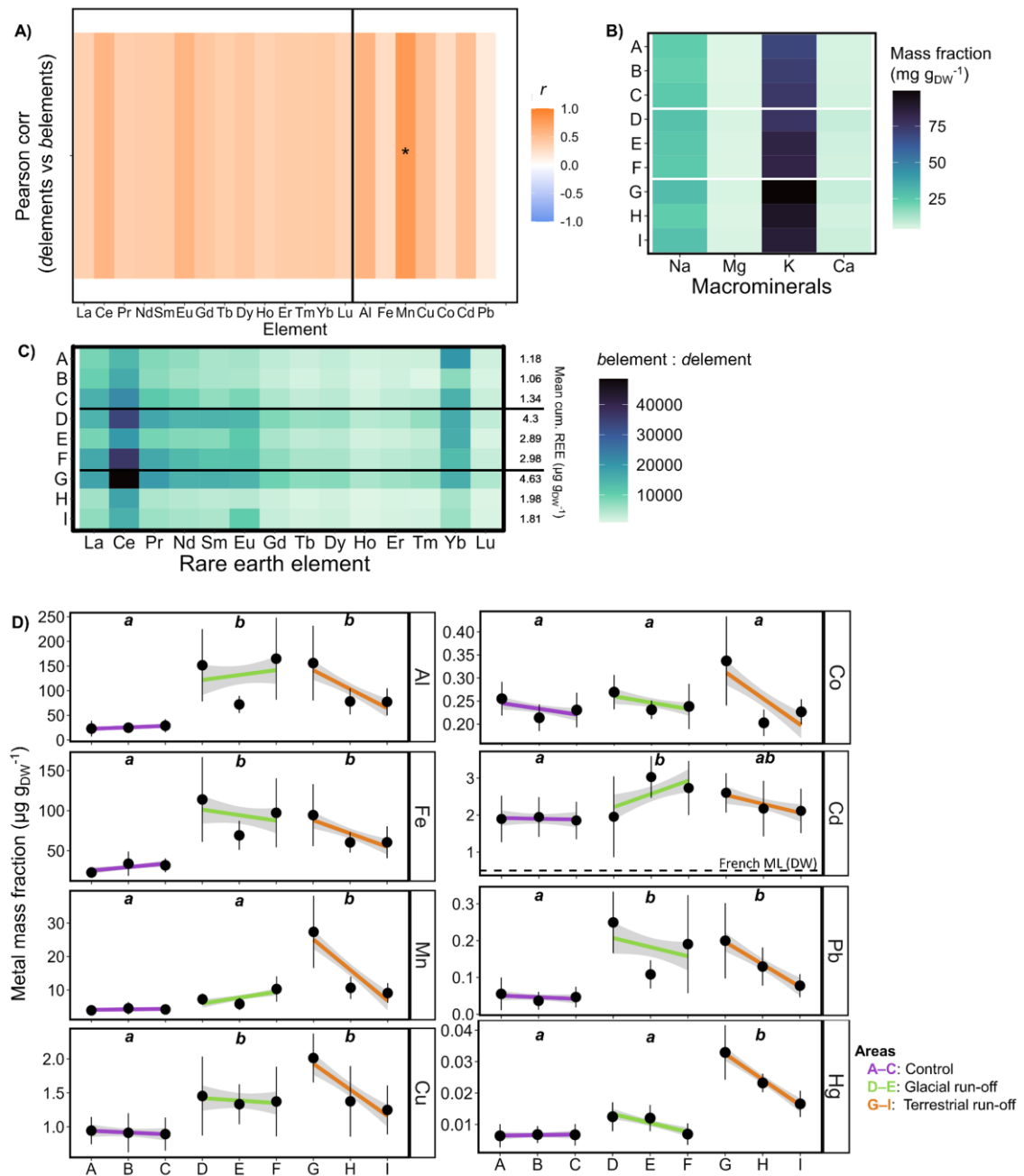
Figure 2: **Element mass fraction in kelps**. The elemental mass fraction in *S. latissima* was analysed in response to control (purple, ABC), glacial run-off (green, DEF) and terrestrial run-off area (orange, GHI) in Billefjorden (*N*=6-9 per sampling station). DEF and GHI are ordered with increasing distance to run-off inflow (see Figure 1A; distance between sampling stations A–I on x-axis are not to scale). **A)** Pearson correlation coefficient *r* between dissolved element concentrations in the water column (5 m depth) and element mass fractions in kelps. Asterisk: Significant correlation (* *P*<0.05). **B)** *b*Element mass fraction of macrominerals (mg g$_{DW}$$^{-1}$) in kelps. **C)** Ratio between biological (μg g$_{DW}$$^{-1}$) and dissolved (μg mL^{-1}) rare earth elements (REE; 88). Right side of the plot: mean cumulative REEs per sampling station (μg g$_{DW}$$^{-1}$). **D)** *b*Metal mass fraction (μg g$_{DW}$$^{-1}$). Linear trend line: visualisation of elemental mass fraction (μg g$_{DW}$$^{-1}$) gradient in sampling area. Grey area: 95 % confidence interval. Different letters within plots: significances between sampling area. Cd subplot: Maximum levels (ML) after Banach et al. (79), based on French recommendations (105).

Kelp biochemical composition changes with run-off intensity

The chlorophyll *a* content was significantly affected by sampling area and station (**Figure 3A**). Mean kelp chlorophyll *a* of the sampling stations ranged between 232–431 µg g_{DW}^{-1}. The chlorophyll *a* content was significantly higher in the glacial run-off area (384±173 µg g_{DW}^{-1}) compared to the control (258±74 µg g_{DW}^{-1}) and terrestrial run-off area (282±121 µg g_{DW}^{-1}). Within the areas, no overall pattern could be detected.

The de-epoxidation state of xanthophyll cycle pigments (DPS) varied significantly among all areas (**Figure 3B**). DPS was highest in the terrestrial run-off area (0.20±0.07) and lowest in the glacial run-off area (0.10±0.04). Within the glacial run-off area, DPS significantly decreased with increasing distance to the run-off inflow. Within the terrestrial run-off area, this was seen as a trend.

The antioxidant activity (**Figure 3C**) differed significantly between areas, being higher in the control area (204±52 TE mM 100 mg_{DW}^{-1}) than in the glacial (181±44 TE mM 100 mg_{DW}^{-1}) and the terrestrial run-off area (152±36 TE mM 100 mg_{DW}^{-1}). We detected no significant differences within the run-off areas.
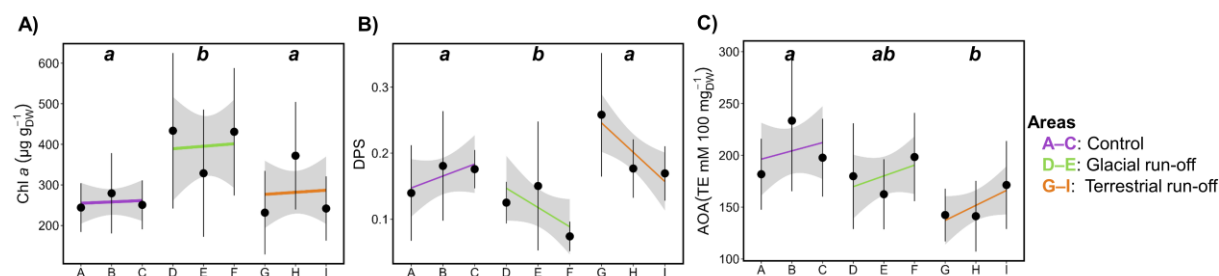
Figure 3: **Biochemical response of kelps**. The kelps biochemical response was analysed in response to control (purple, ABC), glacial run-off (green, DEF) and terrestrial run-off area (orange, GHI) in Billefjorden (*N*=6-9 per sampling station). DEF and GHI are ordered with increasing distance to run-off inflow (see Figure 1A; distance between sampling stations A–I on x-axis are not to scale). Different letters within plots: significances between each area. Linear trend line: visualisation of biochemical composition gradient in sampling area. Grey area: 95 % confidence interval. **A)** Chlorophyll *a* (µg g_{DW}^{-1}). **B)** DPS: De-epoxidation state of xanthophyll cycle pigments. **C)** AOA: Antioxidant activity (TE mM 100 mg_{DW}^{-1}).

Kelp-associated microbial community changes with run-off intensity

Across all samples, we identified 4457 Amplicon Sequence Variants (ASVs). Both Shannon entropy and Pielou evenness were significantly affected by sampling area, being lower in the control area compared to the glacial and terrestrial run-off area (**Figure 4A, B**).

Kelp-associated microbial communities showed distinct clustering between areas (**Figure 4C**). All microbial taxa were significantly affected by sampling area and station (*P*<0.05), except the class

_____

Alphaproteobacteria and the order Rhodobacterales. Most significances between sampling stations were across areas, hence, showing no clear patterns within areas. All kelp-associated microbial communities were dominated by Proteobacteria (especially Gammaproteobacteria) and Bacteriodetes (~58 %; **Figure 4D**). Their abundance was highest in the control area, compared to the glacial and terrestrial run-off area. The same pattern was observed for Flavobacteria (Control: 28.2±12.6 %; Glacial run-off: 14.4±9.7 %; Terrestrial run-off: 16.2±7.8 %) and Tiotrichales (Control: 15.1±10.9 %; Glacial run-off: 4.8±4 %; Terrestrial run-off: 3.1±3.5 %). Planctomycetes (Control: 4.4±2.9 %; Glacial run-off: 12.9±4.9 %; Terrestrial run-off: 10.7±6.1 %) had a lower abundance in the control area compared to the run-off dominated areas. The Saprospirae differed significantly between glacial (8.1±6.7 %) and terrestrial run-off area (4.2±4.1 %), both not differing significantly compared to the control area (5.5±3.3 %). The Rhodobacterales showed no spatial variation in their abundance. The relative abundance of the free-living microbial community is displayed in **Supplementary Figure 3**.
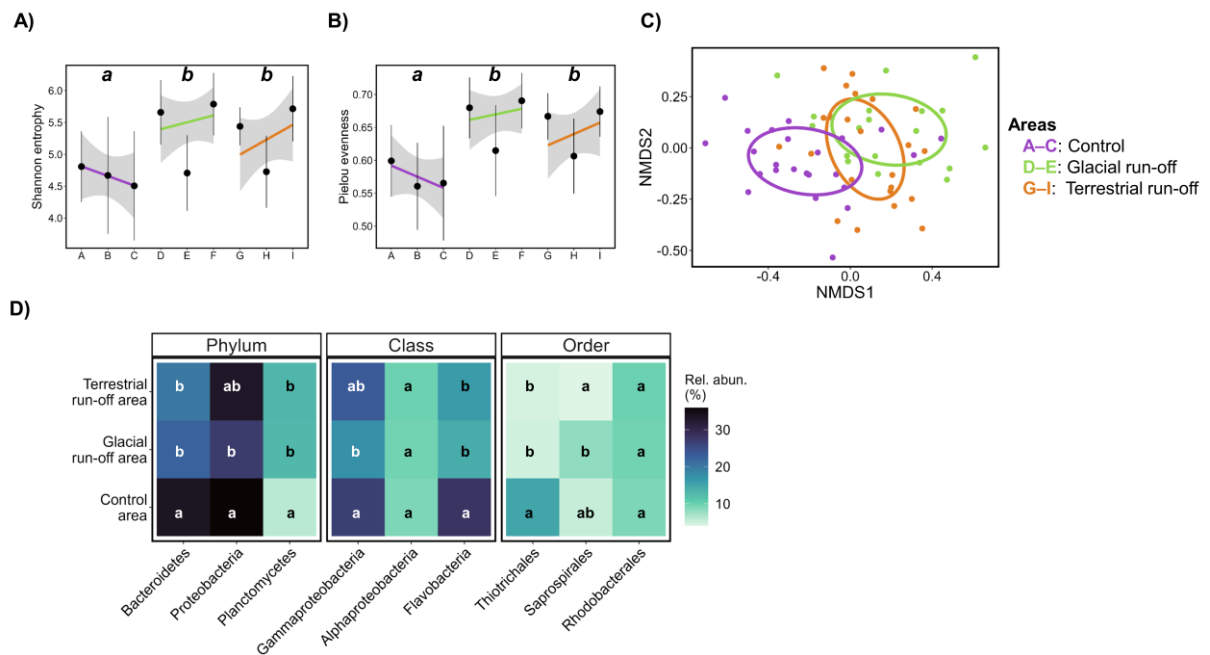
Figure 4: **Kelp-associated microbial community**. The microbial community was analysed in response to control (purple, ABC), glacial run-off (green, DEF) and terrestrial run-off area (orange, GHI) in Billefjorden (*N*=6-9 per sampling station). DEF and GHI are ordered with increasing distance to run-off inflow (Figure 1A; distance between sampling stations A–I on x-axis are not to scale). Different letters within plots: significances between sampling areas. **A, B)** Linear trend line: visualisation of diversity indices in sampling areas. Grey area: 95 % confidence interval. **A)** Shannon diversity index. **B)** Pielou evenness. **C)** Non-metric multidimensional scaling (nMDS) ordinations showing the relative abundance of kelp-associated microbial groups in each area based on Bray-Curtis dissimilarities (stress value ≤ 0.05). **D)** Heatmap showing the mean relative abundance of kelp-associated microbial community taxa (≥ 1%) in each sampling area.

_____

High ecological variability between run-off systems

Kelps significantly differed in their elemental composition, biochemical response, and associated microbial community (**Figure 5**). Their clustering coincided with spatial changes of run-off intensity and associated water parameters (e.g., temperature, light availability, dissolved element concentrations). Responses of kelps from glacial run-off and terrestrial run-off areas were more similar to each other than to the control area. Metal mass fractions in kelps correlated positively with each other and negatively with the relative abundance of microbial taxa, with many of the correlations being significant. The antioxidant activity correlated negatively with metal mass fraction in kelps, which was significant for Hg and Mn.
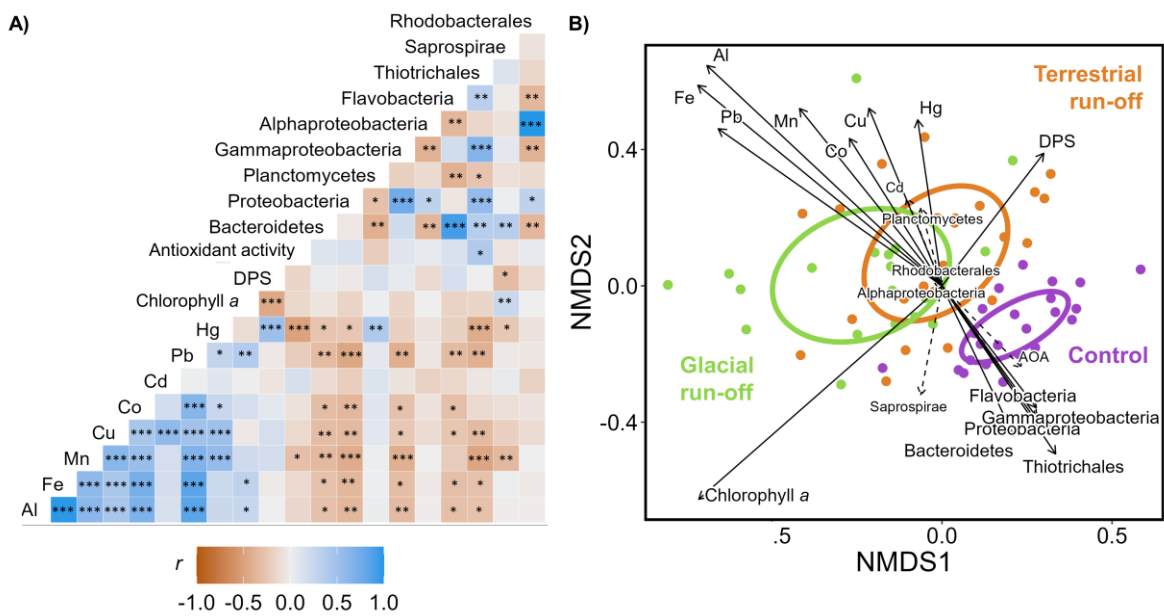
Figure 5: **Correlations between response parameters. A)** Linear dependency between kelp response parameters. Colour scale: Pearson correlation co-efficient (*r*). Asterisk: significance of correlation (*: *P*<0.05; **: *P*<0.01; ***: *P*<0.001. **B)** Non-metric multidimensional scaling (nMDS) ordinations showing kelp responses based on Bray-Curtis dissimilarities. AOA: Antioxidant activity. Significant vectors: solid arrow, larger labelling (stress value ≤ 0.01). Non-significant vectors: dashed arrow, smaller labelling.

Discussion:

In the Arctic, global climate change causes glaciers and permafrost to melt, and increases precipitation rates (14–16), resulting in extensive run-off plumes dominating many coastal areas (20). Run-off plume differences relate both to present-day spatial variations, with the run-off plume influence being highest in the inner fjord region (18), as well as near-future temporal changes, with glaciers retreating (40; 41). Run-off plumes were shown to change the water column physical parameters and carry nutrients, but also be the origin of harmful elements, such as heavy metals (23; 42; 43). Along Arctic rocky coastlines, kelp holobionts function as foundation species, providing the basis for many associated species. If and how kelp holobiont health and functioning changes with variation in run-off is largely unknown, even though their responses can have cascading consequences for the entire ecosystem (38; 39).

We found the element content, biochemistry and associated microbial community of *Saccharina latissima* to strongly respond to changes in run-off influence (clear water vs. glacial and terrestrial run-off), implying high ecological variability between run-off systems (**Figure 5, 6**). We found the dissolved element concentration in the water column to correlate positively with element mass fractions in *S. latissima* specimens, indicating run-off origin, hence, supporting **Hypothesis I**. The element mass fractions in kelps correlated negatively with the antioxidant activity, contradicting **Hypothesis II**. This might be due to the degradation of antioxidants due to chronic heavy metal exposure (44). We detected significantly different abundances of many kelp-associated microbial taxa, correlating negatively with *b*element mass fraction. Altered relative abundances of the microbial community relate to changes in nutritional value of kelps and the ecosystems elemental, e.g., carbon, cycling (**Hypothesis III**).

In this interdisciplinary approach, we highlight the complexity of ecological interactions, presenting new connections and implications of run-off influence on Arctic coastal ecosystem functioning. In the following, we discuss the possible ecological consequences and present potential bio-economical perspectives of our findings. As run-off is predicted to accelerate in the future, the run-off induced change in Arctic coastal ecosystems is likely to intensify.
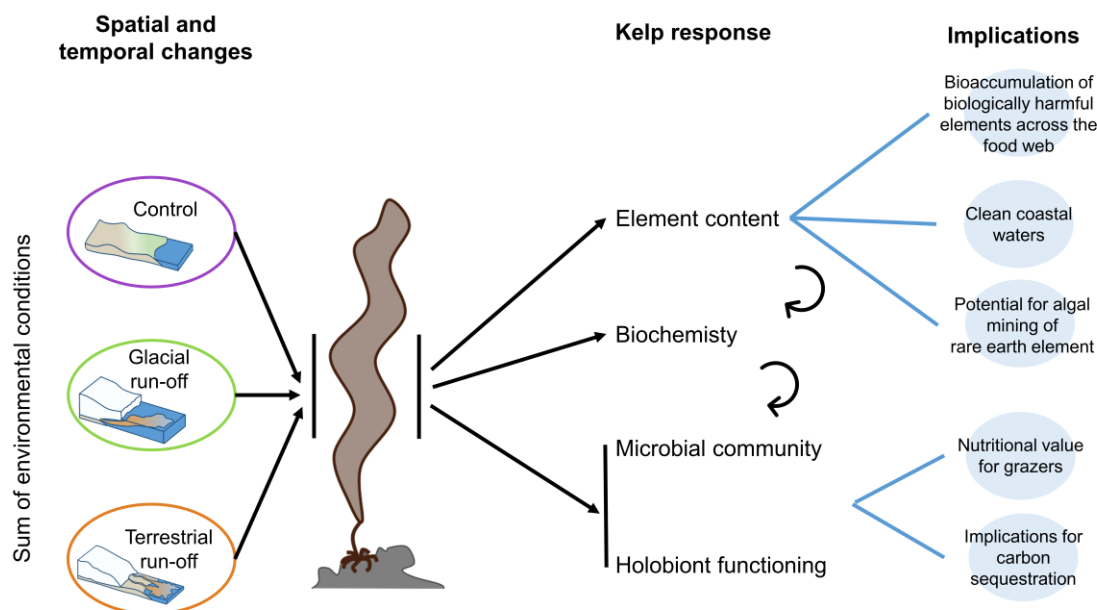
Figure 6: **Run-off influence on Arctic coastal ecosystem functioning and bioeconomy.** The target areas of this study (control area, glacial run-off, terrestrial run-off) relate both to present-day spatial differences, as well as near-future temporal changes, when glaciers retreat. Responding to the sum of environmental conditions in each area (temperature, salinity, light availability, dissolved element concentration), we found significant changes in the kelp element content, biochemistry, and associated microbial community. While we cannot prove the causal dependency between the response parameters (but only correlations), their individual changes pose extensive consequences for high trophic levels, the ecosystem element cycling, but also bioeconomic potential.

Ecosystem functioning

By mapping the environmental conditions of the water column within each area, we validated run-off presence in the glacial and terrestrial run-off area, detecting a stratified water column. In contrast, the water column in the control area was well-mixed. The generally small temperature and salinity amplitudes in all areas (**Figure 1**) can be attributed to the sampling campaign being conducted in late August, hence, at the end of the run-off season (45) with weak run-off plumes being present. However, the sampled kelps were exposed to the environmental conditions of their respective area during the entire run-off season. Hence, we argue that our chosen sampling areas are suitable to draw general conclusions about run-off effects on Arctic kelp holobiont functioning.

Being exposed to different environmental conditions such as light, temperature, salinity and dissolved element concentrations, we found *S. latissima* to strongly respond to the environmental conditions at the different sampling areas (**Figure 5B**) (often even sampling stations). This confirms the conclusion of Diehl et al. (46), reviewing that *S. latissima* is highly plastic in its environmental response. The significant variations across all measured kelp responses implies high ecological variability between run-off systems.

Seaweeds have long been known for their ability to accumulate ions from the surrounding water column (47). We confirmed this by showing that the mass fraction of all elements in kelps correlated positively with dissolved elements in the water column (**Figure 2A**). The positive correlation indicates that the *b*elements were accumulated from run-off discharge. The correlation was only significant for Mn. We attribute this to the high variability of run-off plumes and the dissolved element concentrations being only a point measurement of the whole run-off season. The accumulation of ions makes seaweeds good food sources for macrominerals, e.g., *b*Na, *b*Mg, *b*K and *b*Ca, which we detected to be the most abundant *b*elements in kelps (31; 48) (**Figure 2B**). Further, we found higher metal mass fractions with higher run-off influence, such as *b*Al, *b*Fe, *b*Mn, *b*Cu, *b*Co (**Figure 2D**). Many metals have physiological roles in algae, e.g., are used to stabilise protein structures, catalyse enzymatic reactions or facilitate electron transport (49). Twining & Baines (26) review the requirements of trace metals for marine phytoplankton, e.g., describing *b*Fe and *b*Mn to be essential in the photosynthetic electron transport chain. Overall, the concentration of these essential (trace) metals in the ocean is low and can even limit primary production (50). As Arctic run-off plumes are characterised by increased concentrations of trace metals (11; 29), these habitats might be attractive for algae. However, we also detected harmful elements, such as *b*Cd and *b*Pb in the run-off influenced kelps. Thereby, the toxicity of metals seems to be related to the production of reactive oxygen species and an unbalanced cellular redox status (51). Generally, seaweeds are able to accumulate a certain amount of heavy metals without any toxic effect, as their polysaccharides chelate them (47). Nevertheless, negative effects of heavy metals on their morphology, growth, or photosynthetic and metabolic processes have been described. Cd, Pb or Hg can substitute essential trace elements in proteins or enzymes (52), and we found them in significantly higher mass fraction in the run-off influenced kelps compared to the control area. In freshwater green algae, Al was described to lead to chloroses, necrosis and tissue weakening (53). The interactive stress of Cu and Cd treatments resulted in overall reduced growth in *Macrocystis pyrifera* (54). Kumar et al. (55) described cascading antioxidant responses to mitigate Cd toxicity in the green alga *Ulva lactuca*. Ahamad & Shuhanija (56) reported severe reductions of the maximum quantum yield of photosystem II and membrane disruption as response of a red alga to an increased Hg mass fraction. Costa et al. (33) classified Cu and Pb as stress factors for *Sargassum cymosum*, becoming evident in reduced growth rates, an increase in phenolic compounds acting as antioxidants, and inhibition of the electron transport rate, despite higher chlorophyll *a* content. In this study, the chlorophyll *a* content was significantly higher in the glacial run-off area (**Figure 3A**); however, this might also be due to other abiotic parameters, e.g., reduced light availability in run-off plumes (**Figure 1B**; 57). Further, we found the antioxidant activity to be significantly lower in the run-off areas (**Figure 3C**). This might either be due to reduced light availability in the run-off plumes, leading to less oxidative stress (58), or chronic

_____

heavy metal exposure, resulting in oxidative degradation of antioxidants (44). We conclude that the sum of abiotic factors in the study areas conditioned kelps. The environmental differences and/or altered host conditions might be the reason for changes in the relative abundance of many microbial taxa (35).

Generally, the macroalgal surface is an attractive substrate for heterotrophic microbial communities, as macroalgae generate oxygen during photosynthesis and further excrete carbon-rich mucus (59). Marzinelli et al. (35) described the microbial community from stressed *Ecklonia radiata* individuals to be more similar to each other than to unstressed individuals, which was also confirmed by Burgunter-Delamare et al. (36) for *S. latissima*. We also found the relative abundance of the kelp-associated microbial taxa to depend strongly on the area the kelps were sampled in, with the microbial communities from the two run-off areas clustering closer compared to the control area (**Figure 4C**). Thereby, the Shannon and Pielou indices (**Figure 4A, B**) were lower in the run-off areas compared to the control area, indicating a reduced species richness and evenness. Cundell et al. (60) stated that the kelp-associated microbial community is not directly related to the free-living microbial community in the water column. We also found distinct differences between the kelp-associated and free-living microbial community, e.g., the absence of Planctomycetes in the water column (**Supplementary Figure 3**). Bacteroides, Alphaproteobacteria, and Gammaproteobacteria are considered to be among the most common taxa for macroalgae (59; 61), which we also confirmed in this study. Rhodobacterales have been described as early colonizers of marine surfaces, with the ability to fix nitrogen (62). We detected no significant difference in Rhodobacterales between sampling areas. As we used the kelp surface above the meristem for epiphytic microbial analyses, we assume a later stage of microbial succession on the kelp tissue. High abundances of Planctomycetes have been described to be associated with *Laminaria hyperborea* and *Saccharina latissima* (36; 61; 63). Planctomycetes have a high number of sulfatases, genes that are described to degrade sulphated polysaccharides (64). Saprospiraceae were also described to play an important role in metabolising complex carbon resources (65). We detected them to have highest abundances in the glacial run-off area.

While this study can neither untangle which (interacting) environmental parameter(s) triggered which kelp response, nor prove a causal link between kelp responses, but only correlations, our data clearly show high variability in kelp holobiont composition and functioning between run-off systems. This highlights the complexity of kelp responses to Arctic climate change.

Environmental implications

Being primary producers, kelps serve as food sources for many associated species along Arctic coastlines. As also shown in this study, Pinto et al. (51) stated that algae accumulate heavy metals at chronic exposure. As a consequence, they found the algae pass on heavy metals to higher trophic

levels, indicating bioavailability. The ingestion of metal contaminated kelps was shown to have negative impacts on the fitness of grazers, such as sea urchins (i.e., growth, fertility, development; 66) and might result in bioaccumulation and biomagnification of heavy metals across the Arctic food web, which could already be shown for bHg (67; 68). As we found the bHg mass fractions in the terrestrial run-off area to be 60–70 % higher compared to the other areas, the biomagnification of bHg across the food web might be increased when glaciers retreat on land. Altered pigment composition and consequently photosynthetic output can alter the kelps carbon metabolism (69). Differences in the kelps carbon to nitrogen ratio change the food quality of kelps (70). Further, altered relative abundances of microbial taxa being related to metabolising complex carbohydrates might have consequences for the food web. Brown algae are excreting sulphated polysaccharides as mucus, e.g., fucoidan (71), which are important for micrograzers and filter-feeders. However, due to its complex structure, fucoidan has been described to be difficult to degrade and be stable over centuries in sediments (72). Hence, Buck-Wiese et al. (72) have proposed fucoidan to contribute an underestimated proportion of kelp related blue carbon. Planctomycetes use fucoidan as a carbon source (63). Due to their ability to break down complex sugars, they serve as a crucial link in the food web, contributing to the nutritional value of kelps (38). We found Planctomycetes to have a significantly higher abundance in run-off dominated areas compared to the control area. This indicates a higher nutritional value of kelps; however, it might alter the ecosystem elemental cycling and eventually decrease kelp carbon sequestration.

Being at the basis of the food web and responding strongly to dissolved elements, macroalgae have long been proposed as biomonitors for the bioavailability of heavy metals. Commonly used macroalgae for bioindication are, for example Ulva, Porphyra, and Fucus (73). Biomonitors offer a direct, time-integrated proxy for the bioavailability of heavy metals in its environment. Our study shows a high potential to use *S. latissima* as passive biomonitoring organism for heavy metals, being a sedentary and cosmopolitan species that is easy to taxonomically identify (46). Thereby, age-related exposure time of different phylloid parts have to be considered. While the use of bioindicators poses some risk of under- or overestimating the bioavailability of certain elements due to biological, specific selection, a relative comparison between sites can be performed, as shown by our study or Kim et al. (74), using *S. latissima* to biomonitor heavy metals in the New York region, USA.

To assess the health status of kelps, Burgunter-Delamare et al. (36) propose the development of a kelp's microbiome as a bioindicator. They found distinct differences between healthy and diseased *S. latissima* on amplicon sequence variant (ASV) level. We confirm the potential of using altered microbial communities to resolve environmental influences. While kelp individuals from all sampling stations looked healthy, showing no external sign of physiological stress like

_____

extensive areas of degradation, the associated microbial community responded to the sum of abiotic factors and changes in host conditions. In this context, we emphasise the necessity to conduct studies assessing kelp holobiont functioning in ecological studies. It has long been suggested to study holobionts as one unit, as the microbiome shapes the host's development, morphology, fitness and physiology (reviewed by 75). In this study, we found that altered relative abundances of microbial taxa has consequences for the functional profile of the kelp-associated microbial community, likely responding to host conditions in the respective sampling areas. Higher abundances of certain microbial strains (e.g., Planctomycetes) might also alter the ecosystem services of kelps.

Bio-economical perspectives

The high biosorption potential of kelps holds both risks and potentials for high-latitude bio-economical perspectives. Thereby, further studies have to be conducted to assess the general and local feasibility and ecological consequences of these bioeconomic perspectives. The following discussion is, therefore, neither a risk assessment nor does it provide (policy-based) recommendations for management. However, we specifically advise against the harvest of wild kelp populations, given their crucial ecological role.

In the near future, over 2 billion people are expected to face food insecurity due to climatic and anthropogenic changes (76). Seaweeds have the possibility to increase food yields (76). As high-latitude fjords become tolerable for temperate kelp species with ongoing climate change, seaweeds for human consumption have been discussed to be a sustainable livelihood possibility (31). Thereby, their biosorption potential of heavy metals has to be considered. Currently, European Union legislation concerning heavy metal maximum levels in kelps is limited, with an exception of France (77). Kreissig et al. (31) evaluated the trace metal content of different seaweed groups in Greenland. Even though they found mass fractions of I and Cd to exceed the stricter French regulations, they classified Arctic kelps as promising food source. Shaughnessy et al. (78) found Cd and As levels in S. latissima to reach critical levels for consumption. While we also found the Cd mass fractions of *S. latissima* to exceed the French regulations of 0.5 µg g_{DW}^{-1} in all samples, levels for Pb, Hg, Mn, and Fe were below maximum levels (79). Thereby, the significant differences in kelp metal content within a small area (**Figure 1A, 2D**) are noteworthy and have to be considered regarding the location to implement high-latitude maricultures and the evaluation of the best suited harvest time.

While the biosorption of heavy metals poses a possible risk for food consumption, the cultivation of *S. latissima* in areas with high heavy metal load may serve as biomitigation measure, extracting heavy metals from the water column (32). Costa et al. (80) highlighted that competition with different ions was minor in macroalgae. Hence, they offer an ecologically safe, cheap, and more

efficient method to decontaminate wastewater (32). We argue that harvesting cultivated *S. latissima* in Arctic fjords being dominated by run-off discharge might be a possibility to reduce biologically harmful element biomagnification (e.g., *b*Hg) across the Arctic food web. Further, harvesting cultivated kelps in fjords with high run-off and metal load might pose an eco-friendly method for rare earth element mining (algal mining; 81). We found that rare earth element content (*b*La–*b*Lu) responded strongly to sampling station, showing the ratio between biological and dissolved element content to be in the magnitude of 10^4 (**Figure 2C**). It has to be considered that this ratio depicts a momentary condition during the sampling time, as dissolved element concentrations in run-off are highly variable (23). Measuring mean cumulative rare earth element mass fraction, a maximum of 4.3 mg kg_{DW}^{-1} was reached. The possibility of phytomining rare earth elements was experimentally tested (e.g., 33; 82) in several macroalgal species, who highlighted the capabilities of macroalgae as universal biosorbent for rare earth elements. All studies recorded a high species dependency of the biosorption potential.

_____

Methods:

Experimental design

This study was conducted using *in-situ* samples of the kelp *Saccharina latissima* from Billefjorden. Billefjorden is located on the west coast of Spitsbergen at 78°N. The region between Brucebyen and Kapp Ekholm (**Figure 1**; A–C) is mostly characterised by relatively clear coastal water. The Nordenskjölbreen glacier (NSB) is terminating into Adolfbukta, discharging glacial run-off (**Figure 1**; D–F) (83). Petuniabukta (northernmost bay) is characterised by terrestrial run-off gathered by Hørbyedalen, Ragnardalen and Ebbadalen (**Figure 1**; G–I) (84).

Water column mapping was conducted during mid-day on 30th August 2023. We measured five stations (0–10 m depth; **Figure 1**; purple points) within each area, in proximity to, and in between, kelp sampling stations (**Figure 1**; yellow points).

Kelp samples were collected between the 22–30 August 2022. In each area, similar-sized sporophytes of *S. latissima* were sampled at three sampling stations with a plant rake (Plant rake 19.000, acc. to Sigurd Olsen, KC Denmark, Silkeborg, Denmark) at 5±2 m water depth. A schematic overview of the kelp and water sample preparation in the lab is provided in **Supplementary Figure 4** and **5**.

Physical water parameters

We measured spectrally downwelling irradiance (RAMSES-ACC-UV/VIS radiometer, TriOS Optical Sensor, Oldenburg, Germany) from 400–700 nm in water depths from 0–10 m (alternative calibration). The irradiance of each wavelength was measured. Conversion from mW m^{-2} nm^{-1} to µmol photons m^{-2} s^{-1} and PAR integration were performed after Niedzwiedz & Bischof (21). The light attenuation coefficient (K_d) was calculated for the PAR after Hanelt et al. (85), between the surface and 5 m water depth.

CTD profiles were measured with a SWiFT CTDplus Turbidity (Valeport, St Peters Quay, United Kingdom). On each CTD profile, we measured temperature (°C), salinity, and turbidity (NTU). Outliers were removed from the raw data. Trimmed data were smoothed by the median for each full meter.

Elemental composition

A detailed description of all preparatory work and instrument settings are provided as supporting information. Limits of detection (LODs) and limits of quantification (LOQs) were calculated according to DIN 32645:2008-11 based on method blanks, with LOD defined as 3×standard deviation (SD) and LOQ as 10×SD.

Water samples for *d*element concentration were taken along with the kelp samples from 5 m depth (**Figure 1A**, yellow points), with a trace metal free Niskin bottle (KC Denmark, Silkeborg,

Denmark). Four technical replicates of water samples were filtered (DigiFILTER polytetrafluoroethylene (PTFE) membrane, 0.45 µm pore size, PerkinElmer; Waltham, USA) and stabilised using 100 µL concentrated HNO_3. *d*Elements were measured by using a seaFAST SP2 system (Elemental Scientific; Omaha, USA) coupled online to a triple quadrupole ICP-MS/MS system (Agilent 8900, Agilent Technologies; Tokyo, Japan). Analytes were preconcentrated on two columns filled with Nobias chelate-PA1 resin (HITACHI High-Tech Fielding Corporation; Tokyo, Japan) buffered by 4 mol L^{-1} ammonia acetate buffer (pH = 6.0 ± 0.2) and eluted with 1.5 mol L^{-1} HNO_3. To correct for instrumental drift, a 1 µg L^{-1} Niob (Nb) solution was used as an internal standard. Certified reference material AQUA-1, SLEW-4 and NASS-7 (National Research Council Canada; Ottawa, Canada) were used for method validation (recovery rates; LOD; LOQ: **Supplementary Table 1**).

Kelp material (~10 cm wide stripe above meristem) for *b*element analyses, was rinsed with ultrapure water and freeze-dried, before powdering and homogenising with a ball mill (Agate; Planeten Kugelmühle PM400, Retsch; Düsseldorf, Germany). Of each sample, 100 mg of three technical replicates were weighed into 55 mL TFM (modified PTFE) digestion vessels. For digestion, 0.1 mL HBF_4, 5 mL HNO_3, 2 mL HCl and 1 mL H_2O_2 were added (adapted from 86) and TFM vessels were placed in a closed-vessel microwave-assisted digestion system (Mars 6, CEM Corporation; Matthews, USA). The microwave was set to reach a maximum of 200°C after a suitable and efficient temperature ramping (**Supplementary Table 2**). The sample digests were quantitatively transferred into 50 mL DigiTubes and diluted to 50 mL with ultrapure water. Along with each batch, two blank digestion vessels containing only reagents were processed to monitor procedural contaminations and carry-over effects. For method validation, CRM NIST-3232 (Kelp powder *Thallus laminariae*, National Institute of Standards and Technology, Gaithersburg, USA) was digested under the same conditions (recovery rates; LOD; LOQ: **Supplementary Table 3**). The digested samples were measured with a triple quadrupole ICP-MS/MS system (Agilent 8800, Agilent Technologies; Tokyo, Japan) coupled to an ESI SC-4DX FAST autosampler (Elemental Scientific; Omaha, USA). The recovery of all certified elements was between 80–120 %. The standard deviation of all non-certified elements between measurements was 2–90 % of the mean (**Supplementary Table 3**).

Ratio *b*elements : *d*elements. To estimate the transfer potential of rare earth elements from the water column to kelps (87), we calculated the ratio of biological rare earth element mass fraction (µg g_{DW}^{-1}) to dissolved element concentration in 5 m water depth (µg mL^{-1}) (88).

Biochemical composition

Algal pigment content responds to light availability and cellular energy requirements (89). Pigment composition was determined after Koch et al. (90). 30 mg silica-dried, powdered,

_____

meristematic material (N=6–9) were analysed and dark extracted in 1 mL 90 % acetone for 24 h at 4°C. The filtered supernatant was analysed by a High-Performance Liquid Choromatography (HPLC; LaChromElite® system, L-2200 autosampler (chilled), DA-detector L-2450; VWR-Hitachi International GmbH, Darmstadt, Germany). The pigments were separated after a gradient according to Wright et al. (91), by a Spherisorb® ODS-2 column (250×4.6 mm, 5 μm; Waters, Milford, MA, USA). Respective standards were used to identify and quantify pigment peaks (DHI Lab Products, Hørsholm, Denmark). The accessory pigments were calculated as the sum of chlorophyll c, fucoxanthin and β-carotene. The ratio of accessory pigments to chlorophyll a was calculated. Pigment contents were calculated in μg g_{DW}^{-1}. The de-epoxidation state of xanthophyll cycle pigments (DPS) was calculated after Colombo-Pallotta et al. (92).

Antioxidants serve as a mechanism of protection against abiotic stressors (58). Antioxidant activity was determined after Re et al. (93), following the ABTS$^{.+}$ (2,2'-azino-bis-3-ethylbenzthiazoline-6-sulphonic acid, 7 mM in biDest H$_2$O) assay. One aliquot of 50 mg silica-dried, powdered, meristematic material (N=6–9) was dark extracted in 1 mL 70 % ethanol for 4 h at 47°C. 10 μL of the supernatant were mixed with 1 mL ABTS$^{.+}$-working-standard (absorption range: 0.740±0.01;734 nm). The absorption (734 nm) was measured after 6 min incubation. Antioxidant activity was calculated as Trolox-equivalents (TE) by calibrating the ABTS$^{.+}$-working-solution with a Trolox dilution series (6-hydroxy-2,5,7,8-tetramethychroman-2-carboxylic acid; 2.5 mM in 70 % ethanol).

Microbial community

An area of 10×10 cm above the meristem was swabbed with a sterile cotton swab and immediately frozen at -80°C until analysis. Bacterial DNA was extracted using the QIAamp DNA Mini Kit (QIAGEN, Hilden, Germany) following the manufacturer's instructions. Qubit (ThermoFisher Scientific, Darmstadt, Germany) was used to detect the concentrations of extracted DNA. For microbial community composition analysis, the V4–V5 regions (515F: 5'-GTGCCAGCMGCCGCGGTAA-3' and 907R: 5'-CCGTCAATTCMTTTRAGTTT-3') of the bacterial 16S rRNA gene from DNA extracts were amplified using the PCR procedure (94; 95). Quantified amplicons were sequenced using the Illumina Nova platform (Shanghai Hanyu Biotech lab, Shanghai, China), generating 250 bp paired-end reads. Raw reads were quality filtered using Trimmomatic (v.39) with standard parameters (96). Amplicon Sequence Variant (ASV) were clustered based on high-quality sequences with a 100 % similarity and taxonomically classified based on the Greengenes database (v13.8) (97). To ensure comparability of subsequent analysis, these ASVs were rarified to 49,918 sequences per sample for α diversity analyses.

Statistical analysis

All statistical analyses were run in RStudio (V 2023.12.1 using R-4.3.2-win; 98). Data were evaluated and plotted within "tidyverse" (99). Section plots and maps were created with "PlotSvalbard" (100). All reported values were rounded to significant digits.

The normality (Shapiro-Wilk text, $P>0.05$) and homoscedasticity (Levene's test, $P>0.05$) of the raw data and model's residuals were tested. Outliers were removed from the dataset, if they were classified as extreme (function: identify_outliers; package: rstatix; 101). As the data met requirements, a linear model was fit on each parameter (function: lm; package: stats; 98). Sampling area and station were modelled as single fixed effect, to analyse spatial differences of kelp responses. Analysis of variance was tested on the model by using the "anova" function. Pairwise performance (function: emmeans; package: emmeans; 102) was used to calculate the degrees of freedom, with Tukey adjustment of the p-value. Pearson correlation analyses were calculated (function: cor.test; package: stats; 98). Correlogram was plotted using the ggcorr-function (package: GGally; 103).

Using non-metric multidimensional scaling (nMDS), kelp population structures between areas were tested, based on Bray-Curtis dissimilarities. Variables were fit onto unconstrained ordinations (function: envfit; package: vegan, 104) to explore relationships between kelp responses and environmental drivers.

Data availability:

All data supporting this study are openly available. Water parameters (temperature, salinity, turbidity, available light, element concentration):
https://doi.pangaea.de/10.1594/PANGAEA.968625

Kelp responses (pigments, antioxidant activity, elemental mass fraction):
https://doi.pangaea.de/10.1594/PANGAEA.968627

Elemental content of certified reference material is provided as Supporting information.

The microbial sequences obtained in this study have been deposited in the NCBI SRA database under the ID number: PRJNA1097779

_____

References:

1.   Teagle H., Hawkins, S.J., Moore, P.J., Smale, D.A. The role of kelp species as biogenic habitat formers in coastal marine systems. *J. Exp. Mar. Biol. Ecol*. **492** 81-98 (2017).

2.   Steneck, R.S., Graham, M.H., Bourque, B.J., Corbett, D., Erlandson, J.M., Estes, J.A., Tegner, M.J. Kelp forest ecosystems: biodiversity, stability, resilience and future. *Environ. Conserv*. **29**, 436-459 (2002).

3.   Krumhansl, K.A., Scheibling, R.E. Production and fate of kelp detritus. *Mar. Ecol. Prog. Ser*. **467**, 281-302 (2012).

4.   Krumhansl, K.A., Okamoto, D.K., Rassweiler, A., Novak, M., Bolton, J.J., Cavanaugh, K.C., Connell, S.D., Johnson, C.R., Konar, B., Ling, S.D., Micheli, F., Norderhaug, K.M., Pérez-Matus, A., Sousa-Pinto, I., Reed, D.C., Salomon, A.K., Shears, N.T., Wernberg, T., Anderson, R.J., Barrett, N.S., Buschmann, A.H., Carr, M.H., Caselle, J.E., Derrien-Courtel, S., Edgar, G.J., Edwards, M., Estes, J.A., Goodwin, C., Kenner, M.C., Kushner, D.J., Moy, F.E., Nunn, J., Steneck, R.S., Vásquez, J., Watson, J., Witman, J.D., Byrnes, J.E.K. Global patterns of kelp forest change over the past half-century. *PNAS*. **113**, 13785-13790 (2016).

5.   Filbee-Dexter, K., Wernberg, T., Grace, S.P., Thormar, J., Fredriksen, S., Narvaez, C.N., Feehan, C.J., Norderhaug, K.M. Marine heatwaves and the collapse of marginal North Atlantic kelp forests. *Sci. Rep*. **10**: 13388 (2020).

6.   England, M.R., Eisenman, I., Lutsko, N.J., Wagner, T.J.W. The recent emergence of Arctic Amplification. *Geophys. Res. Lett*. **48**, e2021GL094086 (2021).

7.   Chylek, P., Folland, C., Klett, J.D., Wang, M., Hengartner, N., Lesins, G., Dubey, M.K. Annual mean Arctic Amplification 1970-2020: observed and simulated by CMIP6 climate models. *Geophys. Res. Lett*. **49**, e2022GL099371 (2022).

8.   Bolton, J.J., Lüning, K. Optimal growth and maximal survival temperatures of Atlantic Laminaria species (Phaeophyta) in culture. *Mar. Biol*. **66**, 89-94 (1982).

9.   Araújo, R.M., Assis, J., Aguillar, R., Airoldi, L., Bárbara, I., Bartsch, I., Bekkby, T., Christie, H., Davoult, D., Derrien-Courtel, S., Fernandez, C., Fredriksen, S., Gevaert, F., Gundersen, H., Le Gal, A., Lévêque, L., Mieszkowska, N., Norderhaug, K.M., Oliveira, P., Ouente, A., Rico, J.M., Rinde, E., Schubert, H., Strain, E.M., Valero, M., Viard, F., Sousa-Pinto, I. Status, trends and drivers of kelp forests in Europe: an expert assessment. *Biodivers. Conserv*. **25**, 1319-1348. (2016)

10. Diehl, N., Bischof, K. Coping with a changing Arctic: mechanisms of acclimation in brown seaweed *Saccharina latissima* from Spitsbergen. *Mar. Ecol. Prog. Ser*. **657**, 43-57 (2021).

11. Krause-Jensen, D., Duarte, C.M. Expansion of vegetated coastal ecosystems in the future Arctic. *Front. Mar. Sci*. **1**, 1-10 (2014).

12. Krause-Jensen, D., Archambault, P., Assis, J., Bartsch, I., Bischof, K., Filbee-Dexter, K., Dunton, K.H., Maximova, O., Ragnarsdóttier, S.B., Sejr, M.K., Simakova, U., Spiridonov, V., Wegeberg, S., Winding, M.H.S., Duarte, C.M. Imprint of climate change on Pan-Arctic marine vegetation. *Front. Mar. Sci*. **7**: 617324 (2020).

13. Assis, J., Serrão, E.A., Duarte, C.M., Fragkopoulou, E., Krause-Jensen, D. Major expansion of marine forests in a warmer Arctic. *Front. Mar. Sci*. **9**: 850368 (2022).

14. Bintanja, R., Andry, O. Towards a rain-dominated Arctic. *Nat. Clim. Change*. **7**, 263-268 (2017).

15. Bintanja, R. The impact of Arctic warming on increased rainfall. *Sci. Rep*. **8**:16001 (2018).

16. Milner, A.M., Khamis, K., Battin, T.J., Brittain, J.E., Barrand, N.E., Füreder, L., Cauvy-Fraunie, S., Gíslason, G.M., Jacobsen, D., Hannah, D.M., Hodson, A.J., Hood, E., Lencioni, V., Ólafsson, J.S., Robinson, C.T., Tranter, M., Brown, L.E. Glacier shrinkage driving global changes in downstream systems. *PNAS*. **114**, 9770-9778 (2017).

17. Schmidt, L.S., Schuler, T.V., Thomas, E.E., Westermann, S. Meltwater runoff and glacier mass balance in the high Arctic: 1991-2022 simulations for Svalbard. *Cryosphere*. **17**, 2941-2963 (2023).

18. Schild, K.M., Hawley, R.L., Chipman, J.W., Benn, D.I. Quantifying suspended sediment concentration in subglacial sediment plumes discharging from two Svalbard tidewater glaciers using Landsat-8 and in situ measurements. *Int. J. Remote Sens*. **38**, 6865-6881 (2017).

19. Gattuso, J.-P., Gentili, B., Antoine, D., Doxaran, D. Global distribution of photosynthetically available radiation on the seafloor. *Earth Sys. Sci. Data*. **12**, 1697-1709 (2020).

20. Konik, M., Darecki, M., Pavlov, A.K., Sagan, S., Kowalczuk, P. Darkening of the Svalbard fjords waters observed with satellite ocean color imagery in 1997-2019. *Front. Mar. Sci*. **8**: 699318 (2021).

21. Niedzwiedz, S., Bischof, K. Glacial retreat and rising temperatures are limiting the expansion of temperate kelp species in the future Arctic. *Limnol. Oceanogr*. **68**, 816-830 (2023).

22. Düsedau, L., Fredriken, S., Brand, M., Fischer, P., Karsten, U., Bischof, K., Savoie, A., Bartsch, I. Kelp forest dynamics in Kongsfjorden (Svalbard) across 25 years of Arctic warming. *Ecol. Evol.* **14**, e11606 (2024).

23. McGovern, M., Pavlov, A.K., Deininger, A., Granskog, M.A., Leu, E., Søreide, J., Poste, A.E. Terrestrial inputs drive seasonality in organic matter and nutrient biogeochemistry in a high Arctic fjord system (Isfjorden, Svalbard). *Front. Mar. Sci*. 7**:** 542563 (2020).

24. Krause, J., Hopwood, M.J., Höfer, J., Krisch, S., Achterberg, E.P., Alarcón, E., Carroll, D., González, H.E., Juul-Pedersen, T., Liu, T., Lodeiro, P., Meire, L., Rosing, M.T. Trace element (Fe, Co, Ni and Cu) dynamics across the salinity gradient in Arctic and Antarctic glacier fjords. *Front. Earth Sci*. **9**: 725279 (2021).

25. Pittino, F., Buda, J., Ambrosini, R., Parolini, M., Crosta, A., Zawierucha, K., Franzetti, A. Impact of anthropogenic contamination on glacier surface biota. *Curr. Opin. Biotech.* **80**: 102900 (2023).

26. Twining, B.S., Baines, S.B. The trace metal composition of marine phytoplankton. *Annu. Rev. Mar. Sci*. **5**, 191-215 (2012).

27. Davis, T.A., Voleska, B., Mucci, A. A review of the biochemistry of heavy metal biosorption by brown algae. *Water Res*. **37**, 4311-4330 (2003).

28. Holdt, S.L., Kraan, S. Bioactive compounds in seaweed: functional food applications and legislation. *J. Appl. Phycol*. **23**, 543-597 (2011).

29. Leitch, D.R., Carrie, J., Lean, D., Macdonal, R.W., Stern, G.A., Wand, F. The delivery of mercury to the Beaufort Sea of the Arctic Ocean by the Mackenzie River. *Sci. Total Environ*. **373**, 178-195 (2007).

_____

30. Rudnicka-Kępa, P., Bełdowska, M., Zaborska, A. Enhanced heavy metal discharges to marine deposits in glacial bays of two Arctic fjords (Hornsund and Kongsfjorden). *J. Marine Syst.* **241**, 103915 (2024).

31. Kreissig, K.J., Truelstrup Hansen, L., Erland Jensen, P., Wegeberg, S., Geertu-Hansen, O., Sloth, J.J. Characterisation and chemometric evaluation of 17 elements in ten seaweed species from Greenland. *PLoS ONE*. **16**, e0243672 (2021).

32. Zeraatkar, A.K., Ahmadzadeh, H., Talebi, A.F., Moheimani, N.R., McHenry, M.P. Potential use of algae for heavy metal bioremediation, a critical review. *J. Environ. Manage.* **181**, 817-831 (2016).

33. Costa, G.B., de Felix, M.R.L., Simioni, C., Pamlov, F., Oliverira, E.R., Pereira, D.T., Maraschin, M., Chow, F., Horta, P.A., Lalau, C.M., da Costa, C., Matias, W.G., Bouron, Z.L., Schmidt, É.C. Effects of copper and lead exposure on the ecophysiology of the brown seaweed *Sargassum cymosum*. *Protoplasma*. **253**, 111-125 (2016).

34. Bengtsson, M.M., Sjøtun, K., Lanzén, A., Øvreås, L. Bacterial diversity in relation to secondary production and succession on surfaces of the kelp *Laminaria hyperborea*. *ISME J*. **6**, 2188-2198 (2012).

35. Marzinelli, E.M., Campbell, A.H., Valdes, E.Z., Vergés, A., Nielsen, S., Wernberg, T., de Bettignies, T., Bennett, S., Caporaso, J.G., Thomas, T., Steinberg, P.D. Continental-scale variation in seaweed host-associated bacterial communities is a function of host condition, not geography. *Environ. Microbiol.* **17**, 4078-4088 (2015).

36. Burgunter-Delamare, B., Rousvoal, S., Legeay, E., Tanguy, G., Fredriksen, S., Boyen, C., Dittami, S.M. The *Saccharina latissima* microbiome: effects of region, season and physiology. *Front. Microbiol.* **13**: 1050939 (2023).

37. Bengtsson, M.M., Sjøtun, K., Øvreås, L. Seasonal dynamics of bacterial biofilms on the kelp *Laminaria hyperborea*. *Aquat. Microb. Ecol.* **60**, 71-83 (2010).

38. Norderhaug, K.M., Fredriksen, S., Nygaard, K. Trophic importance of Laminaria hyperborea to kelp forest consumers and the importance of bacterial degradation to food quality. *Mar. Ecol. Prog. Ser.* **255**, 135-144 (2003).

39. Bengtsson, M.M., Sjøtun, K., Storesund, J.E., Øvreås, L. Utilization of kelp-derived carbon sources by kelp surface-associated bacteria. *Aquat. Microb. Ecol.* **62**, 191-199 (2011).

40. Geyman, E.C., van Pelt, W.J.J., Maloof, A.C., Faste Aas, H., Kohler, J. Historical glacier change on Svalbard predicts doubling of mass loss by 2100. *Nature*. **601**, 374-379 (2022).

41. Greene, C.A., Gardner, A.S., Wood, M., Cuzzone, J.K. Ubiquitous acceleration on Greenland Ice Sheet calving from 1985 to 2022. *Nature*. **625**, 523-528 (2024).

42. Bazzano, A., Ardini, F., Terol, A., Rivaro, P., Soggia, F., Grotti, M. Effects of the Atlantic water and glacier run-off on the spatial distribution of particulate trace elements in the Kongsfjorden. *Mar. Chem.* **191**, 16-23 (2017).

43. Chételat, J., McKinney, M.A., Amyot, M., Dastoor, A., Douglas, T.A., Heimbürger, L.-E., Kirk, J., Kahilainen, K.K., Outridge, P.M., Pelletier, N., Skov, H., St. Pierre, K., Vuorenmaa, J., Wang, F. Climate change and mercury in the Arctic: abiotic interactions. *Sci. Total Environ.* **824**, 153715 (2022).

44. Nowicka, B. Heavy metal-induced stress in eukaryotic algae – mechanisms of heavy metal toxicity and tolerance with particular emphasis on oxidative stress in exposed cells and the role of antioxidant response. *Environ. Sci. Pollut. R.* **29**, 16860-16911 (2022).

_____

45.   Nowak, A., Hodson, A. Changes in meltwater chemistry over a 20-year period following a thermal regime switch from polythermal to cold-based glaciation at Austre Brøggerbreen, Svalbard. *Polar Res.* **33**, 22779 (2014).

46.   Diehl, N., Li, H., Scheschonk, L., Burgunter-Delamare, B., Niedzwiedz, S., Forbord, S., Sæther, M., Bischof, K., Monteiro, C. The sugar kelp *Saccharina latissima* I: recent advances in a changing climate. *Ann. Bot.* **133**, 183-211 (2024).

47.   Chung, I.K., Lee, J.A. The effects of heavy metals in seaweeds. *Korean J. Phycol.* **4**, 221-238 (1989).

48.   Schiener, P., Black, K.D., Stanley, M.S., Green, D.H. The seasonal variation in the chemical composition of the kelp species *Laminaria digitata*, *Laminaria hyperborea*, *Saccharina latissima* and *Alaria esculenta. J. Appl. Phycol.* **27**, 363-373 (2014).

49.   Torres, M.A., Barros, M.P., Campos, S.C.G., Pinto, E., Rajamani, S., Sayre, R.T., Colepicolo, P. Biochemical biomarkers in algae and marine pollution: a review. *Ecotox. Environ. Safe.* **71**, 1-15 (2008).

50.   Ash, C., Stone, R. A question of dose. *Science.* 300, 5621 (2003).

51.   Pinto, E., Sigaud-Kutner, T.C.S., Leitão, M.A.S., Okamoto, O.K., Morse, D., Colepicolo, P. Heavy metal-induced oxidative stress in algae. *J. Appl. Phycol.* **39**, 1008-1018 (2003).

52.   Vallee, B.L., Ulmer, D.D. Biochemical effects of mercury, cadmium and lead. *Annual Reviews.* **41**, 91-128. (1972)

53.   Rybak, M., Kołodziejczyk, A., Joniak, T., Ratajczak, I, Gąbka, M. Bioaccumulation and toxicity studies of macroalgae (Charophyceae) treated with aluminium: experimental studies in the context of lake restoration. *Ecotox. Environ. Safe.* **145**, 359-366 (2017).

54.   Jara-Yáñez, R., Meynard, A., Acosta, G., Latorre-Padilla, N., Oyarzo, C., Castañeda, F., Piña, J., Bulboa, C., Contreras-Porcia, L. Negative consequences on the growth, morphology and community structure of the kelp *Macrocystis pyrifera* (Phaeophyceae, Ochrophyta) by a short pollution pulse of heavy metals and PAHs. *Toxics.* **9**, 190 (2021).

55.   Kumar, M., Kumari, P., Gupta, V., Anisha, P.A., Reddy, C.R.K., Jha, B. Differential responses to cadmium induced oxidative stress in marine macroalga *Ulva lactuca* (Ulvales, Chlorophyta. *Biometals.* **23**, 315-325 (2010).

56.   Ahamad, Z.H., Shuhanija, S.N.,Physiological and biochemical responses of a Malaysian red alga, *Gracilaria manilaensis* treated with copper, lead and mercury. *J. Environ. Res. Develop.* **7**, 1246-1253 (2013).

57.   Niedzwiedz, S., Vonnahme, T.R., Juul-Pedersen, T., Bischof, K., Diehl, N. Light-mediated temperature susceptibility of kelp species (*Agarum clathratum*, *Saccharina latissima*) in an Arctic summer heatwave scenario. *Cambridge Prisms: Coastal Future.* **2**, e6 (2024).

58.   Bischof, K., Rautenberger, R. "Seaweed responses to environmental stress: reactive oxygen and antioxidant strategies" in *Seaweed Biology* (Springer, Berlin-Heidelberg, 2012), pp. 109-132.

59.   Egan, S., Harder, T., Burke, C., Steinberg, P., Kjelleberg, S., Thomas, T. The seaweed holobiont: understanding seaweed-bacteria interactions. *FEMS Microbiol. Rev.* **37**, 462-476 (2013).

60.   Cundell, A.M., Sleeter, T.D., Mitchell, R. Microbial populations associated with the surface of the brown algae *Ascophyllum nodosum. Microb. Ecol.* **4**, 81-91 (1977).

61.   King, N.G., Moore, P.J., Thorpe, J.M., Smale, D.A. Consistency and variation in the kelp microbiota: patterns of bacterial community structure across spatial scales. *Microb. Ecol.* **85**, 1265-1275 (2023).

62.   Dang, H., Li, T., Chen, M., Huang, G. Cross-ocean distribution of Rhodobacterales bacteria as primary surface colonizers in temperate coastal marine waters. *Appl. Environ. Microb.* **74**, 52-60 (2008).

63.   Bengtson, M.M., Øvreås, L. Planctomycetes dominate biofilms on surfaces of the kelp *Laminaria hyperborea*. *BMC Microbiol.* **10**:261 (2010).

64.   Wegner, C.-E., Richter-Heitmann, T., Klindworth, A., Klockow, C., Richter, M., Achstetter, T., Glöckner, F.O., Harder, J. Expression of sulfatases in *Rhodopirellula baltica* and the diversity of sulfatases in the genus Rhodopirellula. *Mar. Genom.* **9**, 51-61 (2013).

65.   Weigel, B.L., Pfister, C.A. Succession dynamics and seascape-level patterns of microbial communities on the canopy-forming kelps *Nereocystis luetkeana* and *Macrocystis pyrifera*. *Front. Microbiol.* **10**: 346 (2019).

66.   Latorre-Padilla, N., Meynard, A., Oyarzun, F.X., Contreras-Procia, L. Ingestion of contaminated kelps by the herbivore *Tetrapygus niger*: negative effects on food intake, growth, fertility and early development. *Mar. Poll. Bull.* **147**, 112365 (2021).

67.   Atwell, L., Hobson, K.A., Welch, H.E. Biomagnification and bioaccumulation of mercury in an Arctic marine food web: insights from stable nitrogen isotope analysis. *Can. J. Fish. Aquat. Sci.* **55**, 1114-1121 (1998).

68.   Dastoor, A., Angot, H., Biesner, J., Christensen, J.H., Douglas, T.A., Heimbürger-Boavida, L.-E., Jiskra, M., Mason, R.P., McLagan, D.S., Obrist, D., Outridge, P.M., Petrova, M.V., Ryjkov, A., St. Pierre, K.A., Schartup, A.T., Soerensen, A.L., Toyota, K., Travnikov, O., Wilson, S.J., Zdanowicz, C. Arctic mercury cycling. *Nat. Rev. Earth Environ.* **3**, 270-386 (2022).

69.   Falkowski, P. G., Raven, J.A. *Aquatic photosynthesis* (Princeton Univ. Press, Princeton, ed 2, 2007).

70.   Lowman, H.E., Emery, K.A., Dugan, J.E., Miller, R.J. Nutritional quality of giant kelp declines due to warming ocean temperatures. *OIKOS*, e08619 (2022).

71.   Evans, L.V., Simpson, M., Collow, M.E. Sulphated polysaccharide synthesis in brown algae. *Planta*. **110**, 237-252 (1973).

72.   Buck-Wiese, H., Andskog, M.A., Nguyen, N.P., Bligh, M., Asmala, E., Vidal-Melgosa, S., Liebeke, M., Gustafsson, C., Hehemann, J.-H. Fucoid brown algae inject fucoidan carbon into the ocean. *PNAS*. **120**, e2210561119 (2023).

73.   Rainbow, P.S. Biomonitoring of heavy metal availability in the marine environment. *Mar. Pollut. Bull.* **31**, 183-192 (1995).

74.   Kim, J.K., Kraemer, G., Yarish, C. Evaluation of the metal content of farm grown *Gracilaria tikvahiae* and *Saccharina latissima* from Long Island Sound and New York estuaries. *Algal Res.* **40**, 101484 (2019).

75.   Rosenberg, E., Zilber-Rosenberg, I. Microbes drive evolution of animals and plants: the hologenome concept. *mBIO*. **7**, e01395-15 (2016).

76.   Cavallo, G., Lorini, C., Garamella, G., Bonaccorsi, G. Seaweeds as a "palatable" challenge between innovation and sustainability: a systematic review of food safety. *Sustainability*. **13**, 7652 (2021).

77. Mabeau, S., Fleurence, J. Seaweed in food products: biochemical and nutritional aspects. *Trends Food Sci. Tech.* **4**, 103-107 (1993).

78. Shaughnessy, B.K., Jackson, B.P., Byrnes, J.E.K. Evidence of elevated heavy metals concentrations in wild and farmed sugar kelp (*Saccharina latissima*) in New England. *Sci. Rep.* **13**:17644 (2023).

79. Banach, J.L., Hoek-van den Hill, E.F., van der Feld-Klerx, H.J. Food safety hazards in the European seaweed chain. *Compr. Rev. Food. Sci. Food. Saf.* **19**, 332-364 (2019).

80. Costa, M., Henriques, B., Pinto, J., Fabre, E., Dias, M., Soares, J., Carvalho, L., Vale, C., Pinheiro-Torres, J., Pereira, E. Influence of toxic elements on the simultaneous uptake or rare earth elements from contaminated waters by estuarine macroalgae. *Chemosphere.* **252**, 126562 (2020).

81. Dinh, T., Dobo, Z., Kovacs, H. Phytomining of rare earth elements – a review. *Chemosphere.* **197**, 134259 (2022).

82. Pinto, J., Henriques, B., Soares, J., Coasts, M., Dias, M., Fabre, E., Lopes, C.B., Vale, C., Pinheiro-Torres, J., Pereira, E. A green method based on living macroalgae for the removal of rare-earth elements from contaminated waters. *J. Environ. Manage.* **263**, 110376 (2020).

83. Szczuciński, W., Zajączkowski, M., Scholten, J. Sediment accumulation rates in subpolar fjords – impact of post-Little Ice Age glaciers retreat, Billefjorden, Svalbard. *Estuar. Coast. Shelf S.* **85**, 345-356 (2009).

84. Pinseel, E., Van de Vijer, B., Kavan, J., Verleyen, E., Kopalová, K. Diversity, ecology and community structure of the freshwater littoral diatom flora from Petuniabukta (Spitsbergen). *Polar Biol.* **40**, 533-551 (2017).

85. Hanelt, D., Tüg, H., Bischof, K., Groß, C., Lippert, H., Sawall, T., Wiencke, C. Light regime in an Arctic fjord: a study related to stratospheric ozone depletion as a basis for determination of UV effects on algal growth. *Mar. Biol.* **138**, 649-658 (2001).

86. Trimmel, S., Meisel, T.C., Lancaster, S.T., Prohaska, T., Irrgeher, J. Determination of 48 elements in 7 plant CRM by ICP-MS/MS with a focus on technology-critical elements. *Anal. Bioanal. Chem.* **415**, 1159-1172 (2023).

87. Conder, J.M., Gobas, F.A.P.C., Borgå, K., Muir, D.C.G., Powell, D.E. Use of trophic magnification factors and related measured to characterize bioaccumulation potential of chemicals. *Integr. Environ. Asses.* **8**, 85-97 (2011).

88. Chernova, E.N., Shulkin, V.M. Concentrations of metals in the environment and in algae: the bioaccumulation factor. *Russ. J. Mar. Biol.* **45**, 191-201 (2019).

89. Blain, C.O., Shears, N.T. Seasonal and spatial variation in photosynthetic response of the kelp Ecklonia radiata across a turbidity gradient. *Photosynth. Res.* **140**, 21-38 (2019).

90. Koch, K., Thiel, M., Tellier, F., Hagen, W., Graeve, M., Tala, F., Laeseke, P., Bischof, K. Species separation within the *Lessonia nigrescens* complex (Phaeophyceae, Laminariales) is mirrored by ecophysiological traits. *Bot. Mar.* **58**, 91-92 (2015).

91. Wright, S.W., Jeffrey, S.W., Mantoura, R.F.C., Llewellyn, C.A., Bjørnland, T., Repeta, D., Welschmeyer, N. Improved HPLC method for the analysis of chlorophylls and carotenoids from marine phytoplankton. *Mar. Ecol. Prog. Ser.* **77**, 183-196 (1991).

_____

92. Colombo-Pallotta, M.F., García-Mendoza, E., Ladah, L.B. Photosynthetic performance, light absorption, and pigment composition of *Macrocystis pyrifera* (Laminariales, Phaeophyceae) blades from different depths. *J. Phycol*. **42**, 1225-1234 (2006).

93. Re, R., Pellegrini, N., Proteggente, A., Pannala, A., Yang, M., Rice-Evans, C. Antioxidant activity applying an improved ABTS radical cation decolorization assay. *Free Radical Bio. Med*. **26**, 1231-1237 (1999).

94. Li, J., Pang, S., Shan, T., Su, L. Changes of microbial community structure associated with seedlings of Saccharina japonica at early stage of outbreak of green rotten disease. *J. Appl. Phycol.* **32**, 1323-1327 (2020).

95. Chen, Q., Lønborg, C., Chen, F., Gonsior, M., Li, Y., Cai, R., He, C., Chen, J., Wang, Y., Shi, Q., Jiao, N., Zheng, Q. Increased microbial and substrate complexity result in higher molecular diversity of the dissolved organic matter pool. *Limnol. Oceanogr*. **67**, 2360-2373 (2022).

96. Bolger, A.M., Lohse, M., Usadel, B. Trimmomatic: a flexible trimmer for Illumina Sequence Data. *Bioinformatics.* **15**:2114–2120 (2014).

97. DeSantis, T.Z., Hugenholtz, P., Larsen, N., Rojas, M., Brodie, E.L., Keller, K., Huber T., Dalevi, D., Hu, P., Andersen, G.L. Greengenes, a chimera-checked 16S rRNA gene database and workbench compatible with ARB. *Appl. Environ. Microb*. **72**, 5069-5072 (2006).

98. R Core Team, R: A language and environment for statistical computing. R Foundation for Statistical Computing, https://www.R-project.org/ (2023). [no author]

99. Wickham, H., Averick, M., Bryan, J., Chang, W., McGowan, L.D., François, R., Grolemund, G., Hayes, A., Henry, L., Hester, J., Kuhn, M., Pedersen, T.L., Miller, E., Bache, S.M., Müller, K., Ooms, J., Robinson, D., Seidel, D.P., Spinu, V., Takahashi, K., Vaughan, D., Wilke, C., Woo, K., Yutani, H. Welcome to the tidyverse. *JOSS*. **4**, 1686 (2019).

100. Vihtakari, M. PlotSvalbard – plot research data from Svalbard on maps. R package version 0.9.2. https://github.com/MikkoVihtakari/PlotSvalbard (2020).

101. Kassambara, A. rstatix: Pipe-Friendly Framework for Basic Statistical Tests. R package version 0.7.2, https://CRAN.R-project.org/package=rstatix (2023).

102. Lenth, R., emmeans: Estimated Marginal Means, aka Least-Squares Means. R package version 1.10.0, https://CRAN.R-project.org/package=emmeans (2024).

103. Schloerke, B., Cook, D., Larmarange, J., Briatte, F., Marbach, M., Thoen, E., Elberg, A., Crowley, J. GGally: Extension to 'ggplot2'. R package version 2.2.0, https://CRAN.R-project.org/package=GGally (2023).

104. Oksanen, J., Simpson, G., Blanchet, F., Kindt, R., Legendre, P., Minchin, P., O'Hara, R., Solymos, P., Stevens, M., Szoecs, E., Wagner, H., Barbour, M., Bedward, M., Bolker, B., Borcard, D., Carvalho, G., Chirico, M., De Caceres, M., Durand, S., Evangelista, H., Fitz John, R., Friendly, M., Furneaux, B., Hannigan, G., Hill, M., Lahti, L., McGlinn, D., Ouellette, M., Ribeiro Cunha, E., Smith, T., Stier, A., Ter Braak, C., Weedon, J. vegan: Community Ecology Package. R package version 2.6-4, https://CRAN.R-project.org/package=vegan (2022).

105. ANSES – French Agency for Food, Environmental and Occupational Health and Safety. "Opinion of the French Agency for Food, Environmental and Occupational Health and Safety: on the risk of excess iodine intake from the consumption of seaweed in foodstuffs" (Maisons-Alfort; 2018). [no author]

_____

106. DIN e.V. "Chemical analysis – Decision limit, detection limit and determination limit under repeatability conditions: Terms, methods, evaluation". DIN 32645:2008-11 (2008). [no author]

Acknowledgements:

Author contribution:

SN conceptualised the study under the supervision of KB. SN and SA conducted the field work with advice and support of BD. Parameter analyses and data evaluation were conducted as follows: physical water parameters: SN and SA. Biochemical parameters: SN. Elemental composition of kelps and water: SN, CS, LH, with advice and support of DP and TH. Microbial community of kelps and water: SN, YY, BB-D and RZ. SN wrote the manuscript, which was revised, reviewed and accepted by all co-authors.

Competing interests:

The authors declare no conflict of interest.

_____

<div align="center">

Supplementary material to:

Run-off impacts on Arctic kelp holobionts have strong implications on ecosystem functioning and bioeconomy

Running title: Run-off impacts on Arctic kelp holobionts

</div>

Authors: Sarina Niedzwiedz[1*], Claudia E. Schmidt[2,3], Yunlan Yang[4], Bertille Burgunter-Delamare[5], Sebastian Andersen[6], Lars Hildebrandt[7], Daniel Pröfrock[7], Helmuth Thomas[2,3], Rui Zhang[4,8], Børge Damsgård[6], Kai Bischof[1]

*corresponding author: sarina@uni-bremen.de

Supplementary Methods

<u>Preparatory laboratory work</u>

Preparatory laboratory work was performed in a class 10000 or 1000 clean room. Type I reagent-grade water (18.2 MΩ cm, ultrapure water) was obtained from a Milli-Q Integral water purification system equipped with a Q-Pod Element and a 100 nm endfilter (Merck; Darmstadt, Germany). P.a. grade concentrated nitric acid ($HNO3$; ROTIPURAN®, w = 65 %, Carl Roth GmbH + Co. KG; Karlsruhe, Germany) and hydrochloric acid (HCl; ROTIPURAN®, w = 37 %, Carl Roth GmbH + Co. KG; Karlsruhe, Germany) were purified by double sub-boiling using a perfluoroalkoxy alkane (PFA) acid purification systems (Savillex; Eden Prairie, USA) operated under clean room conditions. Glacial acetic acid ($C_2H_4O_2$; Optima™, Fisher Scientific GmbH; Schwerte, Germany), Ammonia solution (NH3; Optima™, w = 20–22 %, Fisher Scientific; Schwerte, Germany), hydrogen peroxide solution (H2O2; ROTIPURAN® Ultra, w = 31 %, Carl Roth GmbH + Co. KG; Karlsruhe, Germany) and tetrafluoroboric acid (HBF_4; ultrapure, w = 38 %, Chem-lab NV; Zedelgem, Belgium) were used without further purification. For quantification of analytes, external calibrations were performed using single element standards (Carl Roth GmbH; Karlsruhe, Germany or Sigma-Aldrich; Missouri, USA) and custom-made multi-element standards (all traceable to NIST standards) of different compositions (Inorganic Ventures; Christiansburg, USA) to cover the targeted analyte concentration ranges. All plastic consumables were pre-cleaned in solutions of HNO_3 (w = 1–2 %) for a minimum of one week and rinsed with ultrapure water prior to use. Microwave digestion vessels were cleaned (2×) in a steam cleaner at 90°C for 8 h (65 % HNO_3; Easy Trace Cleaner Evolution II, ANALAB, Paris, France).

<u>Analysis of dissolved elements in water samples</u>

Water samples (elemental composition, microbial community) were taken along with the kelp samples (**Figure 1**; yellow points), with a trace metal free Niskin bottle (KC Denmark, Silkeborg, Denmark). In total, 18 fjord water samples were collected using a 1.7 L trace-metal free Niskin water sampler (KC Denmark; Silkeborg, Denmark), filled into 0.5 L high-density polyethylene (HDPE) bottles and kept frozen (-20°C) until further processing. Prior to multi-element analysis, water samples were filtered through DigiFILTERs™ (polytetrafluoroethylene (PTFE) membrane, 0.45 μm pore size, PerkinElmer; Waltham, USA) and collected in 50 mL DigiTUBE®s (PerkinElmer; Waltham, USA). After filtration, water samples were stabilised using 100 μL purified concentrated HNO3 and stored in the dark at 4°C until analysis.

Elements in seawater were measured by using a seaFAST SP2 system (Elemental Scientific; Omaha, USA) coupled online to a triple quadrupole ICP-MS/MS system (Agilent 8900, Agilent Technologies; Tokyo, Japan). Analytes were preconcentrated on two columns filled with Nobias

_____

chelate-PA1 resin (HITACHI High-Tech Fielding Corporation; Tokyo, Japan) buffered by 4 mol L^{-1} ammonia acetate buffer (pH = 6.0±0.2) and eluted with 1.5 mol L^{-1} HNO$_3$. To correct for instrumental drift, a 1 µg L^{-1} Niob (Nb) solution was used as an internal standard.

The ICP-MS instrument was optimised daily using a tuning solution containing Li, Co, Y, Ce and Tl to maintain a reliable day-to-day performance. The system was operated in He/H$_2$ mode and equipped with a x-lense. The certified reference materials (CRMs) AQUA-1 for drinking water, SLEW-4 for estuarine water and NASS-7 for open ocean seawater (all provided by National Research Council Canada; Ottawa, Canada) were used for method validation. Recovery rates (between 80 % and 150 %) are provided in **Table S1**.

Analysis of elements in kelp samples

After sampling, the kelp material (approx. 10 cm wide stripe above meristem; cut with ceramic knife) was rinsed with ultrapure water and freeze-dried for 72 h. It was powdered and homogenised using a ball mill (Agate; Planeten Kugelmühle PM400, Retsch; Düsseldorf, Germany). Of each sample, three aliquots of 100 mg were weighed into 55 mL TFM (modified PTFE) digestion vessels (MARS6, CEM Corporation; Matthews, USA). For digestion, 0.1 mL HBF$_4$, 5 mL HNO$_3$, 2 mL HCl and 1 mL H$_2$O$_2$ were added (adapted from 85). Afterwards, the TFM vessels were placed in a closed-vessel microwave-assisted digestion system (Mars 6, CEM Corporation; Matthews, USA). The microwave was set to reach a maximum of 200°C after a suitable and efficient temperature ramping (**Table S2**).

The sample digests were transferred quantitatively into 50 mL DigiTUBE®s (PerkinElmer; Waltham, USA) and diluted to 50 mL with ultrapure water to reduce acid concentration. Along with each batch, two blank digestion vessels containing only reagents were processed to monitor procedural contaminations and carry-over effects. Furthermore, two vessels containing the CRM NIST-3232 (Kelp powder *Thallus laminariae*, National Institute of Standards and Technology; Gaithersburg, USA) were digested for method validation. Recovery rates are contained in **Table S3** (between 80–121 %). In addition to the certified elements numerous non-certified elements were quantified.

The digested samples were measured by means of a triple quadrupole ICP-MS/MS system (Agilent 8800, Agilent Technologies; Tokyo, Japan) coupled to an ESI SC-4DX FAST autosampler (Elemental Scientific; Omaha, USA). To correct for instrumental drift, an Iridium(Ir)/Rhodium(Rh) solution (10 µg L^{-1}) was used as an internal standard. The ICP-MS instrument was optimised daily using a tuning solution containing Li, Co, Y, Ce and Tl to maintain a reliable day-to-day performance. The system was operated in 5 different gas modes and equipped with a x-lense. In addition to the CRM, an in-house reference multi-element solution comprising different single-element standards and custom-made multi-element standards was used for validation with respect to elements not certified for the CRM.

_____
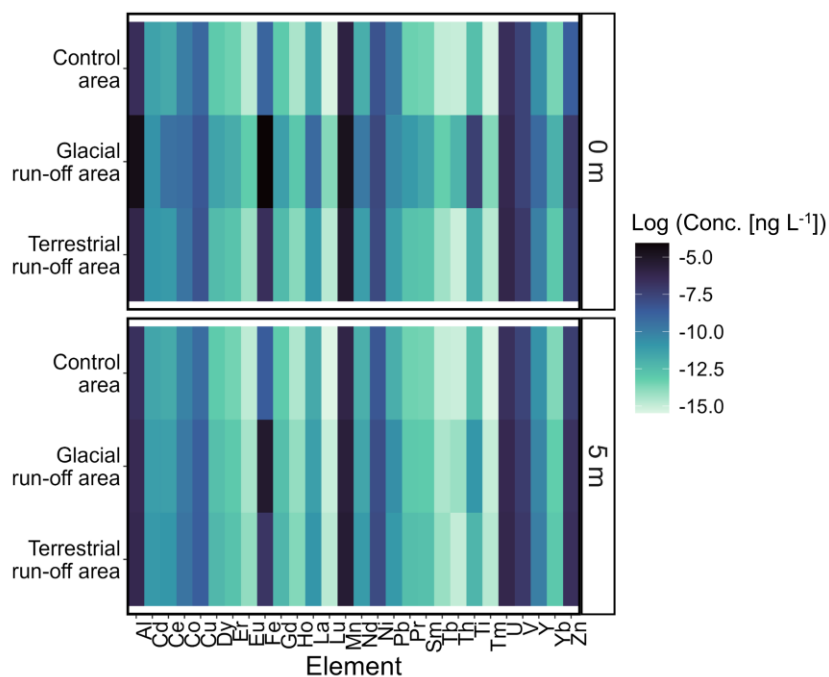
Supplementary Figure 1: Concentration (ng L^{-1}) of dissolved elements on 0 m and 5 m depth in the control, glacial run-off and terrestrial run-off area. Concentration is shown as log(ng L^{-1}) to highlight low concentrations.
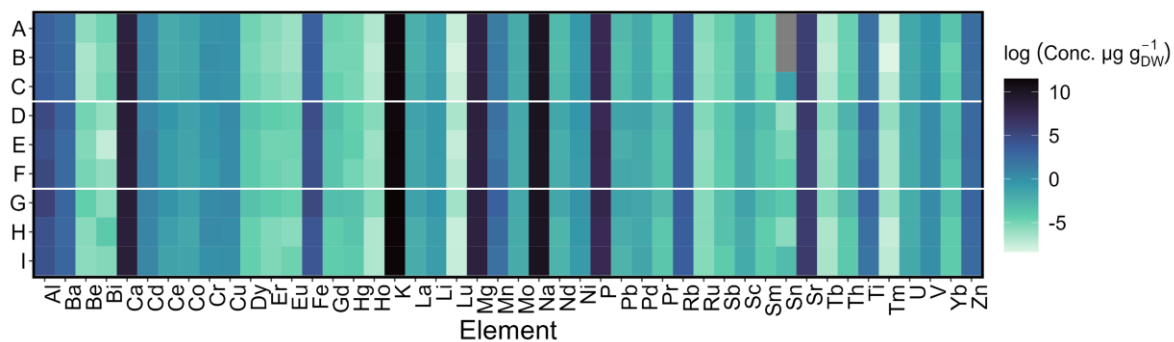
Supplementary Figure 2: Mass fractions (µg g$_{DW}^{-1}$) of kelp elements depending on sampling station. A–C: Control area. E–F: Glacial run-off- G–I: Terrestrial run-off. A) Heatmap of all determined elements (alphabetically ordered) in kelps. Mass fraction is shown as log(µg g$_{DW}^{-1}$) to highlight low mass fractions.
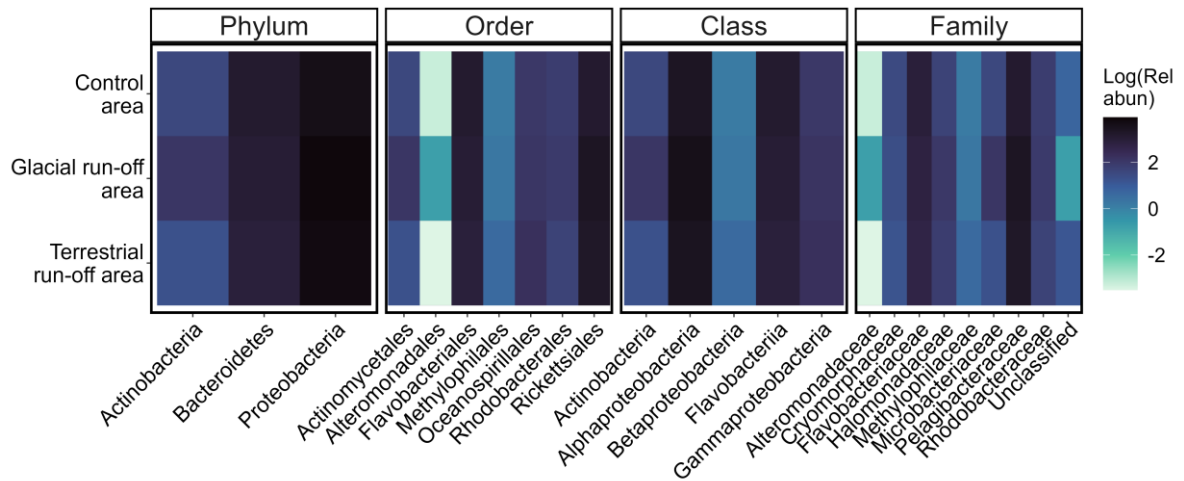
Supplementary Figure 3: Heatmap showing the mean relative abundance of free-living microbial community taxa (≥ 1 %) in each sampling area on 5 m water depth. Relative abundance is shown as Log(Rel abun) to highlight low abundances.
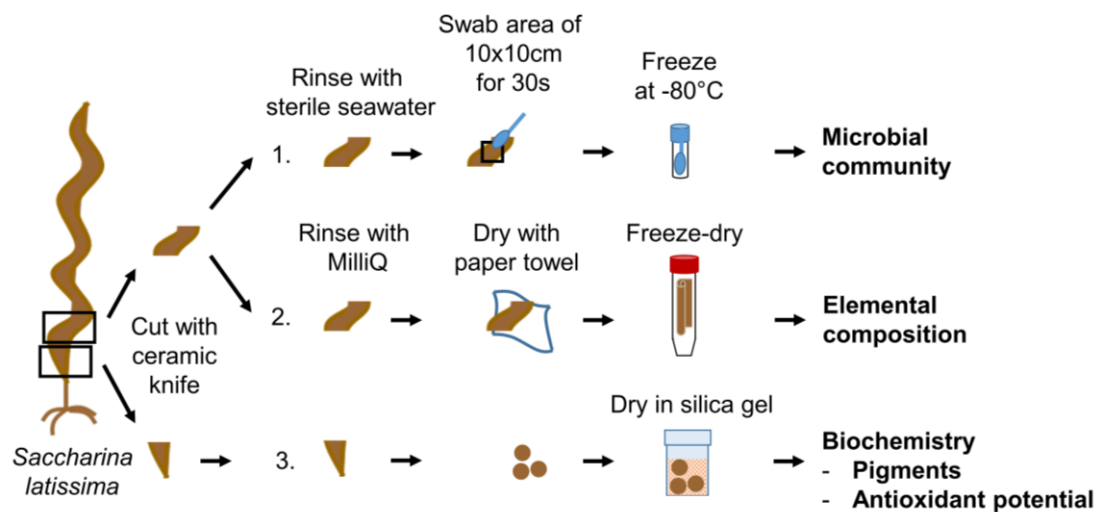
Supplementary Figure 4: Schematic preparation of kelp samples. 1. Microbial community: Swab area of 10×10 cm above meristem with a sterile cotton swab for 30 s and freeze samples on -80°C until analysis. 2. Elemental composition: Rinse area above meristem with type I reagent grade water and freeze-dry. 3. Biochemistry: Dry meristematic discs in silica gel for pigment analysis and antioxidant activity.

_____
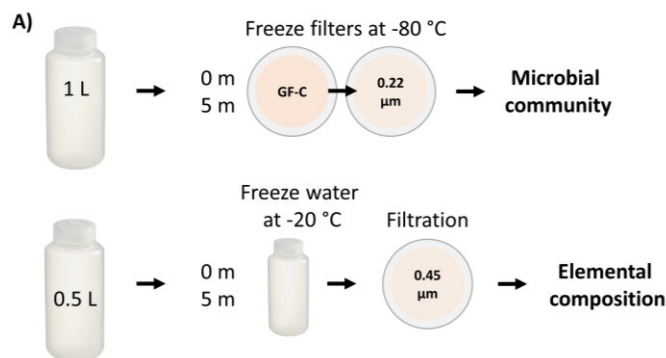
Supplementary Figure 1: Schematic procession of water samples from surface and 5 m depth. Microbial community: Prefilter on GF-C before sterile filtration on 0.22 µm sterile filter. Elemental composition: Freeze water on -20°C and filter on 0.45 µm filter before analyses.

Supplementary Table 1. Recovery (%) of all certified and non-certified elements of CRM AQUA-1 SLEW-4, NASS-7 (*N*=4). Limits of detection (LOD; ng L^{-1}) and limits of quantification (LOQ; ng L^{-1}) were calculated according to DIN 32645:2008-11 (106) based on 14 method blanks (*N*=14), with LOD defined as 3 × standard deviation (SD) and LOQ as 10 × SD of the blank.

Element	Recovery (%)			Concentration (ng L^{-1})	
	AQUA-1	SLEW-4	NASS-7	LOD	LOQ
Al	85.42	-	163.15	30.86	43.91
Ti	83.26	-	136.72	1.62	2.39
V	110.12	103.24	94.37	0.34	0.80
Mn	107.94	96.98	98.35	4.40	13.77
Fe	104.69	96.83	99.90	71.18	79.66
Co	94.74	103.38	97.46	0.05	0.12
Ni	108.09	101.59	95.41	0.79	1.21
Cu	105.75	103.67	95.33	2.81	8.39
Zn	108.57	104.43	102.84	12.00	32.19
Y	116.89	-	108.50	0.00	0.01
Cd	148.43	104.84	94.73	0.06	0.11
La	111.04	-	105.08	0.01	0.02
Ce	110.45	-	105.59	0.02	0.05
Pr	111.49	-	105.87	0.00	0.00
Nd	104.53	-	100.45	0.01	0.02
Sm	103.25	-	98.62	0.00	0.00
Eu	110.34	-	104.22	0.01	0.02
Gd	142.35	-	108.24	0.01	0.02
Tb	135.24	-	115.18	0.00	0.01
Dy	111.11	-	102.73	0.00	0.00
Ho	112.63	-	106.29	0.00	0.01
Er	106.80	-	101.24	0.00	0.01
Tm	111.67	-	110.32	0.00	0.01
Yb	105.84	-	100.57	0.00	0.01
Lu	120.95	-	114.46	0.00	0.01

_____

Pb	110.82	110.76	122.38	0.33	0.86
Th	38.87	-	69.45	0.09	0.27
U	113.15	89.29	79.99	0.04	0.12

Supplementary Table 2: Microwave temperature ramping for kelp digestion.

Stage	Ramp (min)	Hold (min)	Temperature (°C)	Power (W)
1	05:00	10:00	50	400
2	10:00	30:00	20	400
3	30:00	30:00	50	400
4	30:00	59:59	200	1600
5	10:00	30:00	100	800

Supplementary Table 3: Mass fractions (mg g_{DW}^{-1}) of all certified and non-certified elements of CRM Kelp powder *Thallus laminariae*, SKU: 3232, NIST, USA (*N*=19). Limits of detection (LODs) and limits of quantification (LOQs) were calculated according to DIN 32645:2008-11 (106) based on 14 method blanks (*N*=14), with LOD defined as 3 × standard deviation (SD) and LOQ as 10 × SD of the blank.

Elements	Mean (µg g_{DW}^{-1})	±SD	Recovery CRM 3232 (%)	LOD (µg g_{DW}^{-1})	LOQ (µg g_{DW}^{-1})
Certified elements					
Ca	12 473 000	1 084 001	102	9.98	33.3
Cd	390	60	93	0.0155	0.0517
Cr	6000	970	101	1.07	3.57
Cu	3 100	580	80	0.547	1.82
Fe	685 000	36 600	102	7.26	24.2
Hg	110	12	93	0.115	0.382
K	77 000 000	8 126 000	101	1110	3690
Mg	5 915 000	498 100	97	3.64	12.1
Mn	29 660	3 780	121	5.53	18.4
Mo	230	23	94	0.0545	0.182
Na	15 500 000	1 260 000	95	13.7	45.8
Pb	1 030	150	99	0.129	0.429
Zn	26 940	1 980	98	1.66	5.52
Non-certified elements			Deviation SD from mean (%)		
Al	1 070 000	20 600	1.9	9.98	33.3
Ba	72 200	6 260	8.7	0.0495	0.165
Be	35	7	20.0	0.000434	0.00145
Bi	27	9	33.3	0.00782	0.0261
Ce	1 550	210	13.5	0.0348	0.116
Co	305	33	10.8	0	0

Dy	75	11	14.7	0.00162	0.00538
Er	42	7	16.7	0.0017	0.00566
Eu	25	3	12.0	0.00596	0.0199
Gd	80	13	16.3	0.000843	0.00281
Ho	13	2	15.4	0.000267	0.00089
La	660	90	13.6	0.0163	0.0544
Li	1 150	220	19.1	0.505	1.68
Lu	7	1.4	20.0	0.000485	0.00162
Nd	480	80	16.7	0.0125	0.0417
Ni	2 700	320	11.9	0.0323	0.108
P	4 200 000	545 000	13.0	20	66.8
Pd	400	50	12.5	0	0
Pr	130	20	15.4	0.000728	0.00243
Rb	25 400	4 490	17.7	0.0175	0.0584
Ru	3	1.4	46.7	0.0178	0.0593
Sb	60	9	15.0	0.000306	0.00102
Sc	440	150	34.1	0.00295	0.00985
Sm	95	17	17.9	0	0
Sn	90	24	26.7	0	0
Sr	820 200	122 700	15.0	0.0859	0.286
Tb	11	1.2	10.9	0	0
Th	170	21	12.4	0.00332	0.0111
Ti	43 300	4 350	10.0	27.5	91.8
Tm	8	4	50.0	0.000348	0.00116
U	230	25	10.9	0.00312	0.0104
V	4 560	610	13.4	0.468	1.56
Yb	95	85	89.5	0.0136	0.0452

References:

106. DIN e.V. "Chemical analysis – Decision limit, detection limit and determination limit under repeatability conditions: Terms, methods, evaluation". DIN 32645:2008-11 (2008). [no author]

PUBLICATION III

Light mediated temperature susceptibility of kelp species (*Agarum clathratum*, *Saccharina latissima*) in an Arctic summer heatwave scenario

Sarina Niedzwiedz, Tobias Reiner Vonnahme, Thomas Juul-Pedersen, Kai Bischof, Nora Diehl

Temperature mitigates high-light stress

Sarina Niedzwiedz[1], Tobias Reiner Vonnahme[2], Thomas Juul-Pedersen[2], Kai Bischof[1], Nora Diehl[1]

[1] University of Bremen, Germany; [2] Greenland Institute for Natural Resources, Greenland

University of Bremen

Nuuk, Greenland

70°N 65°N 60°N 55°N
60°W 30°W
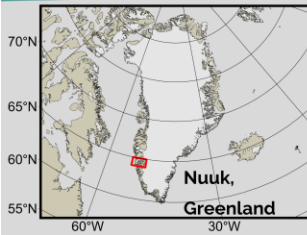
Due to ongoing climate change, Arctic fjords are subject to many environmental changes, e.g. intensification of marine heatwaves or a reduction of the photosynthetically available radiation by high concentrations of suspended particles. Kelps (brown macroalgae) act as foundation species along Arctic rocky shore coastlines, providing the livelihood for many associated species. To be able to understand kelp forest dynamics, we assessed the effect of marine heatwaves under different light regimes on two cold-temperate kelp species (*Agarum clathratum, Saccharina latissima*) at their cold distribution limit.

Research question: How are differences in light availability affecting kelps' susceptibility to marine heatwaves in the Arctic?

Greenlandic kelp forest

12 days heatwave
10°C
7°C
4°C (summer *in-situ*)

High-light conditions
120 µmol photons m⁻² s⁻¹
Conditions in clear Arctic fjords without a sediment plume

Low-light conditions
3 µmol photons m⁻² s⁻¹
Conditions in sediment plume dominated fjord

High-light stress at 4°C, due to exposure of 24 h polar day

High-light stress is mitigated with rising temperature (10°C)

High-light stress, due to formation of reactive oxygen species
⇒ Decreasing of chlorophyll *a* concentrations to reduce oxidative stress
⇒ Reduced photosynthetic rates
⇒ Nevertheless, weight gain

No physiological stress experienced
⇒ No temperature effect due to light-limitation

Low-light limited
⇒ Increasing chlorophyll *a* concentrations during the experiment:
⇒ Positive photosynthetic rates
⇒ Weight gain

Similar response pattern of both species

BUT:

High temperatures promote the expansion of temperate kelps to higher latitudes.

Reduced weight gain in darker fjords
⇒ **Less production**
⇒ **Consequences for carbon cycling?**

More weight gain & less high-light stress

More photosynthetic pigments & feeding deterrents

"Winner" in high-light environments with low grazing pressure

"Winner" in low-light environments with high grazing pressure

Saccharina latissima (Sugar kelp)

Agarum clathratum (Sieve kelp)

Get the publication

Changes in the ecosystems species composition might have cascading effects:
➡ **Changes in the kelp forest associated species community**
➡ **Changes in the of energy transfer to high trophic levels.**

Research Article

Corresponding author:
Sarina Niedzwiedz;
Email: sarina@uni-bremen.de

Light-mediated temperature susceptibility of kelp species (*Agarum clathratum, Saccharina latissima*) in an Arctic summer heatwave scenario

Sarina Niedzwiedz[1] ![ORCID], Tobias Reiner Vonnahme[2], Thomas Juul-Pedersen[2], Kai Bischof[1] and Nora Diehl[1]

[1]Marine Botany, Faculty of Biology and Chemistry & MARUM, University of Bremen, Bremen, Germany and [2]Greenland Climate Research Centre, Greenland Institute for Natural Resources (GINR), Nuuk, Greenland

Abstract

Kelps (Phaeophyceae, Laminariales) are ecosystem engineers along Arctic rocky shores. With ongoing climate change, the frequency and intensity of marine heatwaves are increasing. Further, extensive meltwater plumes darken Arctic fjords. Assessing the effect of a sudden temperature increase at the cold-distribution limit of cold-temperate kelp species, we compared the responses of two kelp species (*Agarum clathratum, Saccharina latissima*) to realistic Arctic summer heatwave scenarios (4–10°C) under low- and high-light conditions (3; 120 μmol photons m^{-2} s^{-1}) for 12 days. We found high-light causing physiological stress in both species (e.g., lower photosynthetic efficiency of photosystem II), which was enhanced by cold and mitigated by warm temperatures. Under low-light conditions, we found no temperature response, probably due to light limitation. Both species acclimated to light variations by adjusting their chlorophyll *a* concentration, meeting cellular energy requirements. *A. clathratum* had ~150% higher phlorotannin concentrations than *S. latissima*, possibly acting as herbivore-deterrent. Our findings suggest competitive advantages of kelps on different Arctic coasts with ongoing warming: *A. clathratum* has advantages in future areas, with low-light intensities, and possibly high grazing pressure and *S. latissima* in areas with high-light intensities and low grazing pressure. Species composition changes might have cascading consequences on ecosystem functioning.

Impact statement

Kelps are brown macroalgae that act as ecosystem engineers on many rocky shore coastlines from temperate to polar regions, covering about 25% of the global coastline. They provide habitat, food, and nursery ground for many associated species, some of which are economically relevant. Kelps in the Arctic experience various climate change related environmental variations, such as intense, sudden short-term temperature increases (heatwave), or a reduction of the available light for photosynthesis due to glacial meltwater with high sediment concentrations being washed into fjords. To be able to preserve these valuable and vulnerable ecosystems, it is important to understand how species dynamics change, responding to single and interacting drivers. In this study, we worked in Nuup Kangerlua, Greenland, assessing how a heatwave affects the sieve kelp (*Agarum clathratum*) and sugar kelp (*Saccharina latissima*), two cold-temperate kelp species, when being exposed to either high-light (clear Arctic fjord) or low-light (meltwater covered Arctic fjord) conditions. We found high-light conditions to inflict most physiological stress in both species, being amplified by cold (in situ) temperatures. Warm temperature during the heatwave scenario had mitigating effects. This finding supports existing models on expansion of temperate kelps to higher latitudes with rising temperatures. When kelps were low-light-limited, temperature had no effect on either species response. Low-light intensities resulted in significantly reduced net photosynthetic rates, indicating less overall production and a reduced contribution to the coastal carbon cycle of kelps. Our results suggest that each kelp species will have competitive advantages in different Arctic coastal areas with increasing warming: The sieve kelp has competitive advantages in areas, with low-light intensities, and possibly high grazing pressure and the sugar kelp in areas with high-light intensities and low grazing pressure. This might have cascading consequences on ecosystem functioning, affecting species-dependent associated species or energy transfer to higher trophic levels.

Introduction

Kelps (Laminariales, Phaeophyceae) form underwater forests on rocky shore coastlines in temperate and polar regions. They act as foundation species and ecosystem engineers, providing

nursery ground, habitat, and food for many associated species (Eckman et al., 1989; Filbee-Dexter et al., 2019; Smale, 2019; Wernberg et al., 2019). Covering about 25% of the world's coastlines, kelp forests provide many socioeconomic services (Teagle et al., 2017; Wernberg et al., 2019). However, being sedentary, kelps cannot actively escape stressors and are susceptible to environmental changes (Ruthrof et al., 2018; Straub et al., 2019). Accordingly, kelp species developed a large range of physiological and biochemical strategies to acclimate to changes in the environment (Hurd et al., 2014). Regarding temperature, for example, each species has a specific physiological optimum within which they exhibit maximal performance at lowest energetic costs (Pörtner et al., 2005). Above or below the optimum, cellular stress and energetic costs are increasing, resulting in decreasing performance (Kültz, 2005).

Temperature is considered a major driver for the latitudinal distribution of kelp species (Lüning, 1990; Adey and Steneck, 2001; Fragkopoulou et al., 2022), as it is directly affecting enzymatic activities (Clarke and Fraser, 2004; Pörtner and Farrell, 2008). Within their genetically set tolerance limits, kelp species can acclimate to increasing temperature by modifying their phenotype (King et al., 2018, Liesner et al., 2020).

As a consequence of climate change, the mean global sea surface temperature is already 0.88°C (0.68–1.01°C) higher comparing 2011–2020 to 1850–1900, with further increasing tendencies (IPCC, 2023). These global changes have consequences for a species entire biogeographical distribution range, as a shift in temperature causes shifts in their performance (e.g., growth) along their reaction norm (Chevin et al., 2010). However, most drastic consequences of rising temperatures become apparent at the species warm and cold distribution limits: Kelp forests were observed to disappear at their warm-edge distribution limits (Sorte et al., 2010; Filbee-Dexter and Wernberg, 2018), as genetically adaptive modifications of the temperature tolerance limits over generations were shown to mismatch with the pace of projected temperature changes (Vranken et al., 2021). With the Arctic warming far beyond the global average (Previdi et al., 2020, 2021; England et al., 2021), habitats in high latitudes become (increasingly more) habitable for temperate kelp species. Both processes combined, a passive northward shift of temperate kelp species is predicted (Assis et al., 2022), potentially outcompeting and replacing cryophilic Arctic kelp species (Bringloe et al., 2020, 2022).

Additional to the long-term temperature increase, the frequency and intensity of extreme temperature events, such as marine heatwaves (MHWs), are expected to increase (Hobday et al., 2016; Oliver et al., 2018; Barkhordarian et al., 2024). Thereby, MHWs are defined as a temperature increase above the 90th percentile of the 30 year mean for more than five consecutive days (Hobday et al., 2016). MHWs have drastic consequences for ecosystems, triggering mortality, demographic and species community disruptions and might be the tipping point for alternative ecosystem states (Wernberg et al., 2016; Filbee-Dexter and Wernberg, 2018; Straub et al., 2019). Filbee-Dexter et al. (2020) highlighted that kelp forest declines in the Atlantic coincided with increasing intensities and frequencies of MHWs, being replaced with low-productive turf algae. Overall, Smale (2019) and Wernberg et al. (2013) evaluated warming and marine heatwaves as major threat for kelp forests worldwide. Further, it was found that even if kelp abundances did not decline due to immediate heat stress, their susceptibility to other stressors increased (Wernberg et al., 2010).

In Arctic coastal areas, elevated temperatures also alter the underwater light availability to primary producers. Increased temperatures lead to an early season breakup of sea ice (increased light availability;

Nicolaus et al., 2012; Payne and Roesler, 2019), while higher terrestrial runoff (Bintanja and Andry, 2017; Milner et al., 2017; Bintanja, 2018) decreases light availability in summer (Gattuso et al., 2020; Konik et al., 2021). Thereby, Schlegel et al. (2023) describe a high interannual variability of light availability. As photoautotrophic organisms, kelps are dependent on the underwater light conditions, driving their depth distribution (Fragkopoulou et al., 2022). They can only grow if their carbon uptake exceeds their carbon loss (Kirk, 2011). The interaction of changes of the underwater light conditions and in temperature is especially important for kelp distribution, as photosynthetic processes are driven by a multitude of (temperature-sensitive) enzymatic reactions (Davison et al., 1991). Therefore, increasing temperatures might also affect kelps' light tolerance.

Agarum clathratum (Nova Scotia; Simonson et al., 2015) and *Saccharina latissima* (Helgoland; Bolton and Lüning, 1982; *S. longicruris* morphology: Long Island; Egan et al., 1989) were described to have a temperature optimum between 10 and 15°C. Fortes and Lüning (1980) monitored *S. latissima* to survive periods at 0°C and Bringloe et al. (2022) classified *A. clathratum* as cryotolerant in areas with temperatures below 0°C. Based on these findings, Nuup Kangerlua (SW Greenland) with a mean annual temperature (upper 5 m water column) of 1.97°C (GEM, 2023) is at the northern cold limit of both species. Nonetheless, it is important to note reported optimum temperature ranges can vary for one species, depending on environmental conditions and geographical location (Bennett et al., 2019). Though this is not evident for *A. clathratum* or *S. latissima* yet.

In this study, we assessed the acclimation of Arctic *A. clathratum* and *S. latissima* in response to summer heatwaves under different light conditions. Thereby, we provide a more detailed understanding of the future dynamics of kelp forests at their northern cold-distribution limit. Based on abiotic in situ measurements, we conducted a 12-day heatwave simulation experiment (4, 7, 10°C) under low light (3 μmol photons m^{-2} s^{-1}) and high light (120 μmol photons m^{-2} s^{-1}), evaluating physiological (growth, photosynthetic efficiency of photosystem II (F_v/F_m), dark respiration rates, net photosynthetic rates), and biochemical (pigments, phlorotannins) parameters. The heatwave was followed by a 5-day recovery phase (Figure 1A). Our study was guided by three hypotheses:

1) *A. clathratum* was observed to grow deeper in the water column (Figure 1B; video transect see Supplement S1). Hence, we expect it to be adapted to low-light conditions, becoming evident by maintaining high physiological performance at low-light conditions.

2) Given the described temperature optimum of 10–15°C (Bolton and Lüning, 1982; Egan et al., 1989; Simonson et al., 2015), we expect an increase in performance of both species with rising temperature.

3) Suboptimal temperatures will increase cellular energy demand (Pörtner et al., 2005). Given the reported temperature tolerance ranges, we consider cold, in situ temperatures suboptimal. Low-light conditions might not provide enough energy. Hence, we hypothesize that the interaction of cold temperatures and low-light causes physiological stress.

Material and methods

Study region, sampling, and experimental setup

Nuup Kangerlua is located between N 64 and 65° south-western Greenland. Similar sized sporophytes of *Agarum clathratum*
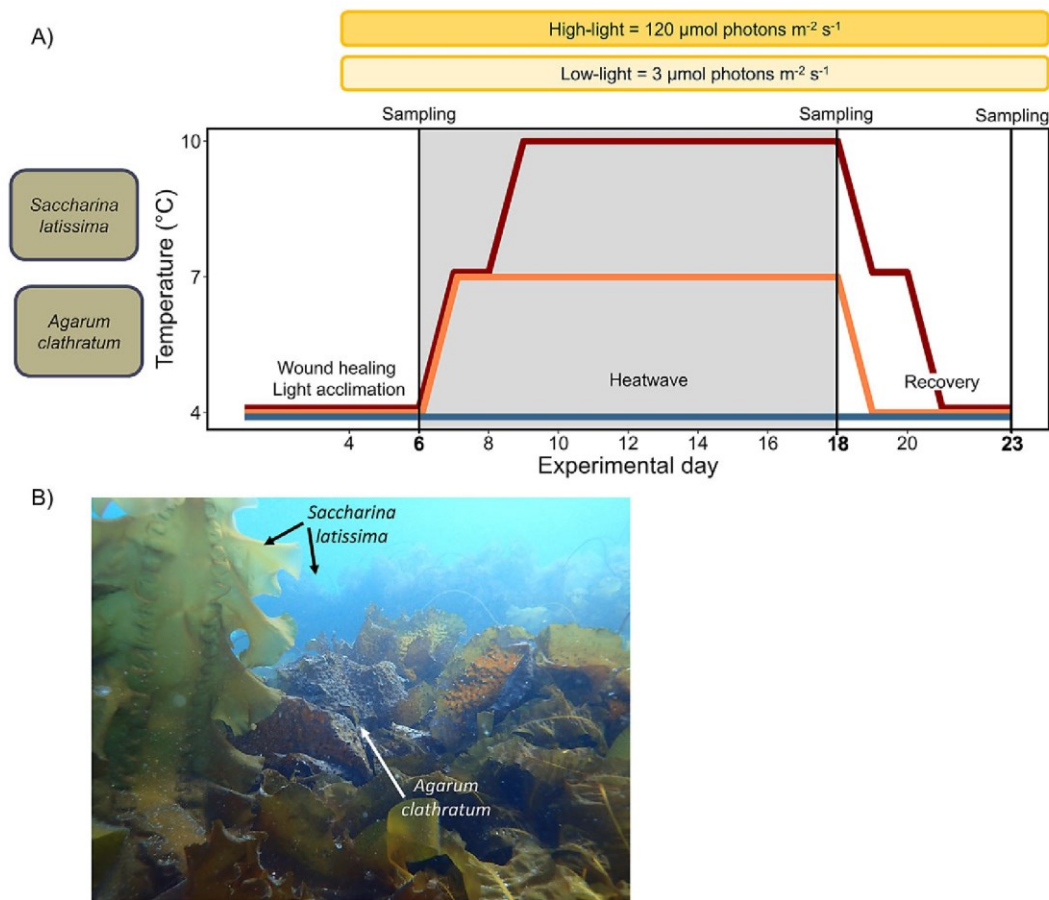
Figure 1. (A) The kelp species *Agarum clathratum* and *Saccharina latissima* were exposed to heatwave scenarios (blue: control, 4°C; orange: 7°C heatwave; red: 10°C heatwave) under low-light (3 μmol photons m^{-2} s^{-1}) and high-light (120 μmol photons m^{-2} s^{-1}) conditions. Days 0–5: wound healing and light acclimation. Days 6–18 (grey): heatwave. Days 19–23: recovery. The photosynthetic efficiency of photosystem II was measured every 2 days; all other parameters were measured on days 6, 18, and 23. (B) In situ photo of the kelp forest around Nuuk, showing *Agarum clathratum* and *Saccharina latissima*. © Sarina Niedzwiedz.

(Dumortier, 1822) were sampled at low tide between 8 and 10 m and *Saccharina latissima* (Lane et al., 2006) between 7 and 8 m at N 64.203° W 51.648° (tidal range: >2 m; Richter et al., 2011). We collected the "*longicruris*" morphology of *S. latissima* (= hollow, very long stipe), contrary to the classic "*latissima*" morphology (= solid, short stipe). McDevit and Saunders (2010) detected no genetic differentiation between both morphotypes. Egan et al. (1989) found a temperature optimum for growth at 10–15°C for "*S. longicruris*" (consistently with Bolton and Lüning (1982) for *S. latissima*). Hence, we consider them the same species – *S. latissima*. We were granted sampling permission by the Government of Greenland under the nonexclusive license no. G23–007.

Meristematic disks (diameter 2 cm; ~10 per individual) were equally distributed between interacting light and temperature treatments (*n* = 4), avoiding pseudoreplication. The disks were cultivated at 24 h LED light in 2 L aerated plastic beakers, filled with fresh, unfiltered seawater (changed every second day, S$_A$ 35). All interacting light-temperature treatments were started in parallel after a 3-day wound healing of experimental specimens and 2 days of light acclimation at 4°C (in situ temperature). Within the heatwave phase (days 6–18), temperatures gradually increased until

treatment temperatures were reached. On day 18, a heatwave recovery was conducted with a gradual temperature decrease until reaching 4°C (Figure 1).

Treatment conditions were based on the 15 years' time series of the Greenland-Ecosystem-Monitoring database (GEM, 2023). Mean summer temperature (June–August) in Nuup Kangerlua in the upper 15 m was 4.2°C. The maximum recorded temperature was 8.5°C in July 2012. Temperature exceeding 7°C were found in July and August in 7 years during the 15 years of monitoring (Supplement S2). Hence, we chose temperature treatments of 4°C (control), 7°C (upper present summer temperature), and 10°C (future temperature). Photosynthetically available radiation (PAR) is typically highest in July with light intensities between ~160 and 2,500 μmol photons m^{-2} s^{-1} at 1 m and ~ 15 to 190 μmol photons m^{-2} s^{-1} at 15 m (GEM, 2023). Referring to the sampling depth, we chose 24 h of 120 μmol photons m^{-2} s^{-1} as high-light conditions (Supplement S2). The chosen low-light conditions (3 μmol photons m^{-2} s^{-1}) should represent light conditions within meltwater plumes on 15 m depth. We used the average light attenuation in sediment-plume-dominated Kongsfjorden, Svalbard as reference (Niedzwiedz and Bischof, 2023a,b; Supplement S3).

Response parameters

All kelp response parameters were measured before (day 6), at the peak of (day 18) and after (day 23) the heatwave (Figure 1). Additionally, maximum quantum yield of photosystem II (F_v/F_m) measurements were measured every second day in $n = 4$. F_v/F_m is a proxy for algal physiological and cellular stress (Murchie and Lawson, 2013) and was measured using pulse amplitude modulated fluorometry (Portable Chlorophyll Fluorometer PAM-2100, Heinz Walz GmbH, Effeltrich, Germany) after 5 min of darkness.

Algal growth (dry weight (g) of freeze-dried disks) is an integrative parameter reflecting an organism's response to the interaction of all environmental parameters.

Dark respiration rates are a proxy for cellular energy requirements. Net photosynthetic rates indicate chemical energy availability of organisms. Both were measured as oxygen concentration evolution responding to different light intensities with a 4-channel optode setup (FireStingO$_2$ Fibre-Optic Oxygen Meter FSO2-C4, PyroScience Sensor technology, Aachen, Germany). As incubation chambers 25-mL Schott bottles were used. The system was one-point-calibrated according to the manufacturers' protocol. A magnetic stirrer ensured homogenic oxygen concentrations. Raw data were corrected for temperature and atmospheric pressure variations using the PyroScience-Calculation-Tool. Linear functions were fitted on the oxygen concentration evolution to calculate the dark respiration and net photosynthetic rates. Linearity of slopes indicated that incubations were not substrate-limited. As we used unfiltered sea water in our experiment, the temperature-dependent mean background (microbes and phytoplankton) respiration and photosynthesis ($n = 4$ per treatment condition) were subtracted. Dark respiration and net photosynthetic rates were normalized to wet weight (g; WW).

Algal pigment content reacts to energy requirements and light availability (Blain and Shears, 2019). Pigment analysis was conducted according to Koch et al. (2015). Thirty to one hundred milligram powdered, freeze-dry material was extracted in 1 mL 90% acetone (v/v) for 24 h in darkness at 4°C. The supernatant was filtered and analyzed by a high-performance liquid chromatography (HPLC; LaChromElite® system, L-2200 autosampler (chilled), DA-detector L-2450; VWR-Hitachi International GmbH, Darmstadt, Germany). A gradient was applied according to Wright et al. (1991), separating the pigments by a Spherisorb® ODS-2 column (250 × 4.6 mm, 5 µm; Waters, Milford, MA, USA). The respective standard for each pigment (DHI Lab Products, Hørsholm, Denmark) was used to identify and quantify pigment peaks. Accessory pigments (Acc) were defined as the sum of chlorophyll *c*, fucoxanthin, and ß-carotin, and the ratio to chlorophyll *a* was calculated (Acc:Chl*a*). The ratio of the xanthophyll cycle pigments, namely the de-epoxidation state (DPS), was calculated after Colombo-Pallotta et al. (2006).

Phlorotannins serve as a mechanism of protection against abiotic stressors and herbivores (Amsler et al., 2009). Total phlorotannin content was determined with the Folin–Ciocalteu assay (Cruces et al., 2013). Twelve to fifteen milligram powdered, freeze-dry material was extracted in 70% acetone (v/v) for 24 h in darkness at 4°C and constant shaking. Two hundred fifty microliter dH$_2$O, 200 µL 20% sodium carbonate (Na$_2$CO$_3$), and 100 µL 2-N-Folin–Ciocalteu reagent (Sigma-Aldrich, Germany) were added to the extract, incubating 45 min in darkness before measuring the absorbance at 730 nm in a microplate reader (FLUOstar OPTIMA, BMG Labtech). The total phlorotannin content was calculated by using a phloroglucinol dilution series (C$_6$H$_6$O$_3$, Sigma-Aldrich: 0–1,000 µg mL^{-1}).

Statistics

Statistical analyses were run in RStudio (Version 2023.06.0; R Core Team, 2021). Each treatment consisted of $n = 4$ biological independent replicates. Normality (Shapiro–Wilk test, $p > 0.05$) and homoscedasticity (Levene's test, $p > 0.05$) of the raw data and model's residuals were tested. As requirements were met, a linear model was fitted on the data, using the "lm" function (Package "stats"; R Core Team, 2021). Temperature (4; 7; 10°C), light (3; 120 µmol photons m^{-2} s^{-1}), species (*A. clathratum; S. latissima*), and day (6; 18; 23) were modelled as multiple fixed effects. The model's fit on the data was assessed. Analysis of variance (ANOVA) was tested on the model by using the "anova" function, assessing the influence of fixed effects. All p-values were fdr-corrected for multiple testing, using "p.adjust" (Package: "stats"; R Core Team, 2021). Pairwise comparisons were performed, using the "emmeans" function (Package: emmeans; Lenth, 2021). The level of significance was set to $p < 0.05$. Using Pearson correlation, linear dependency between response variables was tested (function: cor.test; R Core Team, 2021), after testing for normality.

Results

For overview reasons, all statistical results are shown in Table 1 (ANOVA) and Table 2 (pairwise comparisons) and therefore not given in the text or plots. The fixed effects are abbreviated as

Table 1. Statistical results for all physiological and biochemical parameters. Results of the analysis of variance (ANOVA) to evaluate the effects of the fixed parameter temperature (T), light (L), species (S), and day (D), as well as their interactions on physiological and biochemical parameters. Significant results are highlighted in bold ($p < 0.05$)

Parameter	Fixed effects	numDF	denDF	*F* value	*p* value
Dry weight	**T**	2	108	5.93	**0.009**
	L	1	108	155.24	**0.003**
	S	1	108	29.33	**0.003**
	D	2	108	229.88	**0.003**
	T × L	2	108	8.0	**0.003**
	T × S × D	4	108	0.68	0.76
	L × S × D	2	108	0.1	0.92
	T × L × D	4	108	1.93	0.18
	T × L × S × D	4	108	0.27	0.92
Maximum quantum yield of photosystem II (F_v/F_m)	**T**	2	108	33.55	**0.003**
	L	1	108	295.44	**0.003**
	S	1	108	92.53	**0.003**
	D	2	108	5.36	**0.013**
	T × L	2	108	22.9	**0.003**
	T × S × D	4	108	1.44	0.3
	L × S × D	2	108	6.1	**0.007**
	T × L × D	4	108	1.54	0.32
	T × L × S × D	4	108	0.59	0.78
Dark respiration rate	**T**	2	108	12.76	**0.003**
	L	1	108	59.4	**0.003**
	S	1	108	52.2	**0.003**

(Continued)

Table 1. (*Continued*)

Parameter	Fixed effects	numDF	denDF	F value	p value
	D	2	108	34.5	**0.003**
	T × L	2	108	0.65	0.68
	T × S × D	4	108	3.96	**0.01**
	L × S × D	2	108	0.75	0.64
	T × L × D	4	108	1.12	0.51
	T × L × S × D	4	108	2.74	0.05
Net photosynthetic rate	**T**	2	108	9.93	**0.003**
	L	1	108	408.96	**0.003**
	S	1	108	27.81	**0.003**
	D	2	108	2.61	0.15
	T × L	2	108	2.5	0.16
	T × S × D	4	108	0.52	0.79
	L × S × D	2	108	9.79	**0.002**
	T × L × D	4	108	0.80	0.68
	T × L × S × D	4	108	0.33	0.91
Chlorophyll *a*	T	2	108	2.40	0.2
	L	1	108	115.44	**0.003**
	S	1	108	118.50	**0.003**
	D	2	108	2.35	0.2
	T × L	2	108	1.56	0.35
	T × S × D	4	108	0.59	0.78
	L × S × D	2	108	2.79	0.13
	T × L × D	4	108	0.67	0.66
	T × L × S × D	4	108	1.11	0.52
De–epoxidation state (DPS)	**T**	2	108	6.9	**0.005**
	L	1	108	345.64	**0.003**
	S	1	108	167.16	**0.003**
	D	2	108	40.1	**0.003**
	T × L	2	108	5.27	**0.013**
	T × S × D	4	108	0.6	0.79
	L × S × D	2	108	15.4	**0.003**
	T × L × D	4	108	0.92	0.64
	T × L × S × D	4	108	0.40	0.87
Phlorotannins	**T**	2	108	4.45	**0.02**
	L	1	108	0.95	0.50
	S	1	108	148.17	**0.003**
	D	2	108	4.68	**0.02**
	T × L	2	108	0.14	0.91
	T × S × D	4	108	0.53	0.79
	L × S × D	2	108	0.06	0.95
	T × L × D	4	108	0.58	0.78
	T × L × S × D	4	108	0.61	0.78

Note: Tested values are the mean of means of replicates (*n* = 4). numDF: numerator degrees of freedom. denDF: denominator degrees of freedom.

follows: temperature – T; light – L; species – S; day – D. All values in the text are gives as mean ± standard deviation.

Growth (DW in g) is shown in Figure 2A. T, L, S, and D, as well as the interaction of T × L, significantly affected growth. Meristematic disks from both species showed no significant differences in DW at the beginning of the experiment. Both species gained more weight under high-light conditions compared to low-light conditions. Under high-light conditions, disks of both species became significantly heavier in the course of the experiment. Further, *Saccharina latissima* gained more weight at warm temperatures compared to 4°C. At 10°C, *S. latissima* was significantly heavier than *Agarum clathratum*.

Maximum quantum yield of photosystem II (F_v/F_m) (Figure 2B) was significantly affected by the fixed effects of T, L, S, and D, as well as the interaction between T × L and L × S × D. At the beginning of the experiment, F_v/F_m of all treatments within one species were within the same range, or recovered until the start of the MHW. For both species, F_v/F_m was lower under high light. This trend was intensified by cold temperatures and longer duration of the experiment. Generally, F_v/F_m values were higher for *S. latissima* (0.543–0.744) than for *A. clathratum* (0.409–0.728).

The dark respiration rate (μmol O_2 L^{-1} h^{-1} g_{WW}^{-1}; Figure 2C) was significantly influenced by T, L, S, and D as single fixed effects and T × S × D as interacting effect. For both species, dark respiration rates were lower under low-light compared to high-light conditions. At the peak of the MHW, the dark respiration rate of *A. clathratum* was highest, while after recovery it was lowest. In *S. latissima*, dark respiration rates were lowest under low-light conditions and 10°C throughout the experiment.

Net photosynthetic rates (μmol O_2 L^{-1} h^{-1} g_{WW}^{-1}; Figure 2D) were significantly affected by T, L, and S, as well as L × S × D. Light treatments had the strongest effect on both species' photosynthetic rates. Under high-light conditions, photosynthetic rates decreased during the experiment. Under low-light conditions, photosynthetic rates were negative before the MHW, increasing in the course of the experiment. Overall, the temperature effect on the photosynthetic rate was weak and only observed for *A. clathratum* at the beginning of the experiment (10°C > 4°C).

The chlorophyll *a* concentration (μg g_{DW}^{-1}; Figure 2E) was significantly affected by the fixed effects of L and S. In both species, chlorophyll *a* increased (trend) under low-light conditions, and decreased under high-light conditions in the course of the experiment (significant). Thereby, *A. clathratum* (1,788.4 ± 621 μg g_{DW}^{-1}) had significantly more chlorophyll *a* than *S. latissima* (1,041.1 ± 407 μg g_{DW}^{-1}).

The de-epoxidation state of xanthophyll cycle pigments (DPS; Figure 2F) was significantly affected by T, L, S, and D as well as the interactions of T × L and L × S × D. In both species, DPS was significantly lower under low-light conditions (0.043 ± 0.02) compared to high-light conditions (0.21 ± 0.15). Under low-light conditions, it did not change during the experiment in either species. Under high-light conditions, DPS was significantly higher in *A. clathratum* compared to *S. latissima*. The only temperature response was observed under high-light conditions, with 4°C being higher compared to warmer temperatures in *A. clathratum*.

The total phlorotannin content (mg g_{DW}^{-1}; Figure 2G) was affected by the single effects of T, S, and D. The mean phlorotannin content of *A. clathratum* of all treatments was 65.8 ± 10.2 mg g_{DW}^{-1}, thereby being about 150% higher than in *S. latissima* (30.5 ± 10.8 mg g_{DW}^{-1}), independently of the treatment.

In both species, the net photosynthetic rate correlated positively with the chlorophyll *a* content. This was significant in all cases,

Table 2. Summary of the impact of the interactive fixed effects (T: temperature; L: light; S: species; D: day) on pairwise comparisons of the physiology and biochemistry of kelps ($n = 4$). DW: growth as dry weight. F_v/F_m: maximum quantum yield of photosystem II. Resp: dark respiration rate. PS: net photosynthetic rate. Chl*a*: chlorophyll *a*. DPS: de-epoxidation state of xanthophyll cycle pigments. Phl: total phlorotannin content

T	L	S	D	DW	F_v/F_m	Resp	PS	Chl*a*	DPS	Phl.
TEMPERATURE	Low	Acla	6			–	–	–	–	–
	Low	Acla	18	–	–	(4 = 7) < 10	–	–	–	–
	Low	Acla	23	–	4 > 10	(4 = 7) > 10	–	–	–	–
	High	Acla	6	–	4 < (7 = 10)	(4 = 7) > 10	4 < 10	–	4 > (7 = 10)	–
	High	Acla	18	–	4 < (7 = 10)	–	4 < 10	–	4 > 7	–
	High	Acla	23	–	(4 = 10) < 7	7 > 10	–	–	–	–
	Low	Slat	6	–	–	(4 = 7) > 10	–	–	–	–
	Low	Slat	18		–	–	–	–	–	–
	Low	Slat	23	–	–	4 > 10	–	–	–	–
	High	Slat	6	–	4 < 7	–	–	–	–	–
	High	Slat	18	4 < 10	4 < (7 = 10)	–	–	(4 = 7) < 10	–	–
	High	Slat	23	4 < 7 < 10	4 < (7 = 10)	7 > 10	–	–	–	–
4	LIGHT	Acla	6	–	L > H	L < H	L < H	–	L < H	–
4		Acla	18	–	L > H	L < H	L < H	L > H	L < H	–
4		Acla	23	L < H	L > H	–	L < H	L > H	L < H	–
7		Acla	6	–	–	L < H	L < H	–	–	–
7		Acla	18	L < H	L > H	L < H	L < H	L > H	L < H	–
7		Acla	23	L < H	L > H	–	L < H	L > H	L < H	–
10		Acla	6	–	–	–	L < H	–	–	–
10		Acla	18	L < H	L > H	–	L < H	L > H	L < H	–
10		Acla	23	L < H	L > H	L < H	L < H	L > H	L < H	–
4		Slat	6	–	L > H	–	L < H	–	L < H	–
4		Slat	18	L < H	L > H	L < H	L < H	L > H	L < H	–
4		Slat	23	L < H	L > H	–	L < H	L > H	L < H	–
7		Slat	6	–	–	–	L < H	–	–	–
7		Slat	18	L < H	L > H	–	L < H	L > H	–	–
7		Slat	23	L < H	L > H	L < H	L < H	–	L < H	–
10		Slat	6	–	L > H	L < H	L < H	–	–	–
10		Slat	18	L < H	–	L < H	L < H	–	–	–
10		Slat	23	L < H	L > H	L < H	L < H	L > H	L < H	–
4	Low	SPECIES	6	–	Acla < Slat	–	–	Acla > Slat		Acla > Slat
4	Low		18	–	–	–	–	Acla > Slat		Acla > Slat
4	Low		23	–	–	–	–	Acla > Slat		Acla > Slat
4	High		6	–	Acla < Slat	Acla > Slat	Acla > Slat	Acla > Slat	Acla > Slat	Acla > Slat
4	High		18	–	Acla < Slat	–	–	Acla > Slat	Acla > Slat	Acla > Slat
4	High		23	–	Acla < Slat	–	–	–	Acla > Slat	Acla > Slat
7	Low		6	–	–	–	–	Acla > Slat		–
7	Low		18	–	–	Acla > Slat	–	Acla > Slat		–
7	Low		23	–	–	Acla < Slat	–	Acla > Slat		Acla > Slat
7	High		6	–	–	–	Acla > Slat	–		Acla > Slat
7	High		18	–	Acla < Slat	Acla > Slat	–	–	Acla > Slat	Acla > Slat
7	High		23	–	Acla < Slat	–	–	–	Acla > Slat	Acla > Slat

(Continued)

Table 2. (*Continued*)

T	L	S	D	DW	F_v/F_m	Resp	PS	Chl*a*	DPS	Phl.
10	Low		6	–	Acla < Slat	Acla > Slat	–	Acla > Slat		–
10	Low		18	–	–	Acla > Slat	–	Acla > Slat		Acla > Slat
10	Low		23	Acla < Slat	Acla < Slat	–	–	Acla > Slat		Acla > Slat
10	High		6	–	–	–	Acla > Slat	Acla > Slat		–
10	High		18	Acla < Slat	Acla < Slat	Acla > Slat	–	–	Acla > Slat	Acla > Slat
10	High		23	Acla < Slat	Acla < Slat	–	–	–	Acla > Slat	Acla > Slat
4	Low	Acla	DAY	6 < (18 = 23)	6 < (18 = 23)	–		–		–
4	Low	Slat		6 < 23	–	6 > (18 = 23)		–		–
4	High	Acla		6 < 18 < 23	(6 = 18) > 23	6 > 23	6 > (18 = 23)	6 > 23	(6 = 18) < 23	–
4	High	Slat		6 < 18 < 23	–	–		–		–
7	Low	Acla		–	–	–		–		–
7	Low	Slat		6 < 23	–	6 > 23		–		–
7	High	Acla		6 < 18 < 23	6 > 23	–	6 > (18 = 23)	6 > 23	(6 = 18) < 23	–
7	High	Slat		6 < 18 < 23	–	–		–	(6 = 18) < 23	–
10	Low	Acla		–	(6 = 23) < 18	18 > 6 > 23	6 < 23	6 < (18 = 23)		–
10	Low	Slat		6 < 23	–	–		–		–
10	High	Acla		6 < 18 < 23	(6 = 18) > 23	(6 = 23) < 18	6 > 18 > 23	6 > 23	6 < 18 < 23	–
10	High	Slat		6 < 18 < 23	–	(6 = 18) > 23		18 > 23		–

except for *S. latissima* under higher light conditions (*A. clathratum*: high light: ***p*** = **<0.001**, *t* = 5.01, *df* = 34; low light: ***p*** = **<0.001**, *t* = 3.75, *df* = 34; *S. latissima*: high light: *p* = 0.21, *t* = 1.27, *df* = 34; low light: ***p*** = **0.02**, *t* = 2.36, *df* = 34). Under high-light conditions, the chlorophyll *a* concentration and net photosynthetic rate decreased in the course of the experiment. Under low-light conditions, chlorophyll *a* concentrations and net photosynthetic rates increased during the experiment (Figure 3). In all treatments, disks became heavier over time.

DPS of both species correlated negatively with F_v/F_m in all treatments (*A. clathratum*: high light: ***p*** = **< 0.001**, *t* = −6.77, *df* = 34; low light: ***p*** = **0.03**, *t* = −2.3, *df* = 34; *S. latissima*: high light: ***p*** = **0.02**, *t* = −2.42, *df* = 34; low light: ***p*** = **0.01**, *t* = −2.82, *df* = 34).

Discussion

Due to ongoing climate change, the Arctic is one of the most affected and fastest changing regions in the world, with an increasing frequency of marine heatwaves (IPCC, 2023; Barkhordarian et al., 2024) and deteriorating light conditions in summer (Konik et al., 2021). In Arctic fjord systems, kelps act as foundation species and are challenged by changing conditions. Overall, kelps become more susceptible to additional stressors, when experiencing suboptimal temperature conditions (Wernberg et al., 2010). To be able to conserve these valuable ecosystems, it is important to understand how key species will respond to environmental changes (Lebrun et al., 2022), not only when single drivers change but also when multiple stressors interact. We designed a multifactorial experiment, comparing the reaction of two locally abundant kelp species (*Agarum clathratum, Saccharina latissima*) to summer heatwaves, when exposed to either low- or high-light conditions. The temperature and light treatments were based on measurements,

reflecting MHWs in clear and meltwater dominated fjords (GEM, 2023; Niedzwiedz and Bischof, 2023b). In this setup, tested light amplitudes were the stronger driver (compared to temperature amplitudes), affecting kelp performance. We found *A. clathratum* to be low-light-adapted, confirming Hypothesis 1. Thereby, both species showed the potential to acclimate to varying light conditions by adjusting their pigment composition and concentration. Contradicting Hypothesis 2, the kelps showed no general positive response to increased temperatures, but only in combination with high-light conditions, mitigating physiological stress. Under low-light conditions, we detected no temperature effect, which we consider to be likely due to overall light limitation. Being exposed to high-light conditions, cold temperatures intensified physiological stress levels, contradicting Hypothesis 3. We consider this to be likely due to the photosynthetic electron transport chains being saturated earlier at cold temperatures.

High-light stress is mitigated by warmer temperatures

In our experiment, both kelp species responded stronger to light variations than to the heatwave scenarios (Table 1). We based our treatment conditions on records by GEM (2023), classifying 4°C as summer in situ conditions (Supplement S2). Thereby, maximum quantum yield of photosystem II (F_v/F_m) was below 0.6 of all samples on day 4, indicating that field conditions caused emerging physiological and cellular stress levels in kelps (Dring et al., 1996; Murchie and Lawson, 2013). As optimum growth temperatures were reported between 10 and 15°C for both species (Bolton and Lüning, 1982; Egan et al., 1989; Simonson et al., 2015), this highlights the physiological limits at its cold distribution margins.

Under high-light conditions, F_v/F_m further decreased in the course of the experiment, only recovering under low-light
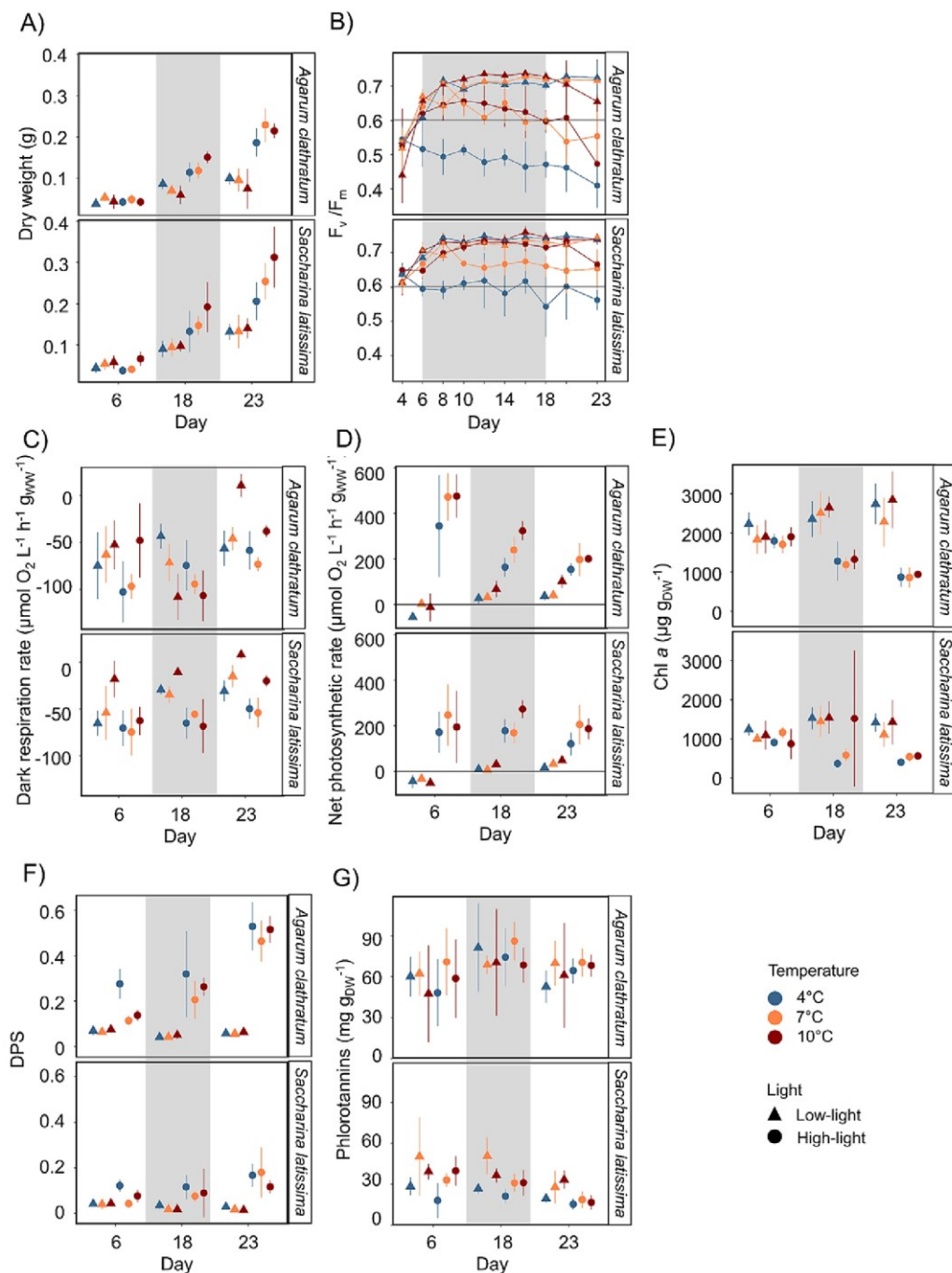
Sarina Niedzwiedz *et al.*

Figure 2. Physiological (A–D) and biochemical response (E–G) of *Agarum clathratum* and *Saccharina latissima* in the course of the experiment. Day 6: Wound healing and light acclimation. Day 18: heatwave (grey area). Day 23: recovery. Heatwave scenario: blue = 4°C; orange = 7°C; red = 10°C). Light conditions: triangle = low light, 3 µmol photon m^{-2} s^{-1}; circle = high light, 120 µmol photons m^{-2} s^{-1} ($n = 4$). Statistical results of the pairwise comparisons are summarized in Table 2. (A) Dry weight (g). (B) Maximum quantum yield of photosystem II (F_v/F_m). (C) Dark respiration rate (µmol O$_2$ L^{-1} h^{-1} g$_{WW}$$^{-1}$). Note that decreasing oxygen concentrations relate to increasing respiration rates. (D) Net photosynthetic rate (µmol O$_2$ L^{-1} h^{-1} g$_{WW}$$^{-1}$). Horizontal black line: 0 µmol O$_2$ L^{-1} h^{-1} g$_{WW}$$^{-1}$. (E) Chlorophyll *a* (µg g$_{DW}$$^{-1}$). (F) De-epoxidation state of xanthophyll cycle pigments (DPS). (G) Total phlorotannin concentration (mg g$_{DW}$$^{-1}$).

conditions (Figure 2B). Additionally, we measured significantly increasing DPS values in both species, when being exposed to high-light conditions (Figure 2F). The DPS of xanthophyll cycle pigments is an immediate reaction to protect the photosystem from

the formation of oxidative stress by the interconversion of violaxanthin to antheraxanthin to zeaxanthin (Demmig-Adams and Adams, 1996). High DPS values have been described as response to high-light stress in kelps (Demmig-Adams and Adams, 1996)
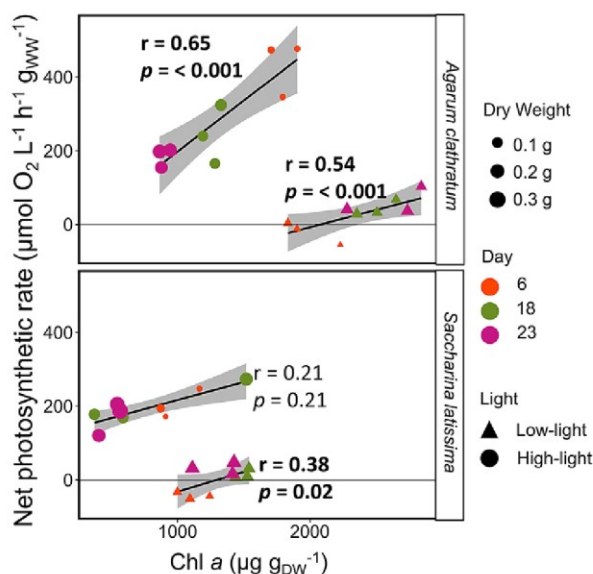
Figure 3. Linear dependency between the net photosynthetic rate (μmol O_2 L^{-1} h^{-1} g_{ww}^{-1}) vs. chlorophyll *a* content (Chl*a*, μg g_{DW}^{-1}) of *Agarum clathratum* and *Saccharina latissima* after different temperature and light treatments. Size: Dry weight (g). Color: day of the experiment: 6 (orange), 18 (green), 23 (pink). Light conditions: low light (3 μmol photon m^{-2} s^{-1}); high light (120 μmol photons m^{-2} s^{-1}) (n = 4). Grey area: 95% confidence interval; *r*: Pearson correlation coefficient. Significant correlations (*p* < 0.05) are marked in bold.

and correlating with decreasing F_v/F_m; this indicates increasing physiological stress levels under high-light conditions. As irradiances up to 186 μmol photons m^{-2} s^{-1} (max) at 15 m were measured in Nuup Kangerlua (Supplement S4), considering 120 μmol photons m^{-2} s^{-1} as "high" light seems contradictory. However, daily PAR cycles have to be considered. In our experiment, we mimicked polar day with 24 h constant light exposure to be able to draw general conclusions on Arctic ecosystems. At the sampling site on 15 m water depth, kelps were not exposed to PAR intensities >120 μmol photons m^{-2} s^{-1} for 24 h but rather 7.5 h (Supplement S4). Hence, the exposure of 120 μmol m^{-2} s^{-1} for 24 h, is causing high-light stress due to long photoperiod and the lack of a low-light recovery period. This emphasizes the necessity to not only consider mean PAR values but also variations in irradiance levels. Especially as variation in day length along the latitudinal gradient is one of the few factors that will not be affected by climate change, day length has to be considered to become a potential interacting stressor.

To mitigate high-light stress, both species acclimated by reducing their chlorophyll *a* concentration, which was significant for *A. clathratum*. This results in less electrons being transmitted into the electron transport chain, reducing the likelihood of reactive oxygen formation, and hence, oxidative stress (Kirk, 2011). The reduced chlorophyll *a* concentration correlated significantly with lower photosynthetic rates, despite which both species gained weight in the course of the experiment (Figure 3).

Thereby, the interaction of high-light conditions with high temperatures enhanced growth in *S. latissima*. As metabolic processes depend on a multitude of enzymatic reactions, they are characterized by the integration of the enzymatic properties, e.g., their temperature optimum for maximum capacity (Davison et al., 1991; Daniel et al., 2008). Highest growth rates for *S. latissima* were described between 10 and 15°C (Bolton and Lüning, 1982).

Therefore, actual temperature conditions during sampling and control temperatures (4°C) are well below its optimum temperature. With increasing temperature, the enzymatic capacity is increasing (Pörtner et al., 2005), leading to higher potential growth rates. Accordingly, temperature-dependent increased respiratory losses have to be considered (Niedzwiedz and Bischof, 2023a). However, as *S. latissima* was not light-limited under high-light conditions, it accumulated carbon, resulting in enhanced weight gain. In *A. clathratum*, we detected no impact of temperature on growth at high-light conditions, even though the optimum growth temperature was also described between 10 and 15°C (Simonson et al., 2015) and disks were not light-limited (high photosynthetic rates). We attribute this to the overall high stress level experienced at high-light conditions and higher respiratory losses (Figure 2C), compared to *S. latissima*.

Under low-light conditions, the increase in weight was lower compared to high-light conditions. This can be explained by lower overall photosynthetic rates (Figures 2D and 3), i.e. less carbon accumulation (Kirk, 2011). Longer exposure to low-light intensities resulted in a low-light acclimation of both species: We measured an increase in chlorophyll *a* concentration that significantly correlated with higher photosynthetic rates to meet cellular energy demands, resulting in a net carbon gain. Overall, light limitation might be a reason why elevated temperatures did not boost growth under low-light conditions.

As both kelp species grew significantly over time in all experimental treatments (Figure 2A), we conclude that they were not starved of nutrients, even though low nutrient concentrations were measured for June water masses in Nuup Kangerlua (Juul-Pedersen et al., 2015).

Herbivore deterrent in A. clathratum

Phlorotannins have been described as antioxidants that also have antimicrobial and antibacterial effects (Ford et al., 2019). Given the strong, correlating response in F_v/F_m and DPS to high-light conditions, we expected higher phlorotannin concentrations under high-light compared to low-light conditions. However, we found no significant response of phlorotannins to light conditions. The only clear overall pattern we detected were mean phlorotannin concentrations of *A. clathratum* being more than twice as high as in *S. latissima*.

In addition to their antioxidant potential, phlorotannins are reported to respond to grazing pressure, acting as herbivore deterrent (Amsler et al., 2009). In the field, we observed high grazing pressure of sea urchins, e.g., *Strongylocentrotus droebachiensis*, on the kelp forest, forming sea urchin barrens. We were not able to quantify the effect of sea urchins on the kelp forests in the course of this study, but observed *S. latissima* to be completely absent on these sea urchin barrens, while *A. clathratum* was regularly found in small stands (Vonnahme, Niedzwiedz, pers. obs.). This interspecific difference in feeding preference was also described by Vadas (1977). A possible reason for that might be the high concentrations of phlorotannins in *A. clathratum*.

Ecological implications – Plastic response

In our study, both kelp species showed stronger responses to the altered light conditions than to temperature changes. When discussing light conditions in Arctic fjords as consequence of climate change, different developments lead to opposing environmental conditions: Increased temperatures are leading to thinner and an early season breakup of sea ice, increasing the underwater

irradiance (Nicolaus et al., 2012; Payne and Roesler, 2019). In combination with cold temperatures, our findings suggest that this seems to reduce the expansion of temperate kelp species to higher latitudes. Glacial melt (Milner et al., 2017), permafrost thaw (Bintanja, 2018) and increased precipitation rates (Bintanja and Andry, 2017) are leading to extensive sediment plumes in summer and darkening fjords (Gattuso et al., 2020; Konik et al., 2021). High terrestrial and glacial runoff rates increase the concentration of suspended particles in the water column, limiting the annual cumulative irradiance (Konik et al., 2021). We detected reduced weight gain of both kelp species, when cultivated under low-light conditions. Niedzwiedz and Bischof (2023a), Bartsch et al. (2016) and Düsedau et al. (n.d.) described the reduction of the kelp maximum distribution depth in meltwater plume dominated fjord systems, indicating reduced kelp primary production in darkening Arctic fjords. Schlegel et al. (2023) highlighted that the interannual in situ PAR variability is too large to project clear long-term developments of Arctic fjord light conditions, strongly depending on season, timescale, and boundary conditions. The high variability in in situ PAR in combination with the strong response of kelps to light variations indicates a high variability of temperate kelp presence along Arctic coastal areas. Thereby, we detected dynamic responses in chlorophyll *a* concentration responding to light conditions to maintain a positive net photosynthetic rate (low-light) or reduce oxidative stress (high-light). We conclude that both kelp species show a high grade of phenotypic plasticity, having the potential to acclimate to low-light conditions, and potentially compensating reduced production rates up to a certain degree. We suggest a long-term experiment specifically targeting the light-dependent production of different kelp species. Additionally, systematic and quantitative studies should be conducted, comparing and monitoring fjords in different stages of cryosphere loss, verifying the experimental results in nature.

In our setup, assessing the effect of summer MHWs in Arctic environments on cold-temperate kelp species, we detect no immediate negative interactions of warm temperature in combination with low-light conditions (Arctic coastal areas in the presence of a sediment plume). On the contrary, elevated temperatures in combination with high-light conditions seemed to have positive effects on the kelps physiological state (e.g., enhanced weight gain), possibly by increasing the enzymatic activities and thereby reducing photo-damaging. This can be explained by temperatures being closer to the species optimum growth temperature of 10–15°C (Bolton and Lüning, 1982; Egan et al., 1989; Simonson et al., 2015). However, these temperature ranges have been described for populations of lower latitudes and Bennett et al. (2019) review that intraspecific temperature susceptibility can change depending on geographic location. While we did not assess temperature reaction norms, our results do not contradict the reported optima, as high physiological stress levels were mitigated by warmer temperatures, being closer to 10–15°C. Thereby, we want to highlight that the positive effect of warmer temperatures during the marine heatwave under high-light stress on kelp physiology and biochemistry only holds true for temperate-adapted species on their cold-distribution edge. Highly detrimental effects of marine heatwaves on kelp forests and ecosystems have been described in other regions (e.g., Wernberg et al., 2013; Smale, 2019; Filbee-Dexter et al., 2020; Smith et al., 2023). As shown by Bass et al. (2023), the effect of sudden temperature increases in combination with varying light conditions on kelp species strongly depends on species and environmental conditions (temperature, light, season).

After conducting an Arctic summer experiment, we further want to highlight the necessity to explore effects of warming temperatures and MHWs during polar night. The studies by Gordillo et al. (2022) and Scheschonk et al. (2019) have described the detrimental effect of Arctic winter warming on kelps, given the monthlong period of darkness. Gagnon et al. (2005) reported *A. clathratum* growing during very low temperatures during spring and fall. Liesner et al. (2020) and Gauci et al. (2022) described reduced plasticity of *Laminaria digitata* when experiencing higher temperatures during development across generations and Martins et al. (2017) showed different thermal optima for different life stages.

Summarizing, we found light to induce stronger physiological and biochemical responses in both kelp species, with temperature either intensifying or mitigating the light-induced species-specific reactions. Thereby, *A. clathratum* was documented to be adapted to lower light intensities than *S. latissima,* enabling *A. clathratum* to maintain a positive net photosynthetic rate at lower light intensities. This enables *A. clathratum* to grow deeper in the water column than *S. latissima* (Vonnahme, Niedzwiedz, pers. obs. in Nuup Kanger-lua), and further implying that it can grow earlier/later in season. However, we found *A. clathratum* to have the potential to acclimate to higher light intensities. Gagnon et al. (2005) reported *A. clathratum* to be very weak in the interspecific competition in shallow waters. Therefore, we hypothesize that *A. clathratum* might have been outcompeted to deeper water depths. Further, Gagnon et al. (2005) reported *A. clathratum* to establish in the presence of grazing pressure.

In an Arctic coastal area with warmer temperatures, less light due to higher sediment inputs and potentially higher grazing pressure, our findings suggest that *A. clathratum* will become more dominant at shallower depths, albeit at lower overall total biomass (assumption based on dry weight measurements). Ameralik fjord, a neighboring fjord to Nuup Kangerlua, represents this scenario (Meire et al., 2023). As expected, *A. clathratum* has indeed been found to acclimate to higher light conditions, occurring at depths up to the intertidal zone and becoming dominant over *S. latissima* (Vonnahme, pers. obs.). These conclusions add to the findings of Simonson et al. (2015), stating that at their warm distribution range (summer sea surface temperature: >18°C; Nova Scotia) *A. clathratum* might have a competitive advantage over *S. latissima* in the future. While the general ecosystem services of a kelp forest would prevail, changes in the kelp forests extent and species composition might have cascading effects on the entire ecosystem, entailing a change in biodiversity and biotic interactions of kelp associated species (Bégin et al., 2004; Smale et al., 2015) or a reduction of energy transfer to high trophic levels (Blain and Gagnon, 2014; Dethier et al., 2014).

References

Adey WH and Steneck RS (2001) Thermogeography over time creates biogeographic regions: A temperature/space/time-integrated model and an abundance-weighted test for benthic marine algae. *Journal of Phycology* 37, 677–698. https://doi.org/10.1046/j.1529-8817.2001.00176.x.

Amsler CD, Iken K, McClintock JB and Baker BJ (2009) Defenses of polar macroalgae against herbivores and biofoulers. *Botanica Marina* 52, 535–545. https://doi.org/10.1515/BOT.2009.070.

Assis J, Serrão EA, Duarte CM, Fragkopoulou E and Krause-Jensen D (2022) Major expansion of marine forests in a warmer Arctic. *Frontiers in Marine Science* 9, 850368. https://doi.org/10.3389/fmars.2022.850368.

Barkhordarian A, Nielsen DM, Olonscheck D and Baehr J (2024) Arctic marine heatwaves forced by greenhouse gases and triggered by abrupt sea-ice melt. *Communications Earth & Environment* 5, 57. https://doi.org/10.1038/s43247-024-01215-y.

Bartsch I, Paar M, Fredriken S, Schwanitz M, Daniel C, Hop H and Wiencke C (2016) Changes in kelp forest biomass and depth distribution in Kongsfjorden, Svalbard, between 1996–1998 and 2012–2014 reflect Arctic warming. *Polar Biology* 39, 2021–2036. https://doi.org/10.1007/s00300-015-1870-1.

Bass AV, Smith KE and Smale DA (2023) Marine heatwaves and decreased light availability interact to erode the ecophysiological performance of habitat-forming kelp species. *Journal of Phycology* 59, 481–495. https://doi.org/10.1111/jpy.13332.

Bégin C, Johnson LE and Himmelman JH (2004) Macroalgal canopies: Distribution and diversity of associated invertebrates and effects on the recruitment and growth of mussels. *Marine Ecology Progress Series* 271, 121–132. https://doi.org/10.3354/meps271121.

Bennett S, Duarte CM, Marbà N and Wernberg T (2019) Integrating within-species variation in thermal physiology into climate change ecology. *Philosophical Transactions of the Royal Society B* 374, 20180550. https://doi.org/10.1098/rstb.2018.0550.

Bintanja R (2018) The impact of Arctic warming on increased rainfall. *Science Reports* 8, 16001. https://doi.org/10.1038/s41598-018-34450-3.

Bintanja R and Andry O (2017) Towards a rain-dominated Arctic. *Nature Climate Change* 7, 263–268. https://doi.org/10.1038/NCLIMATE3240.

Blain C and Gagnon P (2014) Canopy-forming seaweeds in urchin-dominated systems in eastern Canada: Structuring forces or simple prey for keystone species? *PLoS One* 9, e98204. https://doi.org/10.1371/journal.pone.0098204.

Blain CO and Shears NT (2019) Seasonal and spatial variation in photosynthetic response of the kelp *Ecklonia radiata* across a turbidity gradient. *Photosynthesis Research* 140, 21–38. https://doi.org/10.1007/s11120-019-00636-7.

Bolton JJ and Lüning K (1982) Optimal growth and maximal survival temperatures of Atlantic *Laminaria* species (Phaeophyta) in culture. *Marine Biology* 66, 89–94. https://doi.org/10.1007/BF00397259.

Bringloe TT, Verbruggen H and Saunders GW (2020) Unique biodiversity in Arctic marine forests is shaped by diverse recolonization pathways and far northern glacial refugia. *Proceedings of the National Academy of Science* 117, 22590–22596. https://doi.org/10.1073/pnas.2002753117.

Bringloe TT, Wilkinson DP, Goldsmit J, Savoie AM, Filbee-Dexter K, Macgregor KA, Howland KL, McKindsey CW and Verbruggen H (2022) Arctic marine forest distribution models showcase potentially severe habitat losses for cryophilic species under climate change. *Global Change Biology* 28, 3711–3727. https://doi.org/10.1111/gcb.16142.

Chevin L-M, Lande R and Mace GM (2010) Adaptation, plasticity, and extinction in a changing environment: Towards a predictive theory. *PLoS Biology* 8, 4. https://doi.org/10.1371/journal.pbio.1000357.

Clarke A and Fraser KPP (2004) Why does metabolism scale with temperature? *Functional Ecology* 18, 243–251. https://doi.org/10.1111/j.0269-8463.2004.00841.x.

Colombo-Pallotta MF, García-Mendoza E and Ladah LB (2006) Photosynthetic performance, light absorption, and pigment composition of *Macrocystis pyrifera* (Laminariales, Phaeophyceae) blades from different depths. *Journal of Phycology* 42, 1225–1234. https://doi.org/10.1111/j.1529-8817.2006.00287.x.

Cruces E, Huovinen P and Gómez I (2013) Interactive effects of UV radiation and enhanced temperature on photosynthesis, phlorotannin induction and antioxidant activities of two sub-Antarctic brown algae. *Marine Biology* 160, 1–13. https://doi.org/10.1007/s00227-012-2049-8.

Daniel RM, Danson MJ, Eisenthal R, Lee CK and Peterson ME (2008) The effect of temperature on enzyme activity: New insights and their implications. *Extremophiles* 12, 51–59. https://doi.org/10.1007/s00792-007-0089-7.

Davison IR, Greene RM and Podolak EJ (1991) Temperature acclimation of respiration and photosynthesis in the brown algae *Laminaria saccharina*. *Marine Biology* 110, 449–454. https://doi.org/10.1007/s00792-007-0089-7.

Demmig-Adams B and Adams WW (1996) Xanthophyll cycle and light stress in nature: Uniform response to excess direct sunlight among higher plant species. *Planta* 198, 460–470. https://doi.org/10.1007/BF00620064.

Dethier MN, Brown AS, Burgess S, Eisenlord ME, Galloway AWE, Kimber J, Lowe AT, O'Neil CM, Raymond WW, Soik EA and Duggins DO (2014) Degrading detritus: Changes in food quality of aging kelp tissue varies with species. *Journal of Experimental Marine Biology and Ecology* 460, 72–79. https://doi.org/10.1016/j.jembe.2014.06.010.

Dring MJ, Makarov V, Schoschina E, Lorenz M and Lüning K (1996) Influence of ultraviolet-radiation on chlorophyll fluorescence and growth in different life-history stages of three Laminaria species (Phaeophyta). *Marine Biology* 126, 183–191. https://doi.org/10.1007/BF00347443.

Dumortier B-C (1822) *Observations botaniques, dédiées à la Société d'Horticulture de Tourney.* Tourney: Commentationes botanicae.

Düsedau L, Fredriken S, Brand M, Fischer P, Karsten U, Bischof K, Savoie A and Bartsch I (n.d.) *Kelp forest dynamics in Kongsfjorden (Svalbard) across 25 years of Arctic warming. Ecology and Evolution* (in revision).

Eckman JE, Duggins DO and Sewell AT (1989) Ecology of understory kelp environments. I. Effects of kelps on flow and particle transport near the bottom. *Journal of Experimental Marine Biology and Ecology* 129, 173–187. https://doi.org/10.1016/0022-0981(89)90055-5.

Egan B, Vlasto A and Yarish C (1989) Seasonal acclimation to temperature in *Laminaria longicruris* de la Pyl. (Phaeophyta). *Journal of Experimental Marine Biology and Ecology* 129, 1–16. https://doi.org/10.1016/0022-0981(89)90059-2.

England MR, Eisenman I, Lutsko NJ and Wagner TJW (2021) The recent emergence of Arctic amplification. *Geophysical Research Letters* 48, e2021GL094086. https://doi.org/10.1029/2021GL094086.

Filbee-Dexter K and Wernberg T (2018) Rise of turfs: A new battlefront for globally declining kelp forests. *Bioscience* 68, 64–76. https://doi.org/10.1093/biosci/bix147.

Filbee-Dexter K, Wernberg T, Fredriksen S, Norderhaug KM and Pedersen MF (2019) Arctic kelp forests: Diversity, resilience and future. *Global and Planetary Change* 172, 1–14. https://doi.org/10.1016/j.gloplacha.2018.09.005.

Filbee-Dexter K, Wernberg T, Grace, SP, Thormar J, Fredriksen S, Narvaez CN, Feehan CJ and Norderhaug KM (2020) Marine heatwaves and the

collapse of marginal North Atlantic kelp forests. *Scientific Reports* **10**, 13388. https://doi.org/10.1038/s41598-020-70273-x.

Ford L, **Theodoridou K**, **Sheldrake GN and Walsh PJ** (2019) A critical review of analytical methods used for the chemical characterisation and quantification of phlorotannin compounds in brown seaweeds. *Phytochemical Analysis* **30**, 587–599. https://doi.org/10.1002/pca.2851.

Fortes MD and Lüning K (1980) Growth rates of North Sea macroalgae in relation to temperature, irradiance and photoperiod. *Helgoländer Meeresuntersuchungen* **34**, 15–29. https://doi.org/10.1007/BF01983538.

Fragkopoulou E, **Serrão EA**, **De Clerck O**, **Costello MJ**, **Araújo MB**, **Buarte CM**, **Krause-Jensen D and Assis J** (2022) Global biodiversity patterns of marine forests of brown macroalgae. *Global Ecology and Biogeography* **31**, 636–648. https://doi.org/10.1111/geb.13450.

Gagnon P, **Johnson LE and Himmelman JH** (2005) Kelp patch dynamics in the face of intense herbivory: Stability of *Agarum clathratum* (Phaeophyta) stands and associated flora on urchin barrens. *Journal of Phycology* **41**, 498–505. https://doi.org/10.1111/j.1529-8817.2005.00078.x.

Gattuso J-P, **Gentili B**, **Antoine D and Doxaran D** (2020) Global distribution of photosynthetically available radiation on the seafloor. *Earth System Science Data* **12**, 1697–1709. https://doi.org/10.5194/essd-12-1697-2020.

Gauci C, **Bartsch I**, **Martins N and Liesner D** (2022) Cold thermal priming of *Laminaria digitata* (Laminariales, Phaeophyceae) gametophytes enhances gametogenesis and thermal performance of sporophytes. *Frontiers in Marine Science* **9**, 862923. https://doi.org/10.3389/fmars.2022.862923.

GEM (2023) Marine Basis Nuuk – Water column – CTD measurements. https://doi.org/10.17897/KMEK-TK21.

Gordillo FJL, **Carmona R and Jiménez C** (2022) A warmer Arctic compromises winter survival of habitat-forming seaweeds. *Frontiers in Marine Science* **8**, 750209. https://doi.org/10.3389/fmars.2021.750209.

Hobday AJ, **Alexander LV**, **Perkins SE**, **Smale DA**, **Straub SC**, **Oliver ECJ**, **Benthuysen JA**, **Burrows MT**, **Donat MG**, **Feng M**, **Holbrook NJ**, **Moore PJ**, **Scannell HA**, **Gupta AS and Wernberg T** (2016) A hierarchical approach to defining marine heatwaves. *Progress in Oceanography* **141**, 227–238. https://doi.org/10.1016/j.pocean.2015.12.014.

Hurd C, **Harrison PJ**, **Bischof K and Lobban CS** (2014) *Seaweed Ecology and Physiology*. Cambridge: Cambridge University Press.

IPCC (2023) Summary for policymakers. In Lee H and Romero J (eds.), *Climate Change 2023: Synthesis Report. Contribution of Working Groups I, II and III to the Sixth Assessment Report of the Intergovernmental Panel on Climate Change (Core Writing Team)*. Geneva: IPCC, pp. 1–34. https://doi.org/10.59327/IPCC/AR6-9789291691647.001.

Juul-Pedersen T, **Arendt KE**, **Mortensen J**, **Blicher ME**, **Søgaard DH and Rysgaard S** (2015) Seasonal and interannual phytoplankton production in a sub-Arctic tidewater outlet glacier fjord, SW Greenland. *Marine Ecology Progress Series* **524**, 27–38. https://doi.org/10.3354/meps11174.

King NG, **McKeown NJ**, **Smale DA and Moore PJ** (2018) The importance of pheotypic plasticity and local adaptation in driving intraspecific variability in thermal niches of marine macrophytes. *Ecography* **41**, 1469–1484. https://doi.org/10.1111/ecog.03186.

Kirk JTO (2011) *Light and Photosynthesis*. Cambridge: Cambridge University Press.

Koch K, **Thiel M**, **Tellier F**, **Hagen W**, **Graeve M**, **Tala F**, **Laeseke P and Bischof K** (2015) Species separation within the *Lessonia nigrescens* complex (Phaeophyceae, Laminariales) is mirrored by ecophysiological traits. *Botanica Marina* **58**, 81–92. https://doi.org/10.1515/bot-2014-0086.

Konik M, **Darecki M**, **Pavlov AK**, **Sagan S and Kowalczuk P** (2021) Darkening of the Svalbard fjords waters observed with satellite ocean color imagery in 1997–2019. *Frontiers in Marine Science* **8**, 699318. https://doi.org/10.3389/fmars.2021.699318.

Kültz D (2005) Molecular and evolutionary basis of the cellular stress response. *Annual Review of Physiology* **67**, 225–257. https://doi.org/10.1146/annurev.physiol.67.040403.103635.

Lane CE, **Mayes C**, **Druehl LD and Saunders GW** (2006) A multi-gene molecular investigation of the kelp (Laminariales, Phaeophyceae) supports substantial taxonomic re-organization. *Journal of Phycology* **42**, 493–512. https://doi.org/10.1111/j.1529-8817.2006.00204.x.

Lebrun A, **Comeau S**, **Gazeau F and Gattuso J-P** (2022) Impact of climate change on Arctic macroalgal communities. *Global and Planetary Change* **219**, 103980. https://doi.org/10.1016/j.gloplacha.2022.103980.

Lenth RV (2021) emmeans: Estimated marginal means, aka least-squares means. R package version 1.7.0. Available at https://CRAN.R-project.org/package=emmeans.

Liesner D, **Sharma LN**, **Diehl N**, **Valentin K and Bartsch I** (2020) Thermal plasticity of the kelp *Laminaria digitata* (Phaeophyceae) across life cycle stages reveals the importance of cold seasons for marine forests. *Frontiers in Marine Science* **7**, 456. https://doi.org/10.3389/fmars.2020.00456.

Lüning K (1990) *Seaweeds: Their Environment, Biogeography, and Ecophysiology*. New York: John Wiley & Sons.

Martins N, **Tanttu H**, **Pearson GA**, **Serrão E and Bartsch I** (2017) Interactions of daylength, temperature and nutrients affect thresholds for life stage transition in the kelp *Laminaria digitata* (Phaeophyceae). *Botanica Marina* **60**(2), 109–121. https://doi.org/10.1515/bot-2016-0094.

McDevit DC and Saunders GW (2010) A DNA barcode examination of the Laminariaceae (Phaeophyceae) in Canada reveals novel biogeographical and evolutionary insights. *Phycologia* **49**, 235–248. https://doi.org/10.2216/PH09-36.1.

Meire L, **Paulsen ML**, **Meire P**, **Rysgaard S**, **Hopwood MJ**, **Sejr MK**, **Stuart-Lee A**, **Sabbe K**, **Stock W and Mortensen J** (2023) Glacier retreat alters downstream fjord ecosystem structure and function in Greenland. *Nature Geoscience* **16**, 671–674. https://doi.org/10.1038/s41561-023-01218-y.

Milner AM, **Khamis K**, **Battin TJ**, **Brittain JE**, **Barrand NE**, **Füreder L**, **Cauvy-Fraunie S**, **Gíslason GM**, **Jacobsen D**, **Hannah DM**, **Hodson AJ**, **Hood E**, **Lencioni V**, **Ólafsson JS**, **Robinson CT**, **Tranter M and**, **Brown LE** (2017) Glacier shrinkage driving global changes in downstream systems. *Proceedings of the National Academy of Science* **114**, 9770–9778. https://doi.org/10.1073/pnas.1619807114.

Murchie EH and Lawson T (2013) Chlorophyll fluorescence analysis: A guide to good practice and understanding some new applications. *Journal of Experimental Botany* **64**, 3983–3998. https://doi.org/10.1093/jxb/ert208.

Nicolaus M, **Katlein C**, **Maslanik J and Hendricks S** (2012) Changes in Arctic Sea ice result in increasing light transmittance and absorption. *Geophysical Research Letters* **39**, L24501. https://doi.org/10.1029/2012GL053738.

Niedzwiedz S and Bischof K (2023a) Glacial retreat and rising temperatures are limiting the expansion of temperate kelp species in the future Arctic. *Limnology and Oceanography* **68**, 816–830. https://doi.org/10.1002/lno.12312.

Niedzwiedz S and Bischof K (2023b) *Irradiance data at different depths and sites for field sampling the Arctic fjord Kongsfjorden*. Pangaea Database. https://doi.org/10.1594/PANGAEA.951173.

Oliver ECJ, **Donat MG**, **Burrows MT**, **Moore PJ**, **Smale DA**, **Alexander LV**, **Benthuysen JA**, **Feng M**, **Gupta AS**, **Hobday AJ**, **Holbrook NJ**, **Perkins-Kiripatrick SE**, **Scannell HA**, **Straub SC and Wernberg T** (2018) Longer and more frequent marine heatwaves over the past century. *Nature Communications* **9**, 1324. https://doi.org/10.1038/s41467-018-03732-9.

Payne CM and Roesler CS (2019) Characterizing the influence of Atlantic water intrusion on water mass formation and phytoplankton in Kongsfjorden, Svalbard. *Continental Shelf Research* **191**, 104005. https://doi.org/10.1016/j.csr.2019.104005.

Pörtner HO and Farrell AP (2008) Physiology and climate change. *Science* **322**, 690–692. https://doi.org/10.1126/science.116315.

Pörtner HO, **Lucassen M and Storch D** (2005) Metabolic biochemistry: Its role in thermal tolerance and in the capacities of physiological and ecological function. *Fish Physiology* **22**, 79–154. https://doi.org/10.1016/S1546-5098(04)22003-9.

Previdi M, **Janoski TP**, **Chiodo G**, **Smith KL and Polvani LM** (2020) Arctic amplification: A rapid response to radiative forcing. *Geophysical Research Letter* **47**, e2020GL089933. https://doi.org/10.1029/2020GL089933.

Previdi M, **Smith KL and Polvani LM** (2021) Arctic amplification of climate change: A review of underlying mechanisms. *Environmental Research Letters* **16**, 093003. https://doi.org/10.1088/1748-9326/ac1c29.

R Core Team (2021) R: A language and environment for statistical computing. R Foundation for Statistical Computing. Available at https://www.R-project.org/.

Richter A, Rysgaard S, Dietrich R, Mortensen J and Petersen D (2011) Coastal tides in West Greenland derived from tide gauge records. *Ocean Dynamics* **61**, 39–49. https://doi.org/10.1007/s10236-010-0341-z.

Ruthrof KX, Breshears DD, Fontaine JB, Froend RH, Matusick G, Kala J, Miller BP, Mitchell PJ, Wilson SK, van Keulen M, Enright NJ, Law DJ, Wernberg T and Hardy GEStJ (2018) Subcontinental heat wave triggers terrestrial and marine, multi-taxa responses. *Scientific Reports* **8**, 13094. https://doi.org/10.1038/s41598-018-31236-5.

Scheschonk L, Becker S, Hehemann J-H, Diehl N, Karsten U and Bischof K (2019) Arctic kelp eco-physiology during the polar night in the face of global climate warming: A crucial role for laminarin. *Marine Ecology Progress Series* **611**, 59–74. https://doi.org/10.3354/meps12860.

Schlegel R, Singh RK, Gentilli B, Bélanger S, Castro de la Guardia L, Krause-Jensen D, Miller CA, Sejr M and Gattuso J-P (2023) Underwater light environment in Arctic fjords. *Earth System Science Data* (preprint). https://doi.org/10.5194/essd-2023-462.

Simonson EJ, Scheibling RE and Metaxas A (2015) Kelp in hot water: I. Warming seawater temperature induces weakening and loss of kelp tissue. *Marine Ecology Progress Series* **537**, 89–104. https://doi.org/10.3354/meps11438.

Smale DA (2019) Impacts of ocean warming on kelp forest ecosystems. *New Phytologist* **225**, 1447–1454. https://doi.org/10.1111/nph.16107.

Smale DA, Werberg T, Yunnie ALE and Vance T (2015) The rise of *Laminaria ochroleuca* in the Western English Channel (UK) and comparisons with its competitor and assemblage dominant *Laminaria hyperborea*. *Marine Ecology* **36**, 1033–1044. https://doi.org/10.1111/maec.12199.

Smith KE, Burrows MT, Hobday AJ, King NG, Moore PJ, Gupta AS, Thomsen MS, Wernberg T and Smale DA (2023) Biological impacts of marine heatwaves. *Annual Review of Marine Science* **15**, 119–145. https://doi.org/10.1146/annurev-marine-032122-121437.

Sorte CJB, Fuller A and Bracker MES (2010) Impacts of a simulated heat wave on composition of a marine community. *Oikos* **119** 1909–1918. https://doi.org/10.1111/j.1600-0706.2010.18663.x.

Straub SC, Wernberg T, Thomason MS, Moore PJ, Burrows MT, Harvey BP and Smale DA (2019) Resistance, extinction, and everything in between – The diverse responses of seaweeds to marine heatwaves. *Frontiers in Marine Science* **6**, 763. https://doi.org/10.3389/fmars.2019.00763.

Teagle H, Hawkins SJ, Moore PJ and Smale DA (2017) The role of kelp species as biogenic habitat formers in coastal marine ecosystems. *Journal of Experimental Marine Biology and Ecology* **492**, 81–98. https://doi.org/10.1016/j.jembe.2017.01.017.

Vadas RL (1977) Preferential feeding: And optimization strategy in sea urchins. *Ecological Monographs* **47**, 337–371. https://doi.org/10.2307/1942173.

Vranken S, Wernberg T, Scheben A, Severn-Ellis AA, Batley J, Bayer PE, Edwards D, Wheeler D and Coleman MA (2021) Genotype-environment mismatch of kelp forests under climate change. *Molecular Ecology* **30**, 3730–3746. https://doi.org/10.1111/mec.15993.

Wernberg T, Bennett S, Babcock RC, de Bettignies T, Cure K, Depczynski M, Dufois F, Fromont J, Fulton CJ, Hovey RK, Harvey ES, Holmes TH, Kendrick GA, Radford B, Santana-Garcon J, Saunders BJ, Smale DA, Thomsen MS, Tuckett CA, Tuya F, Vanderklift MA and Wilson S (2016) Climate-driven regime shift of a temperate marine ecosystem. *Climate Change* **353**, 169–172. https://doi.org/10.1126/science.aad8745.

Wernberg T, Krumhansl K, Filbee-Dexter K and Pedersen MF (2019) Status and trends for the world's kelp forests. In Sheppard C (ed.), *World Seas: An Environmental Evaluation*. Amsterdam: Elsevier, pp. 57–78. https://doi.org/10.1016/B978-0-12-%20805052-1.00003-6.

Wernberg T, Smale DA, Tuya F, Thomsen MS, Langlois TJ, de Bettignies T, Bennett S and Rousseaux CS (2013) An extreme climatic event alters marine ecosystem structure in a global biodiversity hotspot. *Nature Climate Change* **3**, 78–82. https://doi.org/10.1038/NCLIMATE1627.

Wernberg T, Thomsen MS, Tuya F, Kendrick GA, Staehr PA and Toohey BD (2010) Decreasing resilience of kelp bends along a latitudinal temperature gradient: Potential implications for a warmer future. *Ecology Letters* **13**, 685–694. https://doi.org/10.1111/j.1461-0248.2010.01466.x.

Wright SW, Jeffrey SW, Mantoura RFC, Llewellyn CA, Bjørnland T, Repeta D and Welschmeyer N (1991) Improved HPLC method for the analysis of chlorophylls and carotenoids from marine phytoplankton. *Marine Ecology Progress Series* **77**, 183–196. https://doi.org/10.3354/meps077183.

_____

Supplementary material

Title of Article:

Light-mediated temperature susceptibility of kelp species (*Agarum clathratum*, *Saccharina latissima*) in an Arctic summer heatwave scenario

Authors:

Sarina Niedzwiedz[1*], Tobias Reiner Vonnahme[2], Thomas Juul-Pedersen[2], Kai Bischof[1], Nora Diehl[1*]

*corresponding authors: sarina@uni-bremen.de / ndiehl@uni-bremen.de

Affiliation:

[1]Marine Botany, Faculty of Biology and Chemistry & MARUM, University of Bremen, 28359 Bremen, Germany

[2]Greenland Climate Research Centre, Greenland Institute for Natural Resources (GINR), Nuuk, Greenland

_____

S1: Video transect (by Tobias Reiner Vonnahme) through a kelp forest near Nuuk (01.05.2022) taken 0.5 m (+-0.5m) over the bottom or kelp canopy. The transect starts at about 12 m water depth and ends at the surface. Between ca.12 m and 10 m (2:08 min) the kelp species *Agarum clathratum*, *Saccharina latissima*, and *Alaria esculenta* dominate. Between ca. 5 m (2:35 min) and 2 m, *A. clathratum* is absent, while and first-year *A. esculenta* is most abundant. Laminaria sp. becomes increasingly abundant from ca 3-1m depth.
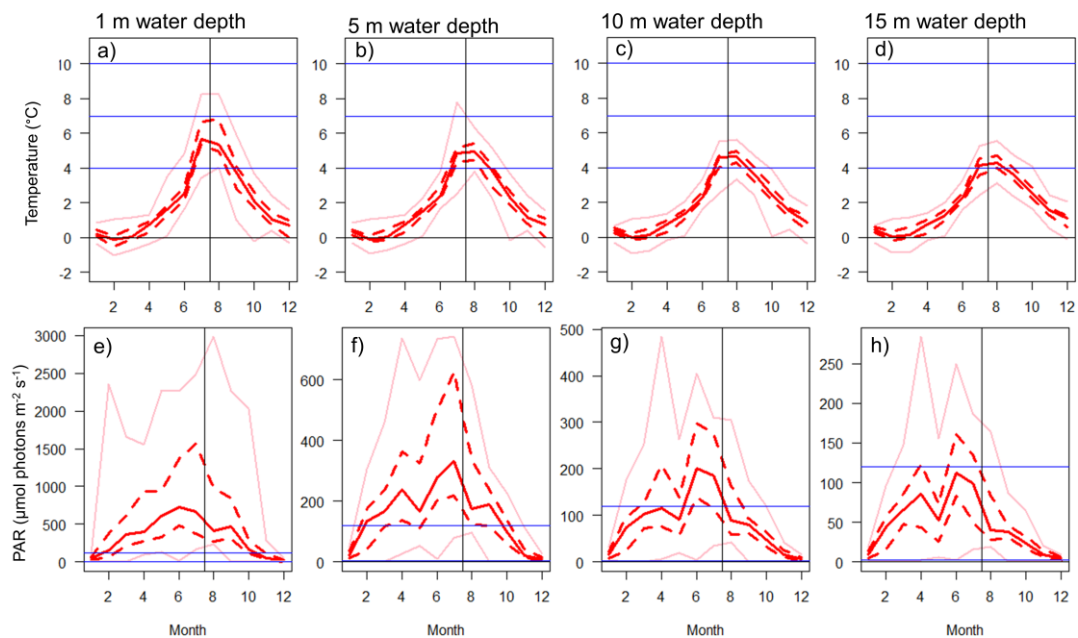
S2: Monthly temperature (a-d) and photosynthetically available radiation (PAR; µmol photons m^{-2} s^{-1}) (e-h) from a marine monitoring station (GF3, G-E-M.dk/data; https://doi.org/10.17897/KMEK-TK21) showing median (solid red line), interquartile ranges (dotted lines), and the total range (light red) of the measurements at 1 m (a,e), 5 m (b,f), 10 m (c,g), and 15 m (d,h) depth between 2005 and 2021 at the nearby marine monitoring station (G-E-M.dk/data). Treatment light intensities and temperatures are shown as blue lines.
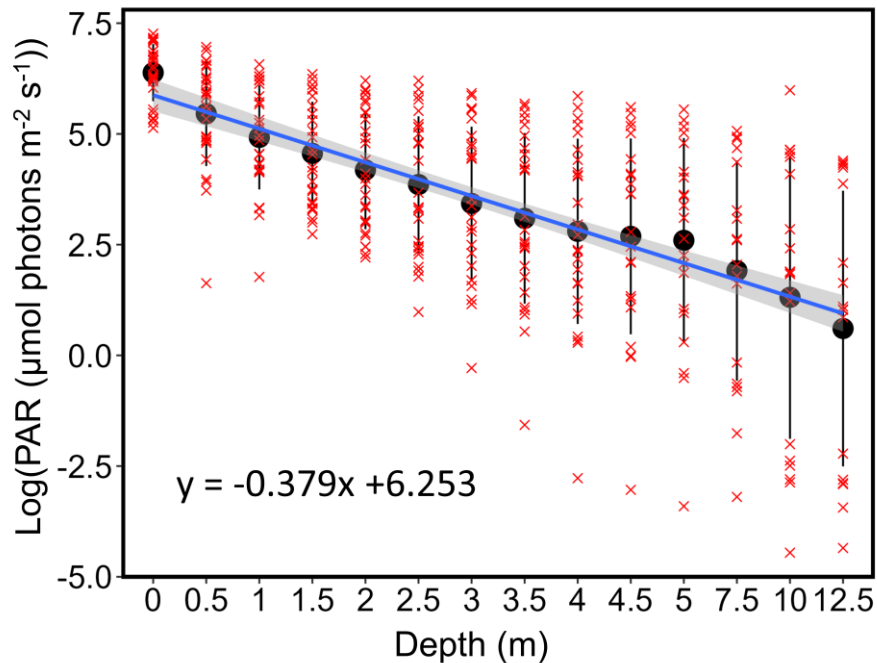
S3: Logarithm of photosynthetically available light (PAR) over water depth (m) in Kongsfjorden, Svalbard. Red crosses: single measurements. Black circles: Mean PAR±SD. Blue line: linear model of PAR intensities over depth ±95 % confidence interval. Data from Niedzwiedz & Bischof (2023b) https://doi.org/10.1594/PANGAEA.951173. The experiment's low-light conditions (3 µmol photons m^{-2} s^{-1}) are at ~15 m water depth.
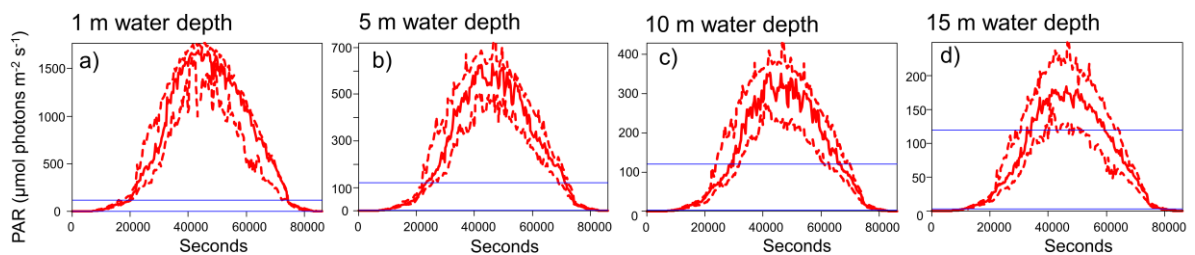
S4: Estimates of mean daily (sec) photosynthetically available radiation (PAR; µmol photons m^{-2} s^{-1}) at 1 (a), 5 (b), 10 (c) and 15 (d) m depth in July since 2008 shown as median (solid red line) and interquartile ranges (dotted red line). Estimates are based on PAR measurements at 2 m over the bottom from ClimateBasis Nuuk (https://doi.org/10.17897/8Z2W-D993, Asiaq) and light attenuation based on PAR profiles measured at a nearby marine monitoring station (GF3, G-E-M.dk/data; https://doi.org/10.17897/KMEK-TK21). Treatment light intensities are shown as blue horizontal lines.

PUBLICATION IV

Photoperiod and temperature interactions drive the latitudinal distribution of kelps under climate change

Nora Diehl, Philipp Laeseke, Inka Bartsch, Margot Bligh, Hagen Buck-Wiese, Jan-Hendrik Hehemann, Sarina Niedzwiedz, Niklas Plag, Ulf Karsten, Tifeng Shan, Kai Bischof

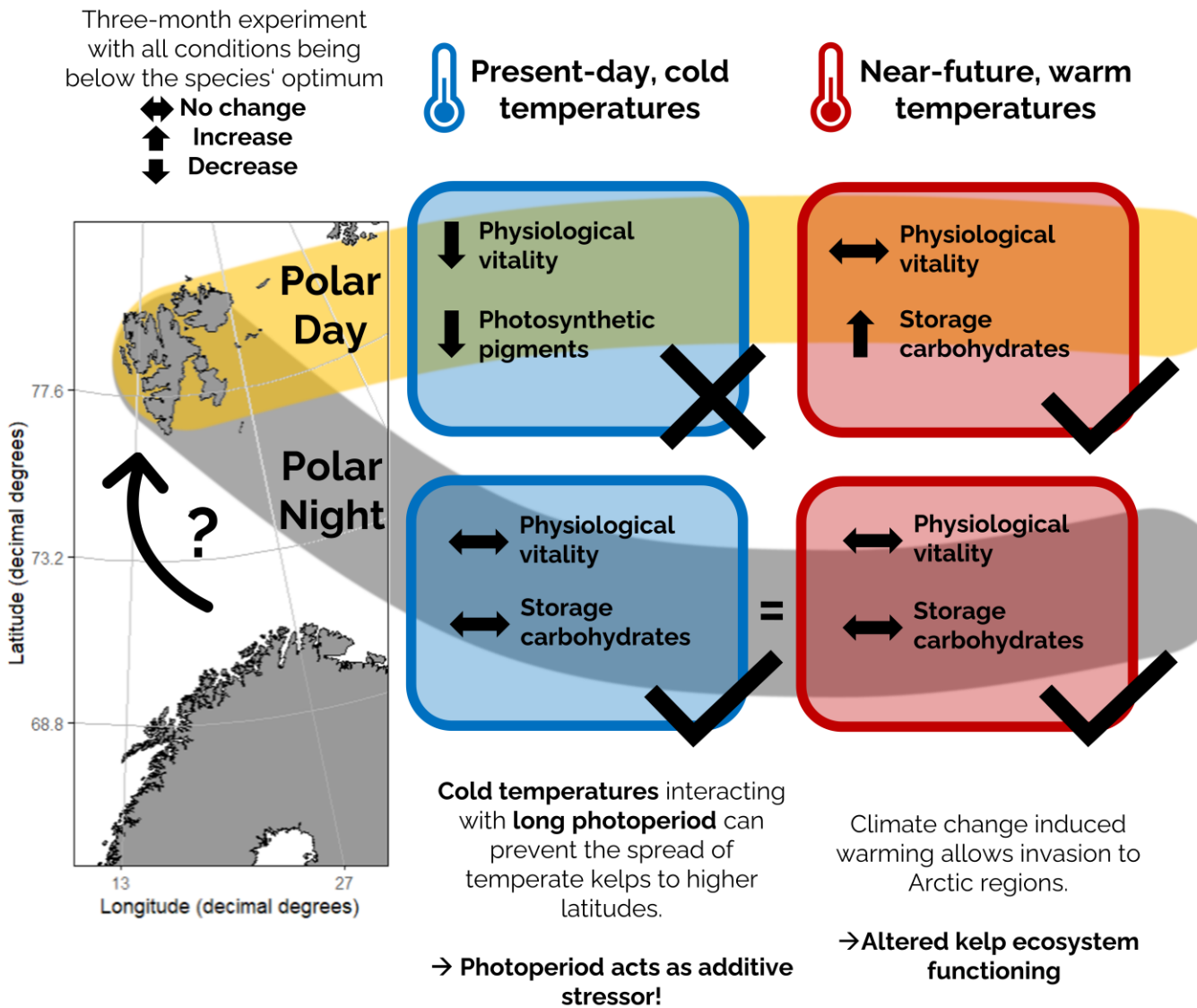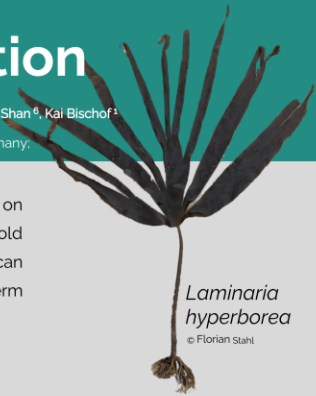# Interactive drivers affect kelp distribution

Nora Diehl [1,2*], Philipp Laeseke, Inka Bartsch [2], Margot Bligh [1,3], Hagen Buck-Wiese [3], Jan-Hendrik Hehemann [1,3], Sarina Niedzwiedz [1], Niklas Plag [4,5], Ulf Karsten [4], Tifeng Shan [6], Kai Bischof [1]

[1]University of Bremen, Germany; [2]Alfred Wegener Institute, Germany; [3]Max Planck Institute for Marine Microbiology, Germany; [4]University of Rostock, Germany; [5]Julius Kühne Institute, Germany; [6]Institute for Oceanology, China

Due to global temperature rises, models predict marine species to expand to higher latitudes. Most models are focusing solely on the thermal requirements of a species, even though it has become clear that temperature alone is a weak predictor for kelps' cold distribution limits: e.g., the ecosystem engineering species *Laminaria hyperborea* has not yet spread to the Arctic, although it can survive and tolerate the prevailing temperatures. To investigate its ability to spread poleward in future, we conducted a long-term experiment, exposing kelp specimens from Northern Norway to different photoperiods at 0°C, 5°C and 10°C.

Research questions: (1) Why has *Laminaria hyperborea* not yet spread to higher latitudes?
(2) Will it spread to polar regions in future?

Laminaria hyperborea
© Florian Stahl

Three-month experiment with all conditions being below the species' optimum
- ↕ No change
- ↑ Increase
- ↓ Decrease

Present-day, cold temperatures

Near-future, warm temperatures

Polar Day

Polar Night

Present-day, cold temperatures:
- ↓ Physiological vitality
- ↓ Photosynthetic pigments

Near-future, warm temperatures:
- ↔ Physiological vitality
- ↑ Storage carbohydrates

Present-day, cold temperatures:
- ↔ Physiological vitality
- ↔ Storage carbohydrates

Near-future, warm temperatures:
- ↔ Physiological vitality
- ↔ Storage carbohydrates

Cold temperatures interacting with **long photoperiod** can prevent the spread of temperate kelps to higher latitudes.

→ **Photoperiod acts as additive stressor!**

Climate change induced warming allows invasion to Arctic regions.

→**Altered kelp ecosystem functioning**

(1) We found cold temperatures interacting with polar day to prevent the spread of *L. hyperborea* to higher latitudes.

(2) Rising temperatures mitigate the high-light stress, potentially facilitating the spread of *L. hyperborea* in the near-future.

Get the publication

_____

Photoperiod and temperature interactions drive the latitudinal distribution of kelps under climate change

Diehl, Nora[1,2*]; Laeseke, Philipp[a]; Bartsch, Inka[2]; Bligh, Margot[1,3]; Buck-Wiese, Hagen[3]; Hehemann, Jan-Hendrik[1,3]; Niedzwiedz, Sarina[1]; Plag, Niklas[4,5]; Karsten, Ulf[4,6]; Shan, Tifeng[7] & Bischof, Kai[1]

[1] *Faculty of Biology and Chemistry & MARUM, University of Bremen, D-28359 Bremen, Germany*

[2] *Alfred Wegener Institute, Helmholtz Centre for Polar and Marine Research, D-27515 Bremerhaven, Germany*

[3] *Max Planck Institute for Marine Microbiology, D-28359 Bremen, Germany*

[4] *Institute of Biological Sciences, University of Rostock, D-18059 Rostock, Germany*

[5] *Julius Kühn-Institute (JKI) – Federal Research Centre for Cultivated Plants, D-38104 Brunswick, Germany*

[6] *Interdisciplinary Faculty, Department of Maritime Systems, University of Rostock, D-18051, Rostock, Germany*

[7] *Institute of Oceanology, Chinese Academy of Sciences, Qingdao 266071, China*

[a] independent

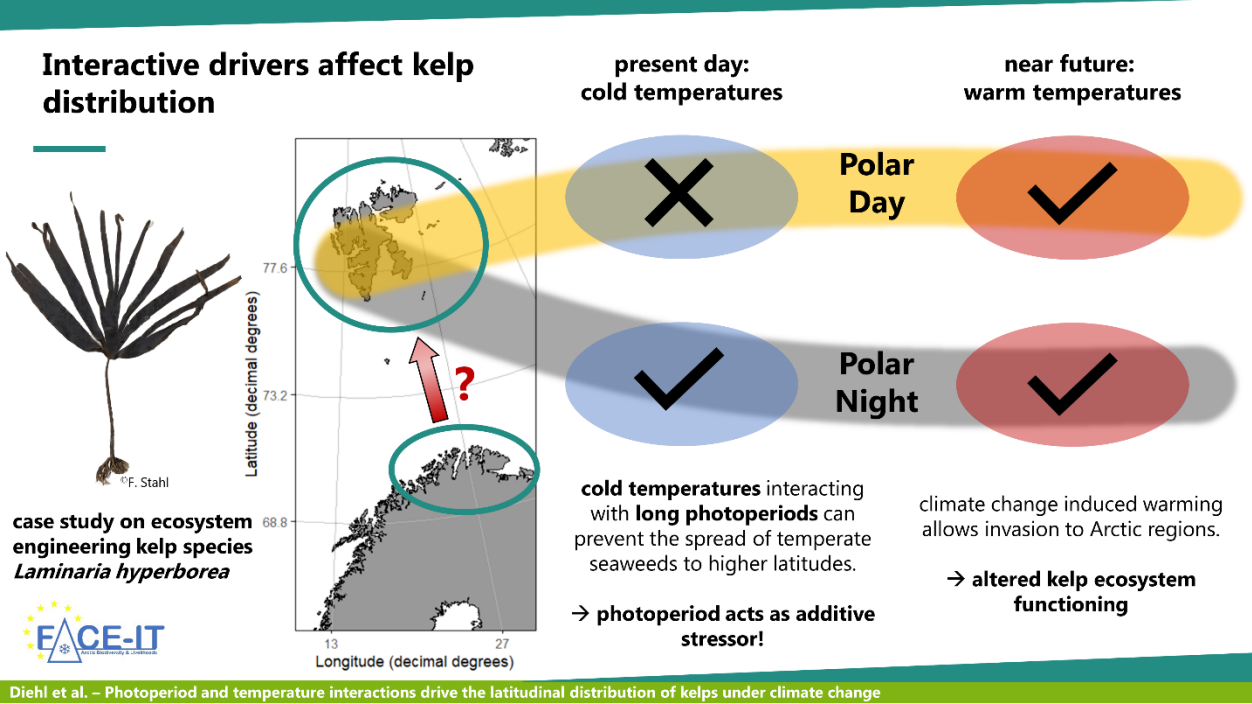*author for correspondence ndiehl@uni-bremen.de (*ORCID iD:* 0000-0002-7245-340X)

Running Head: Interactive drivers affect kelp distribution

ORCID:

Nora Diehl: 0000-0002-7245-340X

Graphical Abstract:

Interactive drivers affect kelp distribution

case study on ecosystem engineering kelp species
Laminaria hyperborea

©F. Stahl

present day:
cold temperatures

near future:
warm temperatures

Polar Day

Polar Night

cold temperatures interacting with **long photoperiods** can prevent the spread of temperate seaweeds to higher latitudes.

→ **photoperiod acts as additive stressor!**

climate change induced warming allows invasion to Arctic regions.

→ **altered kelp ecosystem functioning**

Diehl et al. – Photoperiod and temperature interactions drive the latitudinal distribution of kelps under climate change

_____

Abstract

Due to a global rise in temperature, recent studies predict marine species shifting towards higher latitudes with profound consequences for Arctic ecosystems. We investigated the impact of interacting abiotic drivers (photoperiod × temperature) under climate change scenarios on the northward distribution potential of the temperate kelp *Laminaria hyperborea* (Laminariales, Phaeophyceae) as a case species. The ecosystem engineering *L. hyperborea* is widespread along European coasts, but is not yet found in the High Arctic, although it can survive several months of low temperatures and darkness. To investigate its ability to extend northward in the future, we conducted a long-term multi-factorial experiment using tissue of adult sporophytes collected from Porsangerfjorden, Norway – a site close to the species' currently documented northernmost distribution margin. The samples were exposed to three different photoperiods (PolarDay, LongDay, PolarNight) at 0, 5 and 10°C for three months. Optimum quantum yield of photosynthesis (F_v/F_m), dry weight, pigments, phlorotannins and storage carbohydrates were monitored. Both, physiological and biochemical parameters, revealed that *L. hyperborea* was strongly influenced by the differences in photoperiod and their interaction with temperature, while temperature changes alone exerted only minor effects. The F_v/F_m data were integrated into a species distribution model to project a possible northward expansion of *L. hyperborea*. The combination of extended day lengths and low temperatures in summer appeared to be the limiting reason for further northward spreading of *L. hyperborea* until recently. However, with water temperatures reaching 10°C in summer, this kelp will be able to thrive also in a High Arctic seasonal light regime. Moreover, no indications of physiological or biochemical stress to Arctic winter warming were found. Consequently, *L. hyperborea* has a high potential for spreading northwards under further warming conditions, which may significantly affect the structure and function of Arctic ecosystems.

1. Introduction

Global warming is a main driver of global biodiversity loss and leads to the redistribution of species worldwide (Sunday et al., 2012; Wilson et al., 2019). Compared to the global average, Arctic regions have warmed nearly four times faster over the last four decades (Rantanen et al., 2022), with similar trends observed in air temperature and sea surface temperature (SST) (Skogseth et al., 2020). The rapid temperature increase particularly threatens polar coastal ecosystems, which form an ecologically exceptional environment with a unique biological diversity (Bringloe et al., 2020).

Changes in aquatic temperature regimes directly affect physiological and biochemical processes of organisms and have been identified as a main predictor of biogeographic patterns in seaweeds (Lüning, 1990; Adey and Steneck, 2001; Fragkopoulou et al., 2022). Consequently, temperature changes have drastic effects on the distribution of marine species worldwide, especially at their warm and cold distribution margins (Sunday et al., 2012, 2015). In the Arctic, warming leads to an increase in new substrates and habitats for intertidal and subtidal species due to the associated fast sea ice melting and glacier retreats (Krause-Jensen et al., 2020). Therefore, polar areas are of special interest to ecologists to document and understand the effects of rapid temperature changes on the redistribution of taxa (Callaghan et al., 2004; Bringloe et al., 2020; Assis et al., 2022). Modelling studies provide an excellent approach to predict ongoing northward distributional shifts of temperate seaweeds as a result of increasing SSTs (Assis et al., 2018a, 2022; Krause-Jensen et al., 2020). It is assumed that the higher habitat availability in the Arctic (Krause-Jensen et al., 2020) will favor the invasion for non-polar species with consequences for the structure and function of Arctic communities (Wassmann et al., 2011). Though, to date, we still lack knowledge about changes in seaweed abundance and their effects on the Arctic environment (Filbee-Dexter et al., 2019). Invasive seaweeds or changes in species' diversity can have extensive cascading consequences on the functioning of native ecosystems, such as biotic interactions between habitat formers and epiphytic biota (Thomsen et al., 2010). Thus, what the future brings is still "an uncertain path forward for the Arctic biome" (Bringloe et al., 2020).

While temperature progressively increases in polar environments, seasonal changes in light regimes remain unaltered, with months-long periods of Polar Night and constant light conditions during Polar Day. The annual cycle of photoperiods dictates large-scale periodic changes in reproductive biology and productivity as the latter is the prerequisite for phototrophic carbon acquisition. Thus, light availability and photoperiod affects primary production and ecological processes at the very base of food webs in polar environments, including species composition and reproduction (Wiencke et al., 2009; Berge et al., 2015). In addition, SST also varies strongly over the year (see **Supplementary Table S1**). The fluctuating light and temperature conditions over

_____

the course of the year lead to adaptive responses in polar seaweeds, which adjust their life cycles to the specific polar conditions (Wiencke et al., 2009; Zacher et al., 2009).

The interaction of increasing temperatures under various photoperiodic light conditions has rarely been investigated (Roeber et al., 2021; Lebrun et al., 2022). Physiologically, the interplay of the light regime and temperature conditions is highly important in seaweeds. For example, high photon fluence rates during cold-temperature periods lead to damage at photosystem II (Niedzwiedz et al., 2024), since enzymatic repair mechanisms are too slow to maintain a functioning photosynthetic apparatus under high light stress (Farrugia Drakard et al., 2023).

Seaweeds have developed various physiological and biochemical mechanisms to acclimate to changes in environmental conditions (Hurd et al., 2014; Wiencke and Bischof, 2012 and references therein). However, seaweeds lack mobile life-cycle stages for long-distance migration, and are, hence, particularly affected by ongoing ocean warming (Reed et al., 2016; Straub et al., 2019). As sedentary organisms, seaweeds are dependent on mechanisms that limit dispersal such as release of planktonic spores, transport through external vectors, or long-distance drifting (Tronholm et al., 2012; Hurd et al., 2014). Kelps typically have adaptive mechanisms that are too slow for rapid changes in the environment (Vranken et al., 2021).

Kelp forests provide numerous ecosystem functions to associated organisms, such as shelter and food and also act as a carbon sink (Teagle et al., 2017), but are also of high economic value (Eger et al., 2023). Despite their capability to acclimate to changing environmental conditions, strong declines of kelp forests were reported at their warm-edge distribution limits, mainly as a consequence of SST increase (Sorte et al., 2010; Filbee-Dexter and Wernberg, 2018; Filbee-Dexter et al., 2020), which has far reaching consequences for biodiversity and ecosystem functioning (Wernberg et al., 2024). Concurrently, changed abundances of kelp species, such as *Saccharina latissima* and *Alaria esculenta*, were observed in polar regions (Bartsch et al., 2016; Fredriksen and Kile, 2012; Düsedau et al. in revision). But, it was also observed that warming winters can have negative consequences for their physiological traits, such as photosynthesis and biomass formation (Scheschonk et al., 2019; Gordillo et al., 2022).

The target species for this study, *Laminaria hyperborea*, is an important ecosystem engineering kelp (Phaeophyceae, Laminariales) that forms highly productive ecosystems along rocky shorelines from temperate to polar regions (northern Norway) (Teagle et al., 2017; Wernberg et al., 2019; Smale, 2020). It occurs along European coasts between 40–71°N, i.e., from Northern Portugal to Northern Norway (Lüning, 1985), with a north-easternmost distribution at the Murman coast of the Kola Peninsula, Russia (Schoschina, 1997). As a perennial kelp, it can live up to 18 years in northern Norway (Sjøtun et al., 1993). It survives minimum temperatures of -1.5°C and a maximum of 20°C (Bolton and Lüning, 1982; Lüning, 1986; tom Dieck, 1993), and grows over the entire temperature range between 0 and 20°C, with an optimum at 10–15°C (Bolton and

_____

Lüning, 1982; tom Dieck (Bartsch), 1992). *Laminaria hyperborea* generally reproduces from fall to mid-winter (Kain and Jones, 1975) and may also reproduce during darkness (Lüning, 1980). Moreover, the gametophytes survive and mature, albeit very slowly, down to a temperature of 0°C (Sjøtun and Schoschina, 2002), with the optimum being between 5 and 17°C (Kain, 1979). It is, therefore, surprising that this kelp has not yet been reported from the High Arctic (**see Box**). Lüning (1986) indicated that long photoperiods in the High Arctic could be a limiting factor for the northern occurrence of *L. hyperborea*, as sporophytes thrive during short days and in complete darkness, while formation of new lamina is decreasing with increasing day length and completely inhibited in summer (Lüning, 1986; Bartsch et al., 2008).

In studies on distribution changes of *L. hyperborea*, the species was predicted to expand to Svalbard and further east in the White Sea until the end of the century (Assis et al., 2016, 2018a), determining winter temperatures as the main driver for its distribution. However, experimental data are lacking and the restricted capabilities of statistical models limit such predictions (Fragkopoulou et al., 2022). Seasonality as a critical abiotic factor has not yet been considered in the models on seaweed distribution in the Arctic.

In this study, we evaluated for the first time the effects of photoperiod × temperature interaction by simulating seasonal variations in temperatures and the polar light regime in a three-month multi-factorial experiment. Using *L. hyperborea* as the case species, we investigated how the interplay of both factors affects physiological and biochemical traits. Our study was guided by the hypothesis long photoperiods might be a limiting factor for the further northward distribution of *L. hyperborea*, following Lüning (1986). Accordingly, the extended periods of long days and the Polar Day in the High Arctic could limit the distribution of *L. hyperborea* compared to the Low and Sub-Arctic regions. We incorporated the physiological data into a geographical model to simulate the habitat suitability along the latitudinal gradient under different SST scenarios.

The study was driven by two research questions:

1) How does *L. hyperborea* respond physiologically and biochemically to simulated past, present and future SST conditions during different seasons in the High Arctic?

2) Will *L. hyperborea* be able to spread throughout the High Arctic under future climatic conditions?

BOX:

Gbif.org already lists an occurrence of "*Laminaria hyperborea*" for Spitsbergen as "human observation" (https://www.gbif.org/occurrence/2399478326). Individuals of "*L. hyperborea*" were also reported from Isfjorden and Kongsfjorden (see Fredriksen et al., 2019 and references therein). However, it is important to note that *L. hyperborea* can be difficult to distinguish from *Hedophyllum nigripes* and *Laminaria digitata* due to their similar morphological appearance

_____

(Longtin and Saunders, 2015; Dankworth et al., 2020). Both, *L. digitata* and *H. nigripes* are found widespread in the Arctic from the East (Spitsbergen) to the West (Canadian Arctic) (Bartsch et al., 2016; Dankworth et al., 2020, Düsedau et al. in revision). As *L. hyperborea* may have been misidentified formerly, and so far, there is no molecular evidence of *L. hyperborea* from Svalbard, we are convinced that *L. hyperborea* has not yet spread throughout the High Arctic and that the observations from Spitsbergen are probably erroneous.

2. Material and Methods

2.1. Sampling and Species Identification

SCUBA divers collected adult sporophytes of *Laminaria hyperborea* (Gunnerus) Foslie at approximately 8 m depth near the Holmfjorden Research Station at Porsangerfjord (Finmark, Norway; 70.2°N 25.3°E) in late June 2022. The sporophytes were stored in a tank with fresh deep-water flowthrough (~10°C, S_A 31) for one week and then, due to technical problems, hung in the shade from the pier until further processing (13.7±0.9°C, S_A 30.4±0.8). In mid-July, non-meristematic discs (Ø 28 mm) from the central part (>10 cm above the meristem and >20 cm below the distal end) of 39 sporophytes (10–30 discs per sporophyte) were cut and transported moist, cool (<10°C) and dark to the Alfred Wegener Institute for Polar and Marine Research in Bremerhaven, Germany, where the experiment was conducted.

Due to difficulties in morphological identification for the digitate Laminariaceae (Longtin and Saunders, 2015), we screened all collected specimens genetically. For molecular identification of the individuals, subsamples of each collected sporophyte were preserved in silica gel. Genomic DNA was isolated using a plant genomic DNA extraction kit (DP305, Tiangen Biotech, China) according to the manufacturer's instructions. Species identification was conducted following the method developed by Mauger et al. (2021), which was based on amplification of a fragment of the mitochondrial COI gene (COI-5P). Briefly, two PCR reactions (PCR1 and PCR2) were conducted using a Taq Master Mix kit (Accurate Biology, China) and run on a T-gradient thermocycler (Biometra, Germany). The PCR primers and programs were as described in Mauger et al. (2021). PCR products were visualised under UV light after electrophoresis on agarose gels stained with GelRed. Species were identified according to the patterns of amplified fragments in Mauger et al. (2021).

2.2. Experimental Set-Up

For recovery, the samples were maintained in seawater at 5°C at 30–35 µmol photons m^{-2} s^{-1} (24:0 h light:dark, ProfiLux 3 with LED Mitras daylight 150, GHL Advanced Technology, Kaiserslautern, Germany) for a week (**Fig. 1**). The applied photon fluence rate was based on measurements at a

depth of ~7.5 m in Kongsfjorden, Svalbard (Niedzwiedz and Bischof, 2023b), since Kongsfjorden can be seen as a model ecosystem for the future of Arctic fjord systems (Bischof et al., 2019). After recovery, the samples were exposed to the photoperiod treatments (24:0 h light:dark – PolarDay, 18:6 h light:dark – LongDay, 0:24 h light:dark – PolarNight) and gradually acclimated to the temperature treatments (0, 5, 10°C) over four days. The three temperature set-ups were based on winter (December, January, February) and summer (June, July, August) SSTs measured at 0–20 m in Kongsfjorden, Svalbard between 1980 and 2022 (see **Supplementary Table S1**).
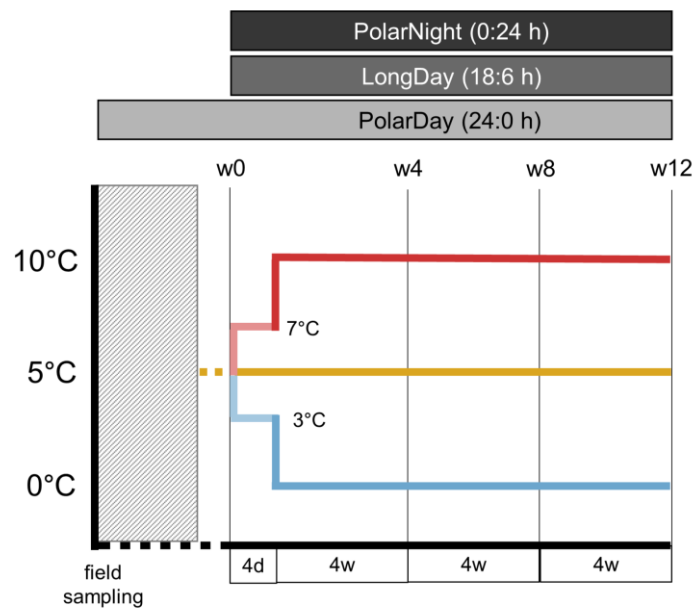

Figure 1: Experimental set-up. Grey-dashed area: maintenance of the sporophytes in the field. Dotted lines: maintenance of samples in the field and recovery in the laboratory. Week 0 (w0), w4, w8, w12: biochemical sampling during the experiment. Photoperiodic treatments: PolarDay = 24h light : 0h dark, Long = 18h light : 6h dark, PolarNight = 0h light : 24h dark. d = days, w = week(s).

Each replicate (n = 4) was set up containing 20 "healthy" discs (F_v/F_m >0.6, data not shown; Dring et al., 1996) from 8–10 individuals, evenly distributed avoiding pseudo-replication. The experiment ran for three months. During the entire experiment, samples were kept in aerated 2 L clear plastic bottles in Provasoli-enriched artificial seawater (S_A 31, 1/40 PES, Provasoli, 1968; modifications: HEPES-buffer instead of Tris). The nutrient conditions of 1/40 PES (13.7 µmol NO_3^- L^{-1}, 0.55 µmol PO_4^{3-} L^{-1}) were based on realistic winter nutrient conditions in Kongsfjorden, Svalbard (Norway) (Bischof et al., 2019). The water was changed twice a week. Experimental sampling was conducted after three days of recovery (w0), in week 4 (w4), week 8 (w8) and at the end of the experiment (w12).

2.3. Physiological Parameters

The physiological vitality of all samples was checked as photosynthetic activity every week by measuring the maximum quantum yield of photosystem II (*in vivo* chlorophyll-fluorescence of photosystem II; F_v/F_m) using a pulse-amplitude-modulated fluorometer (Imaging-PAM, Walz GmbH, Effeltrich, Germany). The Imaging-PAM was set up to an initial fluorescence signal (F_t) between 0.15 and 0.2.

Biomass (dry weight) of the samples was monitored every four weeks (w0, w4, w8, w12). For this purpose, sample discs were randomly picked and freeze-dried (Alpha 1–4 LO plus, Martin Christ Gefriertrocknungsanlagen GmbH, Osterode am Harz, Germany) before weighing (DW in g). In addition, all discs were photographed every two weeks with a 9 cm^2 reference grid and their area (cm^2) analysed with ImageJ (Version 1.52a, Java 1.8.0_112, Wayne Rasband, National Institute of Health, USA).

2.4. Biochemical Parameters

For the biochemical analyses, samples were shock-frozen in liquid N_2 and stored at −80°C until further processing. The samples were freeze-dried before analyses (Alpha 1–4 LO plus, Martin Christ Gefriertrocknungsanlagen GmbH, Osterode am Harz, Germany).

Mannitol and laminarin are the main carbon storage compounds in kelps. Mannitol was analysed after Diehl et al. (2020), using the chromatographic method by Karsten et al. (1991). Laminarin was extracted from freeze-dried material with 50 mM MOPS buffer at 4°C for 5 h and measured following the method of Becker et al. (2017) and Becker and Hehemann (2018).

Pigment composition and photo-protective mechanisms, namely de-epoxidation state of the xanthophyll cycle pigments (DPS) and phlorotannins, were also monitored every four weeks. Absolute pigment content of chlorophyll *a* (Chl*a*), accessory pigments (Acc = Fucoxanthin + Chlorophyll c2 + β-Carotin) and the pool of the xanthophyll cycle pigments (VAZ = Violaxanthin + Antheraxanthin + Zeaxanthin) were determined following Diehl et al. (2021). DPS was calculated following Colombo-Pallotta et al. (2006). The concentration of phlorotannins was measured according Cruces et al. (2012), following the protocol in Springer et al. (2017).

2.5. Geographic Projection of experimental results

We projected F_v/F_m as response variable in a mechanistic approach (Kearney and Porter, 2009). The effect sizes of photoperiod, temperature, exposure time with and without their interaction terms on F_v/F_m were first estimated with a generalised linear model (GLM). We included weights to account for the unequal sample sizes over the course of the experiment. Inclusion of a random term for subsample-structure (i.e., aquariums as nested variable) as tested with a generalised

_____

linear mixed effect model (GLMM) was not significant and thus omitted (not shown). The best model was selected based on the Akaike information criterion (AIC). The parameter estimates for the environmental variables were used to make projections of the algal vitality in response to temperature and photoperiodic conditions across the geographic area of interest to predict potential suitable distribution ranges of the species under current and enhanced SSTs. We chose a conservative threshold of $F_v/F_m \leq 0.3$, as continuous low F_v/F_m result in death for kelps. Thereby, our study focused on changes in habitat suitability along a latitudinal gradient from continental Europe to Svalbard, Norway.

2.5.1. Preparation of environmental layers

For geographic projection of the model results, we prepared raster layers for daily photoperiod (day length) conditions and daily SST with a resolution of 5 arcmin. For daily photoperiod layers we made one raster layer for each day of the year with photoperiod in hours per pixel based on latitude with the daylength()-function from the "geosphere"-package for R (Hijmans et al., 2022). For daily temperature, we first downloaded monthly means of SST averaged over the years 2000–2014 (corresponding to the timespan covered by the widely used BioOracle v2 data set; Assis et al., 2018b) from the NOAA Optimum Interpolation (OI) SST V2 data set as provided by the NOAA PSL, Boulder, Colorado, USA, from their website at https://psl.noaa.gov (downloaded November 28th, 2022; Reynolds et al., 2002). We used a generalised additive model (GAM) to interpolate daily SST values per pixel for our projection raster layers. The period of 2000–2014 reflects the present scenario and baseline SST conditions. To simulate future warming scenarios, we used daily SST and photoperiod data for the year 2023, which was the warmest recorded year in the North Atlantic since 1979 (Copernicus, 2023), and added +1°C.

2.5.2. Geographic projection of F_v/F_m

We used the final model to predict how F_v/F_m of *L. hyperborea* will respond to environmental conditions over a prolonged time period (one year) in the geographic region of interest. F_v/F_m best reflected the overall observed responses of *L. hyperborea* to the experimental treatments, although it is generally a rather dynamic parameter influenced by many external and internal factors (Diehl et al., 2024; Hurd et al., 2014 and references therein). Unlike under constant laboratory conditions, SST and photoperiod change over the course of the year with the seasons. Therefore, we iteratively predicted for every consecutive day of the year how exposure to daily resolved conditions would affect the F_v/F_m. With the final adjusted model we predicted F_v/F_m for each pixel *j* of the temperature and photoperiod layers for each day *n* of the year: $FvFm_{n,j} \sim FvFm_{n-1,j} + \beta_1 \times time_{j,n} + \beta_2 \times temp_{j,n} + \beta_3 \times photoperiod_{j,n} +$ (interaction terms), resulting in a total number of 365 prediction layers per year. For daily predictions, time was set to the constant value of 1. We

_____

further replaced the original model intercept with the F_v/F_m value from the previous day (i.e., with FvFm$_{n-1, j}$), except for $n = 1$, where we used the original intercept of the model. This was done because the original intercept of the model represented the F_v/F_m at the start of the laboratory experiment and, therefore, was equivalent to samples in perfect condition. For a final map, we summed for each pixel the total number of days per year with a predicted F_v/F_m below the chosen threshold of 0.3.

L. hyperborea reproduces (i.e., release of spores) and grows during the fall and winter season, with earliest and latest spore release between middle of September and middle of April, respectively (Kain, 1971; Lüning, 1986). Therefore, starting the year with January 1st as first day and the original intercept was feasible.

2.6. Statistical Analyses and Software

All statistical analyses were done with "R" version 4.2.2 (R Core Team, 2022). The data sets of raw data as well as residuals of models were tested for normal distribution (Shapiro-Wilk test, $p>0.05$), homogeneity of variance (Levene's test, $p>0.05$) and were checked visually with dot plots (Zuur et al., 2013). As the F-statistic is robust to a moderate deviation from the normal distribution for small sample sizes with respect to type I errors and no beneficial effects of the transformation were found (Blanca et al., 2017), the non-normally distributed data sets were not transformed. Linear models were fitted on the data sets, using the "lm" function and significant differences of the response variables to the interactive fixed-effects temperature (T), photoperiod (P) and sampling time (S) were assessed using a fitted linear model using analyses of variances (ANOVA) (Package: stats; R Core Team, 2022). For the parameters F_v/F_m and area repeated measures ANOVAs were applied. Pairwise comparisons were performed, using the "emmeans" function with "sidak" correction (Package: emmeans; Lenth, 2024). The level of significance was set to $p<0.05$. Statistical results are summarised in **Table 1**.

Correlations of the response parameters were tested using Spearman correlation (function: cor.test; R Core Team, 2022), after testing for normality. Data were visualised with the "ggcor" function (Package: GGally; Schloerke et al., 2023).

For all analyses and plotting of the species distribution model, we used "R" version 4.2.2 (R Core Team 2022) with the packages "terra" (Hijmans et al., 2023), "tidyr" (Wickham et al., 2023), "ggplot2" (Wickham, 2016), "mgcv" (Wood, 2023), "tmap" (Tennekes, 2018) and "lme4" (Bates et al., 2015).

_____

3   Results

All statistical results are summarised in **Table 1** and are not given in the plots and the text for overview reasons.

Table 1: Statistics of the physiological and biochemical parameters of *Laminaria hyperborea*. F_v/F_m = optimum quantum yield of photosynthesis, DW = dry weight, Chl*a* = chlorophyll *a*, Acc = accessory pigments, VAZ = pool of xanthophyll cycle pigments, DPS = de-epoxidation state of the xanthophyll cycle. T = temperature, P = photoperiod, S = Sampling Time. PD = PolarDay, LD = LongDay, PN = PolarNight. Significances are highlighted in bold.

Parameter		*p*-value	Direct comparison	
F_v/F_m	T	**< 0.001**	0°C < 5°C < 10°C	
	P	**< 0.001**	PD < LD < PN	
	S	**< 0.001**	w0 > w12	0-PD, 5-PD 0-LD
	T × P	**< 0.001**	strong interaction	
DW	T	**0.009**	0°C ≤ (5°C = 10°C)	
	P	**< 0.001**	PD > LD > PN	
	S	**< 0.001**	w0 < w12	0-PD, 5-PD, 10-PD 0-LD, 5-LD, 10-LD
	T × P	**0.007**	moderate interaction	
	T × S	**0.005**		increasing impact of T throughout the experiment
	P × S	**< 0.001**		increasing impact of P throughout the experiment
	T × P × S	0.335		
Chl*a*	T	**< 0.001**	(0°C = 5°C) < 10°C	
	P	**< 0.001**	(PD = LD) < PN	
	S	**< 0.001**	w0 > w12	0-PD, 5-PD, 10-PD 0-LD, 5-LD
	T × P	0.057	no interaction	
	T × S	**0.002**		increasing impact of T throughout the experiment
	P × S	**0.011**		increasing impact of P throughout the experiment
	T × P × S	0.135		
Acc	T	**< 0.001**	(0°C = 5°C) < 10°C	
	P	**< 0.001**	(PD = LD) < PN	

_____

	S	**< 0.001**	w0 > w12	0-PD, 5-PD, 10-PD 0-LD, 5-LD
	T × P	0.263	no interaction	
	T × S	**< 0.001**		increasing impact of T throughout the experiment
	P × S	**0.004**		increasing impact of P throughout the experiment
	T × P × S	0.228		
VAZ	T	0.086	0°C = 5°C = 10°C	
	P	0.305	PD = LD = PN	
	S	**< 0.001**	w0 > w12	0-PD, 5-PD, 10-PD 0-LD, 5-LD
	T × P	0.923	no interaction	
	T × S	**0.003**		increasing impact of T throughout the experiment
	P × S	**< 0.001**		increasing impact of P throughout the experiment
	T × P × S	**0.029**		
DPS	T	**< 0.001**	0°C > 5°C > 10°C	w12: no sign w8: PD/LD → 0°C > 5°C > 10°C PN → (0°C = 5°C) > 10°C

	P	**< 0.001**	(PD = LD) > PN	w12: no sign
				w8: 0°C → PD-LD (**< 0.001**)
				     0°C → PD-PN (**< 0.001**)
				     5°C → PD-PN (**< 0.001**)

	S	**< 0.001**	w0 = w12	but: w0 < w8
	T × P	**< 0.001**	strong interaction	
	T × S	**< 0.001**		increasing impact of T throughout the experiment
	P × S	**0.001**		increasing impact of P throughout the experiment
	T × P × S	**0.016**		increasing impact of T×P throughout the experiment
Phlorotannins	T	0.319	0°C = 5°C = 10°C	
	P	0.416	PD = LD = PN	
	S	0.177	w0 = w12	exception: 0-PN (w0 < w12 **)
	T × P	0.054	no interaction	
	T × S	0.082		

	P × S	0.661		
	T × P × S	0.164		
Mannitol	T	0.491	0°C = 5°C = 10°C	
	P	**< 0.001**	(PD = LD) > PN	
	S	**0.006**	w0 = w12	exception:10-PN (w0 > w12 ***)
	T × P	0.483	no interaction	
	T × S	0.624		
	P × S	**< 0.001**		increasing impact of P throughout the experiment
	T × P × S	0.557		
Laminarin	T	**< 0.001**	0°C < (5°C = 10°C)	
	P	**< 0.001**	(PD = LD) > PN	
	S	**< 0.001**	w0 < w12	5-PD, 10-PD 5-LD
	T × P	**< 0.001**	strong interaction	
	T × S	**< 0.001**		increasing impact of T throughout the experiment
	P × S	**< 0.001**		increasing impact of P throughout the experiment
	T × P × S	0.185		

3.1 Species Identification

Based on our molecular-genetic data, 37 specimens were identified as *Laminaria hyperborea* (Gunnerus) Foslie, while two specimens were determined as *Laminaria digitata* (Hudson) J.V. Lamouroux (**Supplementary Fig. S1a–c**). Unfortunately, two out of 20 discs were assigned to *L. digitata* in all treatment replicates 2 and 3. These *L. digitata* discs could not be identified during the experiments and, hence, not excluded a priori, but with only 10 % "contamination" by a wrong taxon, we are confident that the data are representative for the target species.

3.2 Physiology

The physiological vitality expressed as optimum quantum yield of photosystem II (F_v/F_m; **Fig. 2**) of *Laminaria hyperborea* was highly affected by temperature (*p*<0.001), photoperiod (*p*<0.001) and their interaction (T×P; *p*<0.001). The samples were particularly stressed when long photoperiods were paired with cold temperatures. Significant decreases in F_v/F_m were determined already after two weeks (w2) at 0°C under Polar Day (= 0-PolarDay) and under Long Day (= 0-LongDay) conditions, while vitality of samples at the 5°C Polar Day treatment (= 5-PolarDay) started to diminish only in w6. After three months (w12), lowest F_v/F_m values were recorded at 0-PolarDay, with values of 0.34±0.07. Both, a shorter photoperiod in combination with very low temperatures of 0°C, as well as higher temperatures under PolarDay conditions resulted in significantly higher F_v/F_m values (0-LongDay: 0.53±0.06; 5-PolarDay: 0.48±0.05) in w12. All 10°C samples, as well as all PolarNight samples and the 5-LongDay treatment, remained above F_v/F_m values of 0.6 during the entire period, independently from the photoperiod.
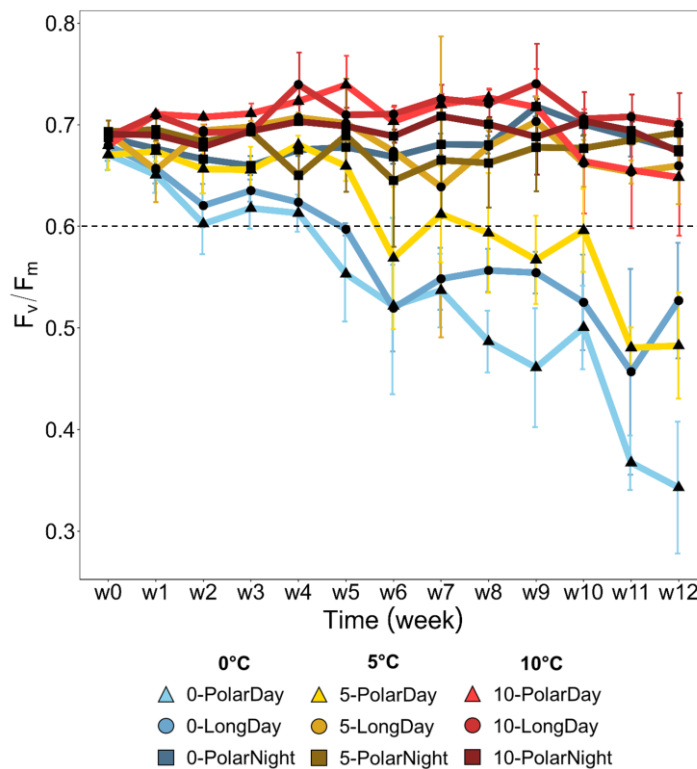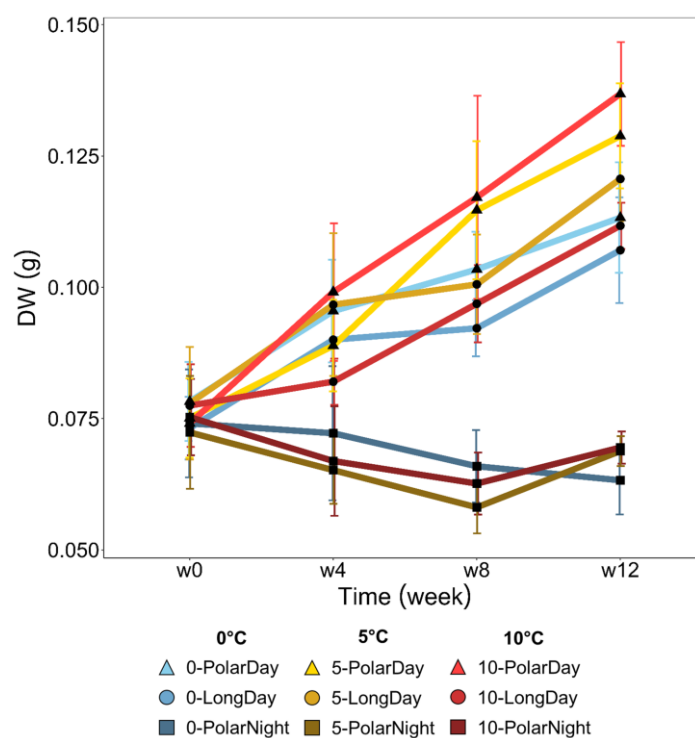

Figure 2: Vitality (maximum quantum yield of photosystem II; F_v/F_m) of *Laminaria hyperborea*, monitored weekly over three months under different temperature and photoperiod combinations. Values are means ± SD (n = 4). The threshold for a "good" (viable) physiological status is marked by the dotted line (Dring et al., 1996).

Dry weight (DW in g; **Fig. 3**) of the samples was mainly affected by the different photoperiods (*p*<0.001) and also by temperature (*p*<0.01). While all samples weighed approx. the same at the

beginning of the experiment (w0, $p>0.05$), significant increases in DW were determined for PolarDay ($p<0.001$) and LongDay ($p<0.001$) over time (sampling (S): $p<0.001$). Further, particularly the interaction of longer photoperiods and higher temperatures resulted in the strongest weight gains with weights up to 184±14% in the 10-PolarDay treatment (T×P; $p<0.01$). Although PolarNight conditions had no significant effect on DW, a trend to weight loss (0-PolarNight 87±18%, 5-PolarNight 90±10%, 10-PolarNight 93±7%) was observed after three months of PolarNight exposure. A change of DW due to growth or shrinking of the samples can be excluded since none of the treatments revealed a significant difference in area (cm^2) between w0 and w12 (data not shown here, but uploaded on PANGAEA).

Figure 3: Dry weight (DW) of *Laminaria hyperborea*, monitored every four weeks over three months under different temperature and photoperiod combinations. Values are means ± SD (n = 4).

_____

3.3 Storage Carbohydrates

Although larger differences in mannitol (mg g^{-1} DW) and laminarin (mg g^{-1} DW) content were measured in the samples in w0, none of the treatments differed significantly regarding both carbohydrates.

We did not measure significant changes in mannitol (**Fig. 4a**) at PolarDay and LongDay, whereas the concentrations decreased at PolarNight, progressively more with increasing temperatures, while the opposite was determined for laminarin (**Fig. 4b**). Its content remained the same for PolarNight, but increased significantly at PolarDay and LongDay.

Mannitol was strongly affected by the different photoperiods ($p<0.001$), whereas neither temperature alone, nor T×P had a significant impact during the experiment. Concentrations in the PolarDay and LongDay treatments remained the same (S: $p>0.05$), while a decrease of mannitol in PolarNight samples was observed over time. Though, with approx. -200 mg g^{-1} DW this decrease was only significant for 10-PolarNight ($p<0.001$), a trend to decreasing mannitol concentrations at 5-PolarNight was detectable (approx. -100 mg g^{-1} DW). Yet, overall mannitol concentrations in the PolarDay and LongDay samples were significantly higher than in the PolarNight samples ($p<0.001$). The significant decrease in the PolarNight treatments resulted in a strong positive correlation with DW over time (**Fig. 6**).

For laminarin, strong impacts of photoperiod ($p<0.001$), temperature ($p<0.001$) and T×P ($p<0.001$) were determined. Contrary to mannitol, laminarin concentration did not decrease in the PolarNight treatments, but increased during LongDay and PolarDay. Significant increases of approx. +200–250 mg g^{-1} DW over time were only detected in treatments combining long photoperiods and enhanced temperatures (S: 5-LongDay $p<0.001$; 5-PolarDay $p<0.01$; 10-PolarDay; $p<0.001$), resulting in significant lower laminarin concentration at 0°C than at 5°C ($p<0.001$) and 10°C ($p<0.01$). Accordingly, a very strong positive correlation between laminarin and DW was detected (**Fig. 6**).
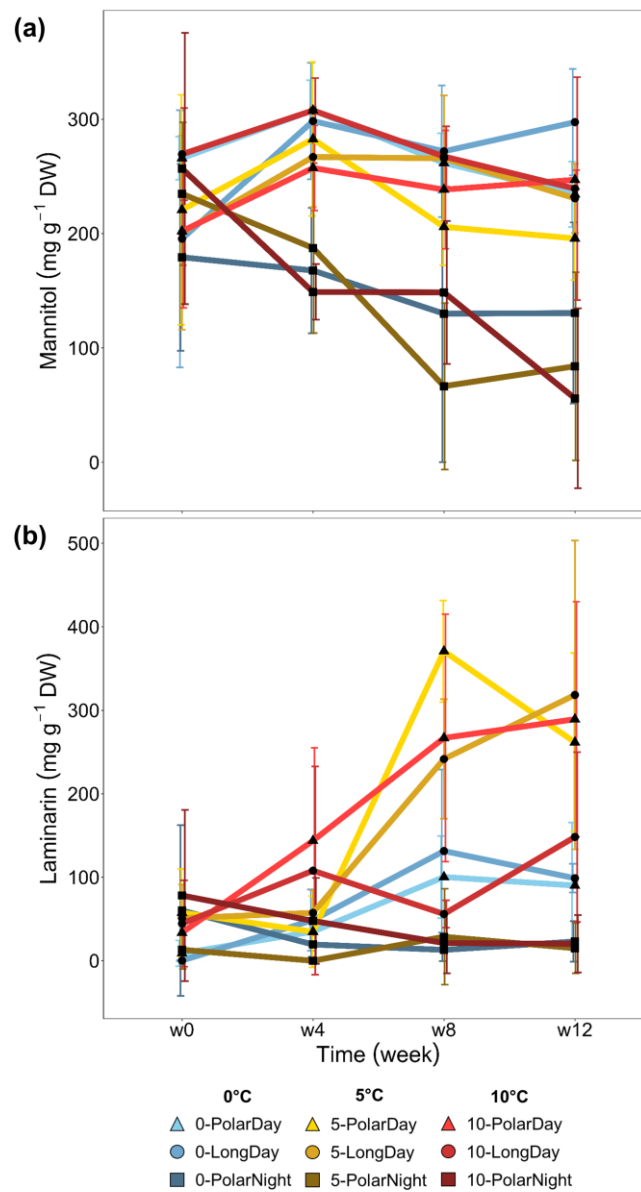
Figure 4: Storage carbohydrates of *Laminaria hyperborea*, monitored every four weeks over three months under different temperature and photoperiod combinations. **(a)** Mannitol **(b)** Laminarin. Values are means ± SD (n = 4).

3.4 Light Response Parameters

Chlorophyll *a* (Chl*a*; µg g^{-1} DW) and the accessory pigments (Acc; µg g^{-1} DW) (**Table 2**) decreased significantly over time under PolarDay conditions and at 0-LongDay and 5-LongDay ($p<0.01$–0.001), while the concentrations in PolarNight-treated samples remained the same. Significant impacts of temperature were found ($p<0.001$), overall resulting in lower Chl*a* and Acc concentrations at 0 and 5°C than at 10°C. While 0-PolarDay and 5-PolarDay resulted in concentrations of about one third of the respective PolarNight treatments, Chl*a* and Acc of 10-PolarDay reached over half the concentrations of 10-PolarNight. Still, a significant effect of T×P was not detected for Chl*a* and Acc. The pool of the xanthophyll cycle pigments (VAZ; µg g^{-1} DW) (**Table 2**) revealed no significant differences between the photoperiods or temperature, but also decreased exclusively in the PolarDay, 0-LongDay and 5-LongDay treatments over time ($p<0.05$–0.001). No significant T×P was detected. All three pigment groups revealed a strong positive correlation with F_v/F_m in the course of the experiment (**Fig. 6**).

Table 2: Biochemical light responses of *Laminaria hyperborea*, monitored every four weeks over three months (w0, w4, w8, w12). Chl*a* = chlorophyll *a*, Acc = accessory pigments, VAZ = pool of xanthophyll cycle pigments. Values are means ± SD (n = 4).

Parameter	Temp-erature	Photo-period	w0	w4	w8	w12
Chl*a* (µg g^{-1} DW)	0°C	PolarDay	1236.4 ± 90.7	610.8 ± 153.1	371.6 ± 106.4	335.4 ± 101.7
		LongDay	1286.6 ± 203.7	847.9 ± 220.2	644.4 ± 133.2	446.3 ± 62.2
		PolarNight	1206.0 ± 177.4	826.3 ± 313.9	815.1 ± 202.5	902.1 ± 146.8
	5°C	PolarDay	1049.6 ± 121.2	910.1 ± 76.5	519.1 ± 119.0	347.9 ± 58.0
		LongDay	1112.6 ± 172.4	672.2 ± 444.2	606.3 ± 116.1	534.6 ± 92.9
		PolarNight	1064.5 ± 194.4	955.9 ± 136.8	862.5 ± 269.7	959.4 ± 171.2
	10°C	PolarDay	1114.7 ± 330.2	1049.5 ± 292.7	1217.8 ± 608.1	428.3 ± 140.1
		LongDay	993.8 ± 357.7	1158.3 ± 134.4	936.4 ± 25.1	653.6 ± 89.8
		PolarNight	1186.5 ± 156.1	1024.6 ± 200.4	868.1 ± 250.2	800.4 ± 203.4
Acc (µg g^{-1} DW)	0°C	PolarDay	835.6 ± 83.9	346.3 ± 89.0	287.6 ± 65.8	263.4 ± 84.5
		LongDay	819.6 ± 132.3	499.9 ± 140.9	455.7 ± 75.1	336.4 ± 47.3
		PolarNight	788.1 ± 140.0	500.5 ± 212.3	518.9 ± 114.5	646.4 ± 70.5
	5°C	PolarDay	661.3 ± 114.0	526.0 ± 51.8	319.2 ± 92.2	264.1 ± 56.8
		LongDay	704.1 ± 135.2	380.9 ± 252.4	385.6 ± 75.2	360.6 ± 54.9
		PolarNight	636.8 ± 133.1	536.2 ± 111.8	420.6 ± 115.5	600.6 ± 120.7
	10°C	PolarDay	671.8 ± 213.3	586.8 ± 181.0	632.8 ± 99.8	326.2 ± 80.4
		LongDay	580.7 ± 234.2	712.4 ± 84.0	607.5 ± 36.1	456.7 ± 58.5
		PolarNight	712.5 ± 79.8	655.3 ± 124.6	549.5 ± 177.9	538.8 ± 162.6

VAZ (µg g⁻¹ DW)	0°C	PolarDay	98.5 ± 33.1	41.0 ± 15.3	31.6 ± 16.7	21.9 ± 7.3
		LongDay	71.7 ± 20.6	55.7 ± 21.2	57.9 ± 14.8	26.4 ± 1.3
		PolarNight	61.3 ± 20.0	28.6 ± 14.6	50.4 ± 19.4	55.3 ± 11.5
	5°C	PolarDay	51.5 ± 15.0	58.0 ± 3.1	43.4 ± 12.0	21.3 ± 4.7
		LongDay	65.7 ± 16.0	34.6 ± 24.1	45.9 ± 10.7	33.5 ± 8.9
		PolarNight	42.1 ± 17.7	40.7 ± 5.7	46.6 ± 7.6	41.4 ± 6.7
	10°C	PolarDay	58.3 ± 20.0	61.7 ± 18.2	47.4 ± 16.0	25.1 ± 7.3
		LongDay	57.4 ± 11.2	66.6 ± 9.8	54.3 ± 5.7	38.4 ± 9.2
		PolarNight	53.2 ± 8.5	54.1 ± 13.3	42.7 ± 13.5	41.5 ± 15.0
Phlorotannins (mg g⁻¹ DW)	0°C	PolarDay	11.6 ± 3.1	11.4 ± 3.5	12.0 ± 7.4	10.7 ± 6.3
		LongDay	10.8 ± 6.2	12.5 ± 2.4	9.6 ± 5.0	15.3 ± 6.7
		PolarNight	11.5 ± 4.8	12.9 ± 7.3	16.5 ± 6.6	24.5 ± 11.9
	5°C	PolarDay	13.4 ± 2.0	7.9 ± 1.2	12.2 ± 8.5	11.6 ± 4.9
		LongDay	13.2 ± 3.0	10.0 ± 1.8	13.3 ± 5.4	12.7 ± 4.8
		PolarNight	14.8 ± 3.9	11.0 ± 4.8	7.8 ± 3.6	11.9 ± 6.4
	10°C	PolarDay	13.8 ± 4.5	11.6 ± 2.1	18.1 ± 7.4	16.4 ± 8.5
		LongDay	12.7 ± 6.9	12.8 ± 3.7	12.2 ± 4.8	8.0 ± 4.4
		PolarNight	19.4 ± 6.1	8.0 ± 4.2	13.1 ± 3.8	9.4 ± 5.6

_____

No significant difference of the de-epoxidation state of the xanthophyll cycle (DPS; **Fig. 5**) was found in any of the treatments between w0 and w12, although significant increases were determined in w8 for 0-PolarDay ($p<0.001$), 0-LongDay ($p<0.001$) and 5-PolarDay ($p<0.01$). In w8, both PolarDay and LongDay at 0°C showed significantly higher DPS than PolarNight ($p<0.001$), while at 5°C only PolarDay differed significantly from PolarNight ($p<0.001$). At 10°C no differences in the photoperiod treatments were found, highlighting the strong impact of T×P on DPS ($p<0.001$). In the first eight weeks of the experiment, lower temperatures in combination with longer photoperiods led to increased DPS, which, however, was compensated after 12 weeks. Nonetheless, it resulted in a strong negative correlation of DPS and F_v/F_m in the course of the experiment (**Fig. 6**).
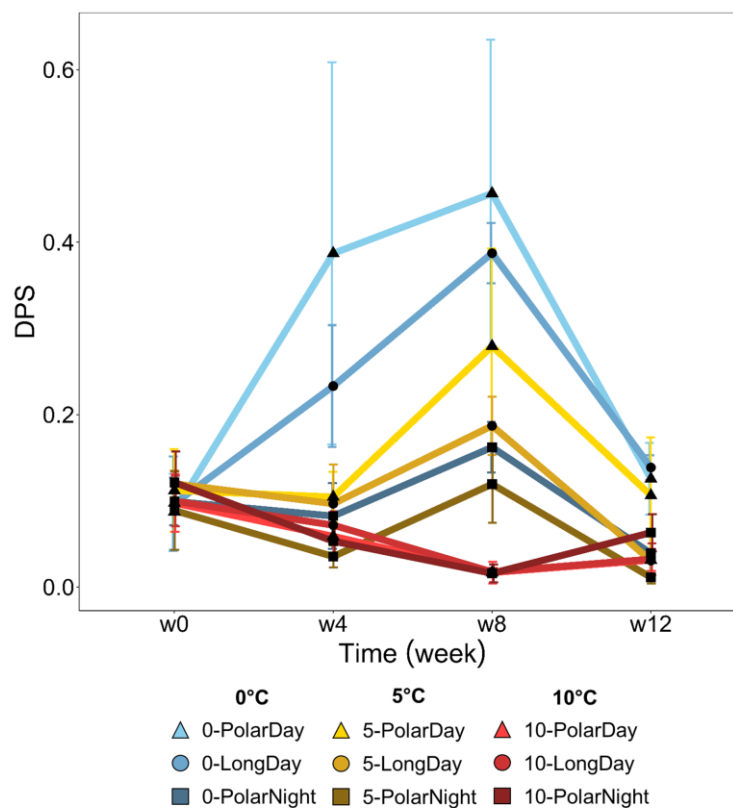
Figure 5: De-epoxidation state of the xanthophyll cycle pigments (DPS) of *Laminaria hyperborea*, monitored every four weeks over three months under different temperature and photoperiod combinations. Values are means ± SD (n = 4).

Concentrations of phlorotannins (mg g^{-1} DW, **Table 2**) in all treatments remained the same over the entire experiments, accordingly were neither affected by the treatment temperatures or photoperiods alone, nor by their interaction (T×P). No significant correlation with F_v/F_m was detected (**Fig. 6**).
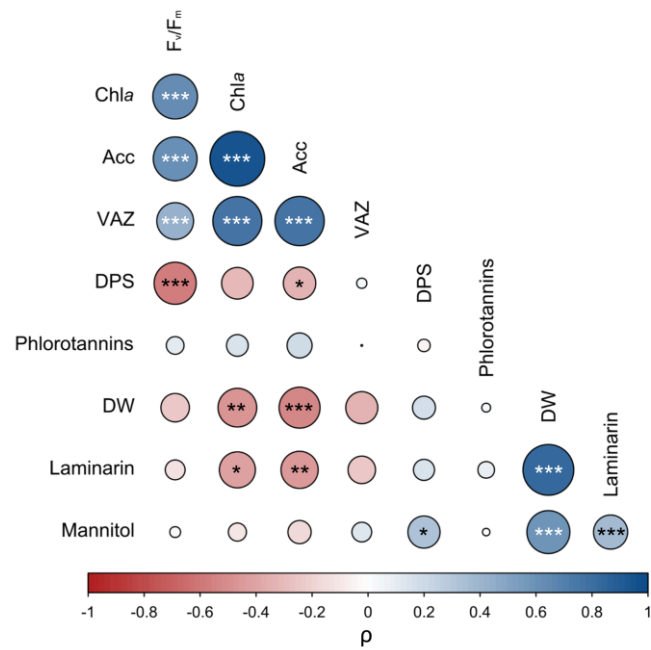
Figure 6: Correlation matrix of the physiological and the biochemical parameters in the course of the experiment. The value of the correlation coefficient Spearsman's Rho (ρ) is represented by color, shading and size of the circles. Significances: $p<0.05$ *, $p<0.01$ **, $p<0.001$ ***.

_____

3.5 Modelling of future distribution

The best model-fit was achieved with *F_v/F_m ~ time × photoperiod + time × temperature × photoperiod*. None of the variables alone had a significant effect on F_v/F_m, but the interaction terms of *time × photoperiod* and *time × temperature × photoperiod* and the intercept were highly significant with *p*<0.0001 (beta-estimate for *time × photoperiod* = -0.0001390 and beta-estimate for *time × temp × photoperiod* = 0.0000193, intercept = 0.68, **Supplementary Table S2**).
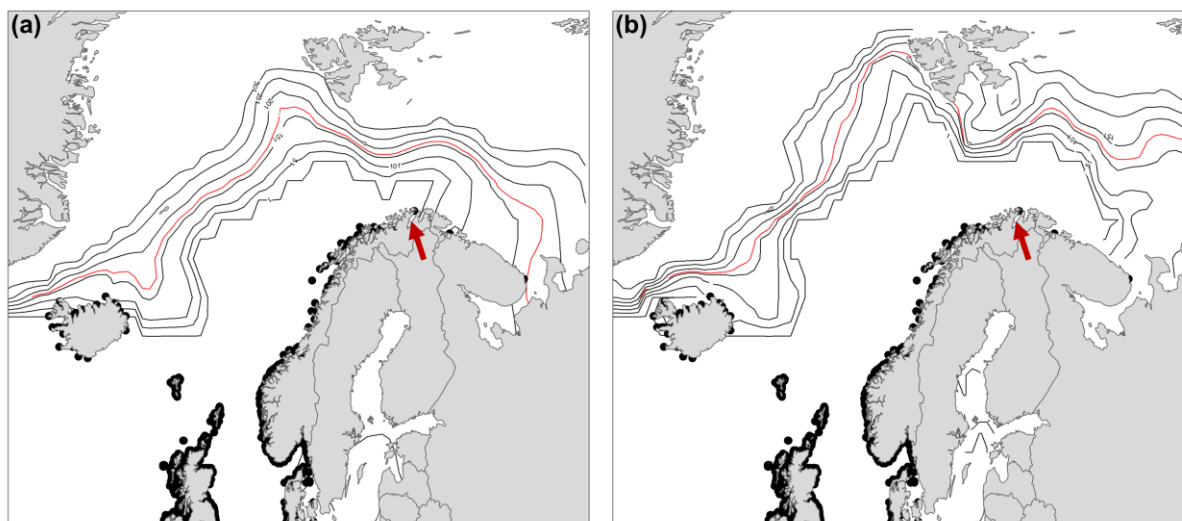
Figure 7: Species distribution model of *Laminaria hyperborea* modeling temperature × photoperiod interactions. Model used for predictions: $FvFm_{n,j}$ ~ $FvFm_{j,\ n-1}$ -0.0001390 * $time_{n,j}$×$photoperiod_{n,j}$ + 0.0000193 * $time_{n,j}$×$temp_{n,j}$×$photoperiod_{n,j}$, with n = day of year and j = pixel. Black dots show the current distribution of *L. hyperborea* in this region as obtained from www.gbif.org excluding the record for Spitsbergen (see Introduction) (https://doi.org/10.15468/dl.jhppyr, November 2022; Mikhaylova, 2010; pers. comm. T.A. Mikhaylova). Red arrows mark the sampling location at Porsangerfjorden, Norway (Finmark). **(a)** Map shows sum of days per year with predicted F_v/F_m ≤0.3 (survival limit for kelps), daily SST averaged over the period 2000–2014. The red line marks the F_v/F_m threshold of 200 days below 0.3, which represents the present-day distribution limit. **(b)** Map shows future prediction for sum of days per year with F_v/F_m ≤0.3, daily SST for 2023+1°C. The red line is shifted under elevated SST.

The geographic projections of the final model show distinctly different results for the two temperature scenarios. For scenario 1 (daily SST averaged over the years 2000–2014, **Fig. 7a**) the area of the Spitsbergen Archipelago is predicted to exhibit environmental conditions under which F_v/F_m is expected to be ≤0.3 for over 289 to 337 days per year. The F_v/F_m threshold was set to 200 days below 0.3, which represents the present-day distribution limit. A continuous F_v/F_m of <0.3 would mean death for kelps. Most of the known distributional range is in areas that experience such conditions for 0 days per year, except for populations from northern Iceland and in northernmost Norway, where populations might be exposed for up to 134 and 110 days, respectively. Under scenario 2 (daily SST in 2023+1°C, **Fig. 7b**), the isoclines shift northward and eastward, following increasing temperatures and indicating less adverse conditions. The isocline of 200 days with predicted F_v/F_m ≤0.3 per year now reaches the western coast of the Spitsbergen

Archipelago. Here, the number of days with F_v/F_m ≤0.3 per year now ranges from 177 to 337 days. For Iceland, northernmost Norway and the Russian coast the environmental conditions are predicted to cause less days of physiological stress per year.

4   Discussion

This study emphasizes the importance of studying the combined effects of abiotic variables on seaweeds and their distribution potential. Our results clearly show that the interaction of photoperiods and temperatures had a greater influence on *L. hyperborea* than either factor alone, and that elevated temperatures lead to an increase in habitat suitability of High Arctic environments for *L. hyperborea*. In fact, increasing temperatures counteracted impairing photoperiodical effects. We showed that photoperiods must especially be included when it comes to predicting distributions of seaweeds and other primary producers under polar conditions.

4.1 Warming of the High Arctic – Curse or blessing for Laminaria hyperborea*?*

Although *L. hyperborea* survives within the temperature ranges of the High Arctic, and could in principle also grow and reproduce (i.e., gametogenesis, sporogenesis) (Bolton and Lüning, 1982; tom Dieck (Bartsch), 1992; Sjøtun and Schoschina, 2002), the species has not yet been found at such high latitudes (Bartsch et al., 2016, Düsedau et al. in revision). Lüning (1986) suggested that the extended periods of long days in High Arctic regions might be a limiting factor for its distribution, as day lengths of 16 h or more inhibited the formation of new fronds. However, the interactive effects of prolonged light availability with rising temperature have not been tested in the latter study. Hence, it remained uncertain whether global warming will lead to an opening of the High Arctic for *L. hyperborea*.

We found a diminished physiological vitality (F_v/F_m <0.6; **Fig. 2**) of *L. hyperborea* at longer photoperiods ≥18 h, confirming our leading hypothesis that long photoperiods act as stressor. Additionally, the photoperiodical stress was intensified by low temperatures (0°C PolarDay: F_v/F_m ~0.3, 0°C LongDay: F_v/F_m ~0.5, 5°C PolarDay: F_v/F_m ~0.5). However, rising temperatures counteracted the impairing effects of extended day length. Temperatures of 5 and 10°C at LongDay resulted in F_v/F_m values >0.6, reflecting "healthy" conditions (Dring et al., 1996), while *L. hyperborea* at 10°C was unaffected even under PolarDay conditions. In this context it is important to point out that all treatment temperatures were below the species' optimum of 15°C (Bolton and Lüning, 1982).

The strong impact by the interaction of photoperiod and temperature was also found in the monitored DW of *L. hyperborea*. Samples exposed to ≥18 h of daylight significantly gained weight, with greater increases measured at ≥5°C. For the treatments, any potential effect of growth can

_____

be excluded, as no change in area of the samples was observed between the start and end of the experiment. Accordingly, *L. hyperborea* must have altered and stored metabolic products causing the weight gain. Since we observed a significant increase in the long-term carbohydrate reserve laminarin at long photoperiods, which was also amplified ≥5°C, we can assume that the gain in DW was mainly caused by the additional storage of laminarin. Laminarin concentration increased strongly by approx. 200 % when light was available, while mannitol as the primary product of photosynthesis and short-term storage carbohydrate did not rise. These findings confirmed that *L. hyperborea* was still able to photosynthesise efficiently and convert mannitol to laminarin (Yamaguchi et al., 1966; Graiff et al., 2018), although it was physiologically stressed during long photoperiods.

The beneficial effects of rising temperatures during conditions of ≥18 h of daylight were also reflected in adjustments of the photosynthetic apparatus. At the end of the experiment, significantly higher concentrations of Chl*a* and Acc were detected at 10°C compared to 0 and 5°C. Moreover, the content of Chl*a*, Acc and VAZ decreased significantly over time during PolarDay and cold LongDay conditions. Comparable patterns with reduced Chl*a* concentration under high light conditions and increased concentrations with enhanced temperatures were also found for kelps from Greenland (Niedzwiedz et al., 2024). Higher plants reduce their pigment content under the combined effect of high light and low temperature to reduce excitation pressure and avoid freezing damage (Lütz, 1996). Accordingly, we assume that the reduced pigment concentrations in *L. hyperborea* and other Arctic kelps at low temperatures and light stress served as photo-protective and anti-freezing mechanism.

The photo-protective mechanism DPS significantly increased up to w8 under low temperature and long photoperiodic conditions. In contrast, at 10°C a decrease in DPS was observed. Yet, the strong disparities between the treatments weakened considerably by w12. This effect might be an indication for an acclimation of *L. hyperborea* to light stress after prolonged exposure. Considering that the antioxidant phlorotannins also act as photo-protectants under prolonged PAR (photosynthetically active radiation) conditions (Steinhoff et al., 2012), it is surprising that we did not observe any response of phlorotannins to the long photoperiods. With means of 8–24 mg g^{-1} DW, *L. hyperborea* generally contained high concentrations of phlorotannins compared to other kelps collected in the High Arctic (1 and 3.5 mg g^{-1} DW; Diehl and Bischof, 2021; Diehl et al., 2023), which probably already provided sufficient protection against the intense light exposure during Polar Day.

Under PolarNight conditions, F_v/F_m of *L. hyperborea* was completely unaffected and independent of temperature. As in the case of the kelp *Saccharina latissima* (Gordillo et al., 2022), which has a similar southern distribution limit as *L. hyperborea* (Araújo et al., 2016), all samples of *L. hyperborea* remained in "healthy" conditions throughout the experiment at PolarNight (F_v/F_m

_____

>0.6; Dring et al., 1996). Also regarding DW, no significant changes were observed after three months of total darkness in *L. hyperborea*. Contrary, other kelp species such as *A. esculenta*, *S. latissima* and *Laminaria solidungula* lost weight during long periods of total darkness and under conditions of increasing temperatures during Polar Night (Scheschonk et al., 2019; Gordillo et al., 2022). Throughout the long Polar Night in the Arctic, mannitol and laminarin in *L. solidungula* and *S. latissima* strongly decreased (Scheschonk et al., 2019), which, however, could not be confirmed for *L. hyperborea* in this study, as it stored laminarin and preferentially utilised mannitol. Also, in contradiction to the findings by Scheschonk et al. (2019), higher temperatures at PolarNight did not result in an enhanced consumption of the storage carbohydrates. *Laminaria hyperborea* was presumably not affected by prolonged Polar Night conditions, as the species can be considered a "season anticipator" (Wiencke et al., 2009), as evidenced by its growth only under photoperiods <12 h (Lüning, 1986).

We did not detect any changes after three months of Polar Night or due to the different temperature treatments, which is in accordance with the *in-situ* observations by Scheschonk et al. (2019) on *L. solidungula* and *S. latissima* before and after the Polar Night period in Kongsfjorden (Svalbard). The fact that we additionally found no differences in the temperature treatments at PolarNight, could be caused by a lack of need of further protection against excitation pressure at low temperatures in total darkness (Lütz, 1996).

Past and current seasonal Arctic environmental conditions so far limited the spread of *L. hyperborea* sporophytes to higher latitudes (**see Box**). However, our experiment clearly indicated that higher SSTs also enable this kelp to cope with so far unfavorable photoperiods ≥18 h, while present and future Polar Night conditions neither impaired nor promoted *L. hyperborea*. Consequently, the physiological and biochemical results of our long-term experiment suggest a possible northward expansion of *L. hyperborea* as a result of climate change in the Arctic.

4.2 Heading Northwards?

Various model studies predicted a strong migration and increase in abundance for many seaweeds northwards in the Arctic, including *L. hyperborea* (Assis et al., 2018a, 2022; Frigstad et al., 2020). However, Arctic photoperiods were not integrated in such seaweed distribution models, while inclusion of physiological data improved the predictive power (Kearney and Porter, 2009; Martínez et al., 2015; Laeseke et al., 2020).

Clear beneficial effects of increasing temperatures during long photoperiods on the physiological or biochemical status of *L. hyperborea* were observed, while this kelp proved to be well adapted to current and future High Arctic winter conditions. The F_v/F_m data set can be treated as an integrated indicator of overall fitness and survival. Therefore, we used these data in a mechanistic species distribution model (Kearney and Porter, 2009). Our model confirmed the assumptions of

_____

the experiments: *L. hyperborea* will be able to spread into the High Arctic if SST continues to increase. When modeling the potential distribution of *L. hyperborea* under the warming scenario, the SST during the year was high enough for the species to spread throughout western Svalbard, albeit the extended photoperiods. However, for the present-day scenario (2000–2014), SST in the High Arctic was not suitable for the colonisation of *L. hyperborea* on the coasts of Svalbard, as physiological performance was impaired during Polar Days.

Nevertheless, there are some limitations in our study that need further exploration. We cannot exclude the possibility that there are other factors limiting the northward expansion of *L. hyperborea*. At low temperatures (0°C), for example, gametogenesis, germination of spores and growth of primary cells of *L. hyperborea* were observed, but development and growth were slow (tom Dieck (Bartsch), 1992; Sjøtun and Schoschina, 2002). Sjøtun and Schoschina (2002) assumed that the strongly delayed development of gametophytes during cold winters and the high mortality risk could be the limiting factor for the spread of *L. hyperborea* in the High Arctic. The development of spores and gametophytes, as well a response of young sporophytes, must therefore be tested under the same experimental conditions to assess the viability of the different life-history stages under High Arctic conditions.

In addition, environmental conditions might further alter habitat suitability for *L. hyperborea*. Sediment inputs lead to changes in underwater light climate along the Arctic coastal regions (Gattuso et al., 2020; Konik et al., 2021) and kelp canopies themselves drastically change the light availability inside kelp communities (Laeseke et al., 2019). Both effects have considerable impact on Arctic kelps, as they reduce incident radiation and thus weaken light stress, but also primary production and maximum depth distribution (Laeseke et al., 2019; Niedzwiedz and Bischof, 2023a). Accordingly, it is possible that decreased light availability further reduces photoperiodic stress for *L. hyperborea* in the High Arctic, leading to a higher habitat suitability. Our model further suffers from a lack of data on recovery of *L. hyperborea* after exposure to unfavorable conditions. Thus, it remains unknown whether *L. hyperborea* can recover from long photoperiods throughout the year. Both these effects must be investigated and considered in the future.

4.3 Ecological Implications

Arctic coastal ecosystems form an exceptional environment with a unique biodiversity that is under high risk due to rapid warming (Bringloe et al., 2020). Warming and consequential loss of sea ice will result in a gain of suitable habitats for intertidal and subtidal species in polar areas (Krause-Jensen et al., 2020), which in turn can lead to an invasion of non-polar species and to a reorganisation of species composition of ecological communities (Wassmann et al., 2011). New species or changes in species' diversity and abundance can have multiple consequences on the

functioning of marine ecosystems, such as changes in the carbon cycle (Vilas et al., 2020), shifts in biotic interactions (Gilson et al., 2021), or changes in the habitat function (Smale et al., 2015; Christie et al., 2022; Gouraguine et al., 2024). *Laminaria hyperborea* is a strong competitor that displaces other kelp species, as has been observed in the Northeast Atlantic (Lüning, 1990). Contrary to other structurally similar kelps that are abundant in the High Arctic, such as *Laminaria digitata*, the stipe of *L. hyperborea* is rich in epibiont assemblages, including Rhodophyta, Bryozoa, Polychaeta, and many more (Schultze et al., 1990; Christie et al., 2003, 2009). The epibiotic community in turn acts, for example, as food source for associated mobile species, such as fish and sea urchins (Norderhaug et al., 2005; King et al., 2021). Hence, the spread of *L. hyperborea* in the High Arctic might have cascading effects on the entire ecosystem.

Authors Contributions

Nora Diehl: original concept, sampling, conducting the experiments, physiological and biochemical analyses, data analyses, writing and editing the manuscript. **Philipp Laeseke:** data analyses with GL(M)M, supporting the statistics, making geographic projections, helping with interpretation of the data. **Inka Bartsch:** providing the facilities for the experiment, helping with concept, interpretation of the data. **Margot Bligh, Hagen Buck-Wiese, Jan-Hendrik Hehemann:** conducting the laminarin analyses. **Sarina Niedzwiedz:** supporting the experiment and statistics. **Niklas Plag, Ulf Karsten:** providing facilities for and supporting the mannitol analyses. **Tifeng Shan:** conducting the DNA barcoding of the samples. **Kai Bischof:** providing facilities for the physiological and biochemical analyses, leader of the project, securement of funding, helping with interpretation. **All authors**: reviewed and revised the manuscript.

_____

Conflict of Interest Statement

No potential conflict of interest was reported by the authors.

References

Adey, W. H., and Steneck, R. S. (2001). Thermogeography over time creates biogeographic regions: A temperature/space/time-integrated model and an abundance-weighted test for benthic marine algae. *J. Phycol.* 37, 677–698. doi:10.1046/j.1529-8817.2001.00176.x.

Araújo, R. M., Assis, J., Aguillar, R., Airoldi, L., Bárbara, I., Bartsch, I., et al. (2016). Status, trends and drivers of kelp forests in Europe: an expert assessment. *Biodivers. Conserv.* 25, 1319–1348. doi:10.1007/s10531-016-1141-7.

Assis, J., Araújo, M. B., and Serrão, E. A. (2018a). Projected climate changes threaten ancient refugia of kelp forests in the North Atlantic. *Glob. Chang. Biol.* 24, e55–e66. doi:10.1111/gcb.13818.

Assis, J., Lucas, A. V., Bárbara, I., and Serrão, E. Á. (2016). Future climate change is predicted to shift long-term persistence zones in the cold-temperate kelp *Laminaria hyperborea*. *Mar. Environ. Res.* 113, 174–182. doi:10.1016/j.marenvres.2015.11.005.

Assis, J., Serrão, E. A., Duarte, C. M., Fragkopoulou, E., and Krause-Jensen, D. (2022). Major expansion of marine forests in a warmer Arctic. *Front. Mar. Sci.* 9. doi:10.3389/fmars.2022.850368.

Assis, J., Tyberghein, L., Bosch, S., Verbruggen, H., Serrão, E. A., and De Clerck, O. (2018b). Bio-ORACLE v2.0: Extending marine data layers for bioclimatic modelling. *Glob. Ecol. Biogeogr.* 27, 277–284. doi:10.1111/geb.12693.

Bartsch, I., Paar, M., Fredriksen, S., Schwanitz, M., Daniel, C., Hop, H., et al. (2016). Changes in kelp forest biomass and depth distribution in Kongsfjorden, Svalbard, between 1996–1998 and 2012–2014 reflect Arctic warming. *Polar Biol.* 39, 2021–2036. doi:10.1007/s00300-015-

1870-1.

Bartsch, I., Wiencke, C., Bischof, K., Buchholz, C. M., Buck, B. H., Eggert, A., et al. (2008). The genus *Laminaria sensu lato*: Recent insights and developments. *Eur. J. Phycol.* 43, 1–86. doi:10.1080/09670260701711376.

Bates, D., Mächler, M., Bolker, B., and Walker, S. (2015). Fitting linear mixed-effects models using lme4. *J. Stat. Softw.* 67, 1–48.

Becker, S., and Hehemann, J.-H. (2018). Laminarin quantification in microalgae with enzymes from marine microbes. *Bio-Protocol* 8, e2666. doi:10.21769/bioprotoc.2666.

Becker, S., Scheffel, A., Polz, M. F., and Hehemann, J. H. (2017). Accurate quantification of laminarin in marine organic matter with enzymes from marine microbes. *Appl. Environ. Microbiol.* 83, 1–14. doi:10.1128/AEM.03389-16.

Berge, J., Renaud, P. E., Darnis, G., Cottier, F., Last, K., Gabrielsen, T. M., et al. (2015). In the dark: A review of ecosystem processes during the Arctic polar night. *Prog. Oceanogr.* 139, 258–271. doi:10.1016/j.pocean.2015.08.005.

Bischof, K., Buschbaum, C., Fredriksen, S., Gordillo, F. J. L., Heinrich, S., Jiménez, C., et al. (2019). "Kelps and environmental changes in Kongsfjorden: Stress perception and responses," in *The ecosystem of Kongsfjorden, Svalbard. Advances in polar ecology*, eds. H. Hop and C. Wiencke (Cham: Springer International, Published AG, Switzerland), 373–422. doi:10.1007/978-3-319-46425-1_10.

Blanca, M. J., Alarcón, R., Arnau, J., Bono, R., and Bendayan, R. (2017). Non-normal data: Is ANOVA still a valid option? *Psicothema* 29, 552–557. doi:10.7334/psicothema2016.383.

Bolton, J. J., and Lüning, K. (1982). Optimal growth and maximal survival temperatures of Atlantic *Laminaria* species (Phaeophyta) in culture. *Mar. Biol.* 66, 89–94. doi:10.1007/BF00397259.

Bringloe, T. T., Verbruggen, H., and Saunders, G. W. (2020). Unique biodiversity in Arctic marine forests is shaped by diverse recolonization pathways and far northern glacial refugia. *Proc. Natl. Acad. Sci. U. S. A.* 117, 22590–22596. doi:10.1073/pnas.2002753117.

Callaghan, T. V., Björn, L. O., Chernov, Y., Chapin, T., Christensen, T. R., Huntley, B., et al. (2004). Biodiversity, distributions and adaptations of arctic species in the context of environmental change. *Ambio* 33, 404–417. doi:10.1579/0044-7447-33.7.404.

Christie, H., Andersen, G. S., Tveiten, L. A., and Moy, F. E. (2022). Macrophytes as habitat for fish. *ICES J. Mar. Sci.* 79, 435–444. doi:10.1093/icesjms/fsac008.

Christie, H., Jørgensen, N. M., Norderhaug, K. M., and Waage-Nielsen, E. (2003). Species distribution and habitat exploitation of fauna associated with kelp (*Laminaria hyperborea*) along the Norwegian coast. *J. Mar. Biol. Assoc. United Kingdom* 83, 687–699. doi:10.1017/S0025315403007653h.

Christie, H., Norderhaug, K. M., and Fredriksen, S. (2009). Macrophytes as habitat for fauna. *Mar. Ecol. Prog. Ser.* 396, 221–233. doi:10.3354/meps08351.

Colombo-Pallotta, M. F., García-Mendoza, E., and Ladah, L. B. (2006). Photosynthetic performance, light absorption, and pigment composition of *Macrocystis pyrifera* (Laminariales, Phaeophyceae) blade from different depths. *J. Phycol.* 42, 1225–1234. doi:10.1111/j.1529-8817.2006.00287.x.

Copernicus (2023). Copernicus - Europe's Eyes on. *Copernicus Clim. Chang. Serv.* Available at: https://climate.copernicus.eu/.

Cruces, E., Huovinen, P., and Gómez, I. (2012). Phlorotannin and antioxidant responses upon short-term exposure to UV radiation and elevated temperature in three South Pacific kelps. *Photochem. Photobiol.* 88, 58–66. doi:10.1111/j.1751-1097.2011.01013.x.

Dankworth, M., Heinrich, S., Fredriksen, S., and Bartsch, I. (2020). DNA barcoding and mucilage ducts in the stipe reveal the presence of *Hedophyllum nigripes* (Laminariales, Phaeophyceae) in Kongsfjorden (Spitsbergen). *J. Phycol.* 56, 1245–1254. doi:10.1111/jpy.13012.

Diehl, N., and Bischof, K. (2021). Coping with a changing Arctic: mechanisms of acclimation in the brown seaweed *Saccharina latissima* from Spitsbergen. *Mar. Ecol. Prog. Ser.* 657, 43–57. doi:10.3354/meps13532.

Diehl, N., Karsten, U., and Bischof, K. (2020). Impacts of combined temperature and salinity stress on the endemic Arctic brown seaweed *Laminaria solidungula* J. Agardh. *Polar Biol.* 43, 647–656. doi:10.1007/s00300-020-02668-5.

Diehl, N., Li, H., Scheschonk, L., Burgunter-Delamare, B., Niedzwiedz, S., Forbord, S., et al. (2024). The sugar kelp *Saccharina latissima* I: recent advances in a changing climate. *Ann. Bot.* 133, 183–211. doi:10.1093/aob/mcad173.

Diehl, N., Roleda, M. Y., Bartsch, I., Karsten, U., and Bischof, K. (2021). Summer heatwave impacts on the European kelp *Saccharina latissima* across its latitudinal distribution gradient. *Front. Mar. Sci.* 8, 695821. doi:10.3389/fmars.2021.695821.

Diehl, N., Steiner, N., Bischof, K., Karsten, U., and Heesch, S. (2023). Exploring intraspecific variability – biochemical and morphological traits of the sugar kelp *Saccharina latissima* along latitudinal and salinity gradients in Europe. *Front. Mar. Sci.* 10, 995982. doi:10.3389/fmars.2023.995982.

Dring, M. J., Makarov, V., Schoschina, E., Lorenz, M., and Lüning, K. (1996). Influence of ultraviolet-radiation on chlorophyll fluorescence and growth in different life-history stages of three species of *Laminaria* (Phaeophyta). *Mar. Biol.* 126, 183–191. doi:10.1007/BF00347443.

Düsedau, L., Fredriksen, S., Brand, M., Fischer, P., Karsten, U., Bischof, K., Savoie, A., Bartsch, I. (in revision). Kelp forest community structure and demography in Kongsfjorden (Svalbard) across 25 years of Arctic warming.

Eger, A. M., Aguirre, J. D., Altamirano, M., Arafeh-Dalmau, N., Arroyo, N. L., Bauer-Civiello, A. M., et al. (2023). The Kelp Forest Challenge: A collaborative global movement to protect and restore 4 million hectares of kelp forests. *J. Appl. Phycol.* doi:10.1007/s10811-023-03103-y.

Farrugia Drakard, V., Hollarsmith, J. A., and Stekoll, M. S. (2023). High-latitude kelps and future oceans: A review of multiple stressor impacts in a changing world. *Ecol. Evol.* 13, e10277. doi:10.1002/ece3.10277.

Filbee-Dexter, K., and Wernberg, T. (2018). Rise of turfs: A new battlefront for globally declining kelp forests. *Bioscience* 68, 64–76. doi:10.1093/biosci/bix147.

Filbee-Dexter, K., Wernberg, T., Fredriksen, S., Norderhaug, K. M., and Pedersen, M. F. (2019). Arctic kelp forests: Diversity, resilience and future. *Glob. Planet. Change* 172, 1–14. doi:10.1016/j.gloplacha.2018.09.005.

Filbee-Dexter, K., Wernberg, T., Grace, S. P., Thormar, J., Fredriksen, S., Narvaez, C. N., et al. (2020). Marine heatwaves and the collapse of marginal North Atlantic kelp forests. *Sci. Rep.* 10, 13388. doi:10.1038/s41598-020-70273-x.

Fragkopoulou, E., Serrão, E. A., De Clerck, O., Costello, M. J., Araújo, M. B., Duarte, C. M., et al. (2022). Global biodiversity patterns of marine forests of brown macroalgae. *Glob. Ecol. Biogeogr.* 31, 636–648. doi:10.1111/geb.13450.

Fredriksen, S., Karsten, U., Bartsch, I., Woelfel, J., Koblowsky, M., Schumann, R., et al. (2019). "Chapter 9: Biodiversity of Benthic Macro- and Microalgae from Svalbard with Special Focus on Kongsfjorden," in *The ecosystem of Kongsfjorden, Svalbard, Advances in polar*

ecology, eds. H. Hop and C. Wiencke (Cham: Springer International, Published AG, Switzerland), 331–371. doi:10.1007/978-3-319-46425-1_9.

Fredriksen, S., and Kile, M. R. (2012). The algal vegetation in the outer part of Isfjorden, Spitsbergen: Revisiting Per Svendsen's sites 50 years later. *Polar Res.* 31, 17538. doi:10.3402/polar.v31i0.17538.

Frigstad, H., Gundersen, H., Andersen, G. S., Borgersen, G., Kvile, K. O., Krause-Jensen, D., et al. (2020). Blue Carbon – climate adaptation, CO_2 uptake and sequestration of carbon in Nordic blue forests - Results from the Nordic Blue Carbon Project. *TemaNord* 541, 541. Available at: http://dx.doi.org/10.6027/temanord2020-541.

Gattuso, J. P., Gentili, B., Antoine, D., and Doxaran, D. (2020). Global distribution of photosynthetically available radiation on the seafloor. *Earth Syst. Sci. Data* 12, 1697–1709. doi:10.5194/essd-12-1697-2020.

Gilson, A. R., Smale, D. A., and O'Connor, N. (2021). Ocean warming and species range shifts affect rates of ecosystem functioning by altering consumer–resource interactions. *Ecology* 102, 1–12. doi:10.1002/ecy.3341.

Gordillo, F. J. L., Carmona, R., and Jiménez, C. (2022). A warmer Arctic compromises winter survival of habitat-forming seaweeds. *Front. Mar. Sci.* 8, 1–18. doi:10.3389/fmars.2021.750209.

Gouraguine, A., Smale, D. A., Edwards, A., King, N. G., Jackson-Bué, M., Kelly, S., et al. (2024). Temporal and spatial drivers of the structure of macroinvertebrate assemblages associated with *Laminaria hyperborea* detritus in the northeast Atlantic. *Mar. Environ. Res.* 198, 106518. doi:10.1016/j.marenvres.2024.106518.

Graiff, A., Ruth, W., and Karsten, U. (2018). "Identification and quantification of laminarins in brown algae," in *Protocols for Macroalgae Research*, eds. B. Charrier, T. Wichard, and C. R. K. Reddy (CRC Press), 189–201.

Hijmans, R., Bivand, R., Pebesma, E., and Sumner, M. (2023). terra: Spatial Data Analysis.

Hijmans, R. J., Karney, C., Williams, E., and Vennes, C. (2022). geosphere: Spherical Trigonometry.

Hurd, C. L., Harrison, P. J., Bischof, K., and Lobban, C. S. (2014). *Seaweed Ecology and Physiology*. Second Edi. Cambridge: Cambridge University Press.

Kain, J. M. (1971). Synopsis of biological data on *Laminaria hyperborea*. *FAO Fish* Synopsis, 68 pp. Available at: http://www.fao.org/3/c3845e/c3845e.pdf.

Kain, J. M. (1979). "A view of the genus *Laminaria*," in *Oceanography and Marine Biology: An Annual Review*, ed. M. Barnes (Aberdeen: Aberdeen University Press), 101–161.

Kain, J. M., and Jones, N. S. (1975). The biology of *Laminaria hyperborea* VII. Reproduction of the sporophyte. *J. Mar. Biol. Assoc. United Kingdom* 55, 567–582. doi:10.1017/S0025315400017264.

Karsten, U., Thomas, D. N., Weykam, G., Daniel, C., and Kirst, G. O. (1991). A simple and rapid method for extraction and separation of low molecular weight carbohydrates from macroalgae using high-performance liquid chromatography, II. Intracellular inorganic ions and organic compounds. *Plant Physiol. Biochem.* 29, 373–378.

Kearney, M., and Porter, W. (2009). Mechanistic niche modelling: Combining physiological and spatial data to predict species' ranges. *Ecol. Lett.* 12, 334–350. doi:10.1111/j.1461-0248.2008.01277.x.

King, N. G., Moore, P. J., Wilding, C., Jenkins, H. L., and Smale, D. A. (2021). Multiscale spatial variability in epibiont assemblage structure associated with stipes of kelp *Laminaria hyperborea* in the northeast Atlantic. *Mar. Ecol. Prog. Ser.* 672, 33–44. doi:10.3354/meps13794.

Konik, M., Darecki, M., Pavlov, A. K., Sagan, S., and Kowalczuk, P. (2021). Darkening of the Svalbard fjords waters observed with satellite ocean volor imagery in 1997 – 2019. *Front. Mar. Sci.* 8, 699318. doi:10.3389/fmars.2021.699318.

Krause-Jensen, D., Archambault, P., Assis, J., Bartsch, I., Bischof, K., Filbee-Dexter, K., et al. (2020). Imprint of climate change on Pan-Arctic marine vegetation. *Front. Mar. Sci.* 7, 617324. doi:10.3389/fmars.2020.617324.

Laeseke, P., Bartsch, I., and Bischof, K. (2019). Effects of kelp canopy on underwater light climate and viability of brown algal spores in Kongsfjorden (Spitsbergen). *Polar Biol.* 42, 1511–1527. doi:10.1007/s00300-019-02537-w.

Laeseke, P., Martínez, B., Mansilla, A., and Bischof, K. (2020). Future range dynamics of the red alga *Capreolia implexa* in native and invaded regions: Contrasting predictions from species distribution models versus physiological knowledge. *Biol. Invasions* 22, 1339–1352. doi:10.1007/s10530-019-02186-4.

Lebrun, A., Comeau, S., Gazeau, F., and Gattuso, J. P. (2022). Impact of climate change on Arctic macroalgal communities. *Glob. Planet. Change* 219, 103980. doi:10.1016/j.gloplacha.2022.103980.

Lenth, R. (2024). emmeans: Estimated Marginal Means, aka Least-Squares Means, R package version 1.10.0.

Longtin, C. M., and Saunders, G. W. (2015). On the utility of mucilage ducts as a taxonomic character in *Laminaria* and *Saccharina* (Phaeophyceae) – The conundrum of *S. groenlandica*. *Phycologia* 54, 440–450. doi:10.2216/15-19.1.

Lüning, K. (1980). Critical levels of light and temperature regulating the gemtogenesis of three *Laminaria* species (Phaeophyceae). *J. Phycol.* 16, 1–15.

Lüning, K. (1985). *Meeresbotanik - Verbreitung, Ökophysiologie und Nutzung der marinen Makroalgen*. Stuttgart - New York: Georg Thieme Verlag.

Lüning, K. (1986). New frond formation in *Laminaria hyperborea* (Phaeophyta): A photoperiodic response. *Br. Phycol. J.* 21, 269–273. doi:10.1080/00071618600650311.

Lüning, K. (1990). *Seaweeds - Their environment, biogeography, and ecophysiology.* , eds. C. Yarish and H. Kirkman Stuttgart: John Wiley & Sons, Inc.

Lütz, C. (1996). Avoidance of photoinhibition and examples of photodestruction in high alpine *Eriophorum*. *J. Plant Physiol.* 148, 120–128. doi:10.1016/S0176-1617(96)80303-8.

Martínez, B., Arenas, F., Trilla, A., Viejo, R. M., and Carreño, F. (2015). Combining physiological threshold knowledge to species distribution models is key to improving forecasts of the future niche for macroalgae. *Glob. Chang. Biol.* 21, 1422–1433. doi:10.1111/gcb.12655.

Mauger, S., Fouqueau, L., Avia, K., Reynes, L., Serrao, E. A., Neiva, J., et al. (2021). Development of tools to rapidly identify cryptic species and characterize their genetic diversity in different European kelp species. *J. Appl. Phycol.* 33, 4169–4186. doi:10.1007/s10811-021-02613-x.

Mikhaylova, T. A. (2010). *Laminaria hyperborea* (Laminariaceae) on the Murman coast of the Barents Sea. *Bot. Zhurnal* 95, 326–338.

Niedzwiedz, S., and Bischof, K. (2023a). Glacial retreat and rising temperatures are limiting the expansion of temperate kelp species in the future Arctic. *Limnol. Oceanogr.*, 1–15. doi:10.1002/lno.12312.

Niedzwiedz, S., and Bischof, K. (2023b). Irradiance data at different depths and sites for field sampling the Arctic fjord Kongsfjorden. Pangaea Database. doi:10.1594/PANGAEA.951173.

Niedzwiedz, S., Vonnahme, T. R., Juul-Pedersen, T., Bischof, K., and Diehl, N. (2024). Light-mediated temperature susceptibility of kelp species (*Agarum clathratum*, *Saccharina latissima*) in an Arctic summer heatwave scenario. *Cambridge Prism. Coast. Futur.* 2, 1–13.

doi:10.1017/cft.2024.5.

Norderhaug, K. M., Christie, H., Fosså, J. H., and Fredriksen, S. (2005). Fish-macrofauna interactions in a kelp (*Laminaria hyperborea*) forest. *J. Mar. Biol. Assoc. United Kingdom* 85, 1279–1286. doi:10.1017/S0025315405012439.

Provasoli, L. (1968). "Media and prospects for the cultivation of marine algae," in *Cultures and collections of algae. In: Proceedings of the Japanese Conference Hakone. Japanese Society of Plant Physiology*, eds. A. Watanabe and A. Hattori (Tokyo), 63–75.

R Core Team, R. (2022). R: A language and environment for statistical computing.

Rantanen, M., Karpechko, A. Y., Lipponen, A., Nordling, K., Hyvärinen, O., Ruosteenoja, K., et al. (2022). The Arctic has warmed nearly four times faster than the globe since 1979. *Commun. Earth Environ.* 3, 168. doi:10.1038/s43247-022-00498-3.

Reed, D., Washburn, L., Rassweiler, A., Miller, R., Bell, T., and Harrer, S. (2016). Extreme warming challenges sentinel status of kelp forests as indicators of climate change. *Nat. Commun.* 7, 1–7. doi:10.1038/ncomms13757.

Reynolds, R. W., Rayner, N. A., Smith, T. M., Stokes, D. C., and Wang, W. (2002). An improved in situ and satellite SST analysis for climate. *J. Clim.* 15, 1609–1625. doi:10.1175/1520-0442(2002)015<1609:AIISAS>2.0.CO;2.

Roeber, V. M., Bajaj, I., Rohde, M., Schmülling, T., and Cortleven, A. (2021). Light acts as a stressor and influences abiotic and biotic stress responses in plants. *Plant Cell Environ.* 44, 645–664. doi:10.1111/pce.13948.

Scheschonk, L., Becker, S., Hehemann, J., Diehl, N., Karsten, U., and Bischof, K. (2019). Arctic kelp eco-physiology during the polar night in the face of global warming: a crucial role for laminarin. *Mar. Ecol. Prog. Ser.* 611, 59–74. doi:https://doi.org/10.3354/meps12860.

Schloerke, B., Cook, D., Larmarange, J., Briatte, F., Marbach, M., Thoen, E., et al. (2023). GGally: Extension to 'ggplot2'_. R package version 2.2.0.

Schoschina, E. V. (1997). On *Laminaria hyperborea* (Laminariales, phaeophyceae) on the murman coast of the barents sea. *Sarsia* 82, 371–373. doi:10.1080/00364827.1997.10413663.

Schultze, K., Janke, K., Krüß, A., and Weidemann, W. (1990). The marcofauna and macroflora associated with *Laminaria digitata* and *L. hyperborea* at the island of Helgoland (German Bight, North Sea). *Helgoländer Meeresuntersuchungen* 4, 39–51. doi:10.1002/ardp.18681830330.

Sjøtun, K., Fredriksen, S., Lein, T. E., Rueness, J., and Sivertsen, K. (1993). Population studies of *Laminaria hyperborea* from its northern range of distribution in Norway. *Hydrobiologia* 260/261, 215–221. doi:10.1007/BF00049022.

Sjøtun, K., and Schoschina, E. V. (2002). Gametophytic development of *Laminaria* spp. (Laminariales, Phaeophyta) at low temperature. *Phycologia* 41, 147–152. doi:10.2216/i0031-8884-41-2-147.1.

Skogseth, R., Olivier, L. L. A., Nilsen, F., Falck, E., Fraser, N., Tverberg, V., et al. (2020). Variability and decadal trends in the Isfjorden (Svalbard) ocean climate and circulation – An indicator for climate change in the European Arctic. *Prog. Oceanogr.* 187, 102394. doi:10.1016/j.pocean.2020.102394.

Smale, D. A. (2020). Impacts of ocean warming on kelp forest ecosystems. *New Phytol.* 225, 1447–1454. doi:10.1111/nph.16107.

Smale, D. A., Wernberg, T., Yunnie, A. L. E., and Vance, T. (2015). The rise of *Laminaria ochroleuca* in the Western English Channel (UK) and comparisons with its competitor and assemblage dominant *Laminaria hyperborea*. *Mar. Ecol.* 36, 1033–1044. doi:10.1111/maec.12199.

_____

Sorte, C. J. B., Fuller, A., and Bracken, M. E. S. (2010). Impacts of a simulated heat wave on composition of a marine community. *Oikos* 119, 1909–1918. doi:10.1111/j.1600-0706.2010.18663.x.

Springer, K., Lütz, C., Lütz-Meindl, U., Wendt, A., and Bischof, K. (2017). Hyposaline conditions affect UV susceptibility in the Arctic kelp *Alaria esculenta* (Phaeophyceae). *Phycologia* 56, 675–685. doi:10.2216/16-122.1.

Steinhoff, F. S., Graeve, M., Bartoszek, K., Bischof, K., and Wiencke, C. (2012). Phlorotannin production and lipid oxidation as a potential protective function against high photosynthetically active and UV radiation in gametophytes of *Alaria esculenta* (Alariales, Phaeophyceae). *Photochem. Photobiol.* 88, 46–57. doi:10.1111/j.1751-1097.2011.01004.x.

Straub, S. C., Wernberg, T., Thomsen, M. S., Moore, P. J., Burrows, M. T., Harvey, B. P., et al. (2019). Resistance, extinction, and everything in between – The diverse responses of seaweeds to marine heatwaves. *Front. Mar. Sci.* 6, 763. doi:10.3389/fmars.2019.00763.

Sunday, J. M., Bates, A. E., and Dulvy, N. K. (2012). Thermal tolerance and the global redistribution of animals. *Nat. Clim. Chang.* 2, 686–690. doi:10.1038/nclimate1539.

Sunday, J. M., Pecl, G. T., Frusher, S., Hobday, A. J., Hill, N., Holbrook, N. J., et al. (2015). Species traits and climate velocity explain geographic range shifts in an ocean-warming hotspot. *Ecol. Lett.* 18, 944–953. doi:10.1111/ele.12474.

Teagle, H., Hawkins, S. J., Moore, P. J., and Smale, D. A. (2017). The role of kelp species as biogenic habitat formers in coastal marine ecosystems. *J. Exp. Mar. Bio. Ecol.* 492, 81–98. doi:10.1016/j.jembe.2017.01.017.

Tennekes, M. (2018). tmap: Thematic Maps in R. Journal of Statistical Software. *J. Stat. Softw.* 84, 1–39.

Thomsen, M. S., Wernberg, T., Altieri, A., Tuya, F., Gulbransen, D., McGlathery, K. J., et al. (2010). Habitat cascades: The conceptual context and global relevance of facilitation cascades via habitat formation and modification. *Integr. Comp. Biol.* 50, 158–175. doi:10.1093/icb/icq042.

tom Dieck (Bartsch), I. (1992). North Pacific and North Atlantic digitate *Laminaria* species (Phaeophyta): hybridization experiments and temperature responses. *Phycologia* 31, 147–163. doi:10.2216/i0031-8884-31-2-147.1.

tom Dieck, I. (1993). Temperature tolerance and survival in darkness of kelp gametophytes (Laminariales, Phaeophyta): ecological and biogeographical implications. *Mar. Ecol. Prog. Ser.* 100, 253–264. doi:10.3354/meps100253.

Tronholm, A., Leliaert, F., Sansón, M., Afonso-Carrillo, J., Tyberghein, L., Verbruggen, H., et al. (2012). Contrasting geographical distributions as a result of thermal tolerance and long-distance dispersal in two allegedly widespread tropical brown algae. *PLoS One* 7, e30813. doi:10.1371/journal.pone.0030813.

Vilas, D., Coll, M., Pedersen, T., Corrales, X., Filbee-Dexter, K., Pedersen, M. F., et al. (2020). Kelp-carbon uptake by Arctic deep-sea food webs plays a noticeable role in maintaining ecosystem structural and functional traits. *J. Mar. Syst.* 203, 103268. doi:10.1016/j.jmarsys.2019.103268.

Vranken, S., Wernberg, T., Scheben, A., Severn-Ellis, A. A., Batley, J., Bayer, P. E., et al. (2021). Genotype-environment mismatch of kelp forests under climate change. *Mol. Ecol.* 30, 3730–3746. doi:10.1111/mec.15993.

Wassmann, P., Duarte, C. M., Agustí, S., and Sejr, M. K. (2011). Footprints of climate change in the Arctic marine ecosystem. *Glob. Chang. Biol.* 17, 1235–1249. doi:10.1111/j.1365-2486.2010.02311.x.

_____

Wernberg, T., Krumhansl, K., Filbee-Dexter, K., and Pedersen, M. F. (2019). "Status and trends for the world's kelp forests," in *World Seas: An environmental evaluation* (Elsevier Ltd.), 57–78. doi:10.1016/b978-0-12-805052-1.00003-6.

Wernberg, T., Thomsen, M. S., Baum, J. K., Bishop, M. J., Bruno, J. F., Coleman, M. A., et al. (2024). Impacts of climate change on marine foundation species. *Annu. Rev. ofMarine Sci.* 16, 247–282. doi:10.1163/9789004204225_008.

Wickham, H. (2016). ggplot2: Elegant Graphics for Data Analysis.

Wickham, H., Vaughan, D., and Girlich, M. (2023). tidyr: Tidy Messy Data.

Wiencke, C., and Bischof, K. (2012). *Seaweed Biology - Novel insights into ecophysiology, ecology and utilization.* Heidelberg New York Dodrecht London: Springer.

Wiencke, C., Gómez, I., and Dunton, K. (2009). Phenology and seasonal physiological performance of polar seaweeds. *Bot. Mar.* 52, 585–592. doi:10.1515/BOT.2009.078.

Wilson, K. L., Skinner, M. A., and Lotze, H. K. (2019). Projected 21st-century distribution of canopy-forming seaweeds in the Northwest Atlantic with climate change. *Divers. Distrib.* 25, 582–602. doi:10.1111/ddi.12897.

Wood, S. (2023). mgcv: Mixed GAM Computation Vehicle with Automatic Smoothness Estimation.

Yamaguchi, T., Ikawa, T., and Nisizawa, K. (1966). Incorporation of radioactive carbon from $H^{14}CO_3$- into sugar constituents by a brown alga, *Eisenia bicyclis*, during photosynthesis and its fate in the dark. *Plant Cell Physiol.* 7, 217–229. doi:10.1093/oxfordjournals.pcp.a079175.

Zacher, K., Rautenberger, R., Hanelt, D., Wulff, A., and Wiencke, C. (2009). The abiotic environment of polar marine benthic algae. *Bot. Mar.* 52, 483–490. doi:10.1515/BOT.2009.082.

Zuur, A. F., Hilbe, J., and Ieno, E. N. (2013). *A Beginner's Guide to GLM and GLMM with R: A frequentist and Bayesian perspective for ecologists.* Newburgh, United Kingdom: Highland Statistics Ltd.

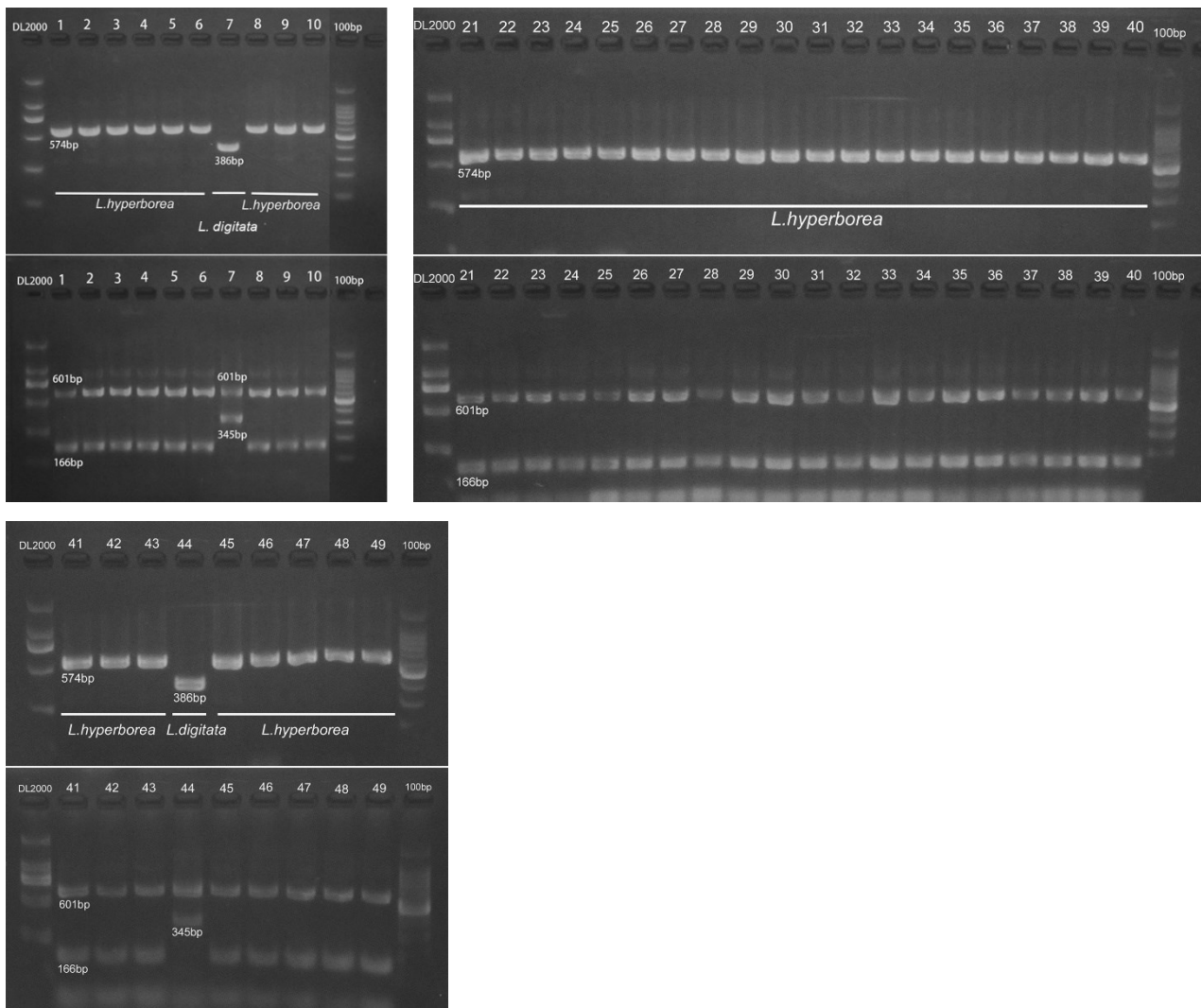**Supplementary Figures & Tables:**

Fig. S1: For species identification of all 39 samples, the amplified fragment patterns of PCR1 and PCR2 were compared to those of Mauger et al. (2021). 37 specimens were identified as *Laminaria hyperborea* (Gunnerus) Foslie, while two specimens were identified as *Laminaria digitata* (Hudson) J.V. Lamouroux. Samples No. 11–20 were part of another experiment and are therefore not included here.

Table S1: Minimum, maximum and mean sea surface temperatures (SST) between 0 and 20 m depth measured in Kongsfjorden between 1980/1982 and 2018/2022. Data downloaded from http://choc.imev-mer.fr/shiny/dataAccess/ (for references see reference list).

in-situ **data:**

year	season	min [°C]	max [°C]	mean [°C]	mean year [°C]
1980 – 2000	winter	-1.97	3.85	-1.67	3.16
	summer	-1.64	7.22	3.50	
2001 – 2018	winter	-1.21	3.82	1.03	4.03
	summer	-0.76	8.14	4.42	

data received from: Skogseth et al. 2019

OISST data:

year	season	min [°C]	max [°C]	mean [°C]	mean year [°C]
1982 – 2000	winter	-1.8	4.86	0.63	1.56
	summer	-0.98	8.71	3.59	
2001 – 2022	winter	-1.8	3.82	0.22	1.75
	summer	-1.43	9.47	3.85	

data received from: Huang et al. 2021

Table S2: Parameter estimates (β) and corresponding *p*-values for the included variables from the final generalised linear model.

$Fv/Fm \sim time * temperature * photoperiod$		
Null deviance: 22.4 on 496 degrees of freedom		
Residual deviance: 6.4 on 489 degrees of freedom		
Variable	**β-Estimate**	***p*-value**
intercept	0.68	**< 0.001**
exposure time	0.0002	0.152
temperature	0.0012	0.193
photoperiods	0.0003	0.469
time × temperature	0.00001292	0.589
time × photoperiod	0.000139	**< 0.001**
temperature × photoperiod	0.00003132	0.581
time × temperature × photoperiod	0.00001393	**< 0.001**

References

Huang, B., Liu, C., Banzon, V., Freeman, E., Graham, G., Hankins, B., Smith, T., Zhang, H.-M. (2021). Improvements of the Daily Optimum Interpolation Sea Surface Temperature (DOISST) Version 2.1. *Journal of Climate, 34,* 2923–2939. https://doi.org/10.1175/JCLI-D-20-0166

Mauger, S., Fouqueau, L., Avia, K., Reynes, L., Serrao, E. A., Neiva, J., Valero, M. (2021). Development of tools to rapidly identify cryptic species and characterize their genetic diversity in different European kelp species. *Journal of Applied Phycology*, *33*, 4169–4186. https://doi.org/10.1007/s10811-021-02613-x

Skogseth, R., Ellingsen, P., Berge, J., Cottier, F., Falk-Petersen, S., Ivanov, B., Nilsen, F., Søreide, J., Vader, A. (2019). UNIS hydrographic database [Data set]. Norwegian Polar Institute. https://doi.org/10.21334/unis-hydrography

PUBLICATION V

Glacial retreat and rising temperatures are limiting the expansion of temperate kelp species in the future Arctic

Sarina Niedzwiedz, Kai Bischof

Glacial run-off opposes Arctic kelp expansion

Sarina Niedzwiedz, Kai Bischof

Marine Botany, Faculty of Biology and Chemistry & MARUM, University of Bremen, D-28359 Bremen, Germany
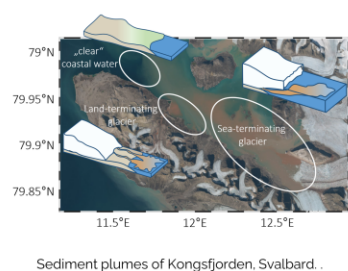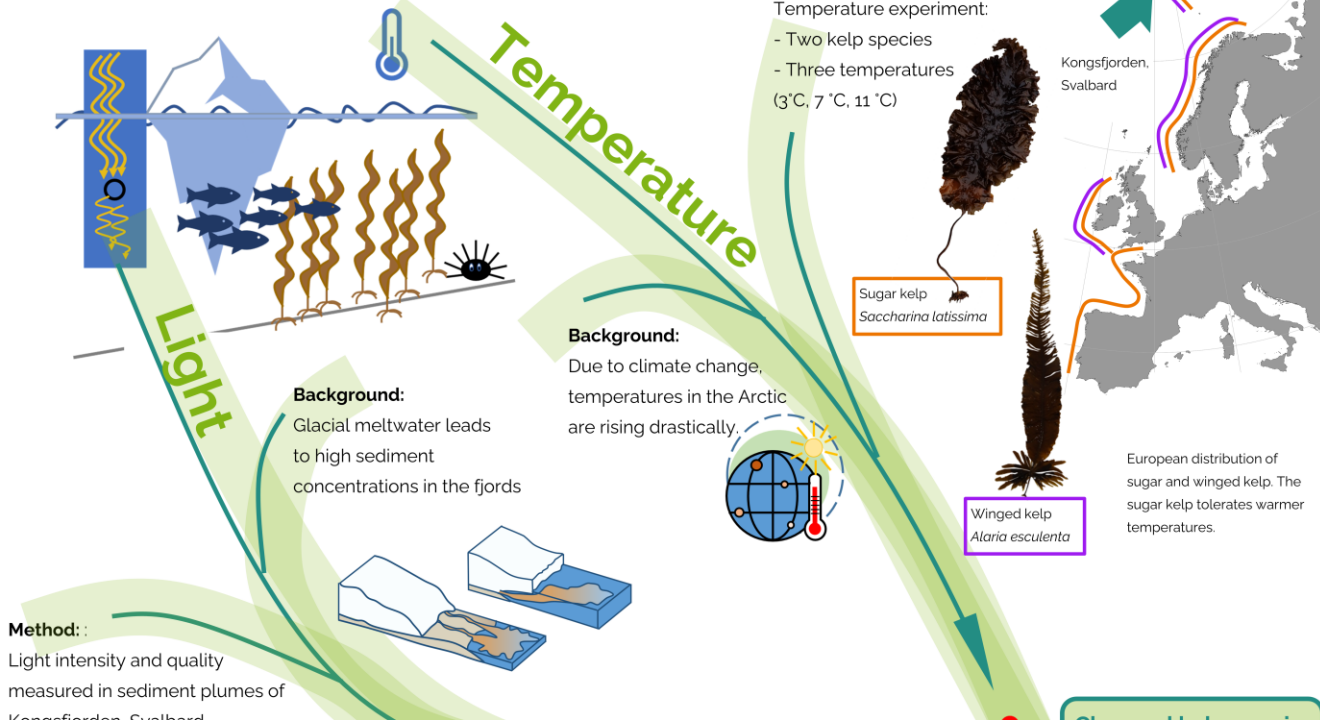
Kelps are brown macroalgae, forming vast submarine forests from temperate to polar regions. Their role in the ecosystem can be compared to trees, as kelps are providing habitat, food and nursery ground for many species. While the water temperature is determining their geographical distribution, light for photosynthesis is determining their depth distribution. Both temperature and light in the Arctic are changing due to climate change.

Research question: How are kelp forests changing in the Arctic in future?

Present

Currently, in the Arctic low temperatures and short light periods prevail.

Temperature

Method:
Temperature experiment:
- Two kelp species
- Three temperatures
(3 °C, 7 °C, 11 °C)

Kongsfjorden, Svalbard

Sugar kelp
Saccharina latissima

Background:
Due to climate change, temperatures in the Arctic are rising drastically.

Winged kelp
Alaria esculenta

European distribution of sugar and winged kelp. The sugar kelp tolerates warmer temperatures.

Light

Background:
Glacial meltwater leads to high sediment concentrations in the fjords

Method: :
Light intensity and quality measured in sediment plumes of Kongsfjorden, Svalbard.

79°N
79.95°N
„clear" coastal water
Land-terminating glacier
79.9°N
Sea-terminating glacier
79.85°N
11.5°E   12°E   12.5°E

Sediment plumes of Kongsfjorden, Svalbard. .

Future

Reduction of kelp depth limit

Drastically reduced light intensity and quality in sediment plumes.

Changed kelp species composition

Polar kelp are constricted; temperate kelps are benefitting.

A changed species composition and reduced depth distribution will have cascading effects on Arctic ecosystems, being also of socio-economic importance.

Get the publication

Check for updates

LIMNOLOGY and OCEANOGRAPHY

ASLO

Glacial retreat and rising temperatures are limiting the expansion of temperate kelp species in the future Arctic

Sarina Niedzwiedz [ID],* Kai Bischof [ID]
Marine Botany, Faculty of Biology and Chemistry & MARUM, University of Bremen, Leobener Straße NW2, Bremen, Bremen, 28359, Germany

Abstract

Kelps act as ecosystem engineers on many polar rocky shore coastlines. The underwater light climate and temperature are the main drivers for their vertical and latitudinal distribution. With temperatures rising globally, an Arctic expansion of temperate kelp species and an accelerating glacial melt is predicted. It was our aim to investigate the effects of retreating glaciers and rising temperatures on the potential habitat of kelps in Arctic fjords. We analyzed the underwater light climate of areas being influenced by different stages of glacial retreat (sea-terminating glacier, land-terminating glacier, coastal water) in Arctic Kongsfjorden. We observed reduced light intensities and a changed spectral composition in glacial meltwater plumes, potentially resulting in an upward shift of the lower depth limit of kelp, counteracting the predicted biomass increase in the Arctic. Furthermore, we studied temperature-related changes in light-use characteristics in two kelp species (*Alaria esculenta*, *Saccharina latissima*) at 3°C, 7°C, and 11°C. Rising temperatures lead to a significant increase of the compensation irradiance of *A. esculenta*. The dark respiration of *S. latissima* increased significantly, correlating with a decreasing carbon content. We detected no differences in photosynthetic rates, although the chlorophyll *a* concentration of *A. esculenta* was ~ 78% higher compared to *S. latissima*. Ultimately, temperature-induced changes in kelps light-use characteristics might lead to a changed species composition, as we found *A. esculenta* better adapted to polar conditions. We conclude that the deterioration of the underwater light climate and the temperature increase may drive substantial changes of the future Arctic kelp forest structure.

Kelps (Laminariales, Phaeophyceae) dominate many rocky shore coastlines in temperate and polar regions, forming submarine forests that are among the most productive ecosystems on our planet (Teagle et al. 2017; Wernberg et al. 2019). Kelps function as ecosystem engineers and foundation species, thereby providing a wide range of ecosystem services that are of vast socioeconomic importance (Eckman et al. 1989; Filbee-Dexter et al. 2019; Wernberg et al. 2019). However, kelp forest distribution and productivity strongly depend on external

biotic and abiotic factors (e.g., Feehan et al. 2012; Smale and Wernberg 2013; Smale 2020). Especially in the context of global climate change, it is important to understand the drivers of kelp forest distribution to conserve these ecosystems and their essential ecological and socioeconomic role.

The underwater light climate, being defined as the intensity of photosynthetically active radiation (PAR) and the spectral composition of the downwelling irradiance, is a key driver of kelps vertical distribution in the water column (Wondraczek et al. 2013; Fragkopoulou et al. 2022). Kelps are dependent on the underwater light climate as they can only accumulate biomass, if their net carbon uptake (photosynthesis) exceeds their carbon loss (respiration), that is, if their net photosynthetic rate is positive (Kirk 2011). The light intensity at which the photosynthetic and respiration rate are balanced is called compensation irradiance. Its ecological application is the compensation depth, above which net carbon uptake is positive and below it is negative (Falkowski and Raven 2007). The underwater light climate is the result of complex interactions, such as the Sun's activity, the Earth orbit geometry and the light transmission through the atmosphere (Kirk 2011), as well as spectral properties of the water and its suspended particles, scattering and absorbing light (Stomp et al. 2007).

Niedzwiedz and Bischof   Glacial run-off opposes Arctic kelp expansion

The influence of suspended particular matter is particularly pronounced in the Arctic (Aksnes et al. 2009; Konik et al. 2021), as permafrost thaw (Bintanja 2018), melting glaciers (Milner et al. 2017) and high precipitation rates (Bintanja and Andry 2017) release sediments to fjord systems. The sediment concentration of the fjord meltwater layer is heterogenous with spatial and temporal (seasonal) variations (Huovinen et al. 2020), which are strongly affected by the glacier type. At sea-terminating glaciers, the meltwater enters the ocean below the surface and rises buoyantly toward the surface once it reaches open water, establishing an upwelling nutrient flux. As the meltwater of land-terminating glaciers discharges into proglacial rivers, entering the fjord on the surface (Schild et al. 2017), this nutrient flux subsides once the glacier becomes land-terminating. Furthermore, the sediment plume dynamics affect the sedimentation patterns. This has consequences to kelp population dynamics and interspecific competition (Traiger and Konar 2017), as the substrate quality and the properties of the downwelling irradiance, reaching the benthos are changed (Huovinen et al. 2020). Whether the effect of glacial retreat and run-off on marine primary production is positive or negative depends on a multitude of interacting factors, for example, fjord-glacier geometry, resource availability, and glacier type (Hopwood et al. 2020). In the near-future, the loss of global glacier mass is predicted to accelerate (Hugonnet et al. 2021), resulting in increasing terrestrial run-off (Bintanja and Andry 2017), sediment release and, consequently, a deterioration of the underwater light climate (Payne and Roesler 2019).

Temperature is a key driver of the latitudinal distribution of kelps (Fragkopoulou et al. 2022). Since the past century, the annual mean global sea surface temperature (SST) is rising drastically (Xu et al. 2021) and sedentary species, such as kelps, have to adapt to thrive under future conditions (Vranken et al. 2021). For many kelp species, rising SSTs have already led to a high mortality at their warm-distribution edge (Krumhansl et al. 2016; Filbee-Dexter et al. 2020) and a poleward range shift of kelps has been recorded (Smale and Wernberg 2013; Bartsch et al. 2016). For many kelp species, SSTs in the Arctic are currently below their optimum growth temperature (Krause-Jensen et al. 2020). Therefore, the species trait characteristics to survive and produce viable offspring in the Arctic environmental setting is not optimal (reduced performance; Pörtner et al. 2005). Hence, kelp biomass accumulation in the Arctic is lower compared to mid-latitudinal regions (Borum et al. 2002; Pessarrodona et al. 2018). However, with the Arctic warming at a rate far beyond the global average (Previdi et al. 2020, 2021; England et al. 2021), near-future SSTs might allow for increasing enzymatic activity and performance (Pörtner et al. 2005). Consequently, models predict a biomass increase of kelps in the Arctic (Krause-Jensen and Duarte 2014; Krause-Jensen et al. 2020; Assis et al. 2022). However, higher temperatures were shown to alter species light-use characteristics (Davison et al. 1991; Atkin and Tjoelker 2003), this might result in rising compensation

irradiances. Depending on the species temperature tolerance, temperature changes affect species light-use characteristics differently, which might result in a changed species community composition (Traiger and Konar 2017).

It was the aim of this study to gain a mechanistic understanding of the interactive effects of deteriorating underwater light climate and rising SSTs in Arctic fjords on the potential habitat of the two cold-temperate kelp species *Alaria esculenta* and *Saccharina latissima*. Both species are forming extensive kelp forests in Kongsfjorden, Svalbard (Bartsch et al. 2016), which is at their cold-distribution edge with summer SSTs below their optimum growth temperature (Munda and Lüning 1977; Bolton and Lüning 1982). We assessed the influence of glacial retreat on the underwater light climate and the effect of temperature on the light-use characteristics of kelps. Our study was guided by two hypotheses:

Hypothesis 1: Given the complex sediment plume dynamics of sea- and land-terminating glacier, we expect a strong spatial gradient of prevailing PAR intensities, decreasing closer to the glaciers, which results in a shallower compensation depth of kelps.

To verify this, we chose Kongsfjorden, Svalbard as model fjord system, analyzing the underwater light climate in three areas, representing different stages of glacial retreat: (1) sea-terminating glacier, (2) land-terminating glacier, (3) coastal water (at the mouth of the fjord). Based on these results, we created a model showing the prevailing PAR intensities in Kongsfjorden. Furthermore, we expect the spectral composition to change with decreasing proximity to the glaciers due to the additional suspended particles in the water column.

Hypothesis 2: Regarding the kelp response to increasing temperatures, we expect *A. esculenta* (optimum: 8–9°C; Munda and Lüning 1977) to be better adapted to lower temperatures compared to *S. latissima* (optimum: 10–15°C; Bolton and Lüning 1982).

To assess this, we exposed *A. esculenta* and *S. latissima* to three short-term temperature treatments (3°C, 7°C, and 11°C) and examined changes in their photosynthesis vs. irradiance curves and biochemical composition. We expect to find increasing respiration and photosynthetic rates with higher temperature due to higher enzymatic and metabolic activities and differences in the kelps pigment concentrations and carbon to nitrogen ratio. We hypothesize that the different temperature tolerance ranges of the kelps to rising temperatures, result in a temperature-induced variation of the compensation depth, leading to a shift of the species composition.

Methods

Study region

Kongsfjorden is one of the best-studied Arctic fjord ecosystems (Bischof et al. 2019). It represents a model system to study links between changes in the physical environment

Niedzwiedz and Bischof   Glacial run-off opposes Arctic kelp expansion

(such as glacial retreat) and their effects on ecological processes, which serve as indicators for future Arctic conditions (Bischof et al. 2019). It is located at 79°N at the west coast of Spitsbergen, Norway, being orientated from southeast to northwest. It is about 20 km long (Fig. 1) and up to 350 m deep. Its tidal range is about 0.5 m. Since 2014, SSTs between -1.8°C in winter and $+8.35$°C in summer were recorded (AWI-Dashboard, https://dashboard.awi.de/?dashboard=2847;15 July 2022). The fjord is characterized by areas being influenced by different stages of glacial retreat: (1) Three sea-terminating glaciers (Kongsvegen, Kronebreen, Kongsbreen) terminate into the fjord at the southeast coast. (2) Brøggerbreen is a land-terminating glacier on the southern coast, discharging melt water into the Bayelva river and the fjord (Svendsen et al. 2002). (3) In the outer fjord region glacial freshwater release is not in close spatial proximity and relatively clear coastal water prevails, depicting the last stage of glacial retreat.

Underwater light climate measurements and water samples

The spectrally resolved downwelling irradiance was measured (RAMSES-ACC-UV/VIS radiometer; TriOS Optical Sensor) from 400 to 700 nm in July 2021 at 17 depth profiles (Fig. 1; Table S1). At each depth profile, 14 spectral measurements in water depths from 0 to 12.5 m were taken (alternative calibration). All depth profiles were taken between midday and early afternoon (highest light intensities) and only on days with stable and constant light conditions to ensure comparability between the measurements. In each area, we measured several depth profiles: Depth profiles A–J represent the sea-terminating glacier fjord area (zone 3 and 4 after Hop et al. 2002). Depth profiles K–O (zone 3 after Hop et al. 2002) are within the land-terminating fjord area. The coastal

water is represented by depth profiles Q and P (zone 2 after Hop et al. 2002). We measured as many depth profiles as possible under the prevailing environmental conditions to ensure the coverage of a large area in the meltwater plume at the highest possible resolution (sea-terminating glacier: 10, land-terminating glacier: 5, coastal water: 2). Due to the presence of ice bergs during July 2021, we were not able to conduct light measurements closer to the sea-terminating glacier than depth profile A. The irradiance of each wavelength was measured in mW m^{-2} nm^{-1} and converted to μmol photons m^{-2} s^{-1} after Eq. 1.

$$I_\lambda = \left[\lambda(\mathrm{m}) \times X_\lambda\left(\mathrm{W\,m}^{-2}\right)\right] \times \left[h(\mathrm{Js}) \times c\left(\mathrm{m\,s}^{-2}\right) \times N_A\left(\mathrm{mol}^{-1}\right)\right]^{-1}$$
$$= \mu\,\mathrm{mol\ photons\ m}^{-2}\,\mathrm{s}^{-1} \tag{1}$$

PAR was calculated by integrating the irradiance (I_λ) from 400 to 700 nm (Eq. 2). As the downwelling irradiance was measured every 2.1 nm, PAR values were corrected by this factor in consultation with the manufacturer.

$$I_{\mathrm{PAR}} = \int_{400}^{700} I_\lambda d_\lambda \times 2.1 = \sum_{400}^{700} I_\lambda \times 2.1 = \mu\,\mathrm{mol\ photons\ m}^{-2}\,\mathrm{s}^{-1} \tag{2}$$

Based on these calculations, the Kongsfjorden underwater light climate in July 2021 was modeled using Ocean Data View, version 5.5.1 (Schlitzer 2021). The model (DIVA gridding, X scale-length: 40 permille, Y scale-length: 30 permille) shows the $\log_{10}$ of PAR irradiances to highlight low irradiances, which are relevant for the kelp's lower depth limit. The kelps compensation depth was based on the measured compensation irradiance
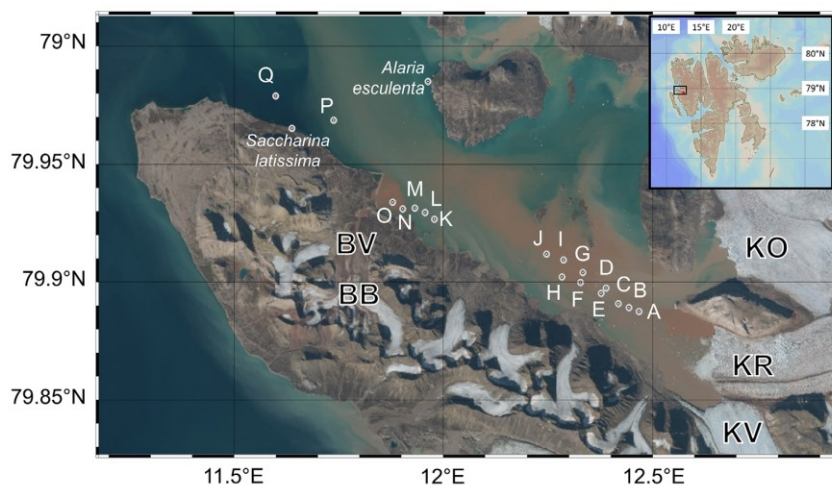

Fig. 1. Sampling sites in Kongsfjorden, Svalbard. Positions of the underwater light climate depth profiles (A–Q) and kelp sampling sites (*Saccharina latissima*, *Alaria esculenta*) in Kongsfjorden, Svalbard. Right upper corner: Overview map of Svalbard; black rectangle marks the position of Kongsfjorden. BB: Brøggerbreen; BV: Bayleva river; KV: Kongsvegen; KR: Kronebreen; KO: Kongsbreen. Brownish water: high concentrations of suspended particles in the water. Map: Ocean Data View (Schlitzer 2021). Satellite image: https://toposvalbard.npolar.no/; 15 July 2022.

Niedzwiedz and Bischof   Glacial run-off opposes Arctic kelp expansion

(*see* paragraph below). It was calculated by fitting a linear function on the $\log_{10}$-PAR irradiance measurements of each depth profile. The mean compensation irradiance of each species and temperature was inserted into the linear function and the equation was solved for the water depth.

The depth profile's spectrum peak describes the wavelength with the maximum irradiance transmission through the water column. It was calculated as the average over the spectral measurements in depth (0–12.5 m) (Eq. 3) and is used as proxy to quantify the overlap of the underwater light climate with the pigment absorption (Wondraczek et al. 2013).

$$\lambda\left(\text{depth profile's spectrum peak}\right)$$
$$= \overline{X}(\max I_\lambda(0\,\text{m}); \max I_\lambda(0.5\,\text{m}); \ldots; \max I_\lambda(12.5\,\text{m})) = \text{nm} \quad (3)$$

At each depth profile, a surface water sample was taken to determine the salinity with a refractometer.

Kelp sampling and temperature experiment

Scientific SCUBA divers collected *S. latissima* and *A. esculenta* sporophytes in Kongsfjorden, Svalbard from 6 to 9 m depth (Fig. 1; Table S1). Sporophytes of the same species were of similar size. Meristematic discs (diameter = 2 cm) were cut and distributed between temperature treatments and replicates ($n = 4$), avoiding pseudo-replication. They were cultivated in 1 L aerated glass beakers, filled with filtered seawater (changed every 2 d), applying 24 h of constant light (24 μmol photons m^{-2} s^{-1}). The experiment ran for 7 d ($t_0 - t_7$), with temperature treatments of 3°C (in situ SST; July 2021, 10 m depth), 7°C (present high SSTs; AWI-Dashboard, https://dashboard.awi.de/?dashboard=2847; 15 July 2022) and 11°C (future SST by the year 2100; Skogseth et al. 2020). Treatment temperature was increased every 2 d by 4°C, allowing for successive acclimation (Fig. 2). After photosynthesis vs. irradiance curves were measured on t_3, t_5, and t_7, the samples were silica-dried and stored in darkness until biochemical analysis.

Kelp response parameters

To quantify the kelp response to rising temperatures, we measured photosynthetic vs. irradiance curves, the maximum quantum yield of photosystem II (F_v/F_m), pigment concentrations and carbon to nitrogen ratio. Photosynthetic vs. irradiance curves were measured on t_3, t_5, and t_7 (Fig. 2) to measure whether increasing temperature changes the kelp light-use characteristics. Therefore, we measured the oxygen concentration evolution under different light intensities, using an optode set-up of PyroScience. Dark respiration and net photosynthetic rates were calculated in μmol O$_2$ L^{-1} cm^{-2} h^{-1}. Subsequently, we analyzed F_v/F_m with a chlorophyll fluorometer of dark-adapted discs, which is used as proxy to quantify algal cellular and physiological stress level. As the algal pigment composition is crucial to absorb light for photosynthesis, we analyzed the chlorophyll *a* (Chl *a*)
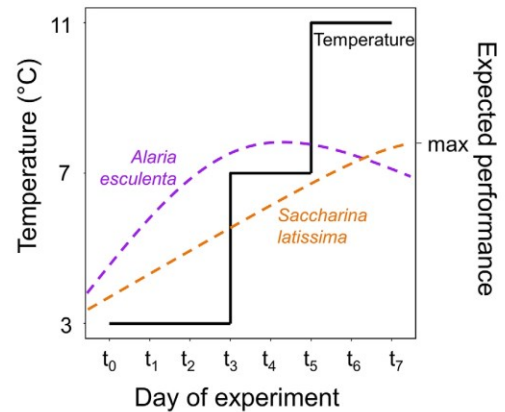

Fig. 2. Experimental set-up. The treatments temperature (°C) (solid black line) was increased by 4°C on t_3 and t_5 of the experiment until the treatment's temperature was reached (3°C, 7°C, and 11°C). Photosynthesis vs. irradiance curve were measured on t_3 (3°C treatment), t_5 (7°C treatment), and t_7 (11°C treatment). Dashed purpled line: expected performance of *Alaria esculenta* based on Munda and Lüning (1977). Dashed orange line: expected performance of *Saccharina latissima* based on Bolton and Lüning (1982).

concentration and ratio of accessory pigments to Chl *a* after Koch et al. (2015) and Wright et al. (1991). Pigment contents were calculated in μg cm^{-2}. Furthermore, we quantified the kelps carbon to nitrogen ratio, to analyze for temperature-induced carbon gain or loss (photosynthesis and respiration). We measured the carbon to nitrogen ratio by combustion of dried kelp material and using Acetanilide as standard (Verardo et al. 1990). Total carbon and nitrogen content were expressed as proportion (%) and ratio. *A. esculenta* and *S. latissima* are morphologically different, with the meristematic discs of *S. latissima* being $\sim$ 85% heavier (fresh weight; data not shown) than *A. esculenta*. To be able to compare the temperature-induced responses, we standardized all parameters to the discs total area (cm^2), including the front- and backside of the discs.

A detailed description of all methods to measure the kelp response parameters can be found as Supporting Information.

Statistics

All statistical analyses of the physiological and biochemical data were run in RStudio (Version 2021.09.0 + 351; R Core Team 2021). A linear model was fit on the data of each parameter, using the "lm" function of the R package "stats". Species (*S. latissima*, *A. esculenta*) and treatment's temperature (3°C, 7°C, 11°C) were modeled as multiple fixed effects. For the analysis of the compensation depth and spectrum peak, the fixed effect of area (sea-terminating glacier; land-terminating glacier; coastal water) was included. Each model's fit on the data was assessed by evaluating the Akaike information criterion and Bayesian information criterion. The normality (Shapiro–Wilk test, $p > 0.05$) and homoscedasticity (Levene's test, $p > 0.05$) of the model's residuals were tested. Analysis of

variance was tested on the model by using the "anova" function, to assess the influence of the fixed effects. Pairwise comparisons were performed, using the "emmeans" function of the R package "emmeans" (Lenth 2021), to calculate the degrees of freedom and Tukey adjustment of the *p* value. Linear dependency of the response variables was determined by calculating the Pearson correlation coefficient, using the "cor. test" function of the R package "stats" (R Core Team 2021) after testing for normality (Shapiro–Wilk test, $p > 0.05$).

Results

Underwater light climate

Comparing the aerial view of Kongsfjorden, distinct meltwater plumes of the sea- and land-terminating glaciers are clearly visible. The brown, sediment-rich water is contrasting the blue, clear water (Fig. 1).

PAR intensities and kelp compensation depth

The modeled PAR intensities of Kongsfjorden in different water depths can be seen in Fig. 3a,b. PAR intensities over depth varied strongly between the three fjord regions. Depth profile Q (coastal water) was characterized by the highest PAR intensities. On 12.5 m, PAR intensities of 81 μmol photons m^{-2} s^{-1} were measured, while in depth profile A (sea-terminating glacier) the lowest PAR intensity was measured ($\sim$ 0.01 μmol photons m^{-2} s^{-1}). Comparing the mean PAR intensities of all areas on 4.5 m, it was highest in the coastal water and lowest near the land-terminating glacier (coastal water: 254.7 $\pm$ 24.55 μmol photons m^{-2} s^{-1} > sea-terminating glacier: 24.8 $\pm$ 30.53 μmol photons m^{-2} s^{-1} > land-terminating glacier: 8.5 $\pm$ 5.58 μmol photons m^{-2} s^{-1}). The
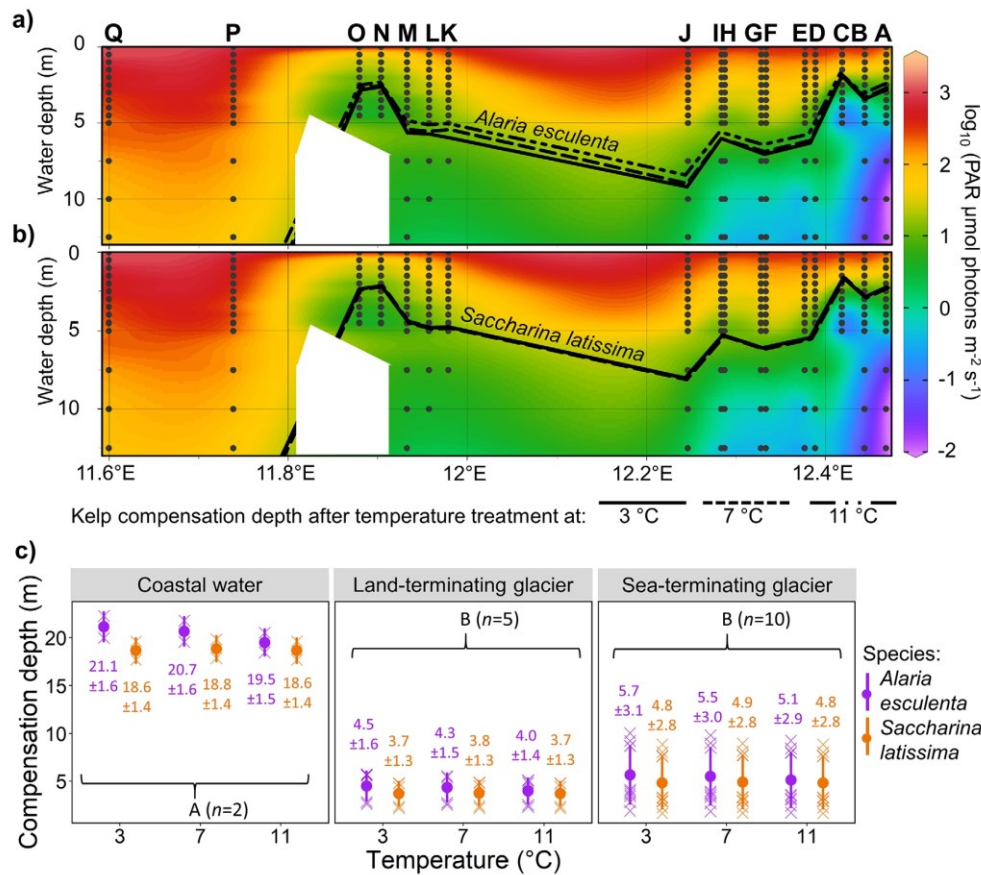

Fig. 3. Photosynthetically active radiation (PAR) in Kongsfjorden, Svalbard. Model of the underwater light climate (log$_{10}$ of PAR irradiances; 400–700 nm) along a longitudinal section through Kongsfjorden, covering all depth profiles (A–Q) and water depths (0–12.5 m). Depth profile P, Q: coastal water. Depth profile O–K: influence of land-terminating glacier. Depth profile A–J: influence of sea-terminating glaciers. Black dots: spectral measurements. White area: insufficient data coverage for model. Black lines in the plots: compensation depth of (**a**) *Alaria esculenta* and (**b**) *Saccharina latissima* being cultivated at 3°C (solid line), 7°C (dashed line) and 11°C (dash-dot-dot line). (**c**) Compensation depth of both species (*A. esculenta*: purple, *S. latissima*: orange) in all fjord areas (coastal water, land-terminating glacier, sea-terminating glacier) after different temperature treatments (3°C, 7°C, 11°C). Temperature mean (dot) $\pm$ SD (number associated to each point) and depth profile response (cross). Different capital letters indicate significant differences between area, temperature, and species.
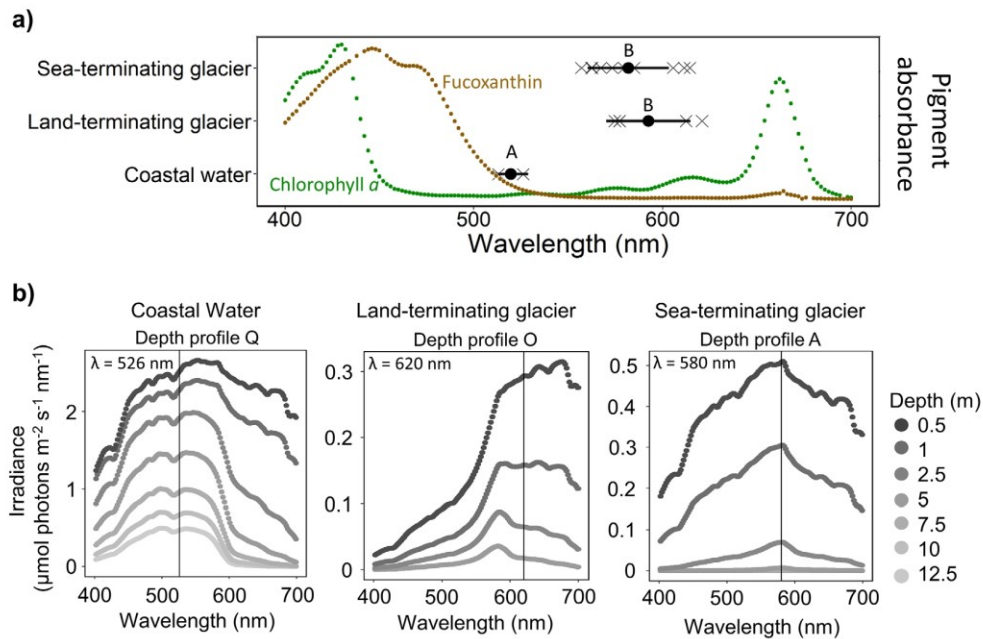
Niedzwiedz and Bischof   Glacial run-off opposes Arctic kelp expansion

Fig. 4. Spectrum peaks. (**a**) Spectrum peaks (wavelength with the highest light transmission trough the water column) of the three fjord areas (sea-terminating glacier, land-terminating glacier, coastal water). Area mean (black dots) $\pm$ SD and depth profile spectrum peak (black cross) ($n = 2$–10). Different capital letters indicate significant differences between areas. Schematic light absorption curve of chlorophyll a (green line) and fucoxanthin (brown line) after Jeffrey et al. (1997). (**b**) Spectrally resolved underwater light climate of different water depths of depth profile Q, O, and A. Vertical black line; λ: depth profiles spectrum peak. Note the different y-axis scales of the subplots.

compensation depth for *A. esculenta* (Fig. 3a) and *S. latissima* (Fig. 3b) was modeled based on the measured compensation irradiance (*see* paragraph below) and follows the variations in PAR intensities. While we detected no significant changes in the compensation depth between species ($p = 0.163$; $F_{1,84} = 1.985$) or temperature ($p = 0.841$; $F_{2,84} = 0.174$), the fjord area showed significant differences ($p < 0.001$; $F_{2,84} = 188.536$). The compensation depths of both species were significantly higher in the coastal area compared to the glacier-influenced areas (Fig. 3c). In the coastal water, the potential compensation depth for both kelp species and all temperature treatments was below 17 m. Furthermore, we detected three trends (Fig. 3): (1) With increasing temperature, the compensation depth of *A. esculenta* shifts to shallower water depths by a mean of $10.4 \pm 0.2\%$ independently of the fjord region. *S. latissima* showed no temperature dependent differences. (2) The compensation depth of *S. latissima* is $11.3 \pm 0.05\%$ shallower compared to *A. esculenta*. (3) Within the glacial areas, the compensation depth of both species increases with increasing distance to the glacier front.

Spectral composition

The spectral characteristics of the underwater light climate in different water depths of each area are shown in Fig. 4. The mean spectrum peak of the areas varied significantly ($p = 0.0032$; $F_{2,14} = 8.925$), with spectrum peak of the coastal water area (519.72 ± 9.30 nm) being significantly lower

compared to the mean spectrum peak of the land-(592.34 ± 22.31 nm, $p = 0.0028$) and sea-terminating glacier (581.70 ± 21.50 nm; $p = 0.0053$) area (Fig. 4a). While the mean spectrum peak of all three areas are within the green gap of Chl a, the spectrum peaks of the coastal area are close to the absorption of fucoxanthin. The spectrum peaks of the areas being influenced by glaciers are out of the spectral absorption range of fucoxanthin. Comparing the spectral light composition of depth profiles for each fjord region (coastal water: depth profile Q; land-terminating glacier: depth profile O; sea-terminating glacier: depth profile A), three characteristics can be seen (Fig. 4b): (1) in all fjord regions, the irradiance of each wavelength is decreasing with increasing water depth. (2) Comparing the same water depth, the irradiance is highest in the outer fjord region (depth profile Q) and lowest near the Bayelva river mouth (depth profile O) and (3) not only the depth profiles spectrum peak is shifting, but the whole spectral composition is changing.

Salinity

The water's surface salinity (S_A) varied significantly between all areas ($p < 0.001$; $F_{2,48} = 11.704$). The coastal water had the highest mean salinity ($S_A = 36.75 \pm 0.82$), followed by the surface salinity of the land-terminating glacier area ($S_A = 27.80 \pm 3.16$) and the sea-terminating glacier area ($S_A = 31.15 \pm 4.46$), which were significantly lower. Within
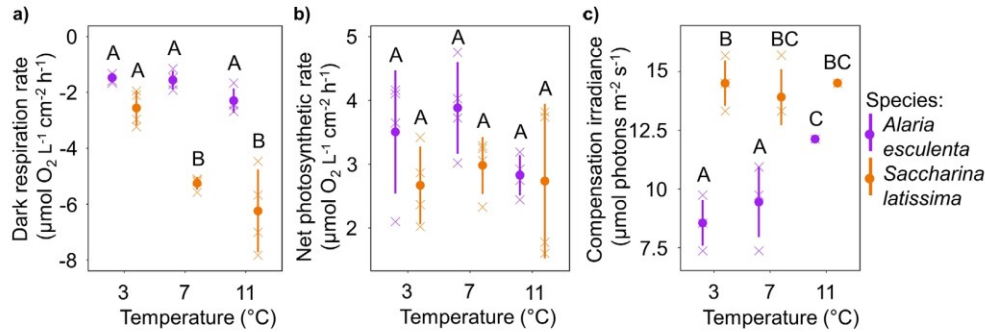
Fig. 5. Respiration and photosynthesis. Photosynthetic responses of *Alaria esculenta* (purple) and *Saccharina latissima* (orange) after different temperature treatments (3°C, 7°C, and 11°C). Treatment mean (dots) $\pm$ SD and average replicate response (cross) ($n = 3$–4). Different capital letters indicate significant ($p < 0.05$) differences between the temperature treatments and species. (**a**) Dark respiration rate (μmol O_2 L^{-1} cm^{-2} h^{-1}). (**b**) Net photosynthetic rate (μmol O_2 L^{-1} cm^{-2} h^{-1}). (**c**) Compensation irradiance (μmol photons m^{-2} s^{-1}). Some error bars are within the diameter of the symbol.

the land-terminating glacier area, the salinity was lowest of depth profile O ($S_A = 26$), showing an increasing trend with increasing distance to the Bayelva river mouth ($S_A = O < N < L < K$). The salinity of the sea-terminating glaciers influenced depth profiles A–J, showed no clear spatial trend.

Kelp response parameters
Dark respiration rate
The dark respiration rate (μmol O_2 L^{-1} cm^{-2} h^{-1}) was significantly affected by species ($p < 0.001$; $F_{1,18} = 102.675$) and temperature ($p < 0.001$; $F_{2,18} = 20.96$), as well as their interaction (S × T) ($p = 0.001$; $F_{2,18} = 10.12$; Fig. 5a). After all temperature treatments, the mean dark respiration rate of *A. esculenta* was between 42% and 71% lower than of *S. latissima*. With increasing temperature, the dark respiration rate of *S. latissima* increased (decreasing oxygen concentrations) significantly ([11°C = 7°C] > [3°C]), while the dark respiration rate of *A. esculenta* only showed an increasing trend.

Net photosynthetic rate
The net photosynthetic rate (μmol O_2 L^{-1} cm^{-2} h^{-1}) was neither significantly affected by species ($p = 0.069$; $F_{1,18} = 3.741$), temperature ($p = 0.268$; $F_{2,18} = 1.417$) nor their interaction ($p = 0.519$; $F_{2,18} = 0.681$; Fig. 5b), being 3.1 ± 0.48 μmol O_2 L^{-1} cm^{-2} h^{-1} on average for both species and temperatures. No significant temperature-induced response was observed. Although the mean net photosynthetic rate of *A. esculenta* was highest after the 7°C treatment, the difference was not significant due to the high variability in the replicates response.

Compensation irradiance
Species ($p < 0.001$; $F_{1,17} = 106.158$), temperature ($p = 0.003$; $F_{2,17} = 8.579$), and their interaction ($p = 0.010$; $F_{2,17} = 6.042$) had a significant effect on the compensation irradiance (μmol photons m^{-2} s^{-1}) (Fig. 5c). Independently of the temperature, the mean compensation irradiance of *A. esculenta* was lower

compared to *S. latissima*, being 41% lower after the 3°C treatment. The compensation irradiance of *A. esculenta* increased significantly by 29% with increasing temperature, while the compensation irradiance of *S. latissima* showed no temperature-induced response, being 14.3 ± 0.35 μmol photons m^{-2} s^{-1} after all temperature treatments.

F_v/F_m
Mean F_v/F_m values of all species and temperature treatments were between 0.72 and 0.76. F_v/F_m was significantly affected by species ($p < 0.001$; $F_{1,18} = 15.219$) and temperature ($p < 0.001$; $F_{2,18} = 13.029$), while their interaction ($p = 0.183$; $F_{1,18} = 1.869$) had no significant effect (Table 1). With increasing temperature, F_v/F_m of *A. esculenta* and *S. latissima* increased significantly.

Chlorophyll a
Species ($p < 0.001$; $F_{1,18} = 250.027$) and temperature ($p = 0.01$; $F_{2,18} = 6.088$) had a significant effect on Chl a concentration (μg cm^{-2}) ($p < 0.05$), while their interaction ($p = 0.191$; $F_{2,18} = 1.8148$) had no effect (Table 1). Independently of the temperature, the Chl a concentration of *A. esculenta* was $\sim 78\%$ higher than the Chl a concentration of *S. latissima*. Chl a of both species was highest after the 11°C treatment, being only significant for *A. esculenta*.

Accessory pigments to Chl a ratio
The ratio of accessory pigments to Chl a was neither significantly affected by species ($p = 0.581$; $F_{1,18} = 0.318$), temperature ($p = 0.235$; $F_{2,18} = 1.589$), nor their interaction ($p = 0.741$; $F_{2,18} = 0.306$; Table 1). No significant differences between *A. esculenta* or *S. latissima* were detected after the temperature treatments.

Carbon
The total carbon content (%) was significantly influenced by species ($p < 0.001$; $F_{1,18} = 96.766$) and the interaction of species and temperature ($p = 0.015$; $F_{2,18} = 5.334$), while the temperature alone had no significant effect ($p = 0.350$; $F_{2,18} = 1.113$;

Niedzwiedz and Bischof   Glacial run-off opposes Arctic kelp expansion

Table 1. Kelp response parameters. Maximum quantum yield of photosystem II (F_v/F_m), chlorophyll *a* (μg cm^{-2}), ratio of accessory pigments to chlorophyll *a*, total carbon content (%), total nitrogen content (%) and carbon to nitrogen ratio of *Alaria esculenta* and *Saccharina latissima* after different temperature treatments (Temp.). Different capital letters indicate significant (Sig.; $p < 0.05$) differences between the temperature treatments and species within one parameter.

Parameter	Temp.	*Alaria esculenta*			*Saccharina latissima*		
		Mean	$\pm$ SD	Sig.	Sig.	Mean	$\pm$ SD
F_v/F_m	3°C	0.72	0.011	A	B	0.741	0.015
	7°C	0.749	0.011	BC	BC	0.754	0.007
	11°C	0.742	0.004	BC	C	0.764	0.006
Chlorophyll *a* (μg cm^{-2})	3°C	7.81	1.45	AC	B	1.66	1.1
	7°C	7.56	1.25	A	B	1.64	0.095
	11°C	10.1	1.14	C	B	2.36	0.295
Accessory pigments to chlorophyll *a* ratio	3°C	0.216	0.025	A	A	0.222	0.012
	7°C	0.213	0.008	A	A	0.207	0.026
	11°C	0.204	0.025	A	A	0.193	0.023
Carbon content (%)	3°C	37.0	1.36	A	B	32.4	2.17
	7°C	37.9	2.09	A	BC	29.6	1.64
	11°C	38.8	2.66	A	C	27.6	1.86
Nitrogen content (%)	3°C	1.27	0.112	A	A	1.36	0.226
	7°C	1.34	0.316	A	A	1.18	0.104
	11°C	1.55	0.324	A	A	1.23	0.326
Carbon to nitrogen ratio	3°C	29.5	3.69	A	A	24.2	3.09
	7°C	29.4	6.81	A	A	25.3	3.47
	11°C	26.3	8.49	A	A	23.5	5.95

F_v/F_m, chlorophyll *a*, ratio of accessory pigments to chlorophyll *a*, total carbon and nitrogen content, and carbon to nitrogen ratio were tested against the single and interactive effects of species and temperature. Values are the treatment means ($n = 4$) $\pm$ SD.
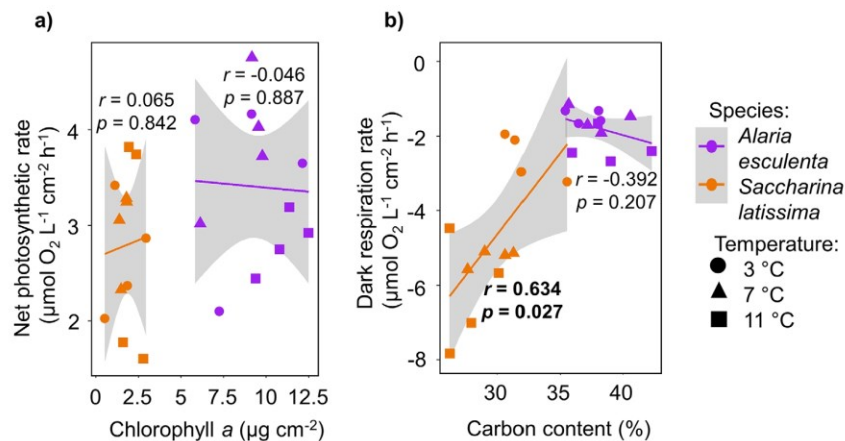

Fig. 6. Correlations. Linear dependency between two response parameters of *Alaria esculenta* (purple) and *Saccharina latissima* (orange) after different temperature treatments (circle: 3°C, triangle: 7°C; box: 11°C; $n = 3$–4). Gray area: 95% confidence interval. *r*: Pearson correlation coefficient. Significant correlations ($p < 0.05$) are marked in bolt. (**a**) Net photosynthetic rate (μmol O$_2$ L^{-1} cm^{-2} h^{-1}) vs. chlorophyll *a* content (μg cm^{-2}). (**b**) Dark respiration rate (μmol O$_2$ L^{-1} cm^{-2} h^{-1}) vs. total carbon content (%).

Table 1). The mean carbon content of *A. esculenta* was 12–29% higher than of *S. latissima*. The carbon content of *S. latissima* decreased significantly with increasing temperature, while the carbon content of *A. esculenta* showed an increasing trend with increasing temperature.

Nitrogen

The total nitrogen content (%) was not significantly affected by the tested fixed effects (species: $p = 0.223$; $F_{1,18} = 1.591$; temperature: $p = 0.599$; $F_{2,18} = 0.527$; interaction: $p = 0.289$; $F_{2,18} = 1.333$; Table 1). No significant

Niedzwiedz and Bischof   Glacial run-off opposes Arctic kelp expansion

differences between *A. esculenta* and *S. latissima* were detected after the temperature treatments.

Carbon to nitrogen ratio

The carbon to nitrogen ratio was not affected by the tested fixed effects (species: $p = 0.094$; $F_{1,18} = 3.127$; temperature: $p = 0.669$; $F_{2,18} = 0.411$; interaction: $p = 0.906$; $F_{2,18} = 0.099$; Table 1). The mean carbon to nitrogen ratio was 26.37 ± 2.57 for both species after all temperature treatments, showing no significant changes.

Correlations

In both species, the photosynthetic rate did not correlate significantly with the Chl *a* concentration (*A. esculenta*: $p = 0.887$, $t = -0.146$, df = 10; *S. latissima*: $p = 0.842$, $t = 0.205$, df = 10; Fig. 6a). The carbon content of *S. latissima* decreased significantly with increasing respiration rate ($p = 0.027$, $t = 2.591$, df = 10). In *A. esculenta* the correlation was not significant ($p = 0.207$, $t = -1.350$, df = 10) (Fig. 6b).

Discussion

Kelps act as important foundation species in Arctic rocky shore ecosystems (Filbee-Dexter et al. 2019). Currently, they are experiencing major changes in their habitat's environment. According to Constable et al. (2022), the SST in Arctic regions is predicted to increase drastically by the end of the century. At a warming rate of $0.7°C$ per decade, a mean summer SST of $11°C$ will be reached in ~ 100 years (Skogseth et al. 2020), although extreme temperature events will reach $11°C$ earlier. While the Arctic endemic marine vegetation is likely to be lost (Bringloe et al. 2020), a poleward expansion of temperate kelp species is projected (Krause-Jensen et al. 2020; Assis et al. 2022). However, with rising SSTs, terrestrial run-off is also increasing (Constable et al. 2022), which was shown to deteriorate the underwater light climate (Konik et al. 2021), impeding net photosynthesis and, hence, result in a shift of the kelp forest to shallower waters (Filbee-Dexter et al. 2019). Our study aimed to address two critical aspects related to Arctic kelp ecophysiology: the characterization of the underwater light climate at different stages of glacial retreat and the response of Arctic kelp species (*A. esculenta*, *S. latissima*) to different light and thermal conditions. We found a strong spatial variation in the underwater light climate within Kongsfjorden, with the light intensity being reduced and the spectral composition shifting toward longer wavelengths near glaciers. That significantly affected the kelp compensation depth, leading to a shoaling of the kelp forest near glaciers (Hypothesis 1). Our results further showed that rising SSTs are affecting kelp light-use characteristics, with *A. esculenta* being better adapted to polar conditions than *S. latissima*. These differences in the responses might result in a future shift in species composition (Hypothesis 2).

Variation of the underwater light climate due to glacial retreat

With ongoing climate change, glaciers were shown to retreat (Hugonnet et al. 2021). Geyman et al. (2022) found that the glacier mass loss is predicted to double until 2100, compared to the 20th century. Concomitantly, species distribution models estimate a current potential distribution of kelp forests in the Arctic of $655,000$ km^2 (Assis et al. 2022), potentially being influenced by glaciers and glacial run-off.

Comparing the underwater light climate of all three fjord areas, we observed distinct differences. Near glaciers (depth profile O, A), the reduction of PAR was much stronger, compared to the clearer water at the outside of the fjord (Fig. 3a,b). This can be explained by the high concentration of suspended particles of the meltwater plumes, which additionally absorb and scatter the available light (Stomp et al. 2007). Hence, high meltwater run-off rates (and consequently sediment concentrations in the water) resultant from retreating glaciers lead to less available light for photosynthesis (Payne and Roesler 2019).

Additional to the PAR intensity, we analyzed the spectral composition of the downwelling irradiance and compared its overlap with the light absorption spectrum of Chl *a* and fucoxanthin (Fig. 4a). The main absorption peaks of Chl *a* are at 430 nm (blue light) and 662 nm (red light), leaving a major green gap in which light absorption is low (Jeffrey et al. 1997). Fucoxanthin and chlorophyll *c*, belonging to the major accessory pigments of brown algae, close this green gap partly, as their main absorption peaks are between 445 and 468 nm (blue light) (Jeffrey et al. 1997). We found that all spectrum peaks (wavelength with the highest light transmission through the water column) were within the green gap of Chl *a* (Fig. 4a). However, the spectrum peaks of coastal water were close to the absorption spectrum of fucoxanthin, resulting in a large overlap of the light spectrum with the pigment absorption spectrum. The spectrum peaks of the glacier-influenced depth profiles were well outside the absorption range of fucoxanthin, leading to a very limited overlap of the spectra. The photosynthetic efficiency is dependent on the overlap between the prevailing light spectrum and the absorption spectrum of the pigments (Wondraczek et al. 2013). Therefore, high meltwater rates and sediment concentrations reduce the quality of the downwelling irradiance for photosynthesis and biomass accumulation of kelps. Loos et al. (2017) described significant variations of the spectral composition, depending on the distance to a river mouth, being correlated to the concentration of suspended particles in the water column. Furthermore, a similar shift of the spectrum was described by Stomp et al. (2007), who compared the spectral niches in the water column and their availability for photosynthetic organisms of clear ocean, costal water, and a peat lake.

Comparing the underwater light climate of all three areas, the variation of the PAR intensities translated into a significant difference in the kelp's compensation depth, showing

Niedzwiedz and Bischof   Glacial run-off opposes Arctic kelp expansion

that an increased run-off results in a shift of the lower depth limit to shallower waters. We found the lowest light intensities and strongest change of the spectral composition near the land-terminating glacier. However, it has to be considered that the distance of depth profile O (closest to land-terminating glacier) to the Bayelva river mouth is much smaller than the distance of depth profile A (closest to sea-terminating glacier) to the sea-terminating glacier front (Fig. 1). In addition, the sediment plume of sea-terminating glaciers was much more pronounced, influencing a larger area of the fjord (Fig. 1). Sediment plumes of land-terminating glacier were influenced by wind direction and currents to a higher degree (pers. obs.).

Therefore, we conclude that the darkening of the water column as well as the change of the spectral composition of the light in the Arctic may lead to a reduction of the available habitat for kelp forests near retreating glaciers. We also found that the strong negative influence of melting sea-terminating glaciers on the underwater light climate may reduce as they become land-terminating.

Kelp responses to rising SST

Metabolic processes depend on enzymatic reactions (Davison et al. 1991) and are characterized by the integration of different intrinsic enzymatic properties. Therefore, metabolic pathways have a temperature optimum at which they are at their maximal capacity (Daniel et al. 2008). Currently, many kelps species are experiencing temperatures below their optimum in the Arctic (Krause-Jensen et al. 2020). Above or below the temperature optimum, the physiological stress increases (Pörtner et al. 2005), leading to smaller kelp individuals in the Arctic compared to mid-latitude range populations (Borum et al. 2002). As proxy for algal cellular and physiological stress level (Murchie and Lawson 2013), we assessed F_v/F_m after all temperature treatments. Despite significant changes of F_v/F_m between species and temperature treatments, all recorded values were > 0.7 (Table 1), which is considered healthy for kelps (Dring et al. 1996). Therefore, no damaging effect on photosystem II occurred during our experiment and the electron transfer was not impaired (Li et al. 2017). Hence, we conclude that the temperature increase during the experiment did not have negative effects on the performance of the kelps.

Nevertheless, we found significant species-specific differences in the temperature responses, depicting a different effect of increasing SSTs on their balance of carbon uptake and loss. The dark respiration rates of *A. esculenta* were lower compared to *S. latissima* after all temperature treatments. While it was significantly lower after the 7°C and 11°C treatment, we detected no significant difference after the 3°C treatment, when the respiration rate of *S. latissima* was comparably low to *A. esculenta*. We interpret the low respiration rate of *S. latissima* at 3°C as a limitation of enzymatic capacities, reducing potential respiration rates (Atkin and Tjoelker 2003). The high dark respiration rates of *S. latissima* at 7°C and 11°C indicate a higher mitochondrial adenosine triphosphate

formation capacity (Pörtner et al. 2005) and therefore more cellular energy. However, we also observed a significant correlation between the increasing dark respiration rates and decreasing carbon content in *S. latissima* (Fig. 6b). As the carbon to nitrogen ratio was determined after the photosynthesis vs. irradiance curves were measured, we conclude that the low carbon content depicts the carbon loss during dark respiration (Saltveit 2019). Neither the dark respiration rate nor the total carbon content of *A. esculenta* did change significantly with higher temperatures (Fig. 5a; Table 1). The carbon content displays kelp storage compounds, such as Mannitol and Laminarin (Scheschonk et al. 2019). Mannitol was shown to be crucial in cellular osmotic regulation, cell turgor control and freezing protection (Iwamoto and Shiraiwa 2005; Elliott et al. 2017) and is converted into the long-term carbon-storage product laminarin (Graiff et al. 2016; Scheschonk et al. 2019). We hypothesize that the high carbon content of *A. esculenta*, enables it to respond to freezing temperatures and salinity fluctuations, which we also observed in Kongsfjorden. Furthermore, the low dark respiration rates of *A. esculenta* prevents carbon loss during dark periods, enabling it to maintain a higher degree of growth and performance (Davison et al. 1991).This confirmed our expectation that *A. esculenta* is better adapted to low temperatures than *S. latissima* (optimal growth temperatures after Munda and Lüning 1977 and Bolton and Lüning 1982). Thereby, it is noteworthy to mention that the optimum temperatures, described for temperate populations, hold also true for Arctic populations. Evidence of a high overall resilience toward low temperatures of *A. esculenta* was reported by Bringloe et al. (2022), showing that *A. esculenta* populations were resilient to past glaciation events and adapted to Arctic conditions.

Based on the low respiration rates of *A. esculenta* during the entire experiment (low carbon loss), we expected that *A. esculenta* would also have higher photosynthetic rates (i.e., higher carbon gain) compared to *S. latissima* (higher performance). However, we detected neither a significant difference between species nor temperature treatments (Fig. 5b). As the net photosynthetic rates were measured at low light conditions (24 μmol photons m^{-2} s^{-1}), we conclude that the photosynthetic rates of both kelp species were restricted by the available light intensity. This implies that the photosynthetic capacity to gain carbon was not limited by the low SSTs but by the prevailing light climate. Hence, in low light conditions, the predicted increasing enzyme activities due to rising temperatures are not causing a higher photosynthetic rate in *A. esculenta* and *S. latissima*.

Considering this, it is striking that the concentration of Chl *a* per area in *A. esculenta* was 78% higher compared to *S. latissima*, as higher Chl *a* concentration indicates higher potential photosynthetic rates. A similar difference in the Chl *a* concentration between both species was reported by Gordillo et al. (2006). We do not think that the observed interspecific difference in the Chl *a* concentration is due to a

low-temperature limitation of Chl *a* synthesis as described by Davison et al. (1991), as we detected neither a temperature-induced change in the absolute Chl *a* concentration nor in the ratio of accessory pigments to Chl *a* (Table 1). The high Chl *a* concentrations of *A. esculenta* in combination with the comparably low photosynthetic rates (Fig. 6a) rather indicate a higher amount of inactive photosynthetic reaction centres compared to *S. latissima*. Falkowski and Raven (2007) described a significant reduction of active photosynthetic reaction centres due to low nutrient environments. In summer, water masses in Arctic fjords are characterized by a strong stratification due to temperature and salinity gradients and the absence of vertical mixing (Cottier et al. 2010), resulting in a nutrient depletion (Gordillo et al. 2006). As no extra nutrients were added to the temperature treatments during the experiment, we found the discs to be nitrogen limited, with a carbon to nitrogen ratio between 23 and 30 (Atkinson and Smith 1983). We interpret the distinct difference in Chl *a* concentration between the species (78% higher in *A. esculenta*) as Arctic adaptation of *A. esculenta*, enabling a fast increase of photosynthetic rates with increasing nutrient concentrations.

Additional to temperature-induced alterations in kelp carbon uptake and loss, we found that rising temperatures have the potential to increase the light requirement to balance both processes (compensation irradiance). Relating the measured compensation irradiance of *A. esculenta* and *S. latissima* to the underwater light climate modeled for the three areas in Kongsfjorden (Fig. 3a,b), we found that the overall compensation depth of both species is between ∼ 2 and 9 m. This corresponds to SCUBA-based field-surveys by Bartsch et al. (2016) and L. Düsedau pers. comm. Therefore, we consider our results of the compensation irradiance to be accurate. While we did not detect a significant change of the dark respiration rate or the photosynthetic rate of *A. esculenta* with increasing treatment temperature, the compensation irradiance increased significantly. However, the compensation irradiance cannot be derived directly from the dark respiration and photosynthetic rate, as respiration rates of plants in light were shown to vary between 25% and 100% from the dark respiration rates (Krömer 1995). Therefore, we conclude that the ratio of respiration during photosynthesis in light of *A. esculenta* changes with rising SSTs, leading to a higher compensation irradiance. At 3°C and 7°C, we found that the mean compensation irradiance of *A. esculenta* was 30–40% lower compared to *S. latissima*. These results suggest that *A. esculenta* is capable of net photosynthesis in low PAR environments and is therefore better adapted to low underwater light climate and temperatures in Arctic fjords. At low temperatures, its potential habitat is bigger compared to *S. latissima*. However, we also found that the compensation irradiance of *A. esculenta* is highly temperature sensitive. After exceeding the temperature optimum of 8–9°C in the 11°C treatment, the compensation irradiance of *A. esculenta* was significantly higher compared to the 3°C treatment. While our results did not indicate a significant

increase of the compensation irradiance for *S. latissima* (Fig. 5c), Davison et al. (1991) found a significantly higher compensation irradiance with increasing temperature, comparing young *S. latissima* sporophytes being exposed to temperatures from 5°C to 25°C. This shows that rising SSTs have the potential to affect the light requirement necessary to balance respiration by photosynthesis of both kelp species.

Thereby, the significant variations of the light-use characteristics, biochemical and physiological parameters between both kelp species in response to increasing temperature, might lead to a changed balance of interspecific competition in future Arctic kelp forests.

Ecological implications

Bartsch et al. (2016) and L. Düsedau pers. comm. analyzed the long-term development of kelp depth distribution in Kongsfjorden, comparing the kelp forest structure from 1996–1998 to 2012–2014 and 2021. They found an overall shift of the kelp forest to shallower water depths. Furthermore, Filbee-Dexter et al. (2022) found a positive correlation between low light condition in the Canadian Arctic with reduced kelp biomass. Both studies support our results of a decreased compensation depth with increasing influence of the glacial meltwater plume and rising temperature. Thereby, our results indicate that sea-terminating glaciers have a greater influence on the underwater light climate than land-terminating glaciers. Hence, the negative effect of retreating glaciers on the underwater light climate might be reduced when the glacier terminates on land (note that the kelp compensation depth was still significantly lower compared to coastal waters). Only regarding the effect of the underwater light climate, the potential kelp habitat might increase again after glaciers become land-terminating. Payne and Roesler (2019) modeled phytoplankton productivity in relation to glacier type, accounting for differences in the underwater light climate and rising SSTs. Their findings result in a three-stage concept: (1) Productivity increase due to less sea-ice (high PAR intensities); (2) productivity reduction due to higher glacier melt and sediment release (low PAR intensities); (3) productivity increase after land-termination of the glacier, due to less run-off (high PAR intensities). Although the availability of other resources (e.g., availability of substrate or nutrients) after glacial retreat would have to be assessed (Filbee-Dexter et al. 2022), our results indicate that this concept also holds true for kelps. Thereby, not just summer irradiances but the cumulative annual irradiance has to be considered, when addressing the future depth distribution and biomass accumulation of photosynthetic organisms (Gattuso et al. 2006). Pedersen et al. (2020) showed that the main biomass accumulation of high-latitude *Laminaria hyperborea* is produced in spring, before the meltwater season. However, high summer irradiances are necessary to build up storage compounds for the polar night to maintain a positive annual carbon balance (Gattuso et al. 2006). Scheschonk et al. (2019) showed that

Niedzwiedz and Bischof   Glacial run-off opposes Arctic kelp expansion

S. latissima used 96% of its storage compounds during the polar night. This implies that a reduced potential to assemble laminarin might result in a negative annual carbon balance (i.e., starvation).

Furthermore, we observed interspecific differences between the species response to high temperatures. A changed balance in competition for resources, such as light, is an important structuring factor of kelp ecosystems (Traiger and Konar 2017). This might translate into a future overlap of the realized ecological niche of *A. esculenta* with other species' habitats (e.g., *S. latissima*). The habitat model of Goldsmit et al. (2021) confirms this hypothesis, showing a higher habitat availability for *S. latissima* than *A. esculenta* in the future Canadian Arctic. As kelps are foundation species, a regime shift has cascading effects on ecosystems: important food sources, and settling- and recruitment ground for local benthic organisms might be reduced; non-indigenous and invasive species might be introduced in the ecosystem and the export production of kelp to deeper water might change. This could affect the overall productivity, light availability for the subcanopy community, biogenic habitat structure and biodiversity (Traiger and Konar 2017). Thereby, the degree of photosynthetic acclimation and thermal plasticity depends significantly on the thermal conditions during development and growth (Atkin and Tjoelker 2003; Liesner et al. 2020; Gauci et al. 2022). Hence, changes in the long-term acclimation processes will further affect kelp metabolism in future and has to be kept in mind when assessing the future kelp expansion and species composition in the Arctic.

While the loss of kelp forests as response to rising temperatures was observed at their warm-distribution edge (Krumhansl et al. 2016; Filbee-Dexter et al. 2019, 2020), major kelp forest expansions were modeled for the future Arctic (Krause-Jensen and Duarte 2014; Krause-Jensen et al. 2020; Assis et al. 2022). However, in this study, we showed that the sum of abiotic changes and their effects on kelps physiological and biochemical processes might lead to a future mismatch between resources and that local drivers can contradict kelp expansion and change the species composition in the future Arctic.

Data availability statement

Data supporting the findings of this study are openly available on the PANGAEA platform: Niedzwiedz, Sarina; Bischof, Kai (2022): Lab experiment on the effects of temperature on kelp respiration rates. PANGAEA, https://doi.pangaea.de/10.1594/PANGAEA.951172. Niedzwiedz, Sarina; Bischof, Kai (2022): Irradiance data at different depths and sites for field sampling in the Arctic fjord Kongsfjorden. PANGAEA, https://doi.pangaea.de/10.1594/PANGAEA.951173.

References

Aksnes, D. L., N. Dupont, A. Staby, Ø. Fiksen, S. Kaartvedt, and J. Aure. 2009. Coastal water darkening and implications for mesopelagic regime shifts in Norwegian fjords. Mar. Ecol. Prog. Ser. **387**: 39–49. doi:10.3354/meps08120

Assis, J., E. A. Serrão, C. M. Duarte, E. Fragkopoulou, and D. Krause-Jensen. 2022. Major expansion of marine forests in a warmer Arctic. Front. Mar. Sci. **9**: 850368. doi:10.3389/fmars.2022.850368

Atkin, O. K., and M. G. Tjoelker. 2003. Thermal acclimation and the dynamic response of plant respiration to temperature. Trends Plant Sci. **8**: 343–351. doi:10.1016/S1360-1385(03)00136-5

Atkinson, M. J., and S. V. Smith. 1983. C:N:P ratios of benthic marine plants. Limnol. Oceanogr. **28**: 568–574. doi:10.4319/lo.1983.28.3.0568

Bartsch, I., M. Paar, S. Fredriksen, M. Schwanitz, C. Daniel, H. Hop, and C. Wiencke. 2016. Changes in kelp forest biomass and depth distribution in Kongsfjorden, Svalbard, between 1996–1998 and 2012–2014 reflect Arctic warming. Polar Biol. **39**: 2021–2036. doi:10.1007/s00300-015-1870-1

Bintanja, R. 2018. The impact of Arctic warming on increased rainfall. Sci. Rep. **8**: 16001. doi:10.1038/s41598-018-34450-3

Bintanja, R., and O. Andry. 2017. Towards a rain-dominated Arctic. Nat. Clim. Change **7**: 263–267. doi:10.1038/nclimate3240

Bischof, K., and others. 2019. Kongsfjorden as harbinger of the future Arctic: Knowns, unknowns and research priorities, p. 537–561. *In* H. Hop and C. Wiencke [eds.], The ecosystem of Kongsfjorden, Svalbard. Advances of polar ecology. Springer. doi:10.1007/978-3-319-46425-1_14

Bolton, J. J., and K. Lüning. 1982. Optimal growth and maximal survival temperatures of Atlantic *Laminaria* species (Phaeophyta) in culture. Mar. Biol. **66**: 89–94. doi:10.1007/BF00397259

Borum, J., M. F. Pedersen, D. Krause-Jensen, P. B. Christensen, and K. Nielsen. 2002. Biomass, photosynthesis and growth of *Laminaria saccharina* in a high-arctic fjord, NE Greenland. Mar. Biol. **141**: 11–19. doi:10.1007/s00227-002-0806-9

Bringloe, T. T., H. Verbruggen, and G. W. Saunders. 2020. Unique biodiversity in Arctic marine forests is shaped by diverse recolonization pathways and far northern glacial refugia. Proc. Natl. Acad. Sci. USA **117**: 22590–22596. doi:10.1073/pnas.2002753117

Bringloe, T. T., and others. 2022. Whole genome population structure of North Atlantic kelp confirms high-latitude glacial refugia. Mol. Ecol. **31**: 6473–6488. doi:10.1111/mec.16714

Constable, A. J., S. Harper, J. Dawson, K. Holsman, T. Mustonen, D. Piepenburg, and B. Rost. 2022. Cross-Chapter Paper 6: Polar regions. *In* H.-O. Pörtner and others [eds.], Climate change 2022: Impacts, adaptation, and vulnerability. Contribution of working group II to the sixth assessment report of the intergovernmental panel on climate. Cambridge Univ. Press.

Niedzwiedz and Bischof   Glacial run-off opposes Arctic kelp expansion

Cottier, F. R., F. Nilsen, R. Skogseth, V. Tverberg, J. Skardhamar, and H. Svendsen. 2010. Arctic fjords: A review of the oceanographic environment and dominant physical processes. Geol. Soc. Spec. Publ. **344**: 35–50. doi:10.1144/SP344.4

Daniel, R. M., M. J. Danson, R. Eisenthal, C. K. Lee, and M. E. Peterson. 2008. The effect of temperature on enzyme activity: New insights and their implications. Extremophiles **12**: 51–59. doi:10.1007/s00792-007-0089-7

Davison, I. R., R. M. Greene, and E. J. Podolak. 1991. Temperature acclimation of respiration and photosynthesis in the brown alga *Laminaria saccharina*. Mar. Biol. **110**: 449–454. doi:10.1007/BF01344363

Dring, M. J., V. Makarov, E. Schoschina, M. Lorenz, and K. Lüning. 1996. Influence of ultraviolet-radiation on chlorophyll fluorescence and growth in different life-history stages of three species of *Laminaria* (Phaeophyta). Mar. Biol. **126**: 183–191. doi:10.1007/BF00347443

Eckman, J. E., D. O. Duggins, and A. T. Sewel. 1989. Ecology of understory kelp environments. I. Effects of kelps on flow and particle transport near the bottom. J. Exp. Mar. Biol. Ecol. **129**: 173–187. doi:10.1016/0022-0981(89)90055-5

Elliott, G. D., S. Wang, and B. J. Fuller. 2017. Cryoprotectants: A review of the actions and applications of cryoprotective solutes that modulate cell recovery from ultra-low temperatures. Cryobiology **76**: 74–91. doi:10.1016/j.cryobiol.2017.04.004

England, M. R., I. Eisenman, N. J. Lutsko, and T. J. W. Wagner. 2021. The recent emergence of Arctic amplification. Geophys. Res. Lett. **48**: e2021GL094086. doi:10.1029/2021GL094086

Falkowski, P. G., and J. A. Raven. 2007. Aquatic photosynthesis, 2nd ed. Princeton Univ. Press.

Feehan, C., R. E. Scheibling, and J. S. Lauzon-Guay. 2012. Aggregative feeding behaviour in sea urchins leads to destructive grazing in a Nova Scotian kelp bed. Mar. Ecol. Prog. Ser. **444**: 69–83. doi:10.3354/meps09441

Filbee-Dexter, K., T. Wernberg, S. Fredriksen, K. M. Norderhaug, and M. F. Pedersen. 2019. Arctic kelp forests: Diversity, resilience and future. Global Planet. Change **172**: 1–14. doi:10.1016/j.gloplacha.2018.09.005

Filbee-Dexter, K., T. Wernberg, S. P. Grace, J. Thormar, S. Fredriksen, C. N. Narvaez, C. J. Feehan, and K. M. Norderhaug. 2020. Marine heatwaves and the collapse of marginal North Atlantic kelp forests. Sci. Rep. **10**: 13388. doi:10.1038/s41598-020-70273-x

Filbee-Dexter, K., and others. 2022. Sea ice and substratum shape extensive kelp forests in the Canadian Arctic. Front. Mar. Sci. **9**: 754074. doi:10.3389/fmars.2022.754074

Fragkopoulou, E., E. A. Serrão, O. De Clerck, M. J. Costello, M. B. Araújo, C. M. Duarte, D. Krause-Jensen, and J. Assis. 2022. Global biodiversity patterns of marine forests of brown macroalgae. Glob. Ecol. Biogeogr. **31**: 636–648. doi:10.1111/geb.13450

Gattuso, J.-P., B. Gentili, C. M. Duarte, J. A. Kleypas, J. J. Middelburg, and D. Antoine. 2006. Light availability in the coastal ocean: Impact on the distribution of benthic photosynthetic organisms and contribution to primary production. Biogeosciences **3**: 895–959. doi:10.5194/bg-3-489-2006

Gauci, C., I. Bartsch, N. Martins, and D. Liesner. 2022. Cold thermal priming of *Laminaria digitate* (Laminariales, Phaeophyvceae) gametophytes enhances gametogenesis and thermal performance of sporophytes. Front. Mar. Sci. **9**: 862923. doi:10.3389/fmars.2022.862923

Geyman, E. C., W. J. J. van Pelt, A. C. Maloof, H. F. Aas, and J. Kohler. 2022. Historical glacier change on Svalbard predicts doubling of mass loss by 2100. Nature **601**: 374–379. doi:10.1038/s41586-021-04314-4

Goldsmit, J., and others. 2021. Kelp in the eastern Canadian Arctic: Current and future predictions of habitat suitability and cover. Front. Mar. Sci. **18**: 742209. doi:10.3389/fmars.2021.742209

Gordillo, F. J. L., J. Aguilera, and C. Jiménez. 2006. The response of nutrient assimilation and biochemical composition of Arctic seaweeds to a nutrient input in summer. J. Exp. Bot. **57**: 2661–2671. doi:10.1093/jxb/erl029

Graiff, A., W. Ruth, U. Kragl, and U. Karsten. 2016. Chemical characterization and quantification of the brown algal storage compound laminarin—A new methodological approach. J. Appl. Phycol. **28**: 533–543. doi:10.1007/s10811-015-0563-z

Hop, H., and others. 2002. The marine ecosystem of Kongsfjorden, Svalbard. Polar Res. **21**: 167–208. doi:10.3402/polar.v21i1.6480

Hopwood, M. J., and others. 2020. Review article: How does glacier discharge affect marine biogeochemistry and primary production in the Arctic? The Cryosphere **14**: 1347–1383. doi:10.5194/tc-14-1347-2020

Hugonnet, R., and others. 2021. Accelerated global glacier mass loss in the early twenty-first century. Nature **592**: 726–731. doi:10.1038/s41586-021-03436-z

Huovinen, P., J. Ramírez, M. Palacios, and I. Gómez. 2020. Satellite derived mapping of kelp distribution and water optics in the glacier impacted Yendegaia Fjord (Beagle Channel, Sourthern Chilean Patagonia). Sci.Total Environ. **703**: 135531. doi:10.1016/j.scitotenv.2019.135531

Iwamoto, K., and Y. Shiraiwa. 2005. Salt-regulated mannitol metabolism in algae. Mar. Biotechnol. **7**: 407–415. doi:10.1007/s10126-005-0029-4

Jeffrey, S. W., R. F. C. Mantoura, and S. W. Wright. 1997. Phytoplankton pigments in oceanography, v. **5**, 1st ed. UNESCO Publishing.

Kirk, J. T. O. 2011. Light and photosynthesis in aquatic systems, 3rd ed. Cambridge Univ. Press.

Koch, K., M. Thiel, F. Tellier, W. Hagen, M. Graeve, F. Tala, P. Laeseke, and K. Bischof. 2015. Species separation within the *Lessonia nigrescens* complex (Phaeophyceae,

Niedzwiedz and Bischof   Glacial run-off opposes Arctic kelp expansion

Laminariales) is mirrored by ecophysiological traits. Bot. Mar. **58**: 81–92. doi:10.1515/bot-2014-0086

Konik, M., M. Darecki, A. K. Pavlov, S. Sagan, and P. Kowalczuk. 2021. Darkening of the Svalbard fjords waters observed with Satellite Ocean color imagery in 1997–2019. Front. Mar. Sci. **8**: 699318. doi:10.3389/fmars.2021.699318

Krause-Jensen, D., and C. M. Duarte. 2014. Expansion of vegetated coastal ecosystems in the future Arctic. Front. Mar. Sci. **1**: 77. doi:10.3389/fmars.2014.00077

Krause-Jensen, D., and others. 2020. Imprint of climate change on pan-Arctic marine vegetation. Front. Mar. Sci. **7**: 617324. doi:10.3389/fmars.2020.617324

Krömer, S. 1995. Respiration during photosynthesis. Annu. Rev. Plant. Physiol. Plant. Mol. Biol. **46**: 45–70. doi:10.1146/annurev.pp.46.060195.000401

Krumhansl, K. A., and others. 2016. Global patterns of kelp forest change over the past half-century. Proc. Natl. Acad. Sci. USA **113**: 13785–13790. doi:10.1073/pnas.1606102113

Lenth, R. V. 2021. emmeans: Estimated marginal means, aka least-squares means. R package version 1.7.0. https://CRAN.R-project.org/package=emmeans

Li, H., H. Xu, P. Zhang, M. Gao, D. Wang, and H. Zhao. 2017. High temperature effects on D1 protein turnover in three wheat varieties with different heat susceptibility. Plant Growth Regul. **81**: 1–9. doi:10.1007/s10725-016-0179-6

Liesner, D., L. N. S. Shama, N. Diehl, K. Valentin, and I. Bartsch. 2020. Thermal plasticity of the kelp *Laminaria digitata* (Phaeophyceae) across life cycle stages reveals the importance of cold seasons for marine forests. Front. Mar. Sci. **7**: 456. doi:10.3389/fmars.2020.00456

Loos, E., M. Coasta, and S. Johannessen. 2017. Underwater optical environment in the coastal waters of British Columbia, Canada. FACETS **2**: 872–891. doi:10.1139/facets-2017-0074

Milner, A. M., and others. 2017. Glacier shrinkage driving global changes in downstream systems. Proc. Natl. Acad. Sci. USA **144**: 9770–9778. doi:10.1073/pnas.1619807114

Munda, I. M., and K. Lüning. 1977. Growth performance of *Alaria esculenta* off Helgoland. Helgolander Wiss. Meeresunters **29**: 311–314. doi:10.1007/BF01614267

Murchie, E. H., and T. Lawson. 2013. Chlorophyll fluorescence analysis: A guide to good practice and understanding some new applications. J. Exp. Bot. **64**: 3983–3998. doi:10.1093/jxb/ert208

Payne, C. M., and C. S. Roesler. 2019. Characterizing the influence of Atlantic water intrusion on water mass formation and phytoplankton distribution in Kongsfjorden, Svalbard. Cont. Shelf Res. **191**: 104005. doi:10.1016/j.csr.2019.104005

Pedersen, M., K. Filbee-Dexter, K. M. Norderhaug, S. Fredriksen, N. L. Frisk, C. W. Fagerli, and T. Wernberg. 2020. Detrital carbon production and export in high latitude kelp forests. Oecologia **192**: 227–239. doi:10.1007/s00442-019-04573-z

Pessarrodona, A., P. J. Moore, M. D. J. Sayer, and D. A. Smale. 2018. Carbon assimilation and transfer through kelp forests on the NE Atlantic is diminished under a warmer ocean climate. Glob. Change Biol. **24**: 4386–4398. doi:10.1111/gcb.14303

Pörtner, H. O., M. Lucassen, and D. Storch. 2005. Metabolic biochemistry: Its role in thermal tolerance and in the capacities of physiological and ecological function. Fish Physiol. **22**: 79–154. doi:10.1016/S1546-5098(04)22003-9

Previdi, M., T. P. Janoski, G. Chiodo, K. L. Smith, and L. M. Polvani. 2020. Arctic amplification: A rapid response to radiative forcing. Geophys. Res. Lett. **47**: e2020GL089933. doi:10.1029/2020GL089933

Previdi, M., K. L. Smith, and L. M. Polvani. 2021. Arctic amplification of climate change: A review of underlying mechanisms. Environ. Res. Lett. **16**: 093003. doi:10.1088/1748-9326/ac1c29

R Core Team. 2021. R: A language and environment for statistical computing. R Foundation for Statistical Computing, https://www.R-project.org/

Saltveit, M. E. 2019. Respiratory metabolism, p. 73–91. *In* E. M. Yahia [ed.], Postharvest physiology and biochemistry of fruits and vegetables. Elsevier.

Scheschonk, L., S. Becker, J.-H. Hehemann, N. Diehl, U. Karsten, and K. Bischof. 2019. Arctic kelp eco-physiology during the polar night in the face of global warming: A crucial role for laminarin. Mar. Ecol. Prog. Ser. **611**: 59–74. doi:10.3354/meps12860

Schild, K. M., R. L. Hawley, J. W. Chipman, and D. I. Benn. 2017. Quantifying suspended sediment concentration in subglacial sediment plumes discharging from two Svalbard tidewater glaciers using Landsat-8 and in-situ measurements. Int. J. Remote Sens. **38**: 6865–6881. doi:10.1080/01431161.2017.1365388

Schlitzer, R. 2021. Ocean data view. Version 5.5.1—64 bit (Windows). https://odv.awi.de/

Skogseth, R., and others. 2020. Variability and decadal trends in the Isfjorden (Svalbard) ocean climate and circulation—An indicator for climate change in the European Arctic. Prog. Oceanogr. **187**: 102394. doi:10.1016/j.pocean.2020.102394

Smale, D. A. 2020. Impacts of ocean warming on kelp forest ecosystems. New Phytol. **225**: 1447–1454. doi:10.1111/nph.16107

Smale, D. A., and T. Wernberg. 2013. Extreme climatic event drives range contraction of a habitat-forming species. Proc. R. Soc. B **280**: 20122829. doi:10.1098/rspb.2012.2829

Stomp, M., J. Huisman, L. J. Stal, and H. C. P. Matthijs. 2007. Colorful niches of phototrophic microorganisms shaped by vibrations of the water molecule. ISME J. **1**: 271–282. doi:10.1038/ismej.2007.59

Svendsen, H., and others. 2002. The physical environment of Kongsfjorden–Krossfjorden, an Arctic fjord system in Svalbard. Polar Res. **21**: 133–166. doi:10.3402/polar.v21i1.6479

_____

Niedzwiedz and Bischof   Glacial run-off opposes Arctic kelp expansion

Teagle, H., S. J. Hawkins, P. J. Moore, and D. A. Smale. 2017. The role of kelp species as biogenic habitat formers in coastal marine ecosystems. J. Exp. Mar. Biol. Ecol. **492**: 81–98. doi:10.1016/j.jembe.2017.01.017

Traiger, S. B., and B. Konar. 2017. Supply and survival: Glacial melt imposes limitations at the kelp microscopic life stage. Bot. Mar. **60**: 603–617. doi:10.1515/bot-2017-003

Verardo, D. J., P. N. Froelich, and A. Mclntyre. 1990. Determination of organic carbon and nitrogen in marine sediments using the Carlo Erba NA-1500 analyzer. Deep-Sea Res. **37**: 157–165. doi:10.1016/0198-0149(90)90034-S

Vranken, S., and others. 2021. Genotype-environment mismatch of kelp forests under climate change. Mol. Ecol. **30**: 3730–3746. doi:10.1111/mec.15993

Wernberg, T., K. Krumhansl, K. Filbee-Dexter, and M. F. Pedersen. 2019. Status and trends for the world's kelp forests, p. 57–78. *In* C. Sheppard [ed.], World seas: An environmental evaluation. Elsevier. doi:10.1016/B978-0-12-805052-1.00003-6

Wondraczek, L., M. Batentschuk, M. A. Schmidt, R. Borchardt, S. Scheiner, B. Seemann, P. Schweizer, and C. J. Brabec. 2013. Solar spectral conversion for improving the photosynthetic activity in algae reactors. Nat. Commun. **4**: 2047. doi:10.1038/ncomms3047

Wright, S. W., S. W. Jeffrey, R. F. C. Mantoura, C. A. Llewellyn, T. Bjørnland, D. Repeta, and N. Welschmeyer. 1991. Improved HPLC method for the analysis of chlorophylls and carotenoids from marine phytoplankton. Mar. Ecol. Prog. Ser. **77**: 183–196. doi:10.3354/meps077183

Xu, Z., F. Ji, B. Liu, T. Feng, Y. Gao, Y. He, and F. Chang. 2021. Long-term evolution of global sea surface temperature trend. Int. J. Climatol. **41**: 4494–4508. doi:10.1002/joc.7082

Conflict of Interest

None declared.

_____

Manuscript ID: LO-22-0363.R1

Glacial retreat and rising temperatures are limiting the expansion of temperate kelp species in the future Arctic

Supporting Information:

Method description of kelp parameters:

Photosynthesis vs. irradiance curves. The photosynthesis vs. irradiance curves were measured with a 4-channel optode set-up (FireStingO$_2$ Fibre-Optic Oxygen Meter FSO2-01, PyroScience Sensor technology, Aachen, Germany) by analysing the oxygen evolution in response to different light intensities within 25 mL Schott bottles (*n*=4), each containing three meristematic discs. Before each measurement, the system was one-point-calibrated according to the manufacturers protocol. A magnetic stirrer in each Schott bottle ensured a homogenic oxygen concentration and equal illumination of all discs. The chamber's oxygen concentration (μmol O$_2$ L^{-1}) and temperature (°C) were recorded at 1 s intervals. Illumination intensities of the photosynthesis vs. irradiance curves (PAR; 400–700 nm) were measured (RAMSES-ACC-UV/VIS radiometer, TriOS Optical Sensor, Oldenburg, Germany) by integrating the irradiance from 400–700 nm (see **Equation 1**; **Equation 2**). The PyroScience Calculation Tool was used to correct the raw data for variations in temperature, salinity and atmospheric pressure. To calculate the dark respiration and net photosynthetic rates, linear functions were fit on the oxygen concentration changes over time (15–25 min). Linearity of slopes was maintained in all measurements, indicating that the incubation chambers were neither carbon dioxide or nutrient limited nor oxygen super-saturated. The photosynthesis vs. irradiance curves were measured within a range of 0–24 μmol photons m^{-2} s^{-1}. The maximum illumination intensity of 24 μmol photons m^{-2} s^{-1} was based on the prevailing low light intensities in Kongsfjorden. The measurement at 0 μmol photon m^{-2} s^{-1} was evaluated as dark respiration rate and the measurement at 24 μmol photons m^{-2} s^{-1} as the net photosynthetic rate. Photosynthetic rates are shown as net photosynthetic rates, as plant respiration in the light was shown to vary between 25–100% of dark respiration (Krömer 1995). To increase comprehensibility, we labelled the respective plots with "dark respiration rate" and "net photosynthetic rate" rather than "oxygen concentration changes at 0 / 24 μmol photons m^{-2} s^{-1}". Dark respiration and net photosynthetic rates were calculated in μmol O$_2$ L^{-1} cm^{-2} h^{-1}. The compensation irradiance was determined by monitoring the oxygen concentration change as response to illumination intensities between 0–24 μmol photons m^{-2} s^{-1}. The compensation irradiance was defined as the irradiance at which the oxygen decline (respiration) equals the oxygen increase (photosynthesis).

_____

Maximum quantum yield (F_v/F_m). F_v/F_m was measured using pulse amplitude modulated fluorometry (Portable Chlorophyll Fluorometer PAM-2100, Heinz Walz GmbH, Effeltrich, Germany). Before each measurement, the discs were dark adapted for 5 min.

Pigments. Pigment analysis was conducted according to Koch et al. (2015). Three aliquots of 30–100 mg (silica dried) powdered material (*n*=4) were extracted in 1–1.5 mL 90 % acetone (depending on kelp polysaccharide content; volume percent) for 24 h in darkness at 4°C. The supernatant was filtered and analysed by a High-Performance Liquid Choromatography (HPLC; LaChromElite® system, L-2200 autosampler (chilled), DA-detector L-2450; VWR-Hitachi International GmbH, Darmstadt, Germany). A gradient was applied according to Wright et al. (1991), separating the pigments by a Spherisorb® ODS-2 column (250 × 4.6 mm, 5 μm; Waters, Milford, MA, USA). To identify and quantify pigment peaks, the respective standard for each pigment was used (DHI Lab Products, Hørsholm, Denmark). The accessory pigment concentration was determined by the sum of chlorophyll *c* and carotenoids. The ratio of accessory pigments to chlorophyll *a* was calculated. Pigment contents were calculated in μg cm^{-2}.

Carbon to nitrogen ratio. Carbon and nitrogen content of kelp samples was analysed using silica-dried and powdered material (2–6 mg; *n*=4). Samples were weighted into tin cartridges (5×9 mm) and combusted at 1000°C. Acetanilide was used as standard (Verardo et al. 1990). An elemental analyser (Euro EA 3000 Elemental Analyser, EuroVector S.P.A., Milano, Italy) automatically quantified the carbon and nitrogen content. Total carbon and nitrogen content were expressed as proportion (%) and ratio.

Table S 1: Sampling sites
Sampling date, latitude and longitude of ststaions for underwater light climate depth profiles (A–Q) and kelp sampling (S.lat: Saccharina latissima; A.esc: Alaria esculenta).

Station	Date	Latitude	Longitude	Station	Date	Latitude	Longitude
A	19.07.21	N78.888	E12.468	**B**	07.07.21	N78.889	E12.443
C	19.07.21	N78.891	E12.418	**D**	19.07.21	N78.895	E12.377
E	07.07.21	N78.898	E12.388	**F**	07.07.21	N78.904	E12.333
G	19.07.21	N78.899	E12.328	**H**	07.07.21	N78.909	E12.287
I	19.07.21	N78.902	E12.283	**J**	07.07.21	N78.912	E12.246
K	23.07.21	N78.927	E11.978	**L**	23.07.21	N78.930	E11.957
M	23.07.21	N78.932	E11.933	**N**	23.07.21	N78.931	E11.904
O	23.07.21	N78.934	E11.879	**P**	05.07.21	N78.969	E11.738
Q	05.07.21	N78.979	E11.599				
S.lat	06.07.21	N78.965	E11.638	***A.esc***	13.07.21	N78.985	E11.964

_____

_____

7   Synoptic discussion

Ecosystem engineering kelp forests are subject to many rapid environmental changes in the Arctic. Since the 1980s, the rate of sea surface temperature rise is far beyond the global average (Previdi et al. 2021; Rantanen et al. 2022), with marine heatwaves acting upon the gradual temperature increase (Barkhordarian et al. 2024). Consequently, glacial (Milner et al. 2017) and permafrost melt (Bintanja 2018) are accelerating and precipitation rates are expected to increase (Bintanja and Andry 2017), leading to extensive run-off plumes covering fjords. Run-off plumes alter many water column parameters: e.g., high concentrations of suspended particles are changing the irradiance (Konik et al. 2021) and spectral composition (Stomp et al. 2007); terrestrial and lithogenic material alter the macro- and micronutrient concentrations (McGovern et al. 2020; Krause et al. 2021). Acclimatisation and high plasticity are important for the persistence of kelp forests, as the sedentary kelps are not able to migrate, and adaptation is likely outpaced by the rate of environmental changes (Vranken et al. 2021). Acting as foundation species, their response to environmental changes has cascading ecological and economic consequences on the entire ecosystem (Wernberg et al. 2019; 2024). Hence, it is crucial to understand future kelp forest dynamics to be able to make predictions on Arctic coastal ecosystem developments and functioning.

Laeseke et al. (2024) recently reported that physiological temperature limits, i.e., the fundamental thermal niche, are a weak predictor for many seaweeds' cold-distribution limit. Assessing what defines the current and future distribution of kelps in the Arctic, I investigated the current realised niche of Arctic kelps using *in-situ* approaches and assessed trait performance in response to irradiance and temperature in laboratory experiments. I discuss the relevance of my results for present-day seasonal and spatial, as well as near-future climatic changes, global patterns in kelp forest change and socio-economic implications.

7.1   Major findings

In two *in-situ* monitoring studies, I found high intraspecific variability in the biochemical composition of different Arctic kelp populations, being conditioned by their local environment along the west coast of Svalbard (**publication I**). Hence, performance curves must not be considered static and experimental results have to be extrapolated with care. Investigating the *in-situ* effect of run-off on kelp holobiont functioning in a high spatial resolution, I additionally found run-off to change the content of (harmful) elements in kelps. This led to changes of the ecosystem services of kelp forests, such as the nutritious value of kelps for grazers, or the element cycling of the ecosystem (**publication II**). In three experimental studies, I found that the effect of

temperature on kelps is highly interactive with the prevailing PAR availabilities (**publication III**). High-PAR availability caused drastic physiological stress, especially when interacting with cold temperatures, which currently restricts *L. hyperborea* to expand to higher latitudes (**publication IV**). Reduced irradiance resulted in a predicted shift of the kelps' realised niche and results in a local loss of habitat for cold-temperate kelps in the Arctic (**publication V**).

Figure 7.1 displays a graphical overview of the major findings of my doctoral project. I will discuss them in detail in the following chapters.
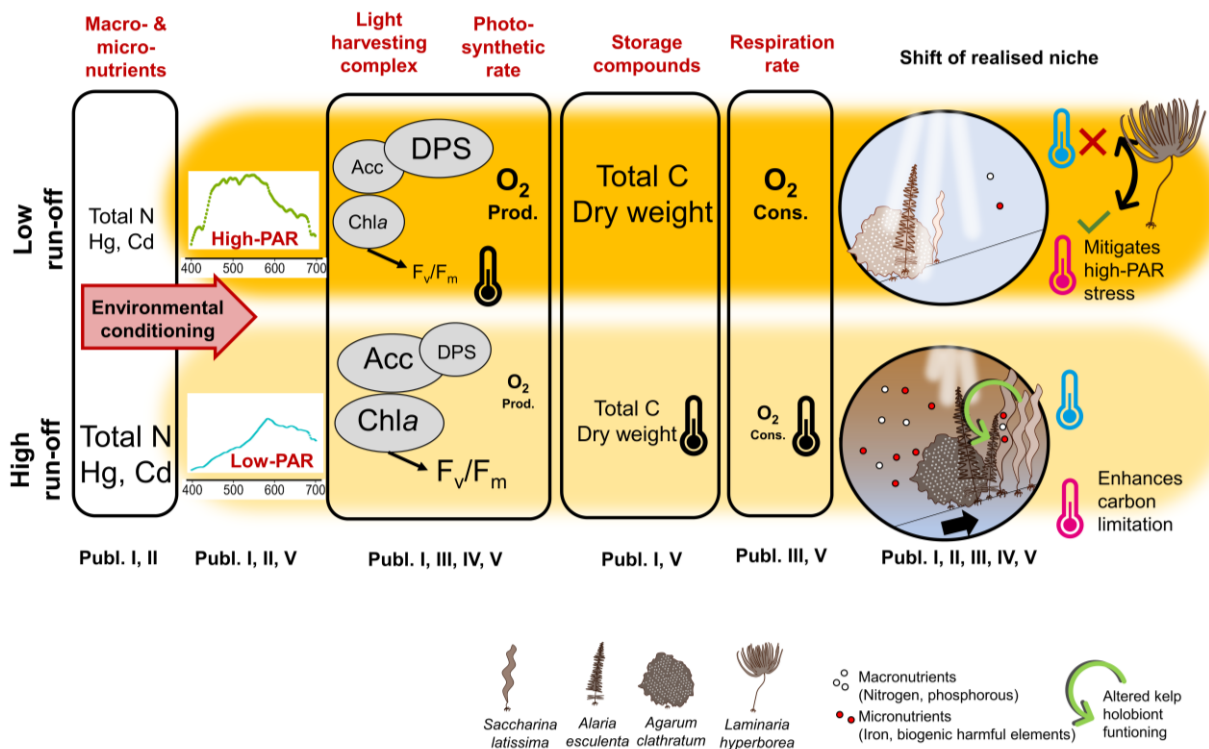
Figure 7.1: Major findings on the influence of coastal run-off on Arctic kelp communities. I measured the following kelp responses (font size refers to the biogenic content, not to scale): total nitrogen (N) and (harmful) elemental composition (e.g., Hg, Cd); the intensity and spectral composition of the photosynthetically active radiation (PAR). Content and composition of the light harvesting complex: Chl*a*: chlorophyll *a*; Acc: accessory pigments; DPS: De-epoxidation state of xanthophyll cycle pigments. F_v/F_m: maximum quantum yield of photosystem II. O_2 Prod.: photosynthetic rate as oxygen production. C: storage compounds as total carbon and dry weight. O_2 Cons.: respiration rate as oxygen consumption. I found a high macro- and micro-nutrient content, i.e., nitrogen but also harmful elements, in kelps being influenced by run-off. High-PAR availabilities prevail under low run-off influence, low-PAR availabilities under high run-off intensity. All kelp physiological and biochemical parameters were highly influenced by varying PAR availabilities. Thermometer: temperature sensitivity. When kelps were exposed to high-PAR, I found the maximum quantum yield to be temperature sensitive. Under low-PAR availabilities, the content of storage compounds and respiration rate were temperature sensitiv. Changing PAR × temperature conditions relate to a shift in the realised niche and interspecific competition balances. High-PAR availabilities interacting with cold temperatures prevent *L. hyperborea* from establishing a high Arctic population. Warm temperatures mitigated high-PAR stress. Under low-PAR availabilities, warm temperatures enhanced PAR-dependent carbon limitation.

_____

7.1.1   Kelps are conditioned by their local environment

Wernberg et al. (2010) showed that susceptibilities of kelps towards stressors are changing when they interact. During my experimental studies I mainly focussed on the effect of PAR × temperature interactions on kelp forests (**chapter 7.1.2**). However, there are more environmental factors related to climate change that are affected by increasing run-off influence, e.g., nutrient availability (McGovern et al. 2020). To investigate the effect of run-off on kelp communities, I conducted two *in-situ* studies (**publication I**, **II**), assessing whether the local environment in Arctic fjords conditions kelp populations and how their holobiont functioning changes when they were exposed to run-off. As introduced in **chapter 1.3.2**, Arctic surface waters in summer are often nutrient depleted (Juul-Pedersen et al. 2015). The re-supply of nutrients and the chemical composition of the water column is dependent on the bedrock composition, glacier type and run-off intensity (Meire et al. 2017; McGovern et al. 2020; Krause et al. 2021). I found kelps to be nitrogen limited, with C:N ratios generally being above 20 (**publication I**, **V**; Atkinson and Smith 1983). Nitrogen limitation reduces the rate of protein synthesis (Falkowski et al. 1989) and further affects photosynthetic and respiration rates, leading to a reduced growth (Falkowski and Raven 2007). As kelps accumulate nutrients from the seawater (Mortensen 2017), their nitrogen content was higher when they were exposed to nutrient-rich run-off (**publication I**). Due to local variations, this correlation was not significant (see discussion **publication I**). While the absorption of nutrients is beneficial for the kelps' performance, I also found kelps to accumulate harmful elements, such as mercury and cadmium, when growing in areas with a high run-off influence (**publication II**). Depending on element, concentration and exposure time, those elements can become toxic (Chung and Lee 1989), by inducing the formation of reactive oxygen species (ROS) (Pinto et al. 2003), substituting trace elements in proteins or enzymes (Vallee and Ulmer 1972), or lead to chloroses (bleaching), necrosis and tissue weakening (Rybak et al. 2017). Further, run-off leads to a significant change of the kelps' associated microbial community (**publication II**), being important for the fitness and functioning of kelps and, therefore, ecosystem health (Burgunter-Delamare et al. 2023). These results clearly indicate that **kelp populations are conditioned by their local environment**. The run-off dependent conditioning influences the susceptibilities and responses of local kelp populations to environmental and climate change related drivers. Hence, responses from one single population have to be extrapolated with care, considering local environmental conditions. Therefore, two main aspects have to be kept in mind when interpreting the effects of experimental PAR × temperature interactions in the following synoptic discussion: 1) I assessed the responses of cold-temperate kelps, as they are forming the majority of Arctic kelp populations (Filbee-Dexter et al. 2019). Hence, the discussion focusses on performance variability of kelps at their cold distribution margin with experimental temperature modifications being below or close to the species' thermal

optimum. 2) As all studies were conducted in Arctic summer, i.e., during 24 h of light availability (except long-day and Polar Night scenario in **publication IV**), the major findings focus on kelp performance during Polar Day. I elaborate on potential effects of climate change on cryophilic kelps, as well as kelp performance during Polar Night in **chapter 7.2**.

7.1.2   Effect of PAR × temperature interactions

Rising temperatures initiate a cascade of associated environmental changes in the Arctic, e.g., the reduction of available PAR in the water column (**chapter 1.3**). How temperature × PAR affect kelps is of high interest, as the carbon gain (photosynthesis) and loss (respiration) of kelps are driven by a multitude of temperature-sensitive processes (Davison et al. 1991, Falkowski and Raven 2007). Hence, the response of kelps to temperature × PAR interactions is not linear. Low values of the maximum quantum yield of photosystem II (F_v/F_m) are a measure for a high physiological and cellular stress level (Dring et al. 1996; Murchie and Lawson 2013). In **publication III** and **IV**, F_v/F_m of *S. latissima*, *A. clathratum* and *L. hyperborea* responded as follows to temperature × PAR interactions:

cold temperature × high-PAR < warm temperatures × high-PAR < cold-temperature × low-PAR.

This sequence is striking, given that warm temperatures are closer to the species' thermal optimum, and would be expected to cause less physiological stress than cold temperatures. However, it confirms that temperature as an isolated driver is a weak predictor (Laeseke et al. 2024). **I argue that PAR availability, i.e., intensity, spectral composition and duration, is a major driver for the distribution limit of cold-temperate kelps in the Arctic**. For context of the following discussion, I displayed a schematic photosynthetic electron transport chain, the net carbon balance, and respiratory electron transport chain in **Figure 7.2** and marked which parameters I measured and which steps are light or temperature sensitive.
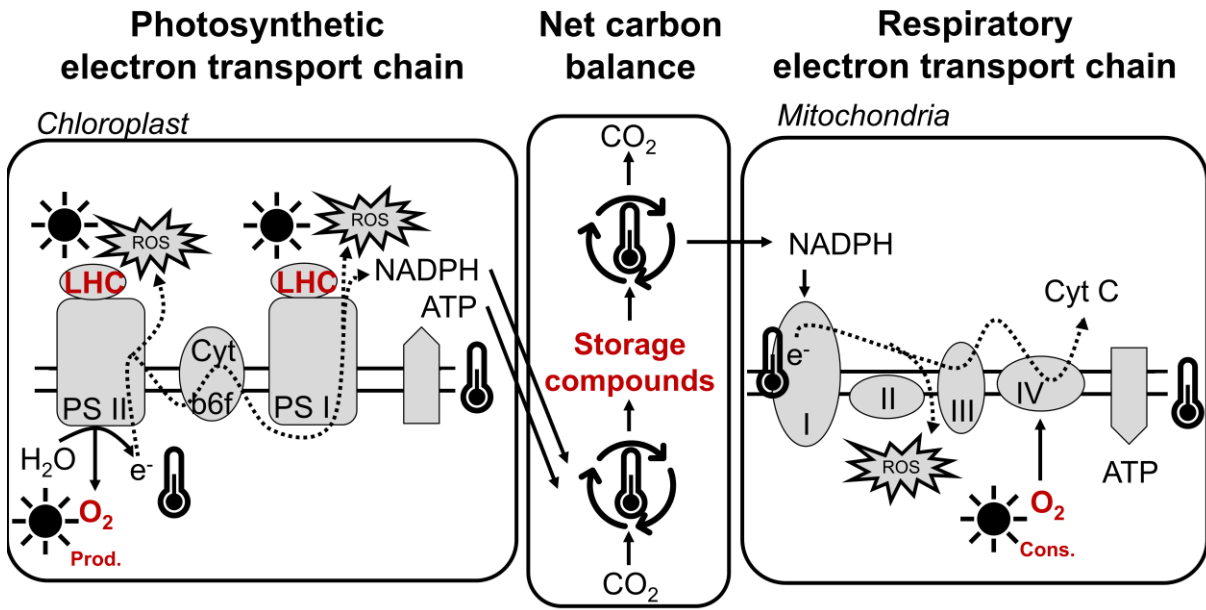
Figure 7.2: Schematic photosynthetic electron transport chain (along thylakoid membrane in chloroplast), net carbon balance and respiratory electron transport chain (along inner mitochondrial membrane). Thermometer symbol: temperature sensitive steps. Sun symbol: light sensitive steps. Red text: measured parameters. e⁻: electrons. Dotted line: e⁻ transport chain. ROS: reactive oxygen species, formed when electrons are transferred to oxygen instead of being processed along the electron transport chain. The photosynthetic electron transport chain is composed of two photosystems (PS II; PS I) and a cytochrome b6f complex (proton pump to establish gradient for ATP synthase). Extraction of electrons (e⁻) is catalysed at PS II, by the oxidation of water. LHC: light harvesting complex consisting of chlorophyll *a* and accessory pigments. At PS I, e⁻ are transferred to reductive equivalent (NADPH). Adenosine triphosphate (ATP; cellular energy unit) is generated as at the ATP synthase, using a proton gradient. NADPH, ATP and carbon dioxide (CO_2) are used to form storage compounds. When storage compounds are used (net carbon balance), CO_2 is released, e⁻ are extracted from NADPH and passed through the respiratory electron transport chain, being composed of complex I–IV to establish a proton gradient for the ATP synthase to generate ATP. Note that there are other physiological and biochemical processes influencing the net carbon balance.

High-PAR availabilities cause physiological stress, when the rate of photon absorption exceeds the rate of the downstream photosynthetic processes and electrons are transferred to oxygen (Bischof and Rautenberger 2012). The formed ROS have a highly destructive potential on macromolecules (Sharma et al. 2012). To prevent ROS formation, brown algae can couple or decouple the light harvesting antenna to redistribute energy (Falkowski and Raven 2007), or dissipate excessive energy in the form of heat by increasing the de-epoxidation state of xanthophyll cycle pigments (DPS; Demmig-Adams and Adams 1996). Both processes are very fast reactions, responding to immediate changes in PAR availability. When kelps are exposed to a longer period of high-PAR, they can photoacclimate to prevent the formation of ROS, e.g., by the overall reduction of chlorophyll *a* or by reducing the light harvesting complex (Franklin and Forster 1997). I detected increased DPS values and modifications of the light harvesting complex in response to high-PAR availabilities experimentally (**publication III**), as well as *in-situ*

_____

monitoring (**publication I**). The reduction of chlorophyll *a* correlated significantly with decreasing photosynthetic rates in the course of the experiment, in both *S. latissima* and *A. clathratum* (**publication III**).

If the formation of ROS cannot be prevented, antioxidants, e.g., phlorotannin (Ford et al. 2019), scavenge ROS, preventing them from reacting with critical macromolecules (Bischof and Rautenberger 2012). Neither phlorotannin concentration in **publication III** nor the antioxidant activity (AOA; determined after Re et al. 1999) in **publication I** correlated significantly with PAR availability, which might indicate that the prevailing high-PAR stress was already effectively mitigated by modifications of the photosystem, preventing an overall cellular stress response. Contrastingly, in **publication II**, I found significant variations in AOA between sampling stations, being higher at sampling stations with lower run-off influence. I hypothesised in the discussion of **publication II** that this might be due to physical or chemical parameters, being associated with run-off, e.g., higher PAR availabilities (Bischof and Rautenberger 2012) or lower concentrations of harmful elements (Nowicka et al. 2022). In **publication II**, I analysed clear gradients of decreasing influence of run-off at high spatial resolution. Hence, it is likely that that run-off related changes of the water column were resolved, which were not detectable in **publication I**.

High-light stress was inflicted by absolute PAR intensities of ~100 µmol photons m^{-2} s^{-1}. This is striking, as kelps are exposed to much higher PAR intensities at lower latitudes (Stahl et al. 2024). However, supraoptimal irradiance levels are defined by the combination of PAR intensity, as well as duration of exposure (Falkowski and Raven 2007). During Polar Day, kelps are exposed to no (or a weak) light-dark cycle (Gattuso et al. 2020; Schlegel et al. 2024). Therefore, **peak high-PAR tolerances of kelp populations from lower latitudes cannot be extrapolated to Arctic kelps, as photoperiod acts as critical driver**. The essential role of photoperiod became especially evident in **publication IV**. Considering the 0°C treatments of *L. hyperborea* to 30–35 µmol photons m^{-2} s^{-1}, a 24 h exposure over several weeks was lethal for the species, while an 18:6 h L:D cycle was tolerable. *S. latissima* and *A. esculenta* did not show extensive signs of physiological stress in response to a continuous exposure to 30–35 µmol photons m^{-2} s^{-1} (**publication V**).

Considering the effect of temperature on kelps under high-PAR exposure, physiological stress levels were generally highest when high-PAR levels interacted with cold temperatures, becoming apparent in low F_v/F_m and high DPS values. Generally, it is assumed that the photosynthetic electron transport chain is not temperature sensitive, as a genuine photochemical reaction would not depend on (temperature-sensitive) intermolecular interactions (Falkowski and Raven 2007). However, the transport processes through the electron transport chain depend on temperature-sensitive membrane fluidity (**Figure 7.2**; Raven and Geider 1988). At cold temperatures, the rate of electron flux is reduced as the independent movement of the electron-transport-chain-

_____

components is impaired, as well as the diffusion of electron carriers (Falkowski and Raven 2007). When the rate of electron transport is reduced in an already electron saturated system, more electrons are being transferred to oxygen and form ROS. Therefore, **cold temperatures are enhancing high-light stress**. With warmer temperature physiological high-PAR stress levels were reduced (**publication III**, **IV**), which I attribute to the ROS formation being mitigated by warmer temperatures. Again, this became especially obvious in **publication IV**. Comparing the response of *L. hyperborea* during 24 h light exposure, its interaction with 0°C proved to be lethal, while warmer temperatures, i.e., 5 and 10°C increased the species performance. *S. latissima* and *A. clathratum* showed the same response pattern in **publication III**. With warmer temperatures, the potential to gain more storage compounds and maintain a positive net carbon balance was increased (i.e., increased weight gain; **publication III**), as it is dependent on temperature-sensitive enzymatic reactions. Hence, **warmer temperatures mitigated high-light stress and, being closer to the species optimum, caused an increase in performance** (Wahl et al. 2020). The temperature increase did not relate to significant changes of the biochemical composition, such as a modification of the light harvesting complex, in neither *S. latissima*, *A. clathratum* nor *L. hyperborea* (**publication III, IV**). It has to be noted that I detected only weak responses of the photosynthetic rate to changes in temperature (**publication III, V**). In the discussion of **publication V**, I attributed this to the photosynthetic rates being light-limited. However, even at 120 μmol photons m^{-2} s^{-1}, the temperature-dependent response of the photosynthetic rate was weak and only significant for a few comparisons (**publication III**). I measured the photosynthetic rate as the oxygen evolution over time, which is formed at PS II by the oxidation of water molecules (**Figure 7.2**). Hence, the oxygen related photosynthetic rate is no measure for the rate of electron transport, which might by a reason why I did not detect a strong temperature sensitivity.

In run-off plumes, the PAR availability changes drastically. Correlating significantly with increasing turbidity, i.e., the concentration of suspended particles in the water column, the light attenuation coefficient of the water column is increasing, reducing the PAR intensity (**publication I**). With increasing distance to the run-off inflow, PAR intensity increases, establishing a strong gradient along fjords (**publication II, V**). An overall darkening of fjords has been described by Konik et al. (2021). Additional to the decrease in PAR intensity in run-off plumes, the spectral composition is changing, as the suspended particles absorb a specific proportion of the PAR spectrum (**publication I, V**; Stomp et al. 2007). The shift of the spectral composition can vary strongly (**publication I**, appendix), as it depends on the prevailing sediment types and their composition of the run-off plume. I found the overlap between the absorption range of photosynthetic pigments with the available light spectrum to decrease with increasing run-off influence (**publication V**). Wondraczek et al. (2013) described the photosynthetic efficiency to be

highly dependent on the spectra overlap. Due to reasons of feasibility, I focussed on the decreasing PAR intensity as interacting driver in the experimental studies. Spectral influences are integrated in the responses monitored in *in-situ* studies. I found the pigment composition to mainly respond to changes in PAR intensity and not the spectral composition (**publication I**).

I found physiological stress levels to be generally low under low-PAR availabilities, independently of the temperature (**publication I, III, IV**). I assume that the photosynthetic electron transport chain was not saturated by low-PAR availabilities (even at cold temperatures), resulting in a low ROS formation. However, kelps can only survive and grow, if their carbon uptake (photosynthesis) exceeds their carbon loss (respiration; carbon excretion) (Kirk 2011). Kelps have to maintain a positive net photosynthetic rate under low-PAR environments to persist in run-off plumes. At the beginning of the experiment in **publication III**, I monitored negative net photosynthetic rates in both *S. latissima* and *A. clathratum*. In the course of the experiment, their net photosynthetic rates became positive, as a result of an increase in chlorophyll *a* content. Integrating the complete experiment, kelps maintained an overall positive net carbon balance and grew. Nevertheless, low-PAR exposed kelps gained significantly less weight compared to high-PAR exposed kelps. I observed a similar response in *in-situ* monitoring (**publication I**). Kelps in fjords with a low-PAR availability increased their chlorophyll *a* content and reduced their antenna complex of the photosynthetic reaction centres to increase light harvesting. Despite the photoacclimation, their total carbon content, too, was significantly lower compared to samples from fjords with a high-PAR availability. Hence, **reduced PAR availabilities in run-off plumes have the potential to cause the net carbon balance of kelps to become negative**, which was confirmed by modelling of the potential depth distribution of kelps along the fjord gradient (**publication V**).

The dark respiration rate, being a proxy for the cellular energy requirement, was highly dependent on the PAR availabilities, being lower under low-PAR intensities (**publication III**). A "light-enhanced-dark-respiration" was also described by Xue et al. (1996). They described the dark respiration rates of *Chlamydomonas reinhardtii* to be dependent on the intensity and duration of light exposure, as well as the photosynthetic rate. I did not detect a clear overall temperature dependency of the dark respiration rate, although it is dependent on membrane fluidity and many enzymatic reactions (**Figure 7.2**). In **publication V**, the respiration rate of *S. latissima* increased significantly with warmer temperatures, correlating with a stronger decrease of the total carbon content. However, this response was not confirmed in any PAR × temperature interaction in **publication III**. I hypothesise that the difference in PAR availability was the predominant driver of the kelps' dark respiration rate in **publication III** masking possible temperature impacts. In *A. esculenta*, warmer temperatures increased the compensation irradiance, i.e., the PAR intensity kelps need to balance respiratory losses (**publication V**;

_____

Falkowski and Raven 2007). The increased light requirements of *A. esculenta* enhanced low-PAR driven habitat loss. *S. latissima* did not show an increase in compensation irradiance. However, considering their thermal performance curve, the optimal growth temperature for *A. esculenta* is below that of *S. latissima* (8–9°C vs. 10–15°C; Munda and Lüning 1977; Bolton and Lüning 1982). Therefore, the experimental temperature increases in **publication V** have larger physiological consequences on *A. esculenta*. Davison et al. (1991) also detected increasing compensation irradiance of *S. latissima* when temperatures increased beyond their thermal optimum. Overall my results suggest, that **temperature effects under low-PAR intensities are species-specific**.

7.1.3   Methodological considerations

The studies I conducted in the course of this dissertation can be categorised in either *in-situ* monitoring studies (**publication I, II**) or experimental studies (**publication III, IV, V**). Both have contrasting advantages and disadvantages.

In experimental studies, the effect of single drivers on kelps can be specifically targeted, untangling the effect towards several interacting drivers. However, basing modelling approaches on a species' response towards a single driver, such as temperature, might lead to mis-extrapolations, as was shown for the kelp *Laminaria hyperborea* (**publication IV**): surviving minimum temperatures of -1.5°C, *L. hyperborea* should be able to occur on Svalbard, when only considering their fundamental thermal niche (Bolton and Lüning 1982; tom Dieck 1993). However, the interaction of cold temperatures with Polar Day conditions has prevented its spread. Consequently, the recorded observation on Svalbard, shown in **Figure 1.3**, is most likely a misidentification. Further, it has to be considered that responses towards single drivers, e.g., temperature, can be gradual, while this relation may not persist when interacting with other environmental factors, as also shown in the studies of this dissertation (**chapter 7.1.2**). In multifactorial experiments, the effect of several interacting drivers can be targeted. However, due to logistical reasons, multifactorial experiments are strongly limited to two or three variables. Drivers that were not accounted for might be limiting in the field. In the discussion of **publication I**, I attribute the overall performance increase of *S. latissima*, Diehl et al. (2021) measured during an Arctic heatwave experiment, to a recovery from high-light stress rather than the response to the experimental conditions. Generally, by selecting and considering only a few (interacting) factors, ecological implications of an experiment should be drawn with care, as species performance curves, as well as tolerance limits might be altered and changed with more interacting factors (Wernberg et al. 2010). By conducting *in-situ* studies, integrated responses of species to their complete environment can be monitored. However, these responses cannot be clearly differentiated between drivers and, therefore, no direct conclusion of future response

patterns can be drawn. Both experimental and *in-situ* studies are powerful tools to investigate the realised niche of species, with contrasting advantages and disadvantages. Hence, **I suggest a combination of experimental and *in-situ* studies to draw reliable conclusions on the trajectories of kelp forest development:** after most important drivers and performance curves were determined experimentally, the resulting ecological implications can be confirmed with *in-situ* monitoring studies and field observations.

A further consideration for both experimental and *in-situ* studies are performance or tolerance differences within species, depending on the geographical region (Bennett et al. 2019), being influenced by the environmental history (e.g., Niedzwiedz et al. 2022). Especially at the cold-distribution margin, species were reported to show large within-species variations (Bennett et al. 2019). Investigating the interacting effects of temperature × PAR on *L. hyperborea*, *L. digitata* and *L. ochroleuca* in the UK, high-PAR availabilities mitigated destructive effects of supraoptimal temperatures, while low-PAR availabilities enhance it (Bass et al. 2023). This finding is in exact opposite to the responses measured for in Arctic kelp populations (**publication III**) and highlights the necessity to consider the environmental context. It further shows the extent of within-species performance differences. Therefore, **the environmental history of kelp specimens, sampled for both experimental and *in-situ* studies has to be considered, when extrapolating results**.

Except **publication II**, all studies conducted in the frame of this thesis are based on the response of meristematic tissue samples from kelps. While this has logistical advantages, the question arises whether the response of the meristematic subsamples is representative for the entire organism, as within-thallus differentiation in kelps has been described (e.g., Scheschonk et al. 2019). While I am not aware of any study that experimentally compared the response of different parts of the phylloid to environmental drivers, the meristem is described as the kelps' metabolically most active region (Wiencke and Bischof 2012). In kelps, photoassimilates, e.g., laminarin, are usually stored in mature, distal parts of the phylloid, which was also shown by Scheschonk et al. (2019) for *S. latissima* in October, in preparation for the Polar Night. For respiratory energy gain, carbon compounds are transported to the meristem as mannitol or amino acids (Wiencke and Bischof 2012). Therefore, the meristem alone is not representative for the total of storage compounds in the entire kelp. I nevertheless consider the direct comparison of meristematic differences in the biochemical compositions between treatments or populations as indication for an overall higher or lower storage compound content. Further, the meristem is the only area of length growth. As growth integrates both physiological and biochemical conditions of the kelp, it is a valuable parameter to determine the performance of kelps. Growth of meristematic subsamples might be limited, as they are not connected to the distal energy supply. Hence, meristematic tissue provides a good proxy for immediate physiological resposes to acute

environmental changes. Regarding the kelps (eco-)physiology, I consider meristematic photoacclimation responses representatively to the rest of the phylloid, provided that illumination is comparable along the phylloid. Different pigmentation and photosynthetic rates have been measured for *Macrocystis pyrifera* along the water column, photoacclimating to the respective PAR availability (Colombo-Palotta et al. 2006). However, in contrast to the here considered species, *M. pyrifera* can occupy the water column for several 10's of meters (Colombo-Palotta et al. 2006). A strong indication of the meristematic part being representative for the tolerance of the entire kelp sporophyte is the fact that the patterns in the depth distribution of kelps modeled in **publication V** were also found in the *in-situ* study by Düsedau et al. (2024).

7.1.4   Summary of major findings

Concluding, I found that the biochemical composition of Arctic kelps is significantly conditioned by the local environment and presence of run-off plumes, with the potential to alter the responses of kelps towards climate change related drivers. Hence, their performance curve is not static and Arctic kelps must not be considered as one biochemical unit (**research question I**). Additional to biochemical changes, run-off alters the kelps' content of harmful elements, as well as their associated microbial community (**research question II**), having consequences on the kelp holobiont functioning and ecosystem services.

Focussing on the impact of PAR × temperature interactions on Arctic kelp populations, I showed that temperature and PAR are highly interactive (**research question III**): Under high-light conditions, warmer temperatures have a mitigating effect on high-light stress, while cold temperatures are enhancing it, to an extent where it restricts the spread of *L. hyperborea* into the Arctic at current environmental conditions (**research question IV**). Under low-PAR availabilities, overall physiological stress levels were reduced. However, low-PAR availabilities also resulted in a reduced weight gain or carbon content in kelps. This relates to a shift of the realised niche of kelps to shallower waters in darkening, run-off dominated fjords. For *A. esculenta* the shift was accelerated, with warming temperatures increasing its light requirement significantly (**research question V**).

7.2   Projections of differences in kelp performance with respect to...

In the following chapter, I will extrapolate the differences in kelp performance in response to changing PAR × temperature interactions to seasonal, spatial and temporal variability. Further, I will explore consequences on kelp ecosystems and the associated local change of ecosystem services. It has to be kept in mind that the influence of many (interacting) drivers are not yet fully understood. Consequently, depending on season, location, the environmental history and species, it is possible that responses are more complex than outlined in the following section.

7.2.1   ...seasonal variability

When extrapolating the results of this dissertation to current seasonal performance of kelps it has to be considered that all results were obtained in summer studies. Liesner et al. (2020) and Gauci et al. (2020) have shown that altered environmental conditions during early kelp development change their phenotypic plasticity and susceptibility towards drivers. Further, Niedzwiedz et al. (2022) found that the immediate environmental history had a large impact on the vulnerability of *S. latissima* towards marine heatwaves, i.e., seasonal conditioning might change the susceptibility of kelps towards changing environmental factors. To clarify the effect of seasonal conditioning on Arctic kelp populations, I propose a seasonal *in-situ* study, monitoring the environmental conditions (temperature, PAR and nutrient availability), and assess the physiological and biochemical response of kelps to the actually prevailing environmental conditions. The results of such a study would contribute to the knowledge of seasonal productivity of Arctic fjord ecosystems and would allow conclusions to be drawn about the impact on the Arctic food web.

I schematically displayed the seasonal variability of environmental conditions in Arctic fjords and the expected overall performance of kelps, based on my results, in **Figure 7.3**.
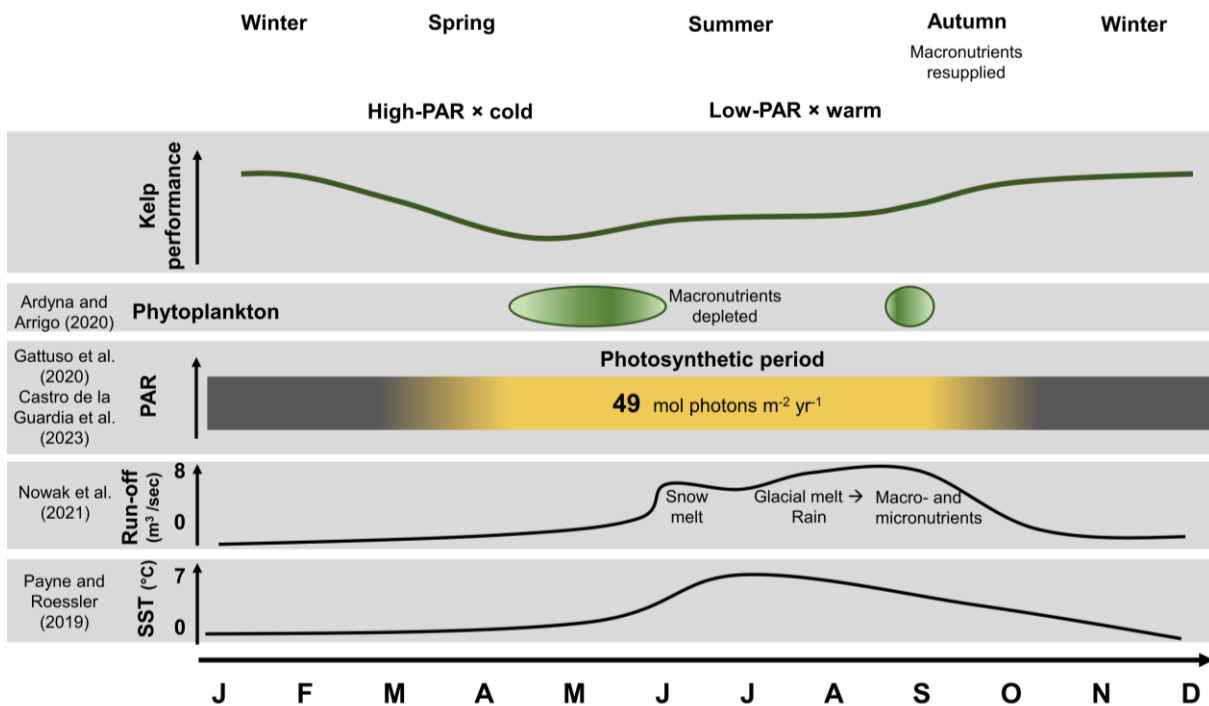
Figure 7.3: Projections of kelp performance with respect to present-day seasonal variability. Arctic coastal areas are marked by annual cycles of substantial environmental changes. Months are marked on the x-axis. Sea surface temperatures (SST) in Isfjorden, Svalbard, vary between ~0–7°C, rising in May/June and reaching their peak in July, before decreasing again (Payne and Roessler 2019). Run-off on Svalbard is sharply inclining end of May / beginning of June with the snow melt, before later in season (July/August) glacial melt and rain are feeding the run-off (Nowak et al. 2021). The pronounced cycle of light availability restricts the photosynthetic period to a few months in summer (Gattuso et al. 2020). A cumulative annual irradiance of 49 mol photons m^{-2} yr^{-1} has to prevail to maintain kelps' survival and growth (Castro de la Guardia et al. 2023). The major phytoplankton bloom is in spring (May), with a smaller bloom in late summer (August); colour gradient: approx. phytoplankton bloom productivity (Ardyna and Arrigo 2020). Early spring and summer conditions are characterised by high-PAR × cold temperatures, changing to low-PAR × warm temperatures in late summer. At the end of the run-off season, kelps contain the highest concentration of harmful elements (**publication II**). I extrapolated the seasonal performance of kelps (schematic) based on my results (green line; **publication I, III, IV**). Polar Night responses of *L. hyperborea* are assessed in **publication IV**.

Arctic seasonal changes are marked by substantial changes in air and water temperature (Timmermans and Marshall 2020) and PAR availability (**chapter 1.1**; Gattuso et al. 2020). Early in the season, after the Polar Night, the water column is characterised by cold temperatures. Due to global climate change, overall rising temperatures have resulted in a significantly reduced sea ice extent in spring, when high-PAR availabilities prevail (Nicolaus et al. 2012; Payne and Roesler 2019). In combination with cold water temperatures, I expect decreasing performance of kelps, becoming evident by decreasing F_v/F_m values and a responding reduction of the light harvesting complex and higher DPS values (**publication III, IV**). However, based on my findings, photosynthetic rates and carbon gain should be high (**publication III**), which might be beneficial for the kelp net carbon balance after Polar Night, being a period of net carbon loss. Further,

_____

photosynthetic rates and carbon gain are probably boosted by relatively high concentrations of nutrients (Falkowski et al. 1989), which were re-supplied during autumn mixing (Cottier et al. 2010).

As water temperatures and PAR availabilities increase, the spring phytoplankton bloom usually depletes the water column of nutrients, also ending their bloom (Ardyna and Arrigo 2020). Additional to the competition for nutrients, the phytoplankton bloom reduces the PAR availability for benthic primary producers, e.g., kelps. I would expect both, the increasing temperatures and reduction of the PAR availability, to increase the performance of kelps. I expect photosynthetic quantum yield to increase, however, no change in the pigment content and composition (**publication III**).

In early June, run-off is starting on Svalbard as warmer air temperatures cause the snow to melt (Nowak et al. 2021). Later in the summer, glacial melt and precipitation are primarily feeding the run-off (Nowak et al. 2021). With higher run-off influence, the available PAR intensity decreases drastically and the spectrum peak shifts to longer wavelengths (**publication I, V**). I would expect a drastic decrease of high-PAR-induced oxidative stress in kelps. The onset of the run-off is eventually accompanied by a short period of negative net photosynthetic rates (**publication III**). After photoacclimating to the low PAR intensities, i.e., increase of the chlorophyll *a* and accessory pigment content, I would expect photosynthetic rates to become positive. However, the photosynthetic rate would be lower compared to spring and early summer conditions, limiting the carbon gain. Depending on the species, warm temperatures might additionally reduce the carbon gain under low-PAR availabilities (**publication V**). Depending on glacier type, bedrock composition and run-off intensity, nutrient availability might have a further effect on the carbon gain potential. I expect the content in kelps of harmful elements to be highest at the end of the run-off season, i.e., late August / September, as kelps accumulated them during the whole run-off season (**publication II**).

During autumn, temperatures are becoming lower and PAR availability is reduced until complete darkness during Polar Night in winter prevails. With the photosynthetic period being restricted to summer months, kelps rely on their storage compounds to survive the Polar Night. Castro de la Guardia et al. (2023) have found a minimum PAR intensity threshold of 49 mol photons m^{-2} yr^{-1}, for kelps to be able to maintain a positive net carbon balance and survive the year. Summers et al. (2023) found in an *in-situ* study in Kongsfjorden, Svalbard that *S. latissima* and *A. esculenta* (as well as other macroalgae), appeared morphologically healthier, with a higher physiological performance in January than in October. This confirms the extrapolation of my results, assuming that **Arctic summer months cause high levels of physiological stress**. Summers et al. (2023) even reported *S. latissima* and *A. esculenta* to grow during Polar Night, suggesting that they use

_____

storage compounds, such as laminarin, and the high nutrient availability to form new tissue. Accordingly, Scheschonk et al. (2019) has shown in an *in-situ* study that *S. latissima* was nearly depleted of storage compounds by the end of the Polar Night. In **publication IV**, *L. hyperborea* discs survived an experimental three months of darkness, mimicking Polar Night conditions. Discs survived the extended period of darkness only using the short-term storage compound mannitol, as long-term storage compounds, e.g., laminarin, is stored in the distal part of the phylloid. This might be an indication that the species might not be susceptible to reduced PAR availability in summer. Overall, **I assume differences in their Polar Night physiology to be highly dependent on species**. As all kelp species maintained a functioning photosynthetic apparatus during present-day Polar Night (**publication IV**; Summers et al. 2023; Gordillo et al. 2022), I expect them to be able to resume phytosynthesis and growth in spring.

7.2.2   ...spatial variability

The currently observed drastic environmental changes in the Arctic have led to the development of models predicting a shift of Arctic ecosystems to a more temperate state, introducing concept terms such as "atlantification" or "borealisation". While it is highly likely that overall temperatures in the future Arctic resemble those of present-days lower latitudes (Rantanen et al. 2022; IPCC 2023), the impact of Arctic Amplification varies regionally (Nordli et al. 2020; Rantanen et al. 2022) and different fjord systems are characterised by different stages of cryosphere loss and PAR × temperature interactions. Further, photoperiod is one of the few factors not changing with ongoing climate change. As photoperiod and PAR intensity are immediate drivers for benthic primary producers, and temperature impacts are dependent on the prevailing PAR availability, I argue that **lower-latitude fjord ecosystems might not serve as direct template for future high-Arctic ecosystems**. To be able to draw conclusions on future trajectories, present-day spatial variability has to be understood. Based on the abiotic data I collected during the studies of my dissertation, my results apply to spatial variations in the performance of kelps, both along the fjord gradients and between fjords being characterised by different PAR × temperature interactions (**Figure 7.4**).
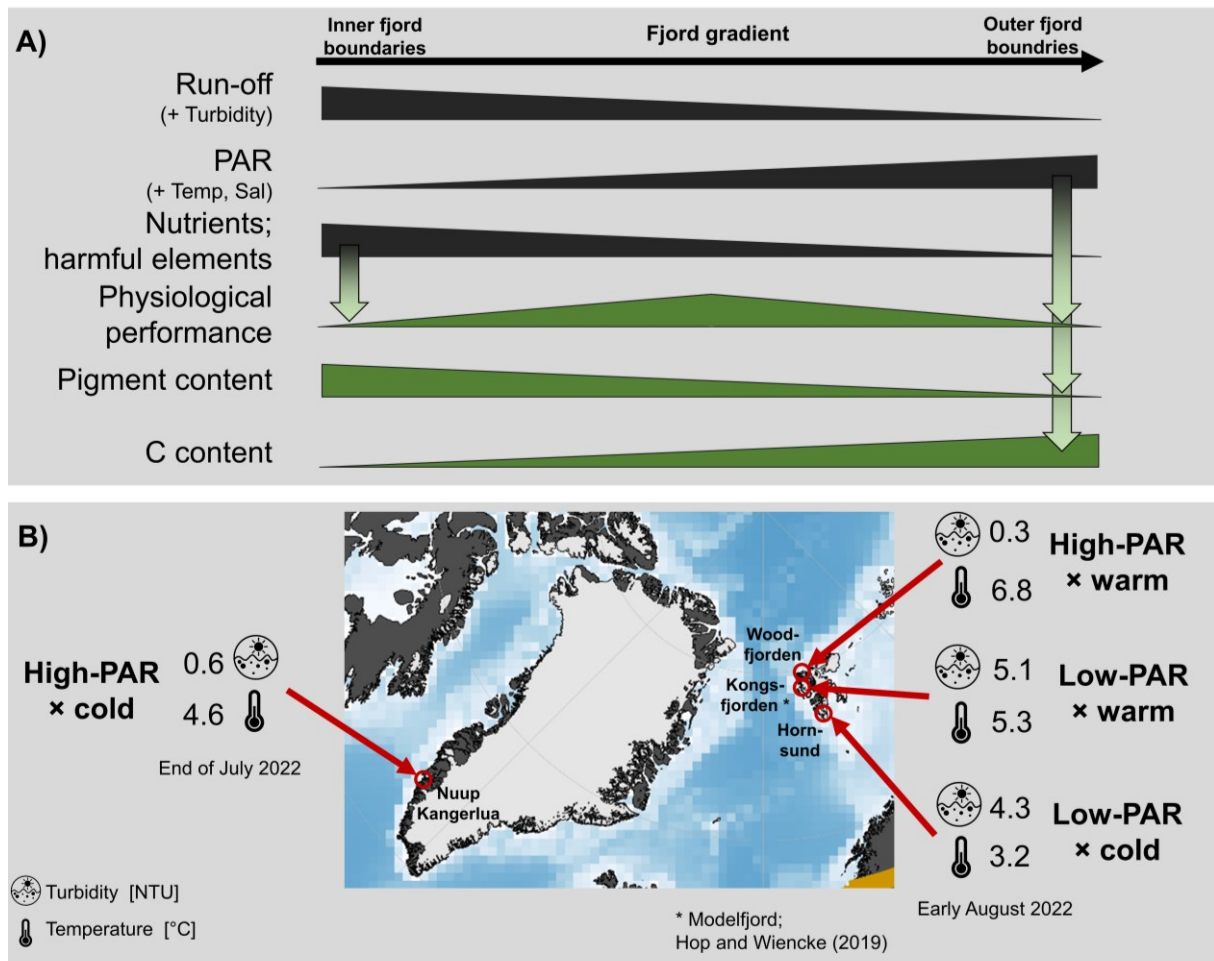
Figure 7.4: Projections of kelp performance with respect to present-day spatial variability. The environmental conditions in Arctic fjords depend on the inner and outer boundary conditions (Cottier et al. 2010). **A)** Fjord gradient. Abiotic conditions: grey colour. Kelp response: green colour. The run-off influence is highest in the inner fjord, decreasing with increasing distance to the run-off inflow. Accordingly, in the inner fjord turbidity values are high; PAR availabilities, water temperature and salinity are low; and the concentration of nutrients and harmful elements are high. Low performance of kelps: in the inner fjord due to high concentrations of harmful elements; in the outer fjord due to high-PAR availabilities. The algal pigment and carbon (C) content follow PAR availability. **B)** Study site comparison. Temperature (°C) and turbidity (NTU) conditions in 3 m water depth summer 2022 in Nuup Kangerlua, Greenland (high-PAR × cold); Woodfjorden, Svalbard (high-PAR × warm); Kongsfjorden, Svalbard (low-PAR × warm); Hornsund, Svalbard (low-PAR × cold). Map was created with ggOceanMaps (Vihtakari 2024). Data for Nuup Kangerlua provided by T.R. Vonnahme; end of July 2022. Data for Svalbard from **publication I**; early August 2022.

In **publication II** and **V**, I showed that PAR intensities, temperature and salinity vary drastically along the fjord gradient (**Figure 7.4A**). Close to the run-off inflow, turbidity values are high, resulting in low PAR intensities, which are increasing along the fjord gradient (**publication II, V**). Water temperatures of the run-off were generally lower compared to marine water masses (**publication II**). Meire et al. (2017) further described that ice berg melt close to sea-terminating glaciers further cools down the surrounding water masses. Both run-off and ice berg melt decrease the salinity of the upper water layer. These abiotic differences along the fjord gradient

have drastic consequences on the fjord productivity. Sejr et al. (2022) described that run-off influences the balance between autotrophic and heterotrophic processes in fjords, showing that the inner fjord was characterised by a net community heterotrophic metabolism. I also showed that the fjord gradient affects the ability of kelps to maintain a positive net carbon balance, their nutritional value as well as their elemental cycling (**publication II, V**). In **publication V**, I modelled the potential maximum distribution of kelps, finding a clear increase in depth with increasing distance to the run-off inflow. In a follow up study to **publication V**, I plan to conduct an *in-situ* monitoring study on kelp and fucoid species productivity along the environmental changes of the fjord gradient, as well as changes in the biodiversity of macroalgal ecosystems. To conduct this study, we chose Woodfjorden in northern Svalbard, being a relatively large fjord system with steep environmental gradients and a high degree of cryosphere loss.

On a larger scale, i.e., comparing the environmental conditions of the study sites for publications of this dissertation, I found the fjords to greatly vary in their PAR × temperature interaction (**Figure 7.4B**). Nuup Kangerlua on Greenland, is characterised by high-PAR × cold temperatures. At the beginning of the experiment in **publication III**, F_v/F_m values of both *S. latissima* and *A. clathratum* were below the threshold of 0.6, which Dring et al. (1996) found for healthy, unstressed kelps. This indicates a high stress level inflicted by field conditions. On Svalbard, southern fjords were dominated by extensive run-off plumes from highly glaciated shorelines; hence, turbidity values were high, i.e., PAR availability was low. Further, temperatures were cold, as the fjords in southern Svalbard were influenced by the Sørkapp current carrying Arctic water masses (Konik et al. 2021). Therefore, Hornsund fjord represented low-PAR × cold temperature conditions. With increasing latitudes, the influence of the West Spitzbergen current increased, carrying warm Atlantic water masses (Cottier et al. 2010). As shorelines were not glaciated, the influence of run-off on the water column was rather low. Northern Svalbard fjord, e.g., Woodfjorden, represented high-PAR × warm temperature conditions. I found *S. latissima* to strongly respond to the environmental gradient along the Svalbard coast (**publication I**).

In the Arctic, Svalbard fjords are the most systematically studied (Cottier et al. 2010). Lebrun et al. (2022) reviewed that even though publications have increased in the past 20 years, only a small proportion of the coastline has been studied with regard to climate change effects on Arctic macroalgal communities. They found a particular emphasis on Kongsfjorden. Amongst other reasons, this can also be attributed to the level of scientific infrastructure available in Kongsfjorden (Hop and Wiencke 2019). Consequently, Kongsfjorden, being situated on the West coast of Svalbard at 78° 59' N, 11–12° E, is established as model fjord to assess Arctic ecosystem functioning and on which to base predictive models of climate changes (Hop and Wiencke 2019). Kongsfjordens' outer boundary is highly influenced by warm Atlantic water from the West

_____

Spitsbergen Current (Cottier et al. 2005), as there is no shallow sill at the entrance of the fjord (Svendsen et al. 2002). The inner part of Kongsfjorden is highly dominated by three sea-terminating glaciers: Kongsvegen, Kronebreen, and Kongsbreen discharging a massive amount of run-off into the fjord each year (Svendsen et al. 2002). I would classify the present-day Kongsfjorden as low-PAR × warm temperature fjord (**Figure 7.4B**). The strong characteristics of Kongsfjordens' boundary conditions, i.e., sill, currents, glaciers, result in a fascinating fjord system being highly variable and, therefore, of high interest to study. Further, the Svalbard region is warming at a rate about twice the Arctic average and seven times the global average (Nordli et al. 2020). Given the extreme environmental changes, Svalbard and Kongsfjorden provide systems to study the vulnerability of ecosystems towards climate change. As kelps show a high potential to be conditioned by their local environment (**publication I**) and environmental history, it is likely that Kongsfjorden is not representative for general dynamics of benthic primary producers in the Arctic. However, Kongsfjorden provides an excellent system for many studies, e.g., the effect of run-off and retreating glaciers on Arctic benthic communities. Further, the relatively high resolution of monitoring studies in Kongsfjorden during the past decades have resulted in highly valuable datasets to describe and monitor ecological changes (e.g., Düsendau et al. 2024) and compare to other fjords. Nevertheless, **to understand general Arctic benthic ecosystem functioning, the research efforts must not be limited to any geographical scale, but rather aim for a pan-Arctic approach**. The comparison I conducted in **Figure 7.4B** is only based on spatial and temporal point measurements, not reflecting the whole fjord. Nevertheless, it shows that while characteristics such as latitude can function as linear predictor for certain aspects of the fjord environments, e.g., photoperiod, it is difficult for others, e.g., temperature. Woodfjorden, the northern-most fjord of this comparison, was characterised by highest temperatures. **"Borealisation" of fjords is mostly determined by outer boundary conditions and not a mere function of latitude**. The high spatial variability makes it complicated to compare fjords.

I am part of an author team, working on the development of a holistic approach to compare primary producer dynamics across present-day fjords. Given their essential ecological role, we focus on kelps and phytoplankton. We use the main driver of kelps and phytoplankton to create a two-dimensional niche model for each group (similar to **Figure 8.1**). To compare their dynamics across fjords, we include the abiotic conditions in fjord in the two-dimensional niche mode. As main drivers for the spatial distribution and responses of kelps we use the prevailing temperature × PAR intensity in fjords. For phytoplankton, we use the prevailing nutrient concentrations × PAR intensity. Based on this work, we suggest two aspects of become highest priority for future research efforts: 1) the establishment of comparable sampling and monitoring methods, and 2) the establishment of year-round monitoring stations representing the fjord gradient, e.g., by monitoring an inner and an outer fjord station.

7.2.3 ...future trajectories

In the following section, I will elaborate on near-future temporal implications of my findings and discuss how Arctic kelp forests might develop (**Figure 7.5**). I base my extrapolations on climate projections for the Svalbard region. It should be noted that climate projections are simplified models based on past changes. The use of linear trends is under debate, as developments are not necessarily linear and rapid changes and extreme events might be masked (Benestadt et al. 2003). While chronic climatic changes are a among the major drivers for global biodiversity alterations and loss (Pereira et al. 2012) and the biogeographical range shift of species (Wilson et al. 2019), sudden extreme events are a more immediate and rapid threat (Filbee-Dexter et al. 2020; Matich et al. 2020). Marine heatwaves (*sensu* Hobday et al. 2016) have been found to cause a mass mortality of kelps and trigger coastal ecosystem regime shifts (Filbee-Dexter et al. 2020). In **publication III**, I found no direct negative effect of marine heatwaves on cold-temperate kelps in the Arctic, on the contrary, warmer temperatures increased kelp performance under high-light stress. Hence, compared to lower latitudes, I assume that destructive effects of Arctic marine heatwaves are not an immediate threat for Arctic kelp forests in the near future, as temperatures do not become supraoptimal for cold-temperate species. Nevertheless, marine heatwaves can cause ecological changes in the Arctic, e.g., the (local) extinction of cryophilic species (Bringloe et al. 2022), or the introduction of warmer adapted species, changing interspecific competition balances. While marine heatwave effects have recently been subject for many studies, less attention has been given to the effect of marine cold-spells (Schlegel et al. 2021), even though they can also lead to high mortality rates and ecosystem changes (Matich et al. 2020). Mora-Soto et al. (2022) have described a positive effect of marine cold-spells on *Macrocystis pyrifera* in southwestern Patagonia, suggesting that these areas might serve as refugia during global warming. Marine cold spells in the Arctic might cause sea ice to form and shift (Meredith et al. 2019), changing the PAR availability and increase ice scouring, shaping the extent and distribution of kelps (Krause-Jensen et al. 2012). A further major risk of ongoing climate change is the passing of tipping points (Lenton et al. 2023), which is also not considered in linear climate projections. One potential tipping point concerns the Atlantic Meridional Overturning Circulation (AMOC), being a part of the global thermohaline circulation, which transports warm water from lower to higher latitudes. As described in **chapter 1.1**, these water masses sink down in the Arctic Ocean, when their density has increased due to cooling and a high salinity. A freshening of the Arctic due to rain and meltwater run-off has weakening effects on the AMOC (salt transport feedback) and the AMOC might eventually break down (AMOC tipping point; Rahmstorf 2024). A collapse of the AMOC would have drastic consequences on a global scale (Lenton et al. 2023). Given our limited understanding on ecosystems resilience and recovery times, predicting populations and ecosystems responses to rapid changes is difficult (Butt et al. 2016). The following discussion is

based on gradual environmental changes in kelp forests. Based on future atmospheric temperature (Hanssen-Bauer et al. 2019; Rantanen et al. 2022) and run-off (Hanssen-Bauer et al. 2019) projections for Svalbard, I arranged five scenarios of different temperature × PAR interactions in fjords along the time scale from 1980–2100 (**Figure 7.5**; 1–5). Note that the rate of change between sequence and stage of cryosphere loss is not (necessarily) to scale. My extrapolations of biological change assume that climatic changes outpace the adaptive capacity of kelps, as suggested by Vranken et al. (2021). Consequently, I assume that performance curves of future kelps are similar to those found in my studies, not referring to a specific geographical region. Further, I want to highlight that the discussion of potential interspecific shifts of competition balances are based on variations in the performance of sporophytes. Different tolerances and performances of early life stages and possible consequences for their reproductive capacity and interspecific competition are only conceptually mentioned in this chapter.
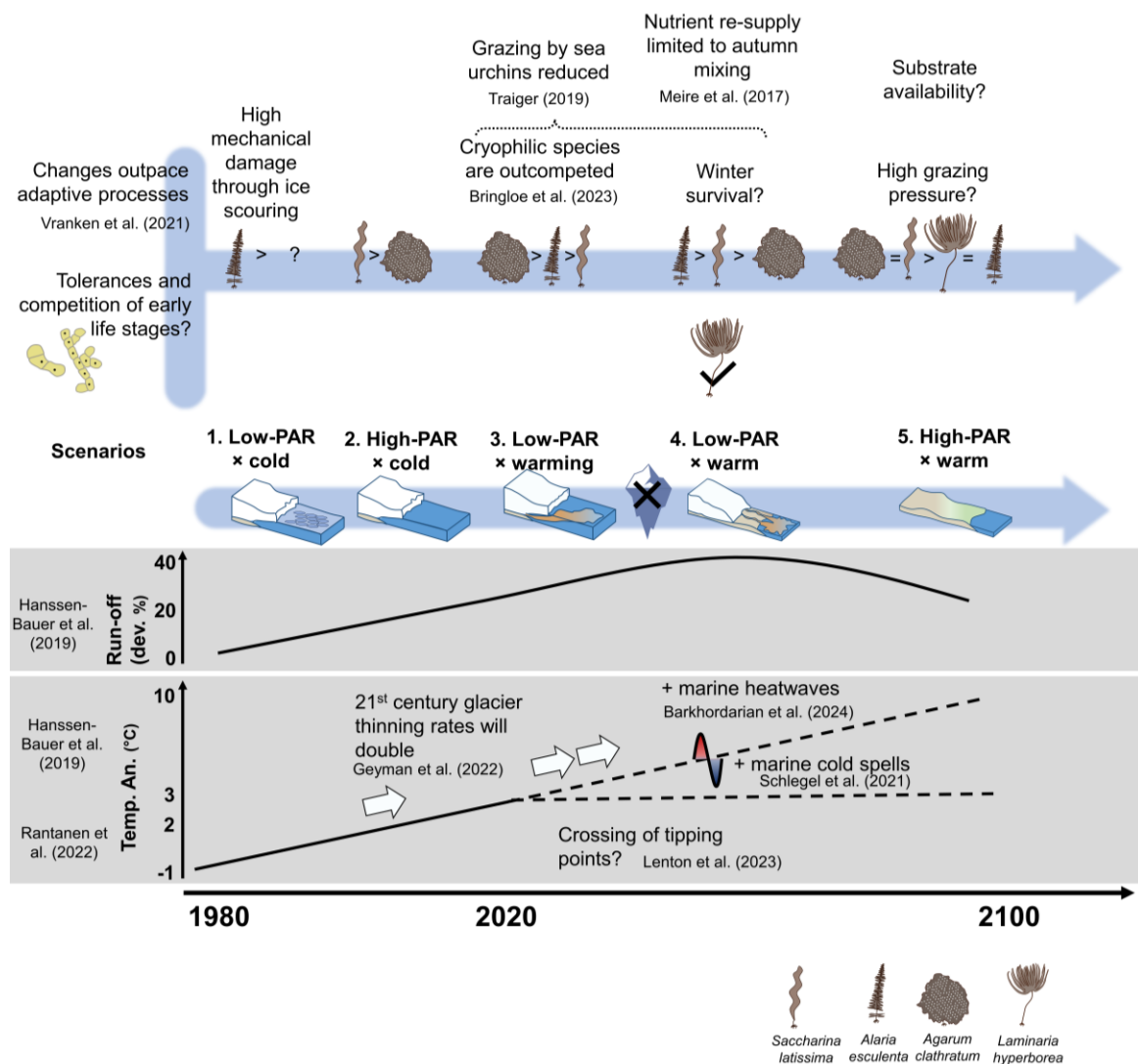
Figure 7.5: Projections of kelp performance until 2100. Annual atmospheric mean temperature anomaly (°C) trend relative to 1980-2010 in the Arctic (66.5–90°N) from 1980–2020 after Rantanen et al. (2022). Depending on the emission scenario, the average increase of the atmospheric annual mean temperature

_____

anomaly is between 3–10°C by 2100 (Hanssen-Bauer et al. 2019). Marine heatwaves (Barkhordarian et al. 2024) and cold spells (Schlegel et al. 2021) will act upon the gradual temperature increase. The crossing of tipping points is unknown (Lenton et al. 2023). Mean annual run-off projections for the river Longyearelva, Svbalbard, are noted in deviation (%) from 1971-2000 as reference period (Hanssen-Bauer et al. 2019). As response to climate projections, a doubling of the glacier thinning rates is projected until 2100, compared to 1936-2010 (Geyman et al. 2022). Based on that I categorised five scenarios of fjords with different stages of cryosphere loss on the time scale. Note that present-day spatial variations represent many of the depicted scenarios (**chapter 7.2.2**). Note that the rate of change between scenarios is schematic and not (necessarily) to scale. Provided that adaptive processes will not change the sporophytes performance curve in the future (Vranken et al. 2021) and neglecting possible change of the competition balance between early life stages, I displayed potential changes of interspecific competition balances between target kelp species of this study, not referring to a specific geographical region.

Scenario 1. Low-PAR × cold. Until the 1980s, Arctic fjords were generally characterised by cold temperatures (Rantanen et al. 2022) and low-PAR availabilities, as extensive sea ice cover during the photoperiod reduced the PAR availability in the water column drastically. When sea ice is covered with snow, the reduction of PAR is even greater and can be less than 2% of the surface irradiance (Wiencke et al. 2006). I did not detect high physiological stress levels in kelps being exposed to cold temperature in combination with low-PAR availabilities, even though photosynthetic rates and the total carbon content were low (**publication I, III, V**), limiting their depth distribution. Krause-Jensen et al. (2012) reported that low annual PAR availabilities might have restrictive consequences on the kelps' maximum distribution depth and productivity. Further, sea ice and ice berg scraping causes mechanical damage to the benthic community in the subtidal area (Krause-Jensen et al. 2012). Keats et al. (1985) reported *A. esculenta* to have a high recolonising potential of ice-scoured areas. Even though not being part of the studies of this dissertation, I expect *Laminaria solidungula* to be a strong competitor, being the only Arctic endemic kelp (Wilce and Dunton 2014).

Scenario 2. High-PAR × cold. Since the 1980s, the rate of climatic changes in the Arctic is faster compared to the global average (Arctic amplification; Rantanen et al. 2022). Warming temperatures have resulted in a thinning of sea ice and a longer period of open water days (Ivanov 2023). This increases the PAR transmission through the water column (Nicolaus et al. 2012; Payne and Roesler 2019), i.e., high-PAR stress in cold-temperate kelps (**publication III, IV**). To reduce high-PAR stress, I expect kelps to have reduced their light-harvesting complex and increased their antioxidant content. Nevertheless, productivity would have increased and a shift in the realised niche would have caused the expansion of the kelp forest to deeper waters (Krause-Jensen et al. 2012). While both *A. clathratum* and *S. latissima* showed a high physiological stress level at high-PAR availabilities × cold temperatures, the performance of *A. clathratum* was significantly lower compared to *S. latissima*. I would, therefore, categorise *A. clathratum* as a weak interspecific

competitor when being exposed to high-PAR availabilities. Gagnon et al. (2005) confirmed this by reporting *A. clathratum* as weak interspecific competitor in shallow waters.

Scenario 3. Low-PAR × warming. For Svalbard, the average increase of the annual mean atmospheric temperature is projected to be between 3–10°C by 2100 (Hanssen-Bauer et al. 2019), as a response to climate forcings, climate feedbacks and changes in the poleward energy transport (**chapter 1.3.1**; Previdi et al. 2021). The recent warming rates have been linked to an accelerated glacier loss (Hugonnet et al. 2021). Geyman et al. (2022) have predicted the rate of glacier thinning on Svalbard to double by 2100 compared to the time period of 1936–2010. With glaciers melting, the run-off increases, carrying high concentrations of suspended particles. As discussed in **chapter 7.1.2**, sediment plumes have severe consequences on the PAR availability, reducing the PAR intensity and causing a shift of the spectrum peak to longer wavelengths (**publication I, II, V**). While this reduces the high-light stress in kelps, low-PAR availabilities also reduce their productivity (Blain et al. 2021). As Arctic regions are characterised by long periods of darkness during Polar Night (Gattuso et al. 2020), the photosynthetic period is restricted to summer months. The cumulative annual irradiance has to be at a minimum of 49 mol photons m^{-2} yr^{-1} (Castro de la Guardia et al. 2023) for kelps to establish a stable population. With the PAR intensity being reduced in summer months by run-off plumes dominating the fjords, large areas are falling below that threshold, and habitat is lost for kelps. Consequently, the maximum distribution depth of kelps will be shallower near the run-off inflow, and deepen with increasing distance (**publication V**). Bartsch et al. (2008) and Düsedau et al. (2024) monitored the upward shift of the Svalbard kelp forest in a 25-year time series, comparing the maximum extent and species composition from 1996–1998 to 2016 and 2021, confirming a shoaling of the kelp forest. In future Greenlandic kelp forests, I consider *A. clathratum* as strong interspecific competitor at low-PAR intensities, as I found the species to be low-light adapted (**publication III**). In **publication V**, I found that *A. esculenta* had a lower compensation irradiance at low-PAR intensities and a significantly higher carbon content compared to *S. latissima*, implying that *A. esculenta* grows deeper in the water column. This extrapolation was confirmed by an *in-situ* monitoring of Düsedau et al. (2024). The thermal optimum of *A. esculenta* is lower than that of *S. latissima* (Bolton and Lüning 1982; Munda and Lüning 1977), indicating that it has an overall performance advantage at cold temperatures (Wahl et al. 2020). Interestingly, the Arctic endemic kelp species *L. solidungula* has neither been found in extensive surveys in Kongsfjorden, Svalbard in 2019 (pers. obs.) nor in 2021 (Düsedau et al. 2024), while Scheschonk et al. (2019) was able to sample it in the winter of 2016/17. Even though specimens are still occurring in (colder) Hornsund (pers. obs. 2022), it highlights the findings of Bringloe et al. (2022), reporting that cryophilic kelp species might be outcompeted in a warming future Arctic.

Scenario 4. Low-PAR × warm. When the temperatures continue to rise, sea-terminating glaciers retreat on land and the re-supply of nutrients is limited to autumn mixing, as subglacial upwelling is stopping (Meire et al. 2017). Depending on the species, warmer temperatures during Polar Day reduced the carbon balance, e.g., by an increase in dark respiration (*A. clathratum* > *S. latissima* > *A. esculenta*; **publication III, V**) or compensation irradiance (*A. esculenta*, **publication V**). Castro de la Guardia et al. (2023) reported the minimum PAR threshold of 49 mol photons m^{-2} yr^{-1} for an area with temperatures between -2–6°C. Hence, when temperatures rise, this minimum PAR threshold might also increase. Yanshuo et al. (2016) reported Arctic Amplification to be especially pronounced during the Polar Night. Scheschonk et al. (2019) found in an *in-situ* study that *S. latissima* uses 96 % of their storage compounds during the Polar Night on Svalbard. A reduced PAR availability in summer, in combination with warm temperatures in winter might cause a shift of the annual net carbon balance to be negative and therefore reduce the winter survival of kelps. While this might have consequences for the phenotypic plasticity of kelps (Liesner et al. 2020; see **chapter 7.2.1**), it further causes physiological changes during the Polar Night. Summers et al. (2023) found kelps to grow new tissue during the Polar Night, making use of their storage compounds and a high nutrient availability in the water column. While Gordillo et al. (2022) confirmed this experimentally for temperatures of 3°C, *S. latissima*, as well as *A. esculenta* were unable to resume growth after being exposed to 8°C during the dark period. Warming further negatively affected the ability of kelps to respond to re-illumination after the Polar Night. Gordillo et al. (2022) concluded that warming Polar Nights might cause a habitat loss in the future Arctic. In **publication IV**, *L. hyperborea* was not negatively influenced by being exposed to Polar Night warming, i.e., no significant changes in dry weight, or carbon storage compounds were detected. Additional to the interspecific competition between kelp species, grazing pressure is a further factor shaping the realised niche of kelp forests. Intense sea urchin herbivory can create barrens, stretching several thousands of kilometres (Filbee-Dexter and Scheibling 2014). Increased sedimentation rates, however, have been reported to reduce the grazing pressure from sea urchins on kelps (Traiger et al. 2019).

Scenario 5. High-PAR × warm. When glaciers have melted completely and run-off is only limited to the spring snow melt and rain run-off, sedimentation rates are also reduced. Only considering the fundamental niche of kelps, kelp forests should thrive under these conditions. However, when it comes to the realised niche, there remain many unknown parameters for this scenario. Given the reduced sedimentation rates, the grazing pressure from sea urchins might increase (Traiger et al. 2019). Porsangerfjorden in northern Norway can be classified as high-PAR × warm Arctic fjord. In July 2023, a mean of 184.5±79.3 sea urchin individuals m^{-2} were found on sea urchin barrens, which is equivalent to a biomass of 1.5±0.7 kg m^{-2}, causing drastic grazing pressure (Koch et al. in rev.). In Greenlandic kelp forests, *A. clathratum* is a very strong competitor under grazing

pressure, being generally avoided by sea urchins (Vadas 1977). On sea urchin barrens where *S. latissima* was completely absent, *A. clathratum* was regularly found in small stands (pers. obs., **Figure 7.6A**). In Ameralik fjord, being close to Nuup Kangerlua, Greenland, *A. clathratum* was found to completely dominate the kelp forest, even in shallower waters, becoming dominant over *S. latissima* (pers. com. T. Vonnahme). A further unknown parameter for future Arctic kelp forest extent, is the availability of hard substrate. The high concentration of suspended particles in the run-off plumes eventually sink down and cover kelps, as well as the hard substrate, filling up the fjord basin. The glacier in Petuniabukta (Billefjorden, Svalbard) has already completely retreated. Compared to neighbouring and sea-terminating glacier dominated Adolfbukta, the maximum water depth in Petuniabukta is approx. 100 m shallower, likely due to glacial sediment deposits (**Figure 7.6B**; Strzelecki et al. 2015). The higher proportion of soft sediment in Petuniabukta and, therefore, reduced suitable hard substrate is likely to be a reason for the significantly reduced coverage of kelps compared to the newly exposed hard substrate in Adolfbukta (Gonzalez Triginer et al. in rev). *S. latissima* might have a competitive advantage in areas with generally soft sediment, as it can grow on gravel (**Figure 7.6C**; Diehl et al. 2024).
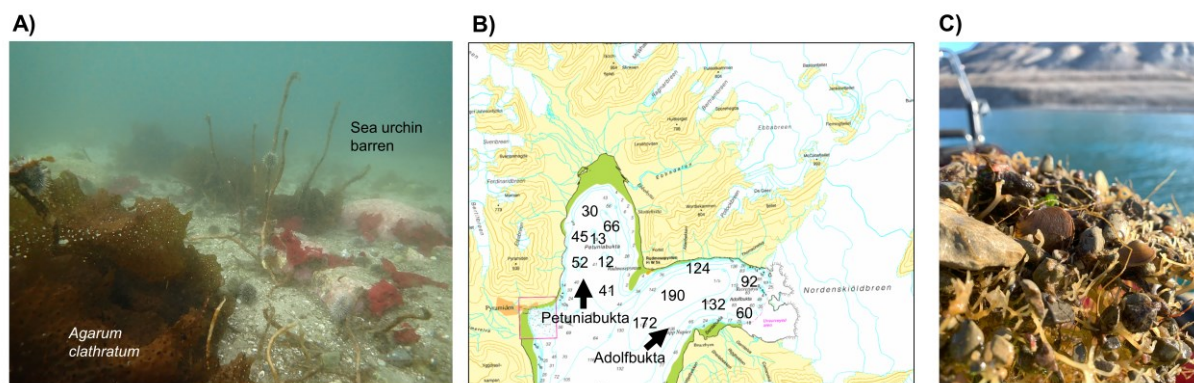
Figure 7.6: **A)** Sea urchin barren in Nuup Kangerlua near Nuuk in June 2023. While all other kelps are being grazed on, *A. clathratum* remains in small stands. © Sarina Niedzwiedz. **B)** Map of Billefjorden, Svalbard. The glacier has retreated from Petuniabukta, leaving it shallower compared to glacier dominated and relatively newly exposed Adolfbukta. Nautical map accessed on accessed 21.06.2024; https://toposvalbard.npolar.no/?lat=78.69640&long=16.87498&zoom=6&layer=map **C)** Rhizoid of sampled *Saccharina latissima* from Billefjorden, Svalbard in August 2022, being attached to gravel. © Sarina Niedzwiedz.

To maintain a stable population despite environmental changes, kelps have to complete their entire life cycle; hence, environmental conditions have to be tolerable for the diplontic, as well as the haplontic stage (**Figure 1.2**). Generally, early life stages of kelps have to be low-PAR adapted, as they grow in the understory of the kelp forest (Laeseke et al. 2019). Coelho et al. (2020) describe a high vulnerability of early life stages of kelps towards climate change related stressors, e.g., warming, increased storm frequencies or pollution, having negative effects on their fertility

and development. Martins et al. (2017) have shown different thermal optima for different life cycle stages and transitions. While Park et al. (2017) have found the gametophytes of *S. latissima* and *A. esculenta* to be able to survive, grow and reproduce when Arctic summer waters reach 10°C, Silva et al. (2022) reported a reduced sexual reproduction when gematophytes were exposed to 9°C instead of 5°C. This difference in response might be due to photoperiod, as it was shown to control gametophyte growth and reproductive success (Martins et al. 2022). While Park et al. (2017) maintained cultures in a 12:12 h L:D cycle, Silva et al. (2022) exposed them to 24:0 h L:D. Gametophytes of *A. esculenta* and *Laminaria digitata* survived long periods of darkness mimicking Polar Night (Silva et al. 2022), though showing species-specific characteristics of reproduction. Additional to temperature × PAR effects on kelps early life stages, Zacher et al. (2016) found detrimental effects as response to increased sedimentation rates, inhibiting sporophyte formation. They found the response to be strongly species-specific, with *A. esculenta* being the only species forming sporophytes under highest sedimentation rates. As many studies focus on the impact of (multiple interacting) drivers on sporophytes, it is essential to improve our understanding of how early life stages will react to drivers to be able to make predictions on future Arctic kelp forest developments (Farrugia Drakard et al. 2023).

Concluding, Krause-Jensen et al. (2012) found sea ice cover a good predictor to explain macrophyte presence along Arctic coasts. I argue that **in near-future fjords, the intensity and extent of sediment plumes serves as integrative predictor for kelp forest distribution in Arctic fjords**. The period of glacial retreat is likely the period during which the rate of environmental changes is highest. **Once the glaciers have melted, the environment in fjord systems is likely to stabilise and a different stable ecosystem state will emerge**.

7.3 Global patterns of change in kelp forests

Anthropogenic climate change is of global consequence, leading to worldwide changes in biodiversity, shifts of species' biogeographical distribution patterns, and, therefore, potential disruptions of ecosystem services (Pecl et al. 2017). The effects of environmental changes become most obvious at the tolerance limits of a species. Massive kelp forest losses have been monitored at their warm distribution margin in response to overall rising temperatures and marine heatwaves (e.g., Wernberg et al. 2013; Smale 2019; Filbee-Dexter et al. 2020; Smith 2023), which were replaced by low-productive filamentous algae (turf; Filbee-Dexter et al. 2020). At their cold-distribution margin, warming temperatures are expected to lead to an increase of kelp habitat (Filbee-Dexter et al. 2019; Manca et al. 2024), even though prevailing PAR availabilities might locally oppose this trend (**publication V**).

As kelps take up and store carbon, their global importance has been recognised due to their contribution to sequestration and long-term storage of carbon (blue carbon; Krause-Jensen et al. 2022). Their carbon storage potential has made kelp ecosystems relevant to mitigate the effect of CO_2-driven climate change. However, the blue carbon contribution of kelp forests is currently under debate. While Gallagher et al. (2022) stated that seaweed ecosystems are a net source of carbon due to consumption and release, Filbee-Dexter et al. (2023) disagreed and provided evidence that kelp ecosystems are a net sink of carbon due to high photosynthetic rates. The contribution of kelps to long-term carbon storage is difficult to quantify (Pedersen et al. 2020), as macroalgae have a relatively short life-span and a large proportion of their biomass enters the trophic food web. There are three established pathways of kelps to contribute to long-term carbon sequestration: As kelps require hard substrate to grow, their sequestered carbon cannot be directly buried, hence, it has to be exported to either 1) sediments, or 2) the deep ocean to be buried. Further, 3) the excretion of fucoidan has been proposed to contribute an underestimated proportion to the carbon export of kelp forests (Buck-Wiese et al. 2023). Based on *in-situ* measurements of the net primary production of seaweeds, Pessarrodona et al. (2022) reported highest production rates at temperate latitudes, however, with increasing export rates towards higher latitudes. The projected emergence of new kelps ecosystems in Arctic regions and temperature-induced increases in seaweed productivity, leads to the assumption that the blue carbon contribution of kelp forest ecosystems can be expected to increase. However, as limited PAR and substrate availability have the potential to oppose Arctic kelp expansion (**chapter 7.2.3**), it also opposes the potential of carbon sequestration of Arctic kelp ecosystems. Blain et al. (2021) confirmed this by reporting that increased turbidity in Arctic fjords leads to a drastic reduction of productivity and, therefore, the potential for blue carbon sequestration in near future. Further, a shift of the species composition was reported to reduce the ecosystems carbon sequestration

_____

(Wright et al. 2022). The contribution of emerging Arctic ecosystems remains subject to current research, e.g., of the recently started EU-project SEA-Quester (Grid Arendal 2024).

Considering global patterns of marine macrophyte dynamics, Manca et al. (2024) reported a substantial habitat loss and a reduction of the current biogeographical extent by 5–6 % until 2100. Hence, the global carbon sequestration of wild kelp forests is likely to decline in near-future (Wright et al. 2022). To enhance carbon sequestration, Gao et al. (2022) suggest the cultivation and harvest of kelps might be an efficient approach. They argue that possible nutrient limitations of the growth of kelps might be overcome by artificial upwelling or the implementation of integrated multi-trophic aquacultures. The carbon of the kelps' biomass could be sequestered if the harvested kelps were buried or transformed to biochar. Biochar is a carbonaceous material that is sustainable with several applications, e.g., as soil fertiliser, for wastewater treatment, potential supercapacitor materials, or act as catalyst (support) (Sun et al. 2022).

Discussing the blue carbon potential of kelp forests in climate change mitigation, **I argue that the blue-carbon-contribution of the secondary production being supported by kelp forests has to be considered**. Being at the basis of the food web and providing habitat for hundreds of associated species (Christie et al. 2003), a large proportion of invertebrates, fish and mammal stocks depend on them. Their export to deep-waters is a significant part of the biological carbon pump and therefore contributes to long-term carbon sequestration (Pershing et al. 2010). Apart from the kelps' ecosystem carbon sequestration, their functioning and maintenance of high biodiversity are of great ecological and economical value (Eger et al. 2023).

7.4   Socio-economic implications

Overall, the Arctic is sparsely populated, and has experienced a net negative migration between 2000-2010, followed by a demographic shift, which is i.a. attributed to the lack of economic opportunities (Larsen and Fondahl 2014). The impacts of climate change are reported to have both positive and negative impacts on Arctic local livelihoods, e.g., the reduced cover and thickness of sea ice could increase the accessibility to the shorelines, but also increase coastal erosion (Larsen and Fondahl 2014). Further, ecological shifts, globalisation and industrial development cause changes in resource availability and local livelihood (Fauchald et al. 2017). The resources of the ocean, including seaweeds, have always been part of the livelihood for Arctic indigenous peoples, e.g., as food source or for pharmaceutical purposes (Rapinski et al. 2018).

Globally, over two billion people are expected to face food insecurity as a consequence of anthropogenic and climatic changes (Cavallo et al. 2021). As Arctic regions are becoming tolerable for temperate seaweeds, the implementation of high-latitude kelp maricultures has lately been

_____

discussed (Kreissig et al. 2021). Traditionally, seaweeds have been wild-harvested (Sæther et al. 2024). Given the crucial and central ecological role of kelps and the global threat, the wild harvest of kelps is controversially discussed (Sæther et al. 2024). Industrial kelp farming and the upscaling of biomass for food and other applications might provide a sustainable method for Arctic livelihood possibilities. Therefore, it is subject of current research; for example, the Greenlandic company "Royal Greenland" has recently received funding to further develop and upscale seaweed production in Greenland (Lindstrøm 2024). In **publication II**, I discussed that the potential of kelps for biosorption of heavy metals from run-off has to be considered in the implementation of Arctic kelp maricultures. High contents of harmful elements (e.g., mercury, cadmium) in kelps growing along run-off dominated coastlines might be passed on to humans. Overall, Kreissig et al. (2021) classified Arctic kelps as promising future food source.

Apart from farming kelps (in the Arctic) for future food provision, the high biosorption potential of kelps for heavy metals also has advantages. It can offer an eco-friendly, cheap method to decontaminate waste waters, serving as biomitigation measure (Zeraatkar et al. 2016). Additionally, in **publication II** I discuss the possibility to use kelps to extract rare earth elements from the water column (phytoming). Rare earth elements are increasingly used for key technologies, e.g., renewable energies or electronics (Costa et al. 2020). Though being species-specific, Costa et al. (2020) and Pinto et al. (2020) highlight macroalgae as universal biosorbant for rare earth elements.

The general and local technical applicability of these socio-economic approaches, as well as their ecological impact has to be closely assessed to evaluate risks and possibilities.

_____

8   Conclusions and

research perspectives in Arctic kelp ecology

The concept of the fundamental thermal niche is a straightforward approach to model the future biogeographical distribution and responses of a species to climate change. A species is expected to survive and establish a population when temperatures are above its lower thermal tolerance limit, with increasing performances until the species' thermal optimum is reached. The studies of my doctoral thesis conclusively confirmed that PAR availability restricts the thermal niche, resulting in a schematic two-dimensional model of the fundamental niche for Arctic kelp populations (**Figure 8.1**). I showed that low-PAR availabilities resulted in a reduced carbon gain, having the potential to result in a negative annual carbon balance. This effect was enhanced, when low-PAR availabilities interacted with warm temperatures. I further showed that high-PAR availabilities had detrimental effects on the survival of kelps, which was enhanced in the interaction with cold temperatures. While I observed this response pattern across all studies, I also detected performance variation between kelp species (interspecific). Further, I found that kelp populations were conditioned by their local environment having the potential to result in performace variation between the populations of a single species (intraspecific).
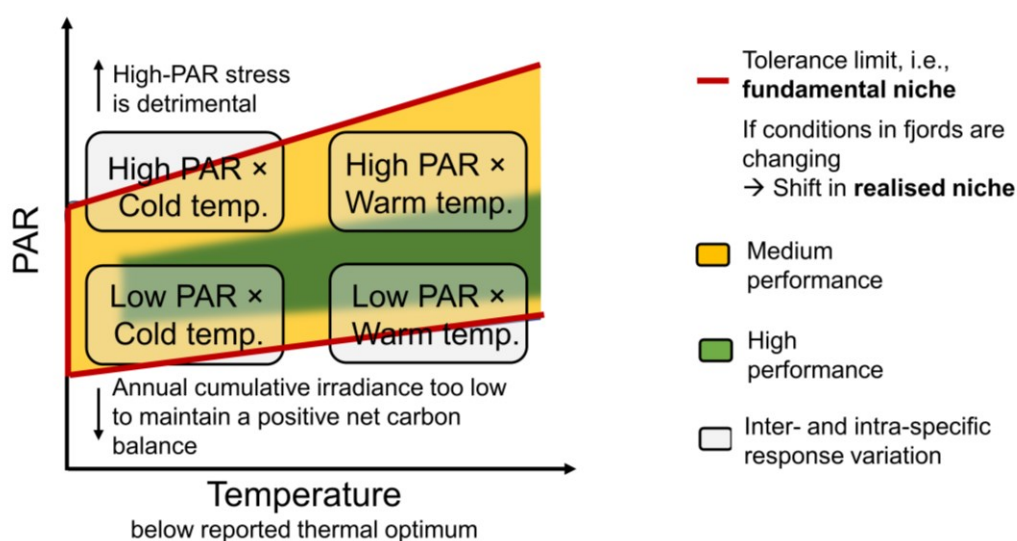
Figure 8.1: Schematic two-dimensional model of the fundamental niche for kelp species in the Arctic, based on performance differences towards temperature × PAR interactions that were investigated in the studies of this doctoral thesis. X-axis: temperatures below the reported thermal optimum of kelp species (investigated range: 3–11°C). Y-axis: Photosynthetically active radiation (PAR) availability (investigated range: 3–120 µmol photons m^{-2} s^{-1}; 24:0 h light:dark). Red line: tolerance limit. Yellow area: medium performance. Green area: high performance. Boxes: inter- and intra-specific performance variability. Climate-change-induced shifts in abiotic conditions of fjords have consequences on the realised niche of kelps in the Arctic.

The boundaries of the fundamental niche have consequences for the realised niche of Arctic kelp forests during climate change, as temperature and PAR availabilities are changing drastically in near future Arctic fjords. Low-PAR (× warm temperature) conditions restrict the vertical extent of the kelp forest in the water column. High-PAR (× cold temperature) conditions restrict the poleward latitudinal spread of kelps. I expect the highest rate of environmental change while glaciers retreat, leading to a dynamic response of kelp forest ecosystems. When Arctic fjords are free of glaciers, I expect abiotic conditions to stabelise and the establishment of alternative ecosystems. The species composition and services of kelp ecosystems depend on the relative position of the conditions in the fjords to the fundamental niche of kelps.

While the studies of this thesis contributed to the knowledge of Arctic kelp forest dynamics and functioning, there remain many unresolved aspects with respect to Arctic kelp ecology. Based on the findings presented in my dissertation, I consider the following three topics as priorities to increase the understanding of Arctic kelp ecosystem dynamics.

1) **Substrate availability**. I investigated the immediate consequences of run-off on the physiology and biochemistry of kelp sporophytes, i.e., the effects of changing PAR availabilities and elemental composition. However, the high concentrations of suspended particles in run-off are drastically increasing sedimentation rates, covering kelp as well as hard substrate in the long-term. Consequently, the potential reduction of hard substrate would limit Arctic kelp forest expansion in future, even if abiotic conditions would otherwise allow the establishment of kelp forests. To improve models on the extent of future Arctic and global kelp forests, research efforts have to integrate habitat loss due to sedimentation rates, i.e., the area of hard substrate that will be covered by soft sediment in the near future. I propose experiments assessing the tolerance of the kelps towards increased sedimentation rates, as well as the development of models predicting the future loss of hard substrate along Arctic coastlines.

2) **Early life stages**. In my studies, I investigated the performance and tolerance of adult kelp sporophytes. However, to establish stable populations, environmental conditions must allow kelps to fulfil their entire life cycle. *In-situ* monitoring studies integrate the life cycle component, as kelp forests would not prevail if conditions were not tolerable for microscopic and early life stages. However, as this is only an indirect extrapolation, I propose a specifically designed multiple stressor experiment with kelp gametophytes, monitoring their reproductive success under varying PAR × temperature interactions. Studies on interspecific fitness differences over consecutive life stages would further contribute significantly to the knowledge of kelp species composition in future Arctic kelp forests.

_____

3) **Space-for-time-substitution**. As present-day Arctic fjords are characterised by different stages of cryosphere loss, ecological processes in fjords with a later stage of cryosphere loss might serve as template for future fjords. However, we have to be able to systematically compare fjord systems to draw the right conclusions, which provides challenges given the high variability in boundary conditions and abiotic factors ampng fjords. Studies of my doctoral thesis, as well as other recent publications, concluded that PAR × temperature interactions serve as good predictor for the realised niche of Arctic kelps and their spatial extent. Therefore, I propose the implementation of long-term *in-situ* monitoring sites in different Arctic fjords. I suggest (at least) one station of PAR and temperature measurements in the inner fjord and one in the outer fjord to cover the fjord gradient.

Kelp forests in Arctic fjords provide the basis for higher trophic levels, contribute to the biological sink of carbon in the ocean and, in some cases, are also crucial for local livelihoods and food provision. Hence, their response to environmental changes has cascading ecological and economic consequences. With this dissertation, I contributed to the knowledge of the boundaries of the fundamental and realised niche of Arctic kelp forests, assessing the drivers of their distribution. The continuation of this research is of high relevance in the light of rapidly changing environmental conditions in the Arctic.

9   Reference list for synoptic chapters

Araújo RM, Assis J, Aguillar R, Airoldi L, Bárbara I, Bartsch I, Bekkby T, Christie H, Davoult D, Derrien-Courtel S, Fernandez C, Fredriksen S, Gevart F, Gundersen H, Le Gal A, Lévêque L, Mieszkowska N, Norderhaug KM, Oliveira P, Puente A, Rico JM, Rinde E, Schubert H, Strain EM, Valero M, Viard F, Sousa-Pinto I (**2016**) Status, trends and drivers of kelp forests in Europe: an expert assessment. *Biodiversity and Conservation.* 25, 1319–1348. Doi: 10.1007/s10531-016-1141-7

Ardyna M, Arrigo KR (**2020**) Phytoplankton dynamics in a changing Arctic Ocean. *Nature Climate Change.* 10, 892–903. Doi: 10.1038/s41558-020-0905-y

Ash C, Stone R (**2003**) A question of dose. *Science.* 300, 925. Doi: 10.1126/science.300.5621.925

Assis J, Serrão E, Duarte CM, Fragkopoulou E, Krause-Jensen D (**2022**) Major expansion of marine forests in a warmer Arctic. *Frontiers in Marine Science.* 9:850368. Doi: 10.3389/fmars.2022.850368

Atkinson MJ, Smith SV (**1983**) C:N:P ratios of benthic marine plants. *Limnology and Oceanography.* 28, 568–574. Doi: 10.4319/lo.1983.28.3.0568

Attard K, Singh RK, Gattuso J-P, Filbee-Dexter K, Krause-Jensen D, Kühl M, Sejr MK, Archambault P, Babin M, Bélanger S, Berg P, Glud RN, Hancke K, Jänicke S, Qin J, Rysgaard S, Sørensen EB, Tachon F, Wenzhöfer F, Ardyna M (**2024**) Seafloor primary production in a changing Arctic Ocean. *Proceedings of the National Academy of Science.* 121, e2303366121. Doi: 10.1073/pnas.2303366121

Barkhordarian A, Nielsen DM, Olonscheck D, Baehr J (**2024**) Arctic marine heatwaves forced by greenhouse gases and triggered by abrupt sea-ice melt. *Communications Earth & Environment.* 5, 57. Doi: 10.1038/s43247-024-01215-y

Bartsch I, Wiencke C, Bischof K, Buchholz C, Buck BH, Eggert A, Feuerpfeil P, Hanelt D, Jacobsen S, Karez R, Karsten U, Molis M, Roleda MY, Schubert H, Schumann R, Valentin K, Weinberger F, Wiese J (**2008**) The genus *Laminaria sensu lato*: recent insights and developments. *European Journal of Phycology.* 43, 1–86. Doi: 10.1080/09670260701711376

Bartsch I, Paar M, Fredriksen S, Schwanitz M, Daniel C, Hop H, Wiencke C (**2016**) Changes in kelp forest biomass and depth distribution in Kongsfjorden, Svalbard, between 1996–1998 and 2012–2014 reflect Arctic warming. *Polar Biology.* 39, 2021–2036. Doi: 10.1007/s00300-015-1870-1

Bass AV, Smith KE, Smale DA (**2023**) Marine heatwaves and decreased light availability interact to erode the ecophysiological performance of habitat-forming kelp species. *Phycological Society of America.* 59, 481–495. Doi: 10.1111/jpy.13332

Benestad RE (**2003**) What can present climate models tell us about climate change? *Climatic Change* 59, 311 331. Doi: 10.1023/A:1024876611259

Bengtsson MM, Sjøtun K, Ørvås L (**2010**) Seasonal dynamics of bacterial biofilms on the kelp *Laminaria hyperborea. Aquatic Microbial Ecology.* 60, 71–83. Doi: 10.3354/ame01409

Bennett S, Duarte CM, Marbà N, Wernberg T (**2019**) Integrating within-species variation in thermal physiology into climate change ecology. *Philosophical Transactions of the Royal Society B.* 374, 20180550. Doi: 10.1098/rstb.2018.0550

Bintanja R, Andry O (**2017**) Towards a rain-dominated Arctic. *Nature Climate Change*. 7, 263–268. Doi: 10.1038/nclimate3240

Bintanja R (**2018**) The impact of Arctic warming on increased rainfall. *Scientific Reports*. 8, 16001. Doi: 10.1038/s41598-018-34450-3

Bischof K, Rautenberger R (**2012**) Seaweed responses to environmental stress: reactive oxygen and antioxidant strategies. In: Wiencke C, Bischof K (eds.) Seaweed Biology. Springer Verlag Berlin-Heidelberg.

Blain CO, Hansen SC, Shears NT (**2021**) Coastal darkening substantially limits the contribution of kelp to coastal carbon cycles. *Global Change Biology*. 27, 5547–5563. Doi: 10.1111/gcb.15837

Bluhm BA, Brown K, Rotermund L, Williams W, Danielsen S, Carmack EC (**2022**) New distribution records of kelp in the Kitikmeot Region, Northwest Passage, Canada, fill a pan-Arctic gap. *Polar Biology*. 45, 719–736. Doi: 10.1007/s00300-022-03007-6

Bolton JJ, Lüning K (**1982**) Optimal growth and maximal survival temperatures of Atlantic *Laminaria* species (Phaeophyta) in culture. *Marine Biology*. 66, 89–94. Doi: 10.1007/BF00397259

Bridle JR, Vines TH (**2006**) Limits to evolution at range margins: when and why does adaptation fail? *Trends in Ecology and Evolution*. 22, 140–147. Doi: 10.1016/j.tree.2006.11.002

Bringloe TT, Starko S, Wade RM, Vieira C, Kawai H, De Clerck O, Cock JM, Coelho SM, Destombe C, Valero M, Neiva J, Pearson GA, Faugeron S, Serrão E, Verbruggen H (**2020**) Phylogeny and evolution of brown algae. *Critical Reviews in Plant Science*. 1–41. Doi: 10.1080/07352689.2020.1787679

Bringloe TT, Wilkinson DP, Goldsmit J, Savoie AM, Filbee-Dexter K, Macgregor KA, Howland KL, McKindsey CW, Verbruggen H (**2022**) Arctic marine forest distribution models showcase potentially severe habitat losses for cryophilic species under climate change. *Global Change Biology*. 28, 3711–3727. Doi: 10.1111/gcb.16142

Buck-Wiese H, Andskog MA, Nguyen NP, Bligh M, Asmala E, Vidal-Melgosa S, Liebeke M, Gustafsson C, Hehemann J-H (**2023**) Fucoid brown algae inject fucoidan carbon into the ocean. *Proceedings of the National Academy of Science*. 120, e2210561119. Doi: 10.1073/pnas.2210561119

Burgunter-Delamare B, Rousvoal S, Legeay E, Tanguy G, Fredriksen S, Boyen C, Dittami SM (**2023**) The *Saccharina latissima* microbiome: effects of region, season, and physiology. *Frontiers in Microbiology*. 13, 1050939. Doi: 10.3389/fmicb.2022.1050939

Burgunter-Delamare B, Shetty P, Vuong T, Mittag M (**2024**) Exchange or eliminate: the secrets of algal-bacterial relationships. *Plants*. 13, 829. Doi: 10.3390/plants13060829

Burrows MT, Schoeman DS, Buckley LB, Moore P, Poloczanska ES, Brander KM, Brown C, Bruno JF, Duarte CM, Halpern BS, Holding J, Kappel CV, Kiessling W, O'Connor MI, Pandolfi JM, Parmesan C, Schwing FB, Sydeman WJ, Richardson AJ (**2011**) The pace of shifting climate in marine and terrestrial ecosystems. *Science*. 334, 652–655. Doi: 10.1126/science.1210288

Butt N, Possingham HP, De Los Rios C, Maggini R, Fuller RA, Maxwell SL, Watson JEM (**2016**) Challenges in assessing the vulnerability of species to climate change to inform conservation actions. *Biological Conservation*. 199, 10–15. Doi: 10.1016/j.biocon.2016.04.020

Callaghan TV, Björn LO, Chernov Y, Chapin T, Christensen TR, Huntley B, Ims, RA, Johansson M, Jolly D, Jonasson S, Matveyeva N, Panikov N, Oechel W, Shaver G, Elster J, Henttonen H, Laine K, Taulavuori K, Taulavuori E, Zöckler C (**2004**) Biodiversity, distribution and adaptations of Arctic species in the context of environmental change. *Royal Swedish Academy of Sciences*. 33, 404–417. Doi: 10.1579/0044-7447-33.7.404

Castro de la Guardia L, Filbee-Dexter K, Reimer J, MacGregor, Garrido I, Singh RK, Bélanger S, Konar B, Iken K, Johnson LE, Archambault P, Sejr MK, Søreide J, Mundy CJ (**2023**) Increasing depth distribution of Arctic kelp with increasing number of open water days with light. *Elementa – Science of the Anthropocene*. 11, 00051. Doi: 10.1525/elementa.2022.00051

Cavallo G, Lorini C, Garamella G, Bonaccorsi G (**2021**) Seaweeds as a "palatable" challenge between innovation and sustainability: a systematic review of food safety. *Sustainability*. 13, 7652. Doi: 10.3390/su13147652

Chevin L-M, Lande R, Mace GM (**2010**) Adaptation, plasticity, and extinction in a changing environment: towards a predictive theory. *PLoS Biology*. 8, e1000357. Doi: 10.1371/journal.pbio.1000357

Christie H, Jørgensen NM, Norderhaug KM, Waage-Nielsen E (**2003**) Species distribution and habitat exploitation of fauna associated with kelp (*Laminaria hyperborea*) along the Norwegian coast. *Journal of the Marine Biological Association of the United Kingdom*. 83, 687–699. Doi: 10.1017/S0025315403007653h

Christie H, Norderhaug KM, Fredriksen S (**2009**) Macrophytes as habitat for fauna. *Marine Ecology Progress Series*. 396, 221–233. Doi: 10.3354/meps08351

Chung IK, Lee JA (**1989**) The effects of heavy metals in seaweeds. *The Korean Journal of Phycology*. 4, 221–238.

Coelho SM, Rijstenbil JW, Brown MT (**2020**) Impacts of anthropogenic stresses on the early development stages of seaweeds. *Journal of Aquatic Ecosystem Stress and Recovery*. 7, 317–333. Doi: 10.1023/A:1009916129009

Collier RJ, Baumgard LH, Zimbelman RB, Xiao Y (**2019**) Heat stress: physiology of acclimation and adaptation. *Animal Frontiers*. 9, 12–19. Doi: 10.1093/af/vfy031

Colombo-Pallotta MF, García-Mendoza E, Ladah LB (**2006**) Photosynthetic performance, light absorption, and pigment composition of *Macrocystis pyrifera* (Laminariales, Phaeophyceae) blades from different depths. *Journal of Phycology*. 42, 1225–1234. Doi: 10.1111/j.1529-8817.2006.00287.x

Costa GB, de Felix MRL, Simoni C, Ramlov F, Oliveira ER, Pereira DT, Maraschin M, Chow F, Horta PA, Lalau CM, da Costa CH, Matias WG, Bouzon ZL, Schmidt EC (**2016**) Effects of copper and lead exposure on the ecophysiology of the brown seaweed *Sargassum cymosum*. *Protoplasma*. 253, 111–125. Doi: 10.1007/s00709-015-0795-4

Costa M, Henriques B, Pinto J, Fabre E, Dias M, Soares J, Carvalho L, Vale C, Pinheiro-Torres J, Pereira E (**2020**) Influence of toxic elements on the simultaneous uptake of rare earth elements from contaminated waters by estuarine macroalgae. *Chemosphere*. 252, 126562. Doi: 10.1016/j.chemosphere.2020.126562

Cottier F, Tverberg V, Inall M, Svendsen H, Nilsen F, Griffiths C (**2005**) Water mass modification in an Arctic fjord through cross-shelf exchange: the seasonal hydrography of Kongsfjorden, Svalbard. *Journal of Geophysical Research*. 10, C125005. Doi: 10.1029/2004JC002757

_____

Cottier FR, Nilsen F, Skogseth R, Tverberg V, Skarđhamar J, Svendsen H (**2010**) Arctic fjords: a review of the oceanographic environment and dominant processes. *Geological Society London Special Publications*. 344, 35–50. Doi: 10.1144/SP344.4

Dankworth M, Heinrich S, Fredriksen S, Bartsch I (**2020**). DNA barcoding and mucilage ducts in the stipe reveal the presence of *Hedophyllum nigripes* (Laminariales, Phaeophyceae) in Kongsfjorden (Spitsbergen). *Journal of Phycology.* 56, 1245–1254. Doi: 10.1111/jpy.13012

Davis TA, Volesky B, Mucci A (**2003**) A review of the biochemistry of heavy metal biosorption by brown algae. *Water Research*. 37, 4311–4330. Doi: 10.1016/S0043-1354(03)00293-8

Davison IR, Greene RM, Podolak EJ (**1991**) Temperature acclimation of respiration and photosynthesis in the brown algae *Laminaria saccharina*. *Marine Biology*. 110, 449–454.

Demmig-Adams B, Adams WW (**1996**) The role of xanthophyll cycle carotenoids in the protection of photosynthesis. *Trends in Plant Science.* 1, 21–26. Doi: 10.1016/S1360-1385(96)80019-7

Diehl N, Roleda MY, Bartsch I, Karsten U, Bischof K (**2021**) Summer heatwave impacts on the European kelp *Saccharina latissima* across its latitudinal distribution gradient. *Frontiers in Marine Science*. 8, 695821. Doi: 10.3389/fmars.2021.695821

Diehl N, Li H, Scheschonk L, Burgunter-Delamare B, Niedzwiedz S, Forbord S, Sæther M, Bischof K, Monteiro C (**2024**) The sugar kelp *Saccharina latissima* I: recent advances in a changing climate. *Annals of Botany*. 133, 183–211. Doi: 10.1093/aob/mcad173

Donelson JM, Sunday JM, Figueira WF, Gaitán-Espitia JD, Hobday AJ, Johnson CR, Leis JM, Ling SD, Marshall D, Pandolfi JM, Recl G, Rodgers GG, Booth DJ, Munday PL (**2019**) Understanding interactions between plasticity, adaptation and range shifts in response to marine environmental change. *Physiological Transactions of the Royal Society B*. 374, 20180186. Doi: 10.1098/rstb.2018.0186

Dring MJ, Makarov V, Schoschina E, Lorenz M, Lüning K (**1996**) Influence of ultraviolet- radiation on chlorophyll fluorescence and growth in different life-history stages of three species of Laminaria (Phaeophyta). *Marine Biology*. 126, 183–191. Doi: 10.1007/BF00347443

Dubi A, Tørum A (**1996**) Wave energy dissipation in kelp vegetation. *Coastal engineering*. Doi: 10.1061/9780784402429.203

Düsedau L, Fredriksen S, Brand M, Fischer P, Karsten U, Bischof K, Savoie A, Bartsch I (**2024**) Kelp forest community structure and demography in Kongsfjorden (Svalbard) across 25 years of Arctic warming. *Ecology and Evolution*. 14, e11606. Doi: 10.1002/ece3.11606

Dumortier B-C (**1822**) Observations botaniques, dédiées à la Société d'Horticulture de Tournay. Commentationes botanicae. Tournay: Imprimerie de Ch. Casterman-Dieu.

Eckman JE, Duggins DO, Sewell AT (**1989**) Ecology of understory kelp environments. I. Effects of kelps on flow and particle transport near bottom. *Journal of Experimental Marine Biology and Ecology*. 129, 173–187. Doi: 10.1016/0022-0981(89)90055-5

Egan B, Vlasto A, Yarish C (**1989**) Seasonal acclimation to temperature and light in *Laminaria longicruris* de la Pyl. (Phaeophyta). *Journal of Experimental Marine Biology and Ecology*. 129, 1–16. Doi: 10.1016/0022-0981(89)90059-2

Egan S, Harder T, Burke C, Steinberg P, Kjelleberg S, Thomas T (**2013**) The seaweed holobiont: understanding sea-weed-bacteria interactions. *FEMS Microbiology Review*. 37, 462-476. Doi: 10.1111/1574-6976.12011

Eger AM, Marzinelli EM, Beas-Luna R, Blain CO, Blamey LK, Byrnes JEK, Carnell PE, Choi CG, Hessing-Lewis M, Young KK, Kumagai NH, Lorda J, Moore P, Nakamura Y, Pérez-Matus A, Pontier O, Smale D, Steinberg PD, Vergés A (**2023**) The value of ecosystem services in global kelp forests. *Nature Communications*. 14, 1894. Doi: 10.1038/s41467-023-37385-0

Eldevik T, Nilsen JEØ (**2013**) The Arctic-Atlantic thermohaline circulation. *Journal of Climate*. 26, 8698–8705. Doi: 10.1175/JCLI-D-13-00305.1

Elsmore K, Nickols KJ, Miller LP, Ford T, Denny MW, Gaylord B (**2024**) Wave damping by giant kelp *Macrocystis pyrifera*. *Annals of Botany*. 133, 29–40. Doi: 10.1093/aob/mcad094

England MR, Eisenman I, Lutsko NJ, Wagner TJW (**2021**) The recent emergence of Arctic Amplification. *Geophysical Research Letters*. 48, e2021GL094086. Doi: 10.1029/2021GL094086

Erlandson JM, Graham MH, Bourque BJ, Corbett D, Estes JA, Steneck RS (**2007**) The kelp highway hypothesis: marine ecology, the coastal migration theory and the peopling of the Americas. *The Journal of Island and Coastal Archaeology*. 2, 161–174. Doi: 10.1080/15564890701628612

ESA (**2019**) Modelling tides in the Arctic Ocean. https://www.esa.int/Applications/ Observing_the_Earth/FutureEO/CryoSat/Modelling_tides_in_the_Arctic_Ocean.   Last access: 10.07.2024

Fabry VJ, Seibel BA, Feely RA, Orr JC (**2008**) Impacts of ocean acidification on marine fauna and ecosystem processes. *ICES Journal of Marine Science*. 65, 414–432. Doi: 10.1093/icesjms/fsn048

Falkowski PG, Sukenik A, Herzig R (**1989**) Nitrogen limitation in *Isochrysis galbana* (Haptophyceae). II. Relative abundance of chloroplast proteins. *Journal of Phycology*. 25, 471–478. Doi: 10.1111/j.1529-8817.1989.tb00252.x

Falkowski PG, Raven JA (**2007**) Aquatic photosynthesis. Princeton University Press. Princeton; Oxford.

Farrugia Drakard V, Hollarsmith JA, Stekoll MS (**2023**) High-latitude kelps and future oceans: A review of multiple stressor impacts in a changing world. *Ecology and Evolution*. 13, e10277. Doi: 10.1002/ece3.10277

Fauchald P, Hausner VH, Schmidt JI, Clark DA (**2017**) Transitions of social-ecological subsistence systems in the Arctic. *International Journal of the Commons*. 11, 275–329. Doi: 10.18352/ijc.698

Fedorov VM, Kostin AA, Frolov DM (**2020**) Influence of the shape of the earth on the characteristics of the irradiation of the earth. *Atmospheric and Oceanic Physics*. 56, 1301–1313. Doi: 10.1134/S0001433820100035

Fernández PA, Gaitán-Espitia JD, Leal PP, Schmid M, Revill AT, Hurd CL (**2020**) Nitrogen sufficiency enhances thermal tolerance in habitat-forming kelp: implications for acclimation under thermal stress. *Scientific Reports*. 10, 3186. Doi: 10.1038/s41598-020-60104-4

Filbee-Dexter K, Scheibling RE (**2014**) Sea urchin barrens as alternative stable states of collapsed kelp ecosystems. *Marine Ecology Progress Series*. 495, 1–25. Doi: 10.3354/meps10573

Filbee-Dexter K, Wernberg T (**2018**) Rise of turfs: a new battlefront for globally declining kelp forests. *BioScience*. 68, 64–76. Doi: 10.1093/biosci/bix147

Filbee-Dexter K, Wernberg T, Fredriksen S, Norderhaug KM, Pedersen MF (**2019**) Arctic kelp forests: diversity, resilience and future. *Global and Planetary Change*. 172, 1–14. Doi: 10.1016/j.gloplacha.2018.09.005

Filbee-Dexter K, Wernberg T, Grace SP, Thormar J, Fredriken S, Narvaez CN, Feehand CJ, Norderhaug KM (**2020**) Marine heatwaves and the collapse of marginal North Atlantic kelp forests. *Scientific Reports*. 10, 13388. Doi: 10.1038/s41598-020-70273-x

Filbee-Dexter K, MacGregor KA, Lavoie C, Garrido I, Goldsmit J, Castro de la Guardia L, Howland KL, Johnson LE, Konar B, McKindsey CW, Mundy CJ, Schlegel RW, Archambault P (**2022**) Sea ice and substratum shape extensive kelp forests in the Canadian Arctic. *Frontiers in Marine Science*. 9, 754074. Doi: 10.3389/fmars.2022.754074

Filbee-Dexter K, Pessarrodona A, Duarte CM, Krause-Jensen D, Hancke K, Smale D, Wernberg T (**2023**) Seaweed forests are carbon sinks that may help mitigate CO_2 emissions: a comment on Gallagher et al. (2022). *ICES Journal of Marine Science*. 80, 1814–1819. Doi: 10.1093/icesjms/fsad107

Ford L, Theodoridou K, Sheldrake GN, Walsh PJ (**2019**) A critical review of analytical methods used for the chemical characterisation and quantification of phlorotannin compounds in brown seaweeds. *Phytochemical Analysis*. 30, 587–599. Doi: 10.1002/pca.2851

Foslie M (**1885**) Ueber die Laminarien Norwegens. *Christiania Videnskabers Selskabs Forhandlinger*. 14, 1-112.

Fox RJ, Donelson JM, Schunter C, Ravasi T, Gaitán-Espitia JD (**2019**) Beyond buying time: the role of plasticity in phenotypic adaptation to rapid environmental change. *Physiological Transactions of the Royal Society B*. 374, 20180174. Doi: 10.1098/rstb.2018.0174

Franklin L, Forster R (**1997**) The changing irradiance environment: consequences for marine macrophyte physiology, productivity and ecology. *European Journal of Phycology*. 32, 207–232. Doi: 10.1080/09670269710001737149

Fraser CI (**2012**) Is bull-kelp kelp? The role of common names in science. *New Zealand Journal of Marine and Freshwater Research*. 46, 279–284. Doi: 10.1080/00288330.2011.621130

Fredersdorf J, Müller R, Becker S, Wiencke C, Bischof K (**2009**) Interactive effects of radiation, temperature and salinity on different life history stages of the Arctic kelp *Alaria esculenta* (Phaeophyceae). *Oecologia*. 160, 483–492. Doi: 10.1007/s00442-009-1326-9

Gagnon P, Johnson LE, Himmelman JH (**2005**) Kelp patch dynamics in the face of intense herbivory: stability of *Agarum clathratum* (Phaeophyta) stands and associated flora on urchin barrens. *Journal of Phycology*. 41, 498–505. Doi: 10.1111/j.1529-8817.2005.00078.x

Gallagher JB, Shelamoff V, Layton C (**2022**) Seaweed ecosystems may not mitigate CO_2 emissions. *ICES Journal of Marine Science*. 79, 585–592. Doi: 10.1093/icesjms/fsac011

Gao G, Beardall J, Jin P, Gao L, Xie S, Gao K (**2022**) A review of existing and potential blue carbon contributions to climate change mitigation in the Anthropocene. *Journal of Applied Phycology*. 59, 1686–1699. Doi: 10.1111/1365-2664.14173

Gattuso J-P, Gentili B, Duarte CM, Kleypas JA, Middelburg JJ, Antoine D (**2006**) Light availability in the coastal ocean of benthic photosynthetic organisms and contribution to primary production. *Biogeosciences Discussions*. 3, 895–959. Doi: 10.5194/bg-3-489-2006

Gattuso J-P, Gentili B, Antoine D, Doxaran D (**2020**) Global distribution of photosynthetically available radiation on the seafloor. *Earth System Science Data*. 12, 1697-1709. Doi: 10.5194/essd-12-1697-2020

Gauci C, Bartsch I, Martins N, Liesner D (**2022**) Cold thermal priming of *Laminaria digitata* (Laminariales, Phaeophyceae) gametophytes enhances gametogenesis and thermal performance of sporophytes. *Frontiers in Marine Science*. 9, 862923. Doi: 10.3389/fmars.2022.862923

Geyman EC, van Pelt WJJ, Maloof AC, Faste Aas H, Kohler J (**2022**) Historical glacier change on Svalbard predicts doubling of mass loss by 2100. *Nature*. 601, 374–379. Doi: 10.1038/s41586-021-04314-4

Goldsmit J, Schlegel RW, Filbee-Dexter K, MacGregor KA, Johnson LE, Mundy CJ, Savoie AM, McKindsey CW, Howland KL, Archambault P (**2021**) Kelp in the Eastern Canadian Arctic: current and future predictions of habitat suitability and cover. *Frontiers in Marine Science*. 18, 742209. Doi: 10.3389/fmars.2021.742209

Gonzales Triginer V, Beck M, Sen A, Bischof K, Damsgård B (**in rev**) Acoustic mapping reveals macroalgal settlement following a retreating glacier front in the High-Arctic. *Frontiers in Marine Science*.

Gordillo FJL, Carmona R, Jiménez C (**2022**) A warmer Arctic compromises winter survival of habitat-forming seaweeds. *Frontiers in Marine Science*. 8, 750209. Doi: 10.3389/fmars.2021.750209

Graham MH (**2004**) Effects of local deforestation on the diversity and structure of southern California giant kelp forest food webs. *Ecosystems*. 7, 341–357. Doi: 10.1007/s10021-003-0245-6

Greville RK (**1830**) *Algae britannicae*, or descriptions of the marine and other inarticulated plants of the British islands, belonging to the order Algae; with plates illustrative of the genera. McLachlan & Stewart; Baldwin & Cradock. Edinburgh; London.

Grid Arendal (**2024**) EU Project SEA-Quester. Latest access: 15.07.2024. https://www.grida.no/activities/1027

Hanelt D, Tüg H, Bischof K, Groß C, Lippert H, Sawall T, Wiencke C (**2001**) Light regime in an Arctic fjord: a study related to stratospheric ozone depletion as a basis for determination of UV effects on algal growth. *Marine Biology*. 138, 649–658. Doi: 10.1007/s002270000481

Hanssen-Bauer I, Førland EJ, Hisdal H, Mayer S, Sandø AB, Sorteberg A (**2019**) Climate in Svalbard 2100 – a knowledge base for climate adaptation. *NCCS report*.

Hobday AJ, Alexander LV, Perkins SE, Smale DA, Straub SC, Oliver ECJ, Benthuysen JA, Burrows MT, Donat MG, Feng M, Holbrook NJ, Moore PJ, Scannell HA, Sen Gupta A, Wernberg T (**2016**) A hierarchical approach to defining marine heatwaves. *Progress in Oceanography*. 141, 227–238. Doi: 10.1016/j.pocean.2015.12.014

Hop H, Wiencke C (eds) (**2019**) The ecosystem of Kongsfjorden, Svalbard. Springer. Cham.

Hopkin R, Kain JM (**1978**) The effects of some pollutants on the survival, growth and respiration of *Laminaria hyperborea*. *Estuarine and Coastal Marine Science*. 7, 531–553. Doi: 10.1016/0302-3524(78)90063-4

_____

Hopwood MJ, Carroll D, Dunse T, Hodson A, Holding JM, Iriarte JL, Ribeiro S, Achterberg EP, Cantoni C, Carlson DF, Chierici M, Clarke JS, Cozzi S, Fransson A, Juul-Pedersen T, Winding MHS, Meire L (**2020**) Review article: how does glacier discharge affect marine biogeochemistry and primary production in the Arctic? *The Cryosphere*. 14, 1347–1383. Doi: 10.5194/tc-14-1347-2020

Horowitz M (**2002**) From molecular and cellular to integrative heat defense during exposure to chronic heat. *Comparative Biochemistry and Physiology Part A: Molecular & Integrative Physiology*. 131, 475–483. Doi: 10.1016/S1095-6433(01)00500-1

Hugonnet R, McNabb R, Berthier E, Menounos B, Nuth C, Girod L, Farinotti D, Huss M, Dussaillant I, Brun F, Kääb A (**2021**) Accelerated global glacier mass loss in the early twenty-first century. *Nature*. 592, 726 – 731. Doi: 10.1038/s41586-021-03436-z

IPCC, 2018: Annex I: Glossary [Matthews, JBR (ed)]. In: Masson-Delmotte V, Zhai P, Pörtner H-O, Roberts D, Skea J, Shukla PR, Pirani A, Moufouma-Okia W, Péan C, Pidcock R, Connors A, Matthews JBR, Chen Y, Zhou X, Gomis MI, Lonnoy E, Maycock T, Tignor M, Waterfield T (eds) Global Warming of 1.5°C. An IPCC Special Report on the impacts of global warming of 1.5°C above pre-industrial levels and related global greenhouse gas emission pathways, in the context of strengthening the global response to the threat of climate change, sustainable development, and efforts to eradicate poverty. Cambridge University Press, Cambridge, New York, USA. Doi: 10.1017/9781009157940.008.

IPCC (**2023**) Summary for Policymakers. In: Core Writing Team, Lee H, Romero J (eds) Climate Change 2023: Synthesis Report. Contribution of Working Groups I, II and III to the Sixth Assessment Report of the Intergovernmental Panel on Climate Change. IPCC, Geneva, Switzerland. Doi: 10.59327/IPCC/AR6-9789291691647.001

Irrgang AN, Bendixen M, Farquharson LM, Baranskaya AV, Erikson LH, Gibbs LH, Ogorodov SA, Overduin PP, Lantuit H, Grigoriev MN, Jones BM (**2022**) Drivers, dynamics and impacts of changing Arctic coasts. *Nature Reviews – Earth & Environment*. 3, 39–54. Doi: 10.1038/s43017-021-00232-1

Ivanov V (**2023**) Arctic sea ice loss enhances the oceanic contribution to climate change. *Atmosphere*. 14, 409. Doi: 10.3390/atmos14020409

Jones CG, Lawton JH, Shachak M (**1977**) Positive and negative effects of organisms as physical ecosystem engineers. *Ecology*. 78, 1946–1957. Doi: 10.1890/0012-9658(1997)078[1946:PANEOO]2.0.CO;2

Juul-Pedersen T, Arendt KE, Mortensen J, Blicher ME, Søraard DH, Rysgaard S (**2015**) Seasonal and interannual phytoplankton production in a sub-Arctic tidewater outlet glacier fjord, SW Greenland. *Marine Ecology Progress Series*. 524, 27–38. Doi: 10.3354/meps11174

Kain JM (**1979**) A view of the genus *Laminaria*. *Oceanography and Marine Biology – An Annual Review*. 17, 101 – 161.

Karsten U (**2007**) Salinity tolerance of Arctic kelps from Spitsbergen. *Phycological Research*. 55, 257–262. Doi: 10.1111/j.1440-1835.2007.00468.x

Keats DW, South GR, Steele DH (**1985**) Algal biomass and diversity in the upper subtidal at a pack-ice disturbed site in eastern Newfoundland. *Marine Ecology Progress Series*. 25, 152–158. Doi: 10.3354/meps025151

King NG, McKeown NJ, Smale DA, Moore PJ (**2017**) The importance of phenotypic plasticity and local adaptation in driving intraspecific variability in thermal niches of marine macrophytes. *Ecography*. 41, 1469–1484. Doi: 10.1111/ecog.03186

Kingsolver JG, Huey RB (**2003**) Introduction: the evolution of morphology, performance and fitness. *Integrative & Comparative Biology*. 43, 361–366. Doi: 10.1093/icb/43.3.361

Kirk JTO (**2011**) Light and photosynthesis in aquatic systems. Cambridge Univ. Press. Cambridge.

Kirst GO (**1990**) Salinity tolerance of eukaryotic marine algae. *Annual Review of Plant Physiology and Plant Molecular Biology*. 40, 21–53. Doi: 10.1146/annurev.pp.41.060190.000321

Kirst GO, Wiencke C (**1995**) Ecophysiology of polar algae. *Journal of Phycology*. 31, 181–199. 1 Doi: 0.1111/j.0022-3646.1995.00181.x

Koch M, Jungblut S, Gütze S, Bock C, Saborowski R (**in rev**) Marine heatwaves in the Subarctic and the effect of acute temperature change on the key grazer *Strongylocentrotus droebachiensis* (Echinoidea, Echinodermata).

Konik M, Darecki M, Pavlov AK, Sagan S, Kowalczuk P (**2021**) Darkening of the Svalbard fjords waters observed with satellite ocean color imagery in 1997–2019. *Frontiers in Marine Science*. 8, 699318. Doi: 10.3389/fmars.2021.699318

Krause J, Hopwood MJ, Höfer J, Krisch S, Achterberg EP, Alarcón E, Carroll D, González HE, Juul-Pedersen T, Liu T, Lodeiro P, Meire L, Rosing MT (**2021**) Trace element (Fe, CO, Ni and Cu) dynamics across the salinity gradient in Arctic and Antarctic glacier fjords. *Frontiers in Earth Science*. 9:725279. Doi: 10.3389/feart.2021.725279

Krause-Jensen D, Marbà N, Olesen B, Sejr MK, Christensen PB, Rodrigues J, Renaud PE, Balsby TJS, Rysgaard S (**2012**) Seasonal sea ice cover as principle driver of spatial and temporal variation in depth extension and annual production of kelp in Greenland. *Global Change Biology*. 18, 2981–2994. Doi: 10.1111/j.1365-2486.2012.02765.x

Krause-Jensen D, Marbà N, Sanz-Martin M, Hendriks IE, Thyrring J, Carstensen J, Sejr MK, Duarte CM (**2016**) Long photoperiods sustain high pH in Arctic kelp forests. *Science Advances*. 2, e1501938. Doi: 10.1126/sciadv.1501938

Krause-Jensen D, Archambault P, Assis J, Bartsch I, Bischof K, Filbee-Dexter K, Dunton KH, Maximova O, Björk S, Sejr MK, Simakova U, Spiridonov V, Wegeberg S, Winding MHS, Duarte CM (**2020**) Imprint of climate change on pan-Arctic marine vegetation. *Frontiers in Marine Science*. 7, 617324. Doi: 10.3389/fmars.2020.617324

Krause-Jensen D, Gundersen H, Björk M, Gullström M, Dahl M, Asplund ME, Boström C, Holmer M, Banta GT, Graversen AWL, Pedersen MF, Bekkby T, Frigstad H, Skjellum SF, Thormar J, Gyldenkærne S, Howard J, Pidgeon E, Ragnarsdóttier SB, Mols-Mortensen A, Hancke K (**2022**) Nordic blue carbon ecosystems: status and outlook. *Frontiers in Marine Science*. 9, 847544. Doi: 10.3389/fmars.2022.847544

Kreissig KJ, Hansen LT, Jensen PE, Wegeberg S, Geertz-Hansen O, Sloth JJ (**2021**) Characterisation and chemometric evaluation of 17 elements in ten seaweed species from Greenland. *PLoS ONE*. 16, e0243672. Doi: 10.1371/journal.pone.0243672

_____

Krumhansl KA, Scheibling RE (**2012**) Production and fate of kelp detritus. *Marine Ecology Progress Series*. 467, 281–302. Doi: 10.3354/meps09940

Krumhansl KA, Okamoto DK, Rassweiler A, Novak M, Bolton JJ, Cavanaugh KC, Connell SD, Johnson CR, Konar B, King SD, Micheli F, Norderhaug KM, Pérez-Matus A, Sousa-Pinto I, Reed DC, Salomon AK, Shears NT, Wernberg T, Anderson RJ, Barrett NS, Buschmann AH, Carr MH, Caselle JE, Derrien-Courtel S, Edgar GJ, Edwards M, Estes JA, Goodwin C, Kenner MC, Kushner DJ, Moy FE, Nunn J, Steneck RS, Vásquez J, Watson J, Witman JD, Byrnes JEK (**2016**) Global patterns of kelp forest change over the past half-century. *Proceedings of the National Academy of Science*. 48, 13785–13790. Doi: 10.1073/pnas.1606102113

Kubelka V, Sandercock BK, Székely T, Freckleton RP (**2021**) Animal migration to northern latitudes: environmental changes and increasing threats. *Trends in Ecology & Evolution*. 37, 30–41. Doi: 10.1016/j.tree.2021.08.010

Kültz D (**2003**) Evolution of the cellular stress proteome: from monophyletic origin to ubiquitous function. *The Journal of Experimental Biology*. 206, 3119–3124. Doi: 10.1242/jeb.00549

Kültz D (**2005**) Molecular and evolutionary basis of the cellular stress response. *Annual Review of Physiology*. 67, 225–257. Doi: 10.1146/annurev.physiol.67.040403.103635

Laeseke P, Bartsch I, Bischof K (**2019**) Effects of kelp canopy on underwater light climate and viability of brown algal spores in Kongsfjorden (Spitsbergen). *Polar Biology*. 42, 1511–1527. Doi: 10.1007/s00300-019-02537-w

Laeseke P, Martínez BD-C, Bischof K (**2024**) Large-scale deviations between realized and fundamental thermal niches in global seaweed distributions. *Diversity and Distributions*. 00, e13868. Doi: 10.1111/ddi.13868

Laliberté J, Bélanger S, Babin M (**2021**) Seasonal and interannual variations in the propagation of photosynthetically available radiation through the Arctic atmosphere. *Elementa Science of the Anthropocene*. 9, 1. Doi: 10.1525/elementa.2020.00083

Lane CE, Mayes C, Druehl LD, Saunders GW (**2006**) A multi-gene molecular investigation of the kelp (Laminariales, Phaeophyceae) supports substantial taxonomic re-organization. *Journal of Phycology*. 42, 593–512. Doi: 10.1111/j.1529-8817.2006.00204.x

Lantuit H, Overduin PP, Couture B, Wetterich S, Aré F, Atkinson D, Brown J, Cherkashov G, Drozdov D, Forbes DL, Graves-Gaylord A, Grigoriev M, Hubberten H-W, Jordan J, Jorgenson T, Ødegård RS, Ogorodov S, Pollard WH, Rachold V, Sedenko S, Solomon S, Steehuisen F, Streletskaya I, Vasikiev A (**2012**) The Arctic coastal dynamics database: a new classification scheme and statistics on Arctic permafrost coastlines. *Estuaries and Coasts*. 35, 383–400. Doi: 10.1007/s12237-010-9362-6

Larsen JN, Fondahl G (eds) (**2014**) Arctic human development report (AHDR) – Regional processes and global linkages. Doi: 10.6027/TN2014-567

Lauvset SK, Carter BR, Pèrez FF, Jiang L-Q, Feely RA, Velo A, Olsen A (**2020**) Processes driving global interior ocean pH distribution. 34, e2019GB006229. Doi: 10.1029/2019GB006229

Lebrun A, Comeau S, Gazeau F, Gattuso J-P (**2022**) Impact of climate change on Arctic macroalgal communities. *Global and Planetary Change*. 2019, 103980. Doi: 10.1016/j.gloplacha.2022.103980

Lenton TM, Laybourn L, Armstrong McKay DI, Loriani S, Abrams JF, Lade SJ, Donges JF, Milkoreit M, Smith SR, Bailey E, Powell T, Fesenfeld L, Zimm C, Boulton CA, Buxton JE, Dyke JG, Ghadiali A (**2023**) Global Tipping Points Report 2023: 'Summary Report'. In: Lenton TM, Armstrong McKay DI, Loriani S, Abrahams JF, Lade SJ, Donges JF, Milkoreit M, Powel T, Smith SR, Zimm C, Buxton JE, Laybourn L, Ghadiali A, Dyke JG (eds) (2023) The Global Tipping Point Report 2023.] University of Exeter. UK.

Liboureau P, Pearson GA, Serrão E, Kreiner A, Martins N (**2024**) A novel sexual system in male gametophytes of *Laminaria pallida* (Phaeophyceae). *European Journal of Phycology*. 59, 232–241. Doi: 10.1080/09670262.2024.2314487

Liesner D, Sharma LNS, Diehl N, Valentin K, Bartsch I (**2020**) Thermal plasticity of the kelp *Laminaria digitata* (Phaeophyceae) across life cycle stages reveals the importance of cold seasons for marine forests. *Frontiers in Marine Science*. 7, 456. Doi: 10.3389/fmars.2020.00456

Liu X, Bogaert K, Engelen AH, Lelilaert F, Roleda MY, De Clercke O (**2017**) Seaweed reproductive biology: environmental and genetic controls. *Botanica Marina*. 60, 89–108. Doi: 10.1515/bot-2016-0091

Lindstrøm M (**2024**) Royal Greenland receives funding for seaweed project in Greenland. https://www.royalgreenland.com/royal-greenland/news-and-seafood-insight/Royal-Greenland-receives-funding-for-seaweed-project-in-Greenland/. Last access: 15.07.2024.

Lüning K (**1985**) Meeresbotanik - Verbreitung, Ökophysiologie und Nutzung der marinen Makroalgen. New York: Georg Thieme Verlag. Stuttgart.

Lüning K (**1990**) Seaweeds: their environment, biogeography, and ecophysiology. John Wiley & Sons. New York.

Ma D, Gregor L, Gruber N (**2023**) Four decades of trends and drivers of global surface ocean acidification. *Global Biogeochemical Cycles*. 37, e2023GB007765. Doi: 10.1029/2023GB007765

Mahner M, Kary M (**1997**) What exactly are genomes, genotypes and phenotypes? And what about phenomes? *Journal of Theoretical Biology*. 186, 55–63. Doi: 10.1006/jtbi.1996.0335

Malanson GP, Westman WE, Yan Y-L (**1992**) Realized versus fundamental niche functions in a model of chaparral response to climatic change. *Ecological Modelling*. 64, 261–277. Doi: 10.1016/0304-3800(92)90026-B

Manca F, Benedetti-Cecchi L, Bradshaw CJA, Cabeza M, Gustafsson C, Norkko AM, Roslin TV, Thomas DN, White L, Strona G (**2024**) Projected loss of brown macroalgae and seagrasses with global environmental change. *Nature Communications*. 15, 5344. Doi: 10.1038/s41467-024-48273-6

Martin RA, da Silva CRB, Moore MP, Diamond SE (**2023**) When will a changing climate outpace adaptive evolution? *WIREs Climate Change*. 14, e852. Doi: 10.1002/wcc.852

Martins N, Tanttu H, Pearson GA, Serrão E, Bartsch I (**2017**) Interactions of daylength, temperature and nutrients affect threshold for life stage transition in the kelp *Laminaria digitata* (Phaeophyceae). *Botanica Marina*. 60, 109–121. Doi: 10.1515/bot-2016-0094

Martins N, Barreto L, Bartsch I, Bernard J, Serrão EA, Pearson GA (**2022**) Daylength influences reproductive success and sporophyte growth in the Arctic kelp species *Alaria esculenta*. *Marine Ecology Progress Series*. 683, 34–52. Doi: 10.3354/meps13950

_____

Matich P, Strickland BA, Heithaus MR (**2020**) Long-term monitoring provides insight into estuarine top predator (*Carcharhinus leucas*) resilience following an extreme weather event. *Marine Ecology Progress Series*. 639, 169–183. Doi: 10.3354/meps13269

McClelland JW, Holmes RM, Dunton KH, Macdonald RW (**2012**) The Arctic Ocean estuary. *Estuaries and Coasts.* 35, 353–368. Doi: 10.1007/s12237-010-9357-3

McDevit DC, Saunders GW (**2010**) A DNA barcode examination of the Laminariceae (Phaeophyceae) in Canada reveals novel biogeographical and evolutionary insight. *Phycologia*. 49, 235–248. Doi: 10.2216/PH09-36.1

McGovern M, Pavlov AK, Deininger A, Grandkog MA, Leu E, Søreide JE, Poste AE (**2020**) Terrestrial inputs drive seasonality in organic matter and nutrient biogeochemistry in a high Arctic fjord system (Isfjorden, Svalbard). *Frontiers in Marine Science*. 7, 542563. Doi: 10.3389/fmars.2020.542563

Meire L, Meire P, Struyf E, Krawczyk DW, Arendt KE, Yde JC, Juul-Pedersen T, Hopwood MJ, Rysgaard S, Meysman FJR (**2016**) High export of dissolved silica from the Greenland ice sheet. *Geophysical Research Letters*. 43, 9173–9182. Doi: 10.1002/2016GL070191.

Meire L, Mortensen J, Meire P, Juul-Pedersen T, Sejr MK, Rysgaard S, Nygaard R, Huybrechts P, Meysman FJR (**2017**) Marine-terminating glaciers sustain high productivity in Greenland fjords. *Global Change Biology*. 23, 5344–5357. Doi: 10.1111/gcb.13801

Meredith M, Sommerhorn M, Cassotta S, Derksen C, Ekaykin A, Hollowed A, Kofinas G, Mackintosh A, Melbourne-Thomas J, Muelbert MMC, Ottersen G, Pritchard H, Schuur EAG (**2019**) Polar regions. In: Pörtner H-O, Roberts DC, Masson-Delmotte V, Zhai P, Tignor M, Poloczanska E, Mintenbeck K, Alegría A, Nicolai M, Okem A, Petzold J, Rama B, WEyner NM (eds) IPCC special report on the ocean and cryosphere in a changing climate. In press.

Milner AM, Khamis K, Battin TJ, Brittain JE, Barrand NE, Füreder L, Cauvy-Frauni é S, Gíslason GM, Jacobsen D, Hannah DM, Hodson AJ, Hood E, Lencioni V, Ólafsson JS, Robinson CT, Tranter M, Brown LE (**2017**) Glacier shrinkage driving global changes in downstream systems. *Proceedings of the National Academy of Science*. 114, 9770–9778. Doi: 10.1073/pnas.1619807114

Mora-Soto A, Aguirre C, Iriarte JL, Palacios M, Macaya EC, Macias-Auria M (**2022**) A song of wind and ice: increased frequency of marine cold-spells in southwestern Patagonia and their possible effects on giant kelp forests. *Advancing Earth and Space Science*. 127, e2021JC017801. Doi: 10.1029/2021JC017801

Mork M (**1996**) The effect of kelp in wave damping. *Sarsia*. 80, 323–327. Doi: 10.1080/00364827.1996.10413607

Morris RL, Graham TDJ, Kelvin J, Ghisalberti M, Swearer SE (**2020**) Kelp beds as coastal protection: wave attenuation of *Ecklonia radiata* in a shallow coastal bay. *Annals of Botany*. 125, 235–246. Doi: 10.1093/aob/mcz127

Mortensen LM (**2017**) Remediation of nutrient-rich, brackish fjord water through production of protein-rich kelp *S. latissima* and *L. digitata*. *Journal of Applied Phycology*. 29, 3089–3096. Doi: 10.1007/s10811-017-1184-5

Munda IM, Lüning K (**1977**) Growth performance of *Alaria esculenta* off Helgoland. *Helgoländer wissenschaftlichen Meresuntersuchungen*. 29, 311–314. Doi: 10.1007/BF01614267

Murchie EH, Lawson T (**2013**) Chlorophyll fluorescence analysis: a guide to good practice and understanding some new applications. *Journal of Experimental Botany*. 64, 3983–3998. Doi: 10.1093/jxb/ert208

Murray JL, Gregor DJ, Loeng H (**1998**) Physical/Geographical Characteristics of the Artic. In Wilson SJ, Murray JL, Huntington HP (eds), AMAP Assessment Report: Arctic Pollution Issues. Arctic Environmental Assessment Programme (AMAP).

Nicolaus M, Katlein C, Maslanik J, Hendricks S (**2012**) Changes in Arctic sea ice result in increasing light transmittance and absorption. *Geophysical Research Letters*. 39, L24501. Doi: 10.1029/2012GL053738

Niedzwiedz S (**2021**) The transcriptomic response of the cold-water coral *Desmophyllum dianthus* to experimental changes in pH. Master thesis. University of Bremen. https://epic.awi.de/id/eprint/55262/

Niedzwiedz S, Diehl N, Fischer P, Bischof K (**2022**) Seasonal and inter-annual variability in the heatwave tolerance of the kelp *Saccharina latissima* (Laminariales, Phaeophyceae). *Phycological Research*. 70, 212–222. Doi: 10.1111/pre.12501

Nordli Ø, Wyszyński P, Gjelten HM, Isaksen K, Łupikasza E, Niedźwiedź T, Przybylak R (**2020**) Revisiting the extended Svalbard Airport monthly temperature series, and the compiled corresponding daily series 1898–2018. *Polar Research*. 36, 3614. Doi: 10.33265/polar.v39.3614

Nowak A, Hodgkins R, Nikulina A, Osuch M, Wawrzyniak T, Kavan J, Łepkowska E, Majaerska M, Romashova K, Vasilevich I, Sobota I, Rachlewicz G (**2021**) From land to fjords: The review of Svalbard hydrology from 1970 to 2019 (SvalHydro). *Svalbard Integrated Arctic Earth Observing System*. Doi: 10.5281/zenodo.4294063

Nowicka B (**2022**) Heavy metal-induced stress in eukaryotic algae – mechanisms of heavy metal toxicity and tolerance with particular emphasis on oxidative stress in exposed cells and the role of antioxidant response. *Environmental Science and Pollution Research*. 29, 16860–16911. Doi: 10.1007/s11356-021-18419-w

Oliver ECJ, Donat MG, Burrows MT, Moore PJ, Smale DA, Alexander LV, Benthuysen JA, Deng M, Sen Gupta A, Hobday AJ, Holbrook NJ, Perkins-Kirkpatrick SE, Scannell HA, Straub SC, Wernberg T (**2018**) Longer and more frequent marine heatwaves over the past century. *Nature Communications*. 9, 1324. Doi: 10.1038/s41467-018-03732-9

Orr HA (**2009**) Fitness and its role in evolutionary genetics. *Nature Reviews Genetics*. 10, 531–539. Doi: 10.1038/nrg2603

Park J, Kim JK, Kong J-A, Depuydt S, Brown MT, Han T (**2017**) Implications of rising temperatures for gametophyte performance of two kelp species from Arctic waters. *Botanica Marina*. 60, 39–48. Doi: 10.1515/bot-2016-0103

Payne CM, Roesler CS (**2019**) Characterizing the influence of Atlantic water intrusion on water mass formation and phytoplankton distribution in Kongsfjorden Svalbard. *Continental Shelf Research*. 191, 104005. Doi: 10.1016/j.csr.2019.104005

_____

Pecl GT, Araújo MB, Bell JD, Blanchard J, Bonebrake TC, Chen I-C, Clark TD, Colwell RK, Danielsen F, Evengård B, Falconi L, Ferrier S, Frusher S, Garcia RA, Griffis RB, Hobday AJ, Janion-Scheepers C, Jarzyna MA, Jennings A, Lenoir J, Linnetved HI, Martin VY, McCormack PC, McDonald J, Mitchell NJ, Mustonen T, Pandolfi JM, Pettorelli N, Popova E, Robinson SA, Scheffers BR, Shaw JD, Sorte CJB, Strugnell JM, Sunday JM, Tuanmu M-N, Vergés A, Villanueva C, Wernberg T, Wapstra W, Williams SE (**2017**) Biodiversity redistribution under climate change: Impacts on ecosystems and human well-being. *Climate Change*. 355, 1389. Doi: 10.1126/ science.aai9214

Pedersen MF, Filbee-Dexter K, Norderhaug KM, Fredriksen S, Frisk NL, Fagerli CW, Wernberg T (**2020**) Detrital carbon production and export in high latitude kelp forests. *Oecologia*. 192, 227–239. Doi: 10.1007/s00442-019-04573-z

Pereira HM, Navarro LM, Martins IS (**2012**) Global biodiversity change: the bad, the good, and the unknown. *Annual Review of Environment and Resources*. 37, 25–50. Doi: 10.1146/annurev-environ-042911-093511

Pershing AJ, Christensen LB, Record NR, Sherwood GD, Stetson PB (**2010**) The impact of whaling on the ocean carbon cycle: why bigger was better. *PLoS one*. 5, e12444. Doi: 10.1371/journal.pone.0012444

Pessarodona A, Assis J, Filbee-Dexter K, Burrows MT, Gattuso J-P, Duarte CM, Krause-Jensen D, Moore PJ, Smale DA, Wernberg T (**2022**) Global seaweed productivity. *Science Advances*. 8, eabn2465. Doi: 10.1126/sciadv.abn2465

Pinto E, Sigaud-Kutner TCS, Leitão MAS, Okamoto OK (**2003**) Heavy metal-induced oxidative stress in algae. *Journal of Phycology*. 39, 1008–1018. Doi: 10.1111/j.0022-3646.2003.02-193.x

Pinto J, Henriques B, Soares J, Coasta M, Dias M, Fabre E, Lopes CB, Vale C, Pinheiro-Torres J, Ereira E (**2020**) A green method based on living macroalgae for the removal of rare-earth elements from contaminated waters. *Journal of Environmental Management*. 263, 110376. Doi: 10.1016/j.jenvman.2020.110376

Pittino F, Buda J, Ambrosini R, Parolini M, Crosta A, Zawierucha K, Franzetti A (**2023**) Impact of anthropogenic contamination on glacier surface biota. *Current Opinion in Biotechnology*. 80, 102900. Doi: 10.1016/j.copbio.2023.102900

Previdi M, Smith KL, Polvani LM (**2021**) Arctic amplification of climate change: a review of underlying mechanisms. *Environmental Research Letters*. 16, 093003. Doi: 10.1088/1748-9326/ac1c29

Rahmstorf S (**2024**) Is the Atlantic overturning circulation approaching a tipping point? *Oceanography*. Doi: 10.5670/oceanog.2024.501

Rantanen M, Karpechko AY, Lipponen A, Nordling K, Hyvärinen O, Ruosteenoja K, Vihma T, Laaksonen A (**2022**) The Arctic has warmed nearly four times faster than the globe since 1979. *Communications Earth & Environment*. 3, 168. Doi: 10.1038/s43247-022-00498-3

Rapinski M, Cuerrier A, Harris C, Elders of Ivujivik, Elders of Kangiqsujuaq, Lemire M (**2018**) Inuit perception of marine organisms: from folk classification to food harvest. *Journal of Ethnobiology*. 38, 333–335. Doi: 10.2993/0278-0771-38.3.333

Raven J, Geider RH (**1988**) Temperature and algal growth. *New Phytologist*. 110, 441–461. Doi: 10.1111/j.1469-8137.1988.tb00282.x

Re R, Pellegrini N, Proteggente A, Pannala A, Yang M, Rice-Evans C (**1999**) Antioxidant activity applying an improved ABTS radical cation decolorization assay. *Free Radical Biology & Medicine*. 26, 1231–1237. Doi: 10.1016/S0891-5849(98)00315-3

Reed TE, Schindler DE, Waples RS (**2011**) Interacting effects of phenotypic plasticity and evolution on population persistence in a changing climate. *Conservation Biology*. 25, 56–63. Doi: 10.1111/j.1523-1739.2010.01552.x

Rezayian M, Niknam V, Ebrahimzadeh H (**2019**) Oxidative damage and antioxidative system in algae. *Toxicological Reports*. 6, 1309–1313. Doi: 10.1016/j.toxrep.2019.10.001

Rivkina EM, Friedmann EI, McKay CP, Gilichinsky DA (**2000**) Metabolic activity of permafrost bacteria below the freezing point. *Applied and Environmental Microbiology*. 66, 3230–3233. Doi: 10.1128/AEM.66.8.3230-3233.2000

Roleda MY, Hurd CL (**2019**) Seaweed nutrient physiology: application of concepts to aquaculture and bioremediation. *Phycologia*. 58,552–562. Doi: 10.1080/00318884.2019.1622920

Rosenberg E, Zilber-Rosenberg I (**2016**) Microbes drive evolution of animals and plants: the hologenome concept. *American Society for Microbiology*. 7, e01395-15. Doi: 10.1128/mBio.01395-15.

Rybak M, Kołodziejczyk A, Joniak T, Ratajczak I, Gąbka M (**2017**) Bioaccumulation and toxicity studies of macroalgae (Charophyceae) treated with aluminium: experimental studies in the context of lake restoration. *Ecotoxicology and Environmental Safety*. 145, 359–366. Doi: 10.1016/j.ecoenv.2017.07.056

Sæther M, Diehl N, Monteiro C, Li H, Niedzwiedz S, Burgunter-Delamare B, Scheschonk L, Bischof K, Forbord S (**2024**) The sugar kelp *Saccharina latissima* II: recent advances in farming and applications. *Journal of Applied Phycology*. Doi: 10.1007/s10811-024-03213-1

Scheschonk L, Becker S, Hehemann J-H, Diehl N, Karsten U, Bischof K (**2019**) Arctic kelp eco-physiology during the polar night in the face of global warming: a crucial role for laminarin. *Marine Ecology Progress Series*. 611, 59–74. Doi: 10.3354/meps12860

Schlegel RW (**2020**) Marine heatwave tracker. https://tracker.marineheatwaves.org/MHW/. Last access: 11.07.2024.

Schlegel RW, Darmaraki S, Benthuysen JA, Filbee-Dexter K, Oliver ECJ (**2021**) Marine cold-spells. *Progress in Oceanography*. 198, 102684. Doi: 10.1016/j.pocean.2021.102684

Schlegel RW, Singh RK, Gentili B, Bélanger S, Castro de la Guardi L, Krause-Jensen D, Miller CA, Sejr M, Gattuso J-P (**2024**) Underwater light environment in Arctic fjords. *Earth System Science Data*. 16, 2773–2788. Doi: 10.5194/essd-16-2773-2024

Sejr MK, Bruhn A, Dalsgaard T, Juul-Pedersen T, Stedmon CA, Blicher M, Meire L, Mankoff KD, Thyrring J (**2022**) Glacial meltwater determines the balance between autotrophic and heterotrophic processes in a Greenland fjord. *Proceedings of the National Academy of Science*. 52, e2207024119. Doi: 10.1073/pnas.2207024119

Serreze MC, Bromwich DH, Clark MP, Etringer AJ, Zhang T, Lammer R (**2003**) Large-scale hydro-climatology of the terrestrial Arctic drainage system. *Journal of Geophysical Research*. 108, 8160. Doi: 10.1029/2001JD000919

Severtsov AS (**2013**) Relationship between fundamental and realized ecological niches. *Biology Bulletin Reviews*. 3, 187–195. Doi: 10.1134/S2079086413030080

_____

Sharma P, Jha AB, Dubey RS, Pessarakli M (**2012**) Reactive oxygen species, oxidative damage, and antioxidative defense mechanism in plants under stressful conditions. *Journal of Botany*. 2012, 217037. Doi: 10.1155/2012/217037

Silva CF, Pearson GA, Serrão EA, Bartsch I, Martins N (**2022**) Microscopic life stages of Arctic kelp differ in their resilience and reproductive output in response to Arctic seasonality. *European Journal of Phycology*. 57, 381–395. Doi: 10.1080/09670262.2021.2014983

Simson EJ, Scheibling RE, Metaxas A (**2015**) Kelp in hot water: I. Warming seawater temperature induces weakening and loss of kelp tissue. *Marine Ecology Progress Series*. 537, 89–104. Doi: 10.3354/meps11438

Smale DA (**2019**) Impacts of ocean warming on kelp forest ecosystems. *New Phytologist*. 225, 1447–1454. Doi: 10.1111/nph.16107

Smith KE, Burrows MT, Hobday AJ, King NG, Moore PJ, Gupta AS, Thomsen MS, Wernberg T, Smale DA (**2023**) Biological impacts of marine heatwaves. *Annual Review of Marine Science*. 15, 119–145. Doi: 10.1146/annurev-marine-032122-121437

Somero GN (**2010**) The physiology of climate change: how potentials for acclimatization and genetic adaptation will determine 'winners' and 'losers'. *The Journal of Experimental Biology*. 2013, 912–920. Doi: 10.1242/jeb.037473

Sørgaard DH, Lund-Hansen LC, López-Blanco E, Schmidt NM, Sichlau Winding MH, Sejr MK, Rysgaard S, Sorrell BK, Christensen TR, Juul-Pedersen T, Tank JL, Riis T (**preprint**) Arctic coastal nutrient limitation linked to tundra greening. Doi: 10.21203/rs.3.rs-2946573/v1

Stahl F, Kappas L, Uhl F, Oppelt N, Bischof K (**2024**) Feasibility study for kelp afforestation in the German Bight: habitat availability and light requirements of *Laminaria hyperborea*. *Journal of Sea Research*. 200, 102512. Doi: 10.1016/j.seares.2024.102512

Steneck RS, Grahm MH, Bourque BJ, Corbett D, Erlandson JM, Estes JA, Tegner MJ (**2002**) Kelp forest ecosystems: biodiversity, stability, resilience and future. *Environmental Conservation*. 29, 436–459. Doi: 10.1017/S0376892902000322

Stomp M, Huisman J, Stal LJ, Metthijs HCP (**2007**) Colorful niches of phototrophic microorganisms shaped by vibrations of the water molecule. *The ISME Journal*. 1, 271–282. Doi: 10.1038/ismej.2007.59

Straub SC, Wernberg T, Thomsen MS, Moore PJ, Burrows MT, Harvey BP, Smale DA (**2019**) Resistance, extinction, and everything in between – the diverse responses of seaweeds to marine heatwaves. *Frontiers in Marine Science*. 6, 763. Doi: 10.3389/fmars.2019.00763

Strzelecki MC, Małecki J, Zagórski P (**2015**). The influence of recent deglaciation and associated sediment flux on the functioning of polar coastal zone – Northern Petuniabukta, Svalbard. In: Maanan M, Robin M (eds) Sediment Fluxes in Coastal Areas. Coastal Research Library. Springer, Dordrecht. Doi: 10.1007/978-94-017-9260-8_2

Summers N, Fragoso GM, Johnsen G (**2023**) Photophysiologically active green, red, and brown macroalgae living in the Arctic Polar Night. *Scientific Reports*. 13, 17971. Doi: 10.1038/s41598-023-44026-5

Sun J, Norouzi O, Mašek O (**2022**) A state-of-the-art review on algae pyrolysis for bioenergy and biochar production. *Bioresource Technology*. 346, 126258. Doi: 10.1016/j.biotech.2021.126258

Svendsen H, Beszczynska-Møller A, Hagen JO, Lefauconnier B, Tverberg V, Gerland S, Ørbæk JB, Bischof K, Papucci C, Zajaczkowski M, Azzolini R, Bruland O, Wiencke C, Winther J-G, Dallmann W (**2002)** The physical environment of Kongsfjorden-Krossfjorden, an Arctic fjord system in Svalbard. *Polar Research*. 21, 133-166. Doi: 10.3402/polar.v21i1.6479

Teagle H, Hawkins SJ, Moore P, Smale DA (**2017**) The role of kelp species as biogenic habitat formers in coastal marine ecosystems. *Journal of Experimental Marine Biology and Ecology*. 492, 81–98. Doi: 10.1016/j.jembe.2017.01.017

Timmermans M-L, Marshall J (**2020**) Understanding Arctic Ocean circulation: a review of ocean dynamics in a changing climate. *Advancing Earth and Space Science*. 125, e2018JC014378. Doi: 10.1029/2018JC014378

tom Dieck I (**1993**) Temperature tolerance and survival in darkness of kelp gametophytes (Laminariales, Phaeophyta): ecological and biogeographic implications. *Marine Ecology Progress Series*. 100, 253–264. Doi: 10.3354/meps100253

Torres MA, Barros MP, Campos SCG, Pinto E, Rajamani S, Sayre R, Colepicolo P (**2008**) Biochemical biomarkers in algae and marine pollution: a review. *Ecotoxicology and Environmental Safety*. 71, 1–15. Doi: 10.1016/j.ecoenv.2008.05.009

Traiger S (**2019**) Effects of elevated temperature and sedimentation on grazing rates of the green sea urchin: implications for kelp forests exposed to increased sedimentation with climate change. *Helgoland Marine Research*. 73, 1–7. Doi: 10.1186/s10152-019-0526-x

Twining BS, Baines SB (**2013**) The trace metal composition of marine phytoplankton. *Annual Review of Marine Science* 5, 191–215. Doi: 10.1146/annurev-marine-121211-172322

Vadas RL (**1977**) Preferential feeding: an optimization strategy in sea urchins. *Ecological Monographs*. 47, 337–371. Doi: 10.2307/1942173

Vallee BL, Ulmer DD (**1972**) Biochemical effects of mercury, cadmium and lead. *Annual Reviews*, 41, 91-128. Doi: 10.1146/annurev.bi.41.070172.000515

Vihtakari M (**2024**) ggOceanMaps: plot data on oceanographic maps using 'ggplot2'. R package version 2.2.0, https://CRAN.R-project.org/package=ggOceanMaps

Vranken S, Wernberg T, Scheben A, Severn-Ellis AA, Batley J, Bayer PE, Edwards D, Wheeler D, Coleman MA (**2021**) Genotype-Environment mismatch of kelp forests under climate change. *Molecular Ecology*. 30, 3730–3746. Doi: 10.1111/mec.15993

Wahl M, Werner FJ, Buchholz B, Raddatz S, Graiff A, Matthiessen B, Karsten U, Hiebenthal C, Hamer J, Ito M, Gülzow E, Rilov G, Guy-Haim T (**2020**) Season affects strength and direction of the interactive impacts of ocean warming and biotic stress in a coastal seaweed ecosystem. *Limnology and Oceanography*. 65, 807–827. Doi: 10.1002/lno.11350

Wernberg T, Thomasen MS, Tuya F, Kendrick GA, Staehr PA, Toohey BD (**2010**) Decreasing resilience of kelp beds along a latitudinal temperature gradient: potential implications for a warmer future. *Ecology Letters*. 13, 685–694. Doi: 10.1111/j.1461-0248.2010.01466.x

Wernberg T, Smale DA, Tuya F, Thomsen MS, Langlois TJ, de Bettignies T, Bennett S, Rousseaux CS (**2013**) An extreme climatic event alters marine ecosystem structure in a global biodiversity hotspot. *Nature Climate Change*. 3, 78–82. Doi: 10.1038/nclimate1627

_____

Wernberg T, Bennett S, Babcock RC, de Bettignies T, Cure K, Depczynski M, Dufois F, Fromont J, Fulton CJ, Hovey RK, Harvey ES, Holmes TH, Kendrick GA, Radford B, Santana-Garcon J, Saunders BJ, Smale DA, Thomsen MS, Tuckett CA, Tuya F, Vanderklift MA, Wilson S (**2016**) Climate-driven regime shift of a temperate marine ecosystem. *Climate Change*. 353, 169–172. Doi: 10.1126/science.aad8745

Wernberg T, Krumhansl K, Filbee-Dexter K, Pedersen MF (**2019**) Status and trends for the world's kelp forests. In: World Seas: An Environmental Evaluation. Academic Press. Doi: 10.1016/B978-0-12-805052-1.00003-6

Wernberg T, Thomsen MS, Baum JK, Bishop MJ, Bruno JF, Coleman MA, Filbee-Dexter K, Gagnon K, He Q, Murdiyarson D, Rogers K, Silliman BR, Smale DA, Starko S, Vanderklift MA (**2024**) Impacts of climate change on marine foundation species. *Annual Review of Marine Science*. 16, 247–282. Doi: 10.1146/annurev-marine-042023-093037

Wiencke C, Clayton MN, Gómez I, Iken K, Lüder K, Amsler CD, Karsten U, Hanelt D, Bischof K, Dunton K (**2006**) Life strategy, ecophysiology and ecology of seaweeds in polar waters. *Reviews in Environmental Science and Bio/Technology*. In: Amils R, Ellis-Evans C, Hinghofer-Szalkay H (eds) Life in Extreme Environments. Springer, Dordrecht. Doi: 10.1007/978-1-4020-6285-8_13

Wiencke C, Bischof K (eds) (**2012**). Seaweed Biology - Novel insights into ecophysiology, ecology and utilization. Heidelberg New York Dodrecht London: Springer.

Wilce RT, Dunton KH (**2014**) The boulder patch (North Alaska, Beufort Sea) and its benthic algal flora. *Arctic*. 67, 43–56. Doi: 10.14430/arctic4360

Wilson KL, Skinner MA, Lotze HK (**2019**) Projected 21st-century distribution of canopy-forming seaweeds in the Northwest Atlantic with climate change. *Diversity and Distribution*. 25, 582–602. Doi: 10.1111/ddi.12897

Wondraczek L, Batentschuk M, Schmidt MA, Borchardt R, Scheiner S, Seemann B, Schweizer P, Brabec CJ (**2013**) Solar spectral conversion for improving the photosynthetic activity in algae reactors. *Nature Communications*. 4, 2047. Doi: 10.1038/ncomms3047

Wright LS, Pessarodona A, Foggo A (**2022**) Climate-drive shifts in kelp forest composition reduce carbon sequestration potential. *Global Change Biology*. 28, 5514–5531. Doi: 10.1111/gcb.16299

Xue X, Gauthier DA, Turpin DH, Weger HG (**1996**) Interactions between photosynthesis and respiration in the green algae *Chlamydomonas reinhardtii*. *Plant Physiology*. 112, 1005–1014. Doi: 10.1104/pp.112.3.1005

Yanshuo W, Fei H, Tingting F (**2017**) Spatio-temporal variations of Arctic amplification and their linkage with the Arctic oscillation. *Acta Oceanologica Sinic.* 36, 42-51. doi: 10.1007/s13131-017-1025-z

Zacher K, Bernard M, Bartsch I, Wiencke C (**2016**) Survival of early life history stages of Arctic kelps (Kongsfjorden, Svalbard) under multifactorial global change scenarios. *Polar Biology*. 39, 2009–2020. Doi: 10.1007/s00300-016-1906-1

Zajączkowski MJ, Legeżyńska J (**2001**) Estimation of zooplankton mortality caused by an Arctic glacier outflow. *Oceanologia*. 43, 341–351.

_____

Zeraatkar AK, Ahmadzadeh H, Talebi AF, Moheimani NR, McHenry MP (**2016**) Potential use of algae for heavy metal bioremediation, a critical review. *Journal of Environmental Management.* 181, 817–831. Doi: 10.1016/j.jenvman.2016.06.059

10   Acknowledgements

always welcoming me at AWI and having time for a cup of coffee! Thank you, **Clément** for joining this PhD adventure, the update calls, Lofoten pictures and data-please-make-sense evenings!

Lots of thanks to everyone who joined me on expedition! Thanks for helping me carry all those heavy boxes, getting frozen and sharing unbelievable moments in the most beautiful Arctic nature. This work would not have been possible without you – at this point, thanks to **Ronny Pelikan**, you made the expeditions possible in the first place with some magic on customs papers! Thanks to the AWI CSD team – and especially, **Markus**, **Lena**, and **Verena** for a wonderful summer in Ny-Ålesund, and for taking me along to the most peaceful place on earth with jumping Minkie whales and pancakes. Thank you, **Alex** for two great weeks on Helgoland! Thank you, **Sebastian** for taking over that very first presentation on board of Hurtigruten, for hour-long water filtrations deep into night and for getting soaking wet with me during a very bumpy boat ride. Thank you, **Ellie** for the most amazing kelp pickles ever!! and thank you both for sharing the excitement for muddy water! Special thanks to the **Hurtigruten crew** for the great support and squeezing in all those amazing sampling opportunities. Thank you, **Tobias** for adopting us in Nuuk and taking us on all those great trips in Nuup Kangerlua – I never ate better fish than in Qorquut. Thank you for sharing one of the most amazing dives of my life! I have never been more frozen! Also thank you, **Dani**, **Ida** and **Ninni** – I miss those fun evenings late into the night with self-hunted reindeer, mussels and Greenlandic coffee.

I thank all my friends for reminding me that there is a world outside of algae in muddy water! **Ivain** and **Rene** – thank you for sharing the adventures, pains and fun, of the scientific diving education and becoming dear friends. I am looking forward to meet you somewhere in Norway or for a burger in Hamburg. **Anncathrin**, ich freue mich schon auf ein nächstes Mädelswochenende. **Finn**, vielen Dank für all die bücherphilosophischen Nachmittage über schönem Tee! Ich freue mich schon auf den Nächsten. **Alexandra**, ich bin sehr dankbar, dass Du schon immer für mich da warst.

Liebsten Dank an **Daniel** für die kleine Welt, ganz egal wo und wie sie mal wieder sehr groß ist und all die vergangen, sowie zukünftigen *Guten-Morgen*-de, nicht nur wenn es um sechs Musikstücke geht.
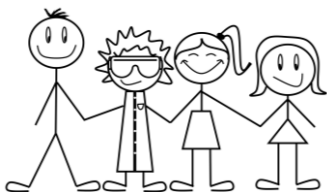
Mama, Papa und **Fenja**, es fällt mir schwer Worte zu finden, deswegen mach ich es kurz – vielen Dank für alles!

11   Versicherung an Eides Statt

Ich, Sarina Niedzwiedz,

versichere an Eides Statt durch meine Unterschrift, dass ich die vorstehende Arbeit selbständig und ohne fremde Hilfe angefertigt und alle Stellen, die ich wörtlich oder dem Sinne nach aus Veröffentlichungen entnommen habe, als solche kenntlich gemacht habe, mich auch keiner anderen als der angegebenen Literatur oder sonstiger Hilfsmittel bedient habe.

Ich versichere an Eides Statt, dass die zu Prüfungszwecken beigelegte elektronische Version der Dissertation identisch ist mit der abgegebenen gedruckten Version.

Ich versichere an Eides Statt, dass ich die vorgenannten Angaben nach bestem Wissen und Gewissen gemacht habe und dass die Angaben der Wahrheit entsprechen und ich nichts verschwiegen habe.

Die Strafbarkeit einer falschen eidesstattlichen Versicherung ist mir bekannt, namentlich die Strafanordnung gemäß § 156 StGB bis zu drei Jahre Freiheitsstrafe oder Geldstrafe bei vorsätzlicher Begehung der Tat bzw. gemäß § 161 Abs. 1 StGB bis zu einem Jahr Freiheitsstrafe bei fahrlässiger Begehung.

Bremen, 26.07.2024   Sarina Niedzwiedz
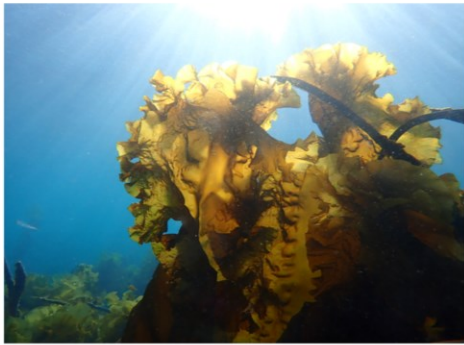
Kelps are brown macroalgae that form marine forests on Arctic rocky shores. They act as foundation species for many associated species and are of vast socio-economic importance.

Due to climate change, temperatures are rising and the frequency of marine heatwaves is increasing. Glacial melt results in extensive coastal run-off, leading to a darkening of fjords.
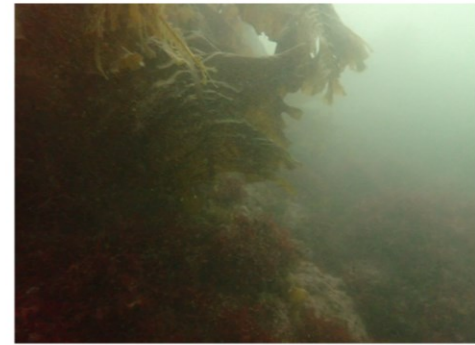
I assessed how coastal run-off affects Arctic kelp populations. I focussed on **temperature × light** interactions, as well as *in-situ* **effects**.

Temperature × light interactions
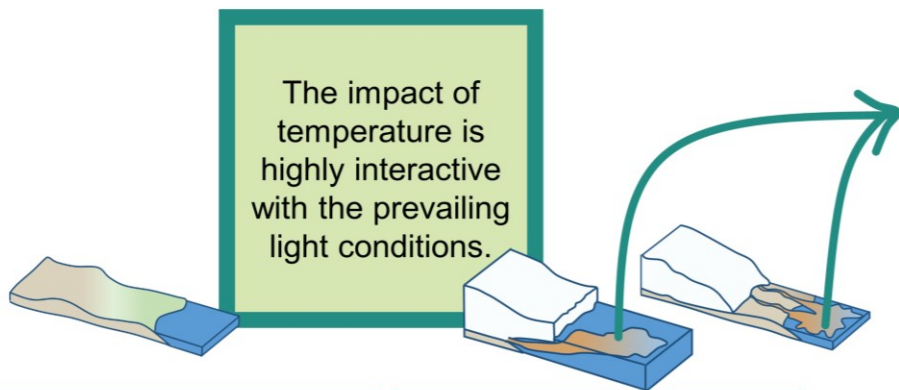
The impact of temperature is highly interactive with the prevailing light conditions.

In-situ effects
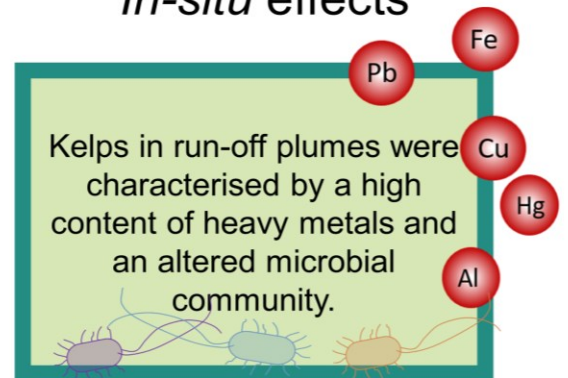
Kelps in run-off plumes were characterised by a high content of heavy metals and an altered microbial community.

Fe
Pb
Cu
Hg
Al

High-light availabilities caused physiological stress.
When interacting with cold temperatures the **northward expansion of kelps was opposed**.

Low-light availabilities **reduced the kelps' maximum depth distribution**.
The effect was accelerated by warm temperatures.

Bioaccumulation of harmful elements in higher trophic levels and
altered functioning of the kelp holobiont have **possible bioeconomic consequences**.

University of Bremen

Sarina Niedzwiedz
Marine Botany
University of Bremen
sarina@uni-bremen.de

EU Polar Cluster

FACE-IT
Arctic Biodiversity & Livelihoods

www.face-it-project.eu
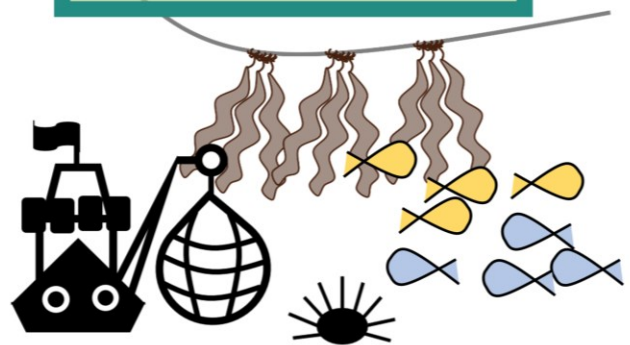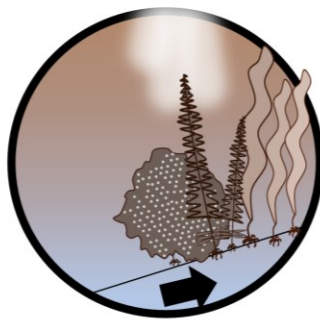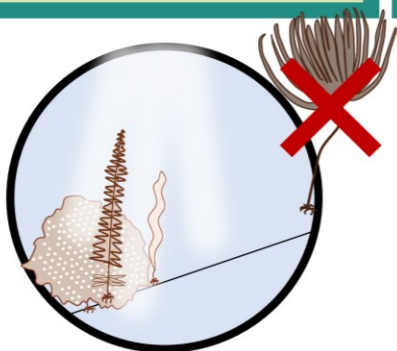
Cover of the printed version: